The Role of N-Acetyl-Aspartyl-Glutamate (NAAG) in the Modulation of NMDA Receptors

PAMELA KHACHO

Thesis submitted to the Faculty of Graduate and Postdoctoral studies in partial fulfillment of the requirements for the Doctorate in Philosophy degree in Neuroscience

Neuroscience Program

Department of Cellular and Molecular Medicine

Faculty of Medicine, University of Ottawa

ABSTRACT

Ischemic strokes cause excessive release of glutamate, leading to overactivation of *N*-methyl-D-aspartate receptors (NMDARs) and excitotoxicity-induced neuronal death. For this reason, inhibition of NMDARs has been a central focus in identifying mechanisms to avert this extensive neuronal damage. *N*-acetyl-aspartyl-glutamate (NAAG), the most abundant neuropeptide in the brain, is neuroprotective in ischemic conditions *in vivo*. Despite this evidence, the exact mechanism underlying its neuroprotection, and more specifically its effect on NMDARs, is currently unknown due to conflicting results in the literature. Here, we uncover a pH-dependent and subunit specific action of NAAG on NMDARs. Using whole-cell electrophysiological recordings on acute hippocampal slices from adult mice and on HEK293 cells, we found that NAAG increases synaptic GluN2A-containing NMDAR excitatory postsynaptic currents (EPSCs), while effectively decreasing extrasynaptic GluN2B-containing NMDAR EPSCs in physiological pH. Intriguingly, the results of our study further show that in low pH, which is a physiological occurrence during ischemia, NAAG depresses GluN2A-containing NMDAR EPSCs and amplifies its inhibitory effect on GluN2B-containing NMDAR EPSCs, as well as upregulates the surface expression of the GluN2A subunit. Altogether, our data demonstrate that NAAG has differential effects on NMDAR function based on subunit composition and extracellular pH levels. These findings suggest that the role of NAAG as a neuroprotective agent during an ischemic stroke is likely mediated by its ability to reduce NMDAR excitation. The inhibitory effect of NAAG on NMDARs and its enhanced function in acidic conditions makes NAAG a prime therapeutic agent for the treatment of ischemic events.

TABLE OF CONTENTS

LIST OF FIGURES

LIST OF TABLES

LIST OF ABBREVIATIONS

2-MPPA	2-(3-mercaptopropyl)pentanedioic acid
2-PMPA	2-(phosphonomethyl)pentanedioic acid
2-PMSA	2-(phosphonomethyl)succinic acid
ACSF	Artifical cerebrospinal fluid
AMPAR	α-amino-3-hydroxy-5-methyl-4-isoxazolepropionic acid receptors
ATP	Adenosine triphosphate
BDNF	Brain-derived neurotrophic factor
CREB	cAMP response element binding protein
CTD	C-terminal domain
DAPK1	Death-associated protein kinase 1
EPSC	Excitatory postsynaptic current
ERK1/2	Extracellular signal-regulated kinase 1/2
GCP-II	Glutamate carboxypeptidase II
GCP-III	Glutamate carboxypeptidase III
GPI-5232	2-[[hydroxy[2,3,4,5,6pentafluorophenyl)methyl] phosphinyl] methyl] pentanedioic acid
GPI-5693	2-(3-mercaptopropyl)pentanedioic acid
i.n.	Intranasal
i.p.	Intraperitoneal
LTD	Long-term depression
LTP	Long-term potentiation
MAGUKs	Membrane-associated guanylate kinases

$mGluR_3$	Metabotropic glutamate receptor 3
mGluR	Metabotropic glutamate receptors
MCAO	Middle cerebral artery occlusion
NAA	N-acetyl-aspartate
NAAG	N-acetyl-aspartyl-glutamate
NMDAR	N-methyl-D-aspartate receptor
nNOS	Neuronal nitric oxide synthase
NO	Nitric oxide
NTD	N-terminal domain
PKA	Protein kinase A
PKC	Protein kinase C
PSD-95	Postsynaptic density-95
ROS	Reactive oxygen species
rt-PA	thrombolytic recombinant tissue plasminogen
SAP102	Synapse associated protein 102
TMD	Transmembrane domain

LIST OF PUBLICATIONS

1. **Khacho P**, Wang B, Ahlskog N, Hristova E, Bergeron R, 2015. Differential effects of N-acetyl-aspartyl-glutamate on synaptic and extrasynaptic NMDA receptors are subunit-and pH-dependent in the CA1 region of the mouse hippocampus. *Neurobiology of Disease*, 82, 580–592
2. Khacho M, Tarabay M, Patten D, **Khacho P**, MacLaurin JG, Guadagno J, Bergeron R, Cregan SP, Harper M-E, Park DS, Slack RS, 2014. Acidosis overrides oxygen deprivation to maintain mitochondrial function and cell survival. *Nature Communications*, 5, Article number: 3550
3. Bakkar W, Ma CL, Pabba M, **Khacho P**, Zhang YL, Muller E, Martina M, Bergeron R, 2011. Chronically saturating levels of endogenous glycine disrupt glutamatergic neurotransmission and enhance synaptogenesis in the CA1 region of the mouse hippocampus. *Synapse*, 65, 1181–1195

AUTHORIZATION FOR THE USE OF PUBLISHED MATERIALS

Neurobiology of Disease

Khacho P, Wang B, Ahlskog N, Hristova E, Bergeron R, 2015. Differential effects of N-acetyl-aspartyl-glutamate on synaptic and extrasynaptic NMDA receptors are subunit-and pH-dependent in the CA1 region of the mouse hippocampus. *Neurobiology of Disease*, 82, 580–592. doi: 10.1016/j.nbd.2015.08.017

"Authors publishing in Elsevier journals retain wide rights to continue to use their works to support scientific advancement, teaching and scholarly communication. An author can, without asking permission, do the following after publication of the author's article in an Elsevier-published journal:

...Include the article in full or in part in a thesis or dissertation"

ACKNOWLEDGEMENTS

First and foremost, I would like to express my sincerest appreciation and gratitude to my PhD supervisor, Dr. Richard Bergeron, for allowing me the opportunity to pursue my graduate studies in his laboratory. Your continued encouragement and mentorship have helped me progress and thrive as a scientist. I am truly grateful for your unending support and expert guidance throughout the years. Your passion, determination, and accomplishments have been inspiring and have surely pushed me towards reaching my goals.

I would like to thank the members of my PhD advisory committee Dr. Jean-Claude Béïque, Dr. Hsiao-Huei Chen, and Dr. Leo Renaud for their critical assessment of my work and insightful comments. A special thanks to Dr. Béïque for his valuable scientific guidance and discussion, which helped me tremendously while pursuing my degree. I would also like to extend my gratitude to all former and present members of Dr. Bergeron's laboratory, including Nina Ahlskog, Dante Biscaro, Elitza Hristova, Dr. Chun Lei Ma, Dr. Marzia Martina, Kieran McCann, Christian Metivier, Dr. Mohan Pabba, Dr. C. Prakash, Dr. Melissa Snyder, Alexandra Sokolovski, Jack Wang, and Dr. Adrian Wong, for their valuable guidance, discussions, and technical assistance. I would like to especially thank Jack, Nina, and Melissa, for their insightful suggestions and in depth analysis and criticism regarding my project and thesis. In addition, I would like to thank Dr. Béïque's lab members, including Saleha Assadzada, Sean Geddes, Kevin Lee, David Lemelin, Sebastian Maille, Wissam Nassrallah, and Cary Soares. You have all been outstanding co-workers and friends, and I thank you for creating such a great working

environment. I would like to take this opportunity to also thank Linda Richard who helped me tremendously in my early years as a graduate student, Nella Bianconi for her academic assistance, and Kelsey Oldland for proofreading my thesis.

Finally, I wish to thank my parents and my sister. I am truly grateful for your constant support, encouragement, and excitement towards my research. The moral support you have given me has been invaluable throughout my degree and for this I am sincerely appreciative.

"However difficult life may seem, there is always something you can do and succeed at."

– *Stephen Hawking*

1. *INTRODUCTION*

1.1. STROKE

Stroke is the leading cause of disability and the third leading cause of death in Canada, ranking behind heart disease and cancer. According to Statistics Canada, each year, over 13,000 Canadians die from stroke, accounting for ~6% of all deaths (Statcan, 2011). Of the 50,000 Canadians that survive a stroke each year, very few recover completely (Heart&Stroke, 2015). The remaining survivors can suffer from a number of disabilities including memory loss, decreased sensation, speech and swallowing difficulties, loss of coordination, and paralysis on one side of the body (Bonita and Beaglehole, 1988; Gresham et al., 1997). Although, in the past six decades, the risk of death following a stroke has been reduced due to improvements in care, the effects of stroke continue to have a significant and long lasting impact on individuals and their families, as well as to the health care system. It is estimated that stroke costs the Canadian economy $3.6 billion a year due to health care costs and decreased economic output. The number of strokes will continue to rise due to population growth, as well as the increasing prevalence of obesity and diabetes, creating further challenges for our health care system (PHAC, 2009). The economic burden of stroke on our society, in addition to diminished quality of life, is justification to find ways to reduce impairment after a stroke.

1.1.1. Pathobiology of stroke

Eighty percent of strokes are ischemic events, while the remaining 20% are caused by hemorrhages. In the case of an ischemic stroke, cerebral blood flow is reduced below the threshold that sustains cell survival, resulting in significant brain damage following a

sequence of pathobiological events. The reduction in blood flow is, in most cases, caused by the occlusion of a cerebral artery either by an embolus or by local thrombosis (Aggarwal et al., 2010). This focal impairment of cerebral blood flow restricts the delivery of substrates, particularly oxygen and glucose, and impedes the normal process of generating energy in the form of adenosine triphosphate (ATP) through oxidative phosphorylation. The resulting decrease in energy supply in neurons impairs the function of energy-dependent Na^+/K^+ ATPase membrane pumps, leading to a disruption in maintaining ionic gradients across the membrane. Consequently, membrane potential is lost and neurons depolarize (Choi, 1987; Martin et al., 1994). Somatodendritic as well as presynaptic voltage-dependent Ca^{2+} channels become activated and excitatory amino acids, such as glutamate, are released into the extracellular space (Choi and Rothman, 1990). Simultaneously, other energy-dependent processes, such as reuptake of glutamate through the use of glutamate transporters, are impeded, which further increases the accumulation of glutamate in the extracellular space (Phillis et al., 2000; Mitani and Tanaka, 2003). Neuronal death following an ischemic stroke is primarily attributed to this accumulation of glutamate (Dirnagl et al., 1999; Camacho and Massieu, 2006).

Glutamate is the most abundant excitatory neurotransmitter found in the mammalian brain (Meldrum, 2000). It acts on two distinct classes of receptors: ionotropic receptors (*N*-mehtyl-D-aspartate receptors (NMDARs), α-amino-3-hydroxy-5-methyl-4-isoxazolepropionic acid receptors (AMPARs), and kainate receptors) and metabotropic glutamate receptors (mGluR) (Hollmann et al., 1989; Keinanen et al., 1990; Hollmann and Heinemann, 1994). Overactivation of these receptors by increased levels of glutamate, such as during a stroke, usually leads to neuronal damage and death in a

process known as glutamate excitotoxicity (Olney and de Gubareff, 1978; Rothman, 1983; Sattler and Tymianski, 2001). Glutamate excitoxicity is primarily Ca^{2+}-dependent and the overactivation of NMDARs play a major role mainly due to their high Ca^{2+} permeability (Choi, 1988; Tymianski, 1996; Tymianski and Tator, 1996; Sattler and Tymianski, 2000). A large influx of Ca^{2+} into the cell results in the activation of Ca^{2+}-dependent enzymes, such as phospholipases, proteases, and endonucleases, which break down phospholipds, proteins, and nucleic acids, respectively, resulting in neuroinflammation and profound damage to the cell structure (Arundine and Tymianski, 2003). In addition, Ca^{2+}-induced activation of second messengers such as neuronal nitric oxide synthase (nNOS) leads to the generation of excessive levels of nitric oxide (NO). NO serves as a substrate for the production of highly reactive free radicals, such as reactive oxygen species (ROS), which can further induce cell death (Beckman and Crow, 1993; Beckman and Koppenol, 1996; Abramov et al., 2007). Excessive Ca^{2+} influx also leads to mitochondrial dysfunction and release of pro-apoptotic proteins from the mitochondrial intermembrane space (Schinder et al., 1996; Vergun et al., 1999). Altogether, the sequence of events resulting from an ischemic stroke and involving excitotoxicity is referred to as the ichemic cascade and ultimately leads to neuronal death (Iadecola, 1997; Dirnagl et al., 1999; Sattler and Tymianski, 2001; Arundine and Tymianski, 2003; Celsi et al., 2009; Aggarwal et al., 2010) (**Fig. 1**).

Following a stroke, the ischemic tissue in the core of the insult and in the surrounding regions is not equally affected by the hemodynamic, metabolic and ionic changes. In the core of the region affected by stroke, anoxic depolarization develops and

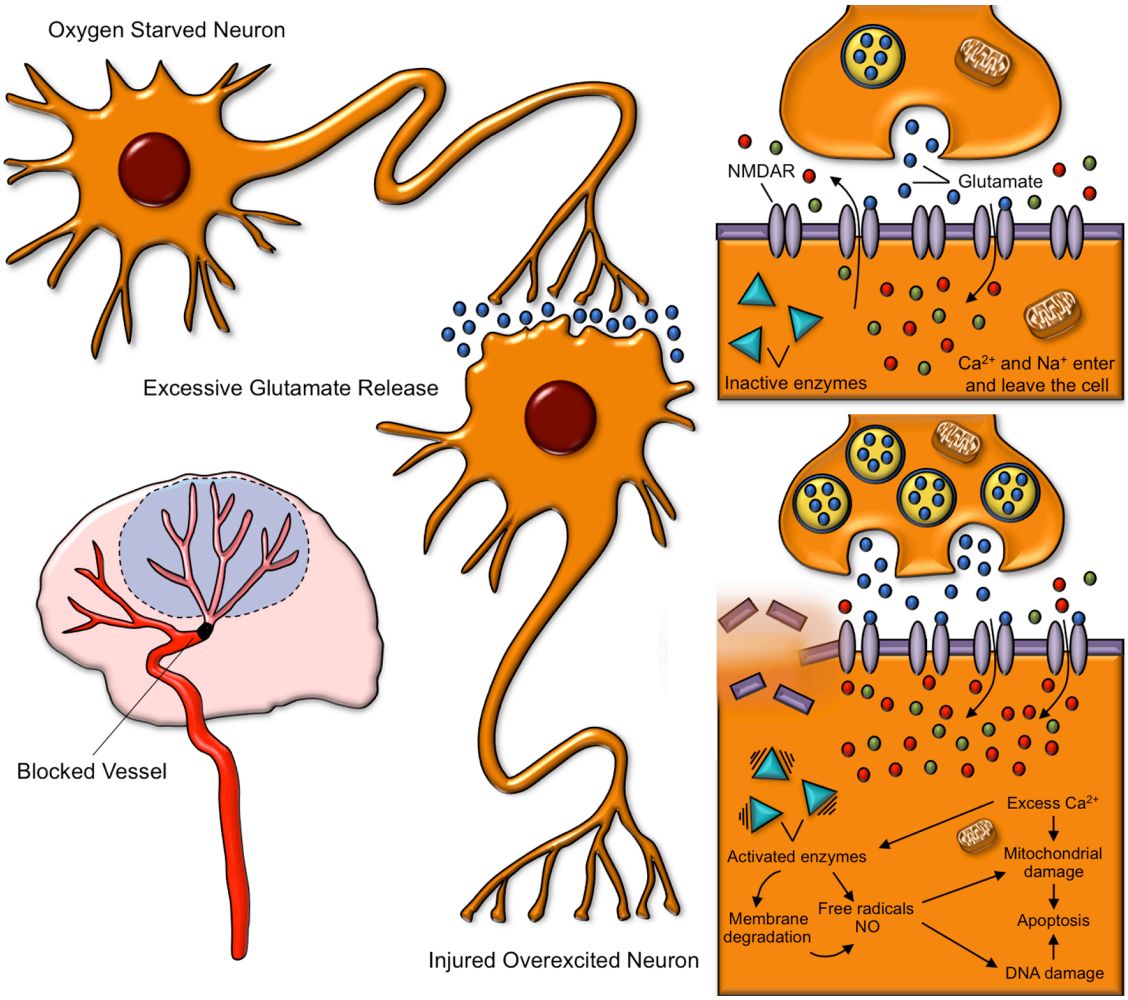

Figure 1. The ischemic cascade. An ischemic stroke occurs when a blood vessel carrying blood to the brain is blocked by a blood clot. The disruption in oxygen delivery causes energy failure leading to excessive glutamate release and overactivation of glutamate receptors. Activation of NMDARs increases Ca^{2+} and Na^{+} levels in the postsynaptic neuron. Excessive Ca^{2+} overactivates degradative enzymes such as proteases, lipases, and endonucleases. As a result free radicals and reactive oxygen species (ROS) are generated causing membrane degradation (lipolysis), as well as mitochondrial and DNA damage, leading to eventual cell death. Adapted from Dirnagl et al., 1999.

cell death occurs rapidly via necrosis. In many cases, once these ischemic pathways have been initiated, re-establishing the oxygen supply is not enough to stop the irreversible effects of free radical production and cellular damage in the ischemic core. Surrounding the lethally damaged ischemic core is the ischemic penumbra, an area with partially preserved energy metabolism due to blood supply from collateral arteries (Kaufmann et al., 1999). This tissue remains viable for several hours and is damaged reversibly, however, without treatment, the ongoing excitotoxicity can eventually lead to secondary detrimental effects, such as spreading depolarization, post-ischemic inflammation, and apoptosis. Hence, the penumbral area is a good target for therapeutic intervention, since there is a window of opportunity to reverse the damage (Obrenovitch, 1995; Dirnagl et al., 1999; Doyle et al., 2008) (**Fig. 2**).

1.1.2. Current stroke treatments

At present, there are two major approaches for the treatment of ischemic stroke: 1) restoration of blood flow to the compromised region, which involves the use of thrombolytic recombinant tissue plasminogen activator (rt-PA), and 2) neuroprotection, which involves the use of drugs to interfere with one or more of the mechanisms in the ischemic cascade and thus minimize the resultant tissue damage. However, only thrombolysis is in clinical use in most parts of the world (Green and Shuaib, 2006).

The basis of thrombolysis is the dissolution of blood clots, thereby restoring blood flow to the affected ischemic tissue. Although thrombolysis with rt-PA is clinically effective for treating acute ischemic stroke (NINDS, 1995), its use is limited by several factors. The restoration of blood flow, also referred to as reperfusion, has been shown to

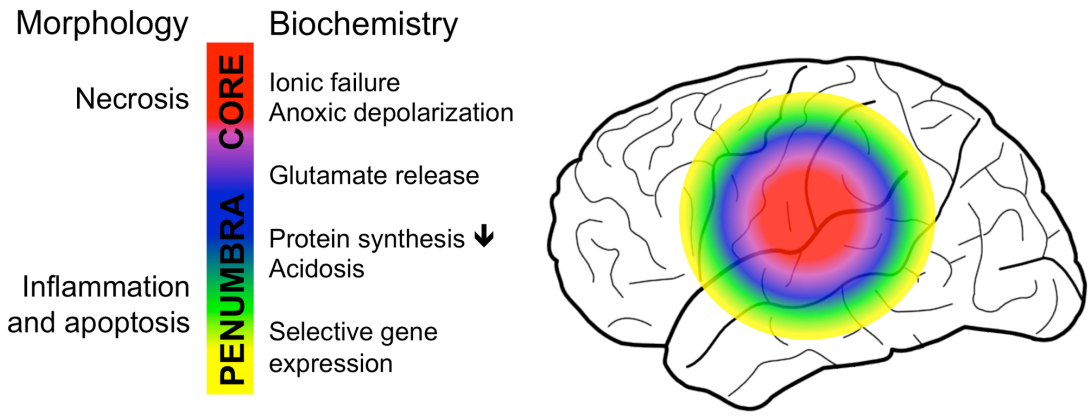

Figure 2. The ischemic core and penumbra. Following an ischemic event there are two zones of injury. The zone closest to the injury is the ischemic core, an area with severe ischemia, ultimately causing neurons and their supportive cells to die within minutes. The zone on the periphery of the core is called the ischemic penumbra, which consists of moderately ischemic tissue that lies between the core and the normally perfused brain. The tissue in the penumbra remains viable due to some continued blood flow from collateral arteries, however, without treatment the neurons will eventually die if the blood flow is not re-established within a few hours. While neurons in the ischemic core cannot be rescued, neurons in the penumbra are potential targets for therapeutic intervention. Modified from Dirnagl et al., 1999.

exacerbate the injury initially caused by ischemia in some patients and animal stroke models. Reperfusion injury is induced by the additional release of free radicals, resulting in further inflammation and oxidative damage (Matsuo et al., 1995; Morimoto et al., 1996; Mori et al., 1999; Nour et al., 2013). There is also an increased risk of symptomatic intracranial hemorrhage, where about 5% of patients will experience hemorrhagic complications as a result of the drug administration (Wardlaw et al., 1997). Furthermore, rt-PA treatment can only be delivered to those with ischemic stroke admitted within three to four and a half hours of definite onset of symptoms, meaning that this treatment is administered to less than 5% of stroke patients (O'Connor et al., 1999; Quaba and Robertson, 2002).

Neuroprotection is an entirely different approach and refers to the process of protecting against neuronal injury and degeneration. Overactivation of glutamate receptors, through the failure of ion homeostasis, and increase in intracellular Ca^{2+} concentration, as explained in section 1.1.1, is a major factor involved in initiating Ca^{2+}-dependent cell death (Aggarwal et al., 2010). Although Ca^{2+} accumulation can occur through voltage-dependent Ca^{2+} channels and the Na^{+}/Ca^{2+} exchanger, as well as being released from neuronal intracellular stores, it appears that the overactivation of NMDARs may be the major route by which glutamate induces toxic Ca^{2+} influx (Murphy et al., 1987; Choi et al., 1988; Finkbeiner and Stevens, 1988; Tymianski et al., 1993; Sattler et al., 1998). One way in which the toxicity of NMDAR-mediated Ca^{2+} entry is governed is by the coupling of NMDARs to neurotoxic intracellular second messengers, such as postsynaptic density-95 (PSD-95) protein (Sattler et al., 1999; Aarts et al., 2002). Therefore, a straightforward therapeutic approach would be to block these NMDARs that

are activated by glutamate. In fact, studies have shown that NMDAR antagonists demonstrate robust neuroprotection when given before or at the time of middle cerebral artery occlusion (MCAO) in animal models of permanent or reperfusion ischemia (Gotti et al., 1988; Park et al., 1989; Gotti et al., 1990; Scatton, 1994; Prass and Dirnagl, 1998). However, at present, no neuroprotective agents are proven to have a definite positive outcome in stroke patients, and all clinical trials, particularly those that block NMDARs, have failed (Grotta, 1995; Lees, 1997; Ginsberg, 2008). There are several possibilities as to why clinical trials have produced negative results, despite the abundance of therapeutic strategies that have decreased injury in animal models when using the same agents. Given that glutamate-mediated activation of NMDARs plays an important physiological role in learning, memory and synaptic plasticity, blocking NMDARs can also have serious side effects, such as psychotomimesis, respiratory depression or cardiovascular dysregulation (Ikonomidou and Turski, 2002). The side effects produced by most anti-excitotoxic compounds severely limit the tolerated dose, such that levels in humans reach only a fifth of the effective concentrations observed in rodent models (Grotta, 1995; Dirnagl et al., 1999; Ikonomidou and Turski, 2002). It is therefore crucial to design neuroprotective drugs with fewer side effects and improved safety profiles and more favourable pharmacokinetics. A possible approach would be to target specific NMDAR subunits and design more selective drugs in the future that are clinically safer (Yamakura and Shimoji, 1999).

1.2. NMDA RECEPTORS (NMDARs)

NMDARs are ligand-gated ion channels involved in a variety of important physiological processes, including synaptogenesis and synaptic plasticity (e.g., long-term potentiation (LTP) and long-term depression (LTD)). However, dysregulation of NMDAR activity can lead to stroke, pathological pain, and neurodegenerative and neuropsychiatric disorders (e.g. Alzheimer's disease, depression, and schizophrenia) (Lau and Zukin, 2007; Paoletti et al., 2013). NMDARs exhibit distinctive characteristics that differentiate them from other ligand-gated ion channels. First, binding of both glutamate and co-agonists D-serine or glycine are required for the activation of the receptor (Johnson and Ascher, 1987; Kleckner and Dingledine, 1988; Schell et al., 1995; Mothet et al., 2000; Papouin et al., 2012). Second, extracellular Mg^{2+}, at resting membrane potential, blocks the NMDAR channel pore, and can only be released upon membrane depolarization (Mayer et al., 1984). Lastly, NMDAR channels are highly permeable to Ca^{2+} (Mayer and Westbrook, 1987; Schneggenburger et al., 1993). This characteristic is the key trigger for many important physiological events (Lynch et al., 1983; Choi, 1987; Dudek and Bear, 1992; Paoletti et al., 2013).

1.2.1. Molecular biology of NMDARs

Functional NMDARs are tetramers composed of two obligatory GluN1 subunits, of which there are eight splice variants encoded by a single gene, combined with two GluN2 subunits, of which there are four subtypes (GluN2A–D), each encoded by four distinct genes. A third family of NMDAR subunits, GluN3, has also been described, which includes subtypes GluN3A and GluN3B (Cull-Candy and Leszkiewicz, 2004; Paoletti et

al., 2013). Each NMDAR subunit consists of four distinct domains: the N-terminal domain (NTD), which contains the binding sites for allosteric modulators; the agonist-binding domain (ABD), which contains the binding sites for glycine/D-serine (GluN1) and glutamate (GluN2), and competitive antagonists; the transmembrane domain (TMD), made of three transmembrane segments (M1, M3, and M4) and a pore loop (M2), and lastly, the C-terminal domain (CTD), which binds to differential intracellular mediators involved in receptor trafficking, anchoring and coupling to signaling molecules (Hollmann and Heinemann, 1994; Kuryatov et al., 1994; Laube et al., 1997; Dingledine et al., 1999; Mayer, 2006; Traynelis et al., 2010; Paoletti et al., 2013) (**Fig. 3**). The subunit composition of the NMDAR is dynamic; changing during synaptic development, synaptic plasticity, and other physiological and pathophysiological processes, and dictates the functional properties of the receptor. Different GluN2 subunits within a heteromeric receptor differentially influence the receptors pharmacology and function depending on their regional and developmental expression, their subcellular location (synaptic or extrasynaptic sites), and their coupling to downstream signaling cascades (Yamakura and Shimoji, 1999; Cull-Candy and Leszkiewicz, 2004; Paoletti et al., 2013; Wyllie et al., 2013).

1.2.2. NMDAR distribution and development: GluN1 and GluN2 subunits

NMDARs are located both synaptically and extrasynaptically on postsynaptic neurons (van Zundert et al., 2004). The GluN1 subunit is expressed throughout the brain and is essential for NMDAR-channel activity (Watanabe et al., 1992; Akazawa et al., 1994).

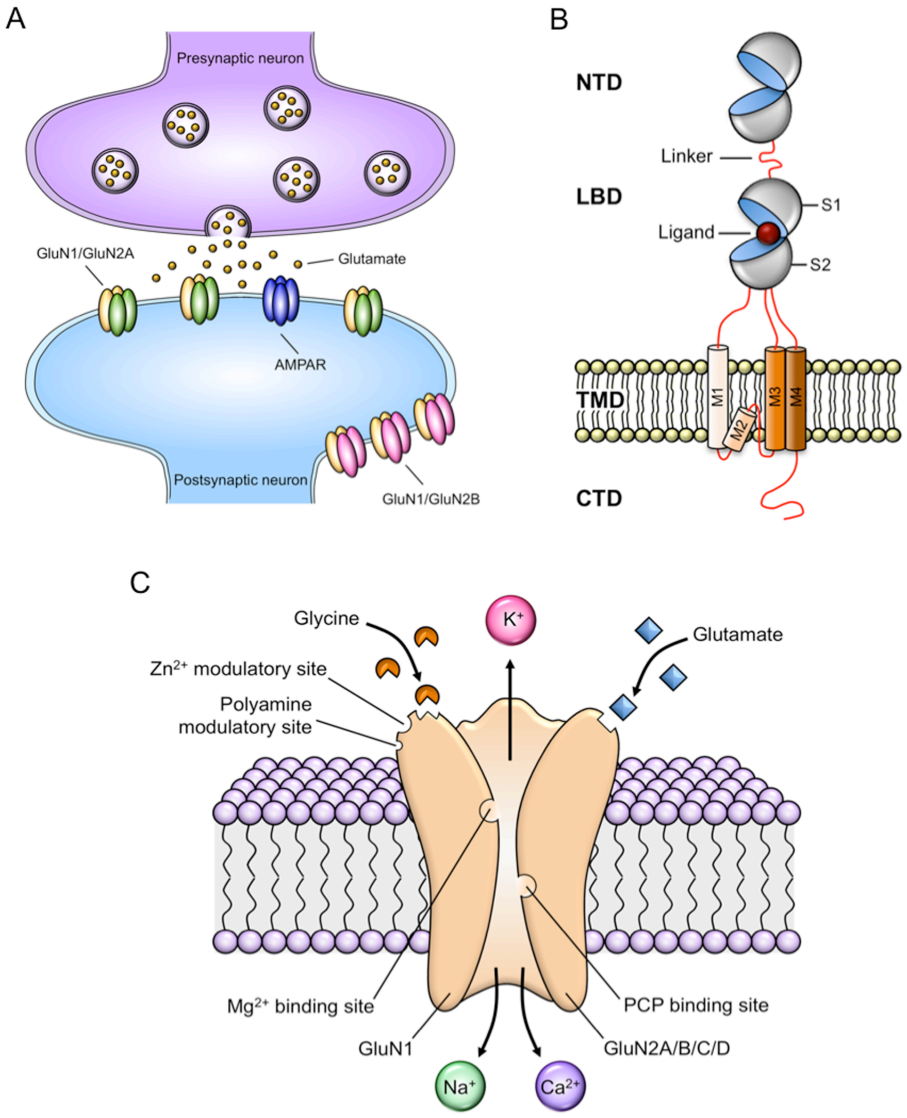

Figure 3. Schematic representation of the NMDAR complex. (A) The differential locations of NMDARs on the postsynaptic neuron (synaptic or extrasynaptic sites) depending on the subunit composition. (B) All GluN subunits are made of four distinct domains: an N-terminal domain (NTD), a ligand-binding domain (LBD) formed from amino acid segments S1 and S2, a transmembrane domain (TMD) formed from four domains (M1–M4) and a P-loop, and a C-terminal tail (CTD). (C) NMDAR structure and binding sites. Adapted from Paoletti et al., 2013.

GluN2A and GluN2B subunits are predominantly expressed in the adult forebrain, while the GluN2C subunit is found particularly in the cerebellum, and the GluN2D subunit expression is limited to the diencephalon and the midbrain (Watanabe et al., 1992, 1993; Monyer et al., 1994).

Developmentally, GluN1 subunits are widespread both pre- and postnatally. GluN2B and GluN2D subunits are present in the prenatal brain. Shortly after birth, GluN2A subunit expression rises steadily and quickly predominates, reaching mature levels by postnatal day 21, while GluN2D subunit expression drops significantly and is expressed in low levels in the adult brain. GluN2B subunit levels remain high following birth, peaking around the first postnatal week and eventually declining to low adult levels. Lastly, the expression of GluN2C subunits appear late in development during postnatal day 10 and continues to be expressed at high levels in the adult brain (Watanabe et al., 1992; Williams et al., 1993; Monyer et al., 1994; Zhong et al., 1994; Portera-Cailliau et al., 1996; Loftis and Janowsky, 2003; Sanz-Clemente et al., 2013). In the adult central nervous system, particularly in the hippocampus and cortex, GluN2A and GluN2B are the predominant subunits (Watanabe et al., 1992; Monyer et al., 1994), signifying their fundamental roles in synaptic function and plasticity, as well as neuronal excitotoxicity (Liu et al., 1996; Paoletti et al., 2013).

1.2.3. Subcellular localization of GluN2A- and GluN2B-containing NMDARs

NMDARs are differentially localized on postsynaptic neurons based on their subunit composition. One of the current controversial theories in the literature is that in the adult forebrain, GluN2A-containing NMDARs are enriched at synaptic sites and GluN2B-

containing NMDARs are more abundant extrasynaptically (Tovar and Westbrook, 1999; Steigerwald et al., 2000; Groc et al., 2006; Martel et al., 2009; Hardingham and Bading, 2010; Sanz-Clemente et al., 2013). However, this separation is by no means absolute, and GluN2A- and GluN2B-containing NMDARs can also be found at extrasynaptic and synaptic sites, respectively (Liu et al., 2004; Thomas et al., 2006; Harris and Pettit, 2007; Petralia et al., 2010). GluN2A and GluN2B subunits exhibit very distinct characteristics. Of the two, GluN2A-containing NMDARs mediate currents with faster rise time and decay kinetics, and exhibit higher open probability and faster deactivation time courses. GluN2B-containing NMDARs mediate slower kinetics, lower open probability, and slower deactivation time courses (Vicini et al., 1998; Chen et al., 1999; Erreger et al., 2005; Wyllie et al., 2013; Shipton and Paulsen, 2014). The differences in decay times have been used to determine the subunit composition of NMDARs during development. Early in brain development, NMDARs containing the GluN2B subunit dominate at the synapse and display long-duration NMDAR-mediated excitatory postsynaptic currents (EPSCs). Throughout development, the subunit composition of NMDARs change to more GluN2A-containing at the synapse and the decay becomes progressively faster (Hestrin, 1992; Monyer et al., 1994; Flint et al., 1997). These changes are accompanied by a decline in the ability of the GluN2B-selective antagonist ifenprodil to inhibit NMDAR currents (Williams et al., 1993; Kew et al., 1996; Quinlan et al., 1999; Mony et al., 2009b). For example, ifenprodil sensitivity in young (P2–9) rats is much higher due to the greater abundance of GluN2B-containing NMDAR subunits as compared to older (P16–21) rats (Bellone and Nicoll, 2007). Additionally, a previous study has reported that ifenprodil sensitivity in immature neurons (mostly GluN2B-containing NMDARs) is

similar to mature NMDAR whole-cell currents following extrasynaptic NMDAR current isolation using MK-801 (a use-dependent NMDAR antagonist) (Tovar and Westbrook, 1999). Furthermore, the ifenprodil sensitivity at synaptic NMDARs was significantly less in mature neurons (Tovar and Westbrook, 1999). These studies demonstrate that NMDAR subunit composition is different depending on the subcellular localization, with GluN2A- and GluN2B-containing receptors dominating synaptic and extrasynaptic sites, respectively, in mature animals.

The differences in localization of GluN2A- and GluN2B-containing NMDARs by surface diffusion to either synaptic or extrasynaptic sites are likely a result of several cellular processes. These may include changes in interactions with scaffolding proteins, subunit phosphorylation status, as well as extracellular factors. GluN2 subunits have divergent cytoplasmic CTDs, which interact with a variety of proteins of the postsynaptic density (Ryan et al., 2008) involved in NMDAR trafficking, clustering, localization and signaling (Collingridge et al., 2004; Kim and Sheng, 2004; Kohr, 2006; Lau and Zukin, 2007). The domains on the C-terminal tail are critical to retain GluN2A- (Steigerwald et al., 2000) and GluN2B-containing NMDARs (Prybylowski et al., 2005) within synapses. Therefore, the lateral shift of subunits that occurs throughout development may be due to variations in lateral mobility and stabilization of the receptors. A particular role in the NMDAR subunit switch during development has been attributed to members of the membrane-associated guanylate kinases (MAGUKs), including synapse associated protein 102 (SAP102) and PSD-95 (van Zundert et al., 2004). SAP102 and PSD-95, which act as synaptic anchors, are preferentially associated with GluN2A- and GluN2B-containing NMDARs. This implies that different NMDAR scaffolding proteins could

underlie the shifting localization of NMDARs with different subunit composition throughout synaptic development (Shi et al., 1997; Sans et al., 2000; Yoshii et al., 2003). The increased levels of PSD-95 throughout development and their preferential association with GluN2A subunits may displace GluN2B subunit-SAP102 complexes to extrasynaptic membranes (Shi et al., 2000; Townsend et al., 2003; Yoshii et al., 2003). In addition, the increased association of GluN2A-containing NMDARs with PSD-95 may underlie their increased stability at mature synapses compared to GluN2B-containing NMDARs, possibly due to a high proportion of PSD-95 compared to SAP-102 in the postsynaptic density (Groc et al., 2006). Thus, there is a progressive shift during development of GluN2B-containing NMDARs from synaptic to extrasynaptic sites. Extrasynaptic NMDARs are activated by excess glutamate spillover from the synaptic cleft during periods of high synaptic activity (Conti and Weinberg, 1999; Kullmann, 1999). Therefore, these receptors may have a specific role during precise patterns of activity or in pathological conditions, such as stroke (Sattler et al., 2000; Hardingham et al., 2002; Vanhoutte and Bading, 2003; Arundine and Tymianski, 2004; Scimemi et al., 2004). Moreover, extrasynaptic NMDARs are the target for neuronal and astrocytic glutamate release as a result of reversed activation of glutamate transporters during ischemia (Fellin et al., 2004; Waxman and Lynch, 2005; Hardingham and Bading, 2010).

1.2.4. Intracellular signaling of synaptic and extrasynaptic NMDARs

NMDARs with different subunit composition and localization have been shown to differentially regulate intracellular signaling cascades. The differences in synaptic and extrasynaptic signaling could be due to a combination of three factors. Firstly, synaptic

and extrasynaptic NMDARs could be coupled to different signaling pathways due to their location. Secondly, differences in signaling could be due to the way in which these distinct pools are activated: brief activation by trans-synaptic glutamate release (synaptic NMDARs) versus chronic low-level activation by ambient glutamate (extrasynaptic NMDARs). Thirdly, NMDAR subunit composition could play a role in the signaling differences between synaptic and extrasynaptic NMDARs due to the cytoplasmic C-termini of the GluN2 subunits (Martel et al., 2009; Hardingham and Bading, 2010).

There is evidence in the literature that GluN2 subtypes influence NMDAR excitotoxicity (Liu et al., 2007). The cytoplasmic CTDs of GluN2 subunits can differentially associate with signaling molecules (Ryan et al., 2008) and influence the toxicity of Ca^{2+} influx through NMDARs (Martel et al., 2012). GluN2A-containing NMDARs are generally associated with neuronal survival, whereas activation of GluN2B-containing NMDARs is coupled to cell death pathways (Liu et al., 2007). In one particular study, constructs were generated which encoded chimeric receptors based on GluN2B and GluN2A but with their respective CTDs replaced with each other's (Martel et al., 2012). In this study it was reported that the CTD of GluN2B promotes excitotoxicity better than that of GluN2A. Furthermore, GluN2B CTD couples to a pro-death PSD-95/nNOS-dependent cAMP response element binding protein (CREB) shut-off pathway (Martel et al., 2012). Other groups have used the 20-mer peptide Tat-NR2B9c, comprising the nine carboxy-terminal amino acids of the NMDAR GluN2B subunit fused to the 11-mer HIV-1 Tat protein transduction domain (Schwarze et al., 1999; Stroke Therapy Academic Industry, 1999; Aarts et al., 2002; Fisher et al., 2009). This peptide acts by perturbing the protein-protein interaction between GluN2B and

PSD-95, the synaptic scaffolding protein that links NMDARs to neurotoxic signaling pathways (Kornau et al., 1995; Sattler et al., 1999; Cui et al., 2007). Treating rats, as well as non-human primates, subjected to MCAO with Tat-NR2B9c was found to be neuroprotective in multiple stroke models (Aarts et al., 2002; Sun et al., 2008; Bratane et al., 2011; Cook et al., 2012), and was also shown to reduce ischemic brain damage in humans (Hill et al., 2012). Moreover, GluN2B-specific antagonists, such as ifenprodil, have demonstrated a role for GluN2B-containing NMDARs in excitotoxicity (Gotti et al., 1988; McDonald and Johnston, 1990; Graham et al., 1992; Shalaby et al., 1992; Tamura et al., 1993; Baskaya et al., 1997; Geng et al., 1997; Picconi et al., 2006; Liu et al., 2007).

Synaptic and extrasynaptic NMDARs have opposing effects on the function of CREB, gene regulation, and cell fate (Vanhoutte and Bading, 2003; Hardingham and Bading, 2010; Parsons and Raymond, 2014). The transcription factor CREB is responsible for regulating the expression of many proteins, including the brain-derived neurotrophic factor (BDNF), which is important for neuronal survival (Shaywitz and Greenberg, 1999). The entry of Ca^{2+} through synaptic GluN2A-containing NMDARs activates the extracellular signal-regulated kinase 1/2 (ERK1/2) pathway, inducing CREB phosphorylation and BDNF gene expression, which initiates a pro-survival program by reducing the expression of pro-apoptotic factors. In contrast, Ca^{2+} entry through extrasynaptic GluN2B-containing NMDARs inactivates the ERK1/2 pathway, triggering the CREB shut-off pathway. This inhibits BDNF gene expression and initiates the cell death pathway causing loss of mitochondrial membrane potential, an early indicator of neuronal damage mediated by glutamate (Hardingham et al., 2002; Ivanov et al., 2006; Cross et al., 2010; Hardingham and Bading, 2010; Kaufman et al., 2012) (**Fig. 4**).

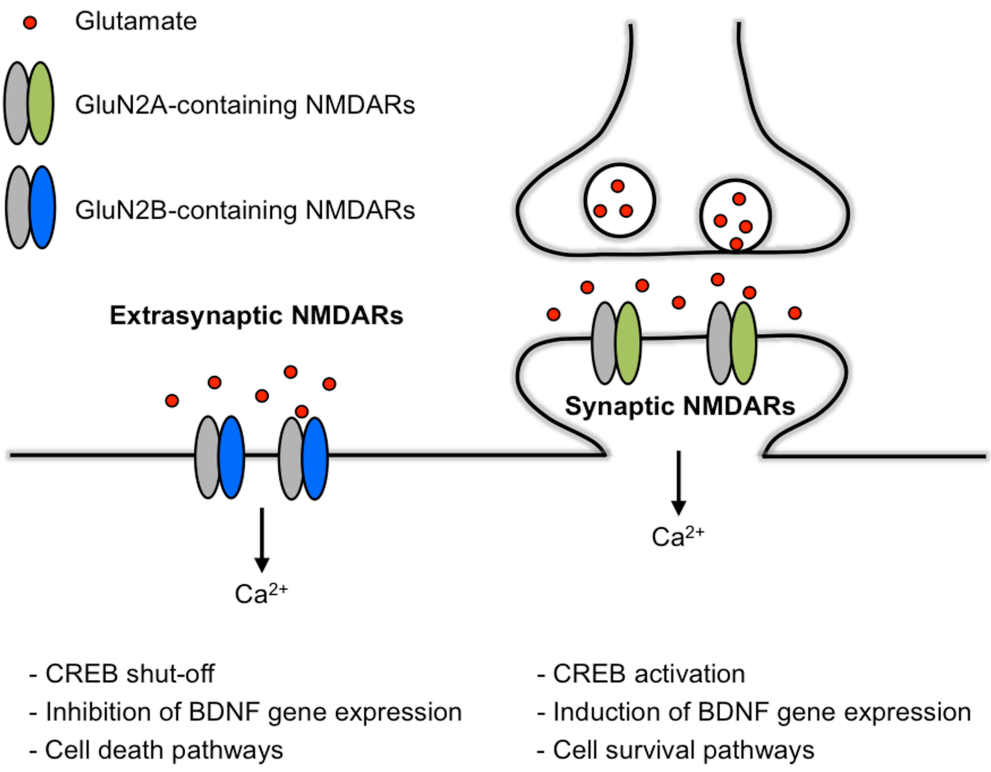

Figure 4. Opposing roles of synaptic and extrasynaptic NMDARs. The activation of synaptic and extrasynaptic NMDARs have opposite effects on CREB function, BDNF gene regulation, and neuronal survival. Modified from Vanhoutte and Bading, 2003.

There is evidence suggesting that increased activation of GluN2B-containing extrasynaptic NMDARs contribute, at least in part, to the toxicity seen in neurodegenerative disorders such as Huntington's and Alzheimer's disease, as well as in ischemic events (Hardingham and Bading, 2010; Lujan et al., 2012; Vizi et al., 2013; Parsons and Raymond, 2014). Therefore, neuroprotective therapies for such conditions should aim to disrupt extrasynaptic NMDAR-dependent death signaling.

1.2.5. NMDARs and protons

In addition to subunit composition, NMDAR function is modulated by protons (Tang et al., 1990; Vyklicky et al., 1990; Traynelis and Cull-Candy, 1991). This is of particular interest since acidic pH occurs as a consequence of ischemia due to the accumulation of lactic acid resulting from an increase in the rate of glycolysis. The extracellular pH in regions subjected to limited oxygen availability, such as the ischemic penumbra following a stroke, can drop by 0.2 to more than 1.0 pH units depending on the severity of the insult (Siemkowicz and Hansen, 1981; Meyer et al., 1986; Kaku et al., 1993; Doyle et al., 2008). Interestingly, studies have shown that acidic pH induces an inhibitory effect on NMDARs, while basic pH enhances NMDAR function. NMDARs have a pH sensitivity with an IC_{50} that is close to physiological pH, meaning that under normal conditions NMDARs are under tonic proton inhibition (Tang et al., 1990; Traynelis and Cull-Candy, 1990; Vyklicky et al., 1990; Traynelis and Cull-Candy, 1991; Low et al., 2003; Dravid et al., 2007). Although many residues, both on GluN1 and GluN2 subunits,

have been shown to control proton inhibition (Kashiwagi et al., 1997; Traynelis et al., 1998; Masuko et al., 1999; Low et al., 2000; Zheng et al., 2001; Low et al., 2003), the precise location of the proton sensor within the ion channel complex remains unknown. Studies have reported that residues that influence proton sensitivity most strongly cluster in two regions closely associated with the activation gate of NMDARs (Low et al., 2003; Chang and Kuo, 2008; Gielen et al., 2008), suggesting that the proton sensor is likely coupled to the gating mechanism of NMDARs (Tang et al., 1990; Banke et al., 2005). Studies have shown that the inhibition of NMDARs by protons is mediated primarily by decreased frequency of channel opening, suggesting that a decrease in pH stabilizes the non-conducting state of NMDARs (Banke et al., 2005).

Interestingly, several NMDAR allosteric modulators have been shown to modify the sensitivity of the proton sensor and alter NMDAR function (Traynelis et al., 1995; Mott et al., 1998; Choi and Lipton, 1999; Low et al., 2000). These compounds have enhanced function in varying pH conditions. For example, ifenprodil is neuroprotective in animal models of stroke, not only by being selective for GluN2B-containing NMDARs, but also by shifting the pKa of the proton sensor, and consequently increasing NMDARs sensitivity to inhibition by protons (Shalaby et al., 1992; Pahk and Williams, 1997; Whittemore et al., 1997; Mott et al., 1998). A recently published study has reported that pH sensitive GluN2B-selective inhibitors are neuroprotective with minimal side effects (Yuan et al., 2015). Researchers found that in a mouse model of ischemic stroke, a GluN2B NMDAR antagonist called 93-31 reduced the volume of damaged brain tissue by more than half, and the mice did not experience the side effects observed with pan-NMDAR antagonists, such as PCP. More importantly they found that this drug was ten

times more potent at acidic pH, typical for ischemic tissue with an insufficient blood supply, than at pH 7.6 (Yuan et al., 2015). Therefore, this suggests that such NMDAR antagonists, whose activity is dependent on acidic environments, would be active only in affected brain regions with decreased pH levels, such as the ischemic penumbra.

Demonstrating that the potency of some compounds is increased at lower pH, as well as exhibiting NMDAR subunit selectivity, provides an interesting pharmacological avenue. This leads the way to the discovery of drugs with optimal pharmaceutical profiles and delivery methods for the treatment of brain injury involving overactivation of NMDARs and extracellular acidification. A drug that selectively targets GluN2B subunits, which is inactive at physiological pH but becomes therapeutically effective in the acidic environment that arises in some pathological conditions, could be the key in the treatment of ischemic stroke events.

1.3. N-ACETYL-ASPARTYL-GLUTAMATE (NAAG)

N-acetyl-aspartyl-glutamate (NAAG) was first discovered in the mammalian nervous system and reported to be present in high micromolar to low millimolar concentrations (Curatolo et al., 1965; Miyamoto et al., 1966). Very little research on NAAG was published for nearly two decades following its discovery until a group published a series of articles further indicating the presence of NAAG in the nervous system and its interaction with a putative excitatory receptor (Zaczek et al., 1983; Koller and Coyle, 1984; Koller et al., 1984; Bernstein et al., 1985; Ffrench-Mullen et al., 1985). According to the established criteria for identification of neurotransmitters, substantial data now support that NAAG is the most prevalent and widely distributed peptide neurotransmitter

in the mammalian nervous system (Miyake et al., 1981; Riveros and Orrego, 1984; Blakely et al., 1988b; Whittemore and Koerner, 1989). NAAG has been shown to modulate the glutamatergic system and is thought to play a key role in neuroprotection and synaptic plasticity (Neale et al., 2005).

1.3.1. Biochemistry of NAAG

NAAG appeared late in evolution with the highest concentration being found in the central nervous system of mammals. NAAG is widely distributed in projection neurons and interneurons in the human brain, particularly in glutamatergic neurons of the human cerebral cortex, amygdala, hippocampus, striatum, brainstem, and spinal cord (Anderson et al., 1986; Cangro et al., 1987; Forloni et al., 1987; Tieman et al., 1988; Tieman et al., 1991; Tsai et al., 1993; Moffett et al., 1994; Moffett and Namboodiri, 1995; Passani et al., 1997; Renno et al., 1997).

Endogenous NAAG is synthesized in neurons by the recently discovered N-acetylaspartate L-glutamate ligase (NAAG synthetase), which joins N-acetyl-aspartate (NAA) and glutamate via a peptide bond in an enzyme-mediated process (Becker et al., 2010; Collard et al., 2010; Lodder-Gadaczek et al., 2011). NAAG is concentrated in neuronal synaptic vesicles, and is released upon depolarization in a Ca^{2+}-dependent manner from synaptic terminals (Forloni et al., 1987; Pittaluga et al., 1988; Tsai et al., 1988; Williamson and Neale, 1988; Zollinger et al., 1988; Sekiguchi et al., 1989; Tsai et al., 1990; Williamson et al., 1991; Williamson and Neale, 1992; Zollinger et al., 1994; Renno et al., 1997; Neale et al., 2005). Studies in animal models of clinical disorders have demonstrated that, following synaptic release, NAAG plays a role in a broad

spectrum of neuronal circuits and nervous system functions, mainly through its action as an agonist at group II metabotropic glutamate receptor 3 ($mGluR_3$), and its mixed agonist/antagonist effect at NMDARs (Fagg et al., 1986; Neale et al., 2005; Tsukamoto et al., 2007; Neale, 2011; Neale et al., 2011). NAAG is degraded by proteolytic cleavage into NAA and glutamate, by the astrocytic glycoproteins glutamate carboxypeptidase II (GCP-II) (Cassidy and Neale, 1993; Fuhrman et al., 1994; Slusher et al., 1999) and glutamate carboxypeptidase III (GCP-III) (Bzdega et al., 2004). A series of studies characterized the pharmacology and biochemistry of GCP-II activity in the rat brain (Robinson et al., 1987; Serval et al., 1990), and found it is widely distributed throughout the central nervous system, consistent with the distribution of NAAG (Blakely et al., 1988a; Fuhrman et al., 1994; Berger et al., 1995; Sacha et al., 2007). The glutamate release from the hydrolytic reaction of NAAG is subject to reuptake by glial and neuronal transporters, while the NAA released is taken up by glial cells (Gehl et al., 2004; Baslow, 2010) (**Fig. 5**).

The release of NAAG, similar to other neuropeptides, is activity dependent (Slusher et al., 1999; Zhong et al., 2006). Under basal conditions, extracellular levels of NAAG in the hippocampus, as measured by microdialysis, are in the 0.5 μM to 1 mM range. Under conditions of enhanced neuronal activity, as was observed following traumatic brain injury, NAAG levels can increase 10- to 15-fold (Zhong et al., 2006). In this study, administration of a GCP-II inhibitor during brain trauma impeded the hydrolysis of NAAG, hence maintaining elevated NAAG concentrations while decreasing glutamate levels. This resulted in a significant reduction of neuronal and glial damage (Zhong et al., 2006). Therefore, GCP-II may have an important neuromodulatory

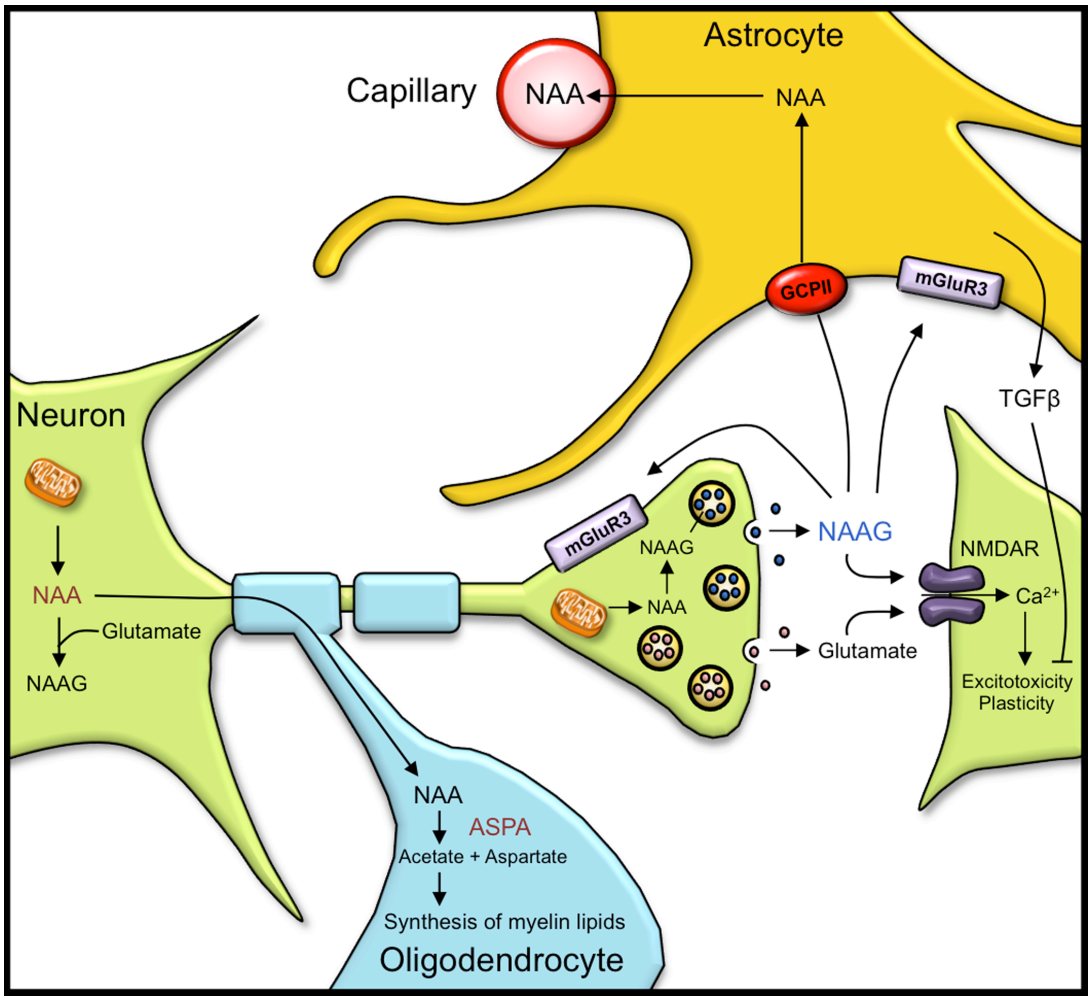

Figure 5. Model of the biochemical process of NAAG and NAA. NAA is combined with glutamate in the neuron to produce NAAG. NAAG is released from synaptic vesicles and acts as a co-transmitter with several other neurotransmitters, including glutamate. NAAG can inhibit glutamate release through its action as an agonist on presynaptic $mGluR_3$, and may also bind to NMDARs, blocking their function during periods of neuronal excitation. NAAG also triggers release of transforming growth factor-β (TGFβ), through its action on $mGluR_3$ in astrocytes. These are all factors possibly contributing to its neuroprotective effect in situations of high glutamatergic activity. Following synaptic release, NAAG is hydrolyzed by GCP-II (found on astrocytes) to NAA and glutamate. Modified from Benarroch E, 2008, Neurology.

and neuroprotective role during high levels of synaptic activity (Slusher et al., 1999).

1.3.2. Clinical implications of NAAG and GCP-II inhibitors: Neuroprotection

A series of pioneering studies have demonstrated the ability of GCP-II inhibitors to be therapeutically beneficial in cases of glutamate-mediated neuronal damage from brain injuries and neurological disorders (Slusher et al., 1999; Lu et al., 2000; Neale et al., 2000; Williams et al., 2001; Neale et al., 2005; Zhou et al., 2005; Barinka et al., 2012). The first potent inhibitor of GCP-II, 2(phosphonomethyl)pentanedioic acid (2-PMPA), is a phosphonate analogue of glutamate (Jackson et al., 1996) and is highly selective for GCP-II with characteristics of low molecular weight and high aqueous solubility (Slusher et al., 1999; Bacich et al., 2002; Hlouchova et al., 2007). Over the last two decades, several more phosphonate-based GCP-II inhibitors have been designed and synthesized (e.g. 2-[[hydroxy[2,3,4,5,6-pentafluorophenyl)methyl]phosphinyl]methyl] pentanedioic acid; GPI-5232), as well as some less selective urea-based compounds (Jackson and Slusher, 2001; Tsukamoto et al., 2002; Oliver et al., 2003; Kozikowski et al., 2004; Maung et al., 2004; Barinka et al., 2008; Choy et al., 2013; Zhong et al., 2014). It has been shown that pre-stroke administration of 2-PMPA or GPI-5232 increased endogenous NAAG concentrations, decreased extracellular glutamate, reduced lesion volume and improved behavioural performance following transient MCAO in rats. In addition, continuous infusion of GPI-5232 was effective even when administered 2 hours after the ischemic injury (Slusher et al., 1999; Vornov et al., 1999; Lu et al., 2000; Williams et al., 2001; Cai et al., 2002; Zhong et al., 2005; Zhong et al., 2006). Numerous studies have also shown that an increase in NAAG is neuroprotective against NMDAR-

mediated neurotoxicity without adverse side effects (Slusher et al., 1999; Vornov et al., 1999; Tortella et al., 2000). Furthermore, GCP-II knockout mice exhibited a significantly smaller infarct volume than control littermates in a model of ischemic injury, and displayed normal neurological function and behaviour (Bacich et al., 2005). Therefore, in contrast to many glutamate receptor antagonist based neuroprotective strategies, GCP-II inhibitors do not cause adverse behavioural changes or deficits in learning and memory in animal models.

Although the currently identified phosphonate- and urea-based GCP-II inhibitors are highly potent compounds and exhibit great potential, they are highly polar with limited oral bioavailability and blood-brain barrier penetration. This led to the discovery of the less polar thiol-based 2-(3-mercaptopropyl)pentanedioic acid (2-MPPA, also known as GPI-5693), which was the first reported orally available GCP-II inhibitor and the first inhibitor to be tested in humans (Majer et al., 2003; van der Post et al., 2005). Although GPI-5693 did not cause any adverse side effects and showed tolerability at plasma concentrations, no further studies were conducted due to its low potency, as well as concerns regarding potential immunological toxicity, which is common to thiol-containing drugs (Durand et al., 2013). Nonetheless, data from this first clinical evaluation of GPI-5693, along with evidence from several studies demonstrating the neuroprotective qualities of GCP-II inhibitors, without the known side effects associated with conventional glutamate receptor antagonists, strengthens the potential of GCP-II inhibitors to serve as a therapeutic target. A recently published study has reported a non-invasive method for delivery of GCP-II inhibitors to the brain via intranasal administration on rodents and non-human primates. Of the three structurally distinct

GCP-II inhibitors that were evaluated, intranasal (i.n.) administration of 2-PMPA exhibited the highest level of brain penetration compared to intraperitoneal (i.p.) administration (Rais et al., 2015). The ability to deliver therapeutic concentrations of 2-PMPA to the brain holds great therapeutic potential and may facilitate its use in clinical studies.

1.3.3. NAAG and glutamatergic receptors

Although it is well established that NAAG provides neuroprotection against ischemic stress, its physiological role at glutamatergic receptors remains complicated and controversial (Bergeron and Coyle, 2012). One of the roles of NAAG in the nervous system is the activation of $mGluR_3$ receptors, which are localized presynaptically on neurons and glia (Wroblewska et al., 1993; Bischofberger and Schild, 1996; Ghose et al., 1997; Wroblewska et al., 1997; Wroblewska et al., 1998; Lea et al., 2001; Sanabria et al., 2004; Wroblewska et al., 2006; Adedoyin et al., 2010; Neale, 2011). When activated, these presynaptic $mGluR_3$ receptors have been shown to inhibit release of neurotransmitters, including glutamate (Cartmell and Schoepp, 2000; Wroblewska et al., 2006). Activation of $mGluR_3$ receptors on glial cells also stimulates the release of neuroprotective growth factors from these cells (Bruno et al., 1998; Ciccarelli et al., 1999). Interestingly, it has also been reported in some studies that NAAG does not have an effect on $mGluR_3$ (Chopra et al., 2009; Fricker et al., 2009).

The literature to date has also reported conflicting results regarding the effect of NAAG on NMDARs (Bergeron and Coyle, 2012). Some groups have described an agonist effect of NAAG on NMDARs (Westbrook et al., 1986; Sekiguchi et al., 1992;

Valivullah et al., 1994; Kolodziejczyk et al., 2009). Westbrook et al. showed that NAAG behaves as a very weak agonist at NMDARs in electrophysiological studies of the rat spinal cord (Westbrook et al., 1986). Additionally, ligand binding studies have shown that NAAG specifically interacts with NMDAR but not AMPAR or kainic acid binding sites (Valivullah et al., 1994). However, other studies have reported that NAAG behaves as an antagonist on NMDARs (Sekiguchi et al., 1989; Puttfarcken et al., 1993; Grunze et al., 1996; Bergeron et al., 2005; Bergeron et al., 2007). Puttfarcken et al. found that NAAG antagonized the release of norepinephrine from hippocampal slices evoked by glutamate and NMDA (Puttfarcken et al., 1993). It was also demonstrated in the hippocampus that NAAG and 2-PMPA reduce NMDAR EPSCs (Bergeron et al., 2005; Bergeron et al., 2007). The NAAG-induced inhibition of NMDARs was still observed even in the presence of LY341495, a potent and selective $mGluR_3$ antagonist, suggesting that the effect of NAAG was not mediated by $mGluR_3$ (Bergeron et al., 2005; Bergeron et al., 2007). Furthermore, whole-cell recordings show that exogenously applied NAAG or treatment with 2-PMPA prevents the induction of LTP at Schaffer collateral–CA1 synapses (Bergeron et al., 2007). On the other hand, some have claimed no significant effect of NAAG on NMDARs (Lea et al., 2001; Losi et al., 2004; Fricker et al., 2009).

Such reported discrepancies, concerning the effect of NAAG on NMDARs, in these studies could be due to multiple factors. These may include differences in NMDAR subunit composition, which depend on the developmental stage of the animal and brain region under investigation, as well as cell type. The differential expression of NMDARs may be responsible for why NAAG has no significant effect on NMDARs in cerebellar granule cells (Losi et al., 2004), while it may have some greater potency at these

receptors with different subunit composition in other systems. For example, a group reported that NAAG potentiated the effect of glutamate on oocytes injected with NMDAR subunit GluN1/2D but not GluN1/2A or 2B (Hess et al., 1999), a result that would suggest that the sensitivity of NMDARs to NAAG is subunit-dependent. Additionally, certain NMDAR complexes, such as those found in the spinal cord or olfactory neurons in culture (Westbrook et al., 1986; Trombley and Westbrook, 1990) may be sensitive to NAAG, while those expressed by cerebellar granule cells or cells in the lateral geniculate nucleus (Jones and Sillito, 1992), or hippocampal granule cells (Lea et al., 2001) may not. Therefore, the difference in sensitivity of NAAG on NMDARs could be due to the GluN2 subunit composition of these receptors. The experimental conditions in which NAAG and NMDARs are studied, such as variations in extracellular pH, could also lead to variability in the results.

2. *OBJECTIVES AND HYPOTHESIS*

OBJECTIVES: Numerous studies have shown that an increase in NAAG, either by exogenous or endogenous manipulation, is neuroprotective against NMDAR-mediated neurotoxicity without adverse side effects (Slusher et al., 1999; Lu et al., 2000; Tortella et al., 2000; Cai et al., 2002). Although it is well established that NAAG has neuroprotective properties, the literature to date has reported conflicting results regarding its effect on NMDARs (Westbrook et al., 1986; Sekiguchi et al., 1989; Sekiguchi et al., 1992; Losi et al., 2004; Bergeron et al., 2005; Bergeron et al., 2007; Fricker et al., 2009). It remains unclear whether the neuroprotective properties of NAAG are mediated through the modification of NMDAR activity, which could depend on the subunit composition and subcellular localization of the receptor, as well as extracellular conditions. To use NAAG therapeutically it is crucial to gain a better understanding of its possible mechanisms of action on NMDARs. Therefore, the objective of this thesis is to determine whether NAAG can have differential effects on NMDARs depending on subunit composition and extracellular pH.

HYPOTHESIS: NAAG modulates NMDAR activity in a subunit-selective and pH-dependent manner

3. *AIMS*

Using electrophysiological and biochemical methods, the present study aims to:

1. Clarify the effect of NAAG on synaptic and extrasynaptic NMDARs

2. Determine the subunit specificity of NAAG on GluN2A- and GluN2B-containing NMDARs
3. Investigate whether the effect of NAAG on NMDARs is pH-dependent
4. Study the influence of NAAG on surface expression of NMDAR subunits

4. *MATERIALS AND METHODS*

4.1. Slice preparation

Acute coronal hippocampal brain slices (300 μm thick) were obtained from wild type Swiss mice of either sex (8–12 weeks old). Prior to decapitation, animals were anaesthetized by isoflurane inhalation, in agreement with the guidelines of the Canadian Council of Animal Care and approved by the University of Ottawa Animal Care Committee. The brain was removed and placed in oxygenated (95% O_2 / 5% CO_2) artificial cerebrospinal fluid (ACSF) at 4°C containing (in mM): 126 NaCl, 2.5 KCl, 2 $CaCl_2$, 1 $MgCl_2$, 26 $NaHCO_3$ and 10 glucose (300 mOsm, pH 7.2). Slices were cut with a vibrating microtome (Leica VT 1000S) and incubated for 1 hour in oxygenated ACSF at room temperature before they were used for experiments.

4.2. Whole-cell electrophysiology on hippocampal slices

Whole-cell voltage-clamp recordings were performed on CA1 pyramidal neurons from acute hippocampal slices using differential interference contrast optics and infrared video microscopy (IR-DIC; Leica DMLFSA). All experiments were performed at room temperature in ACSF and cells were voltage-clamped at –65 mV. A stable baseline recording was first obtained in normal ACSF. To isolate the NMDAR-mediated EPSC, ACSF with a low concentration of Mg^{2+} (0.1 mM) was used containing (in μM): 5 NBQX, 50 picrotoxin, 10 bicuculline and 0.5 strychnine (all purchased from Tocris Bioscience). To isolate for extrasynaptic NMDAR-mediated EPSCs, 30 μM MK-801 (purchased from Abcam) and 30 μM DL-TBOA (purchased from Tocris Bioscience) were included in the low Mg^{2+} ACSF as previously described (Hardingham et al., 2002;

Carpenter-Hyland et al., 2004; Harney et al., 2008; Imamura et al., 2008; Okamoto et al., 2009; Hardingham and Bading, 2010; Xia et al., 2010; Li et al., 2011). When required, additional drugs were bath applied (in μM): 20 NAAG, 10 2-PMPA, 3 ifenprodil, 10 LY341495 (all purchased from Tocris Bioscience) and 10 2-(phosphonomethyl)succinic acid (2-PMSA; a generous gift from Dr. Barbara Slusher). Extracellular solutions with modified pH values were prepared by replacing $NaHCO_3$ in the ACSF with one of two different pH buffers (depending on their pH ranges), PIPES (20 mM) or HEPES (20 mM), and the pH was adjusted to either 6.5, 6.8, or 7.6 with NaOH (Doroshenko and Renaud, 2009). For voltage-clamp recordings, borosilicate glass electrodes were filled with an internal solution containing (in mM): 128 Cs-methanesulfonate, 10 tetraethylammonium-Cl, 10 HEPES, 0.6 EGTA, 2 $MgCl_2$, 2 Mg-ATP, 0.5 Na-GTP (all purchased from Sigma-Aldrich) and 5 QX-314 (purchased from Abcam), and the pH was adjusted to 7.2 (280–290 mOsm). The recording electrodes had a resistance of 4–6 MΩ. The series resistance was continuously monitored throughout the experiment by delivering a 5 mV hyperpolarizing step at the onset of every electrophysiological sweep. Recordings with series resistance higher than 25 MΩ were discarded. EPSCs were evoked by electrical stimulation of the Schaffer collaterals in the CA3 region of the hippocampus with a bipolar stimulating electrode positioned in the Schaffer collaterals. The single stimulation protocol consisted of 100 μs current pulses (10–200 μA) evoked every 12 s. To facilitate the blocking of synaptic NMDAR currents by MK-801 throughout the extrasynaptic NMDAR isolation protocol, the interval of stimulation was changed from 12 to 6 s during MK-801 application only. The intensity of the stimulation

was adjusted to obtain evoked postsynaptic currents in the amplitude range of 100–150 pA.

4.3. HEK293 cells maintenance and whole-cell electrophysiology

HEK293 cells were maintained in minimal essential media supplemented with 10% fetal bovine serum, 100 u/ml penicillin/streptomycin, 100 μM neomycin, and 1× glutaMAX^{TM} (all purchased from Life Technologies) and grown in a humidified 37^{o}C, 5% CO_2 incubator. Twenty-four hours prior to transfection, approximately 0.18 × 10^6 cells were plated on Thermanox plastic coverslips (15 mm diameter, thickness 0.2 mm; Thermo Scientific) in 12-well plates. The cells were then transiently transfected with GluN1 together with either GluN2A or GluN2B cDNAs using the TransIT-2020 transfection reagent (Mirus). For visualization purposes, mCherry fluorescent protein was used as co-transfectant. The total amount of cDNA added for these triple transfections was approximately 1 μg per well at a cDNA molar ratio of 1:2:0.5 (GluN1:GluN2A:mCherry or GluN1:GluN2B:mCherry). Following transfection, the cells were grown in the presence of 100 mM DL-APV (selective NMDAR antagonist; purchased from Tocris Bioscience) to prevent overactivation of expressed receptors and subsequently cell death. Cells were used for electrophysiological recordings 48–72 h after transfection. Individually transfected HEK293 cells were then identified for whole-cell recordings and currents were evoked using pressure ejection (10 psi) from a picospritzer micropipette filled with glutamate (100 μM) and glycine (10 μM; both purchased from Sigma-Aldrich) for a duration of 5–30 ms every 20 s. For HEK293 cell electrophysiological recordings, the external solution contained (in mM): 150 NaCl, 10 HEPES, 3 KCl and 2 $CaCl_2$. The

pH was adjusted accordingly using 5 M NaOH and the osmolality to 290 mOsm using sucrose. The borosilicate electrodes were filled with internal solution containing (in mM): 115 NaCl, 10 NaF, 5 HEPES, 5 Na_4-BAPTA, 0.5 $CaCl_2$, 1 $MgCl_2$ and 10 Na_2-ATP (all purchased from Sigma-Aldrich), and the pH was adjusted to 7.2 (280–290 mOsm).

4.4. Analysis

Data were collected using a Multiclamp 700A amplifier (Axon Instruments), filtered at 2 kHz and digitized at 10 kHz by a Digidata 1320 digitizer (Molecular Devices). Recordings were analyzed using the pClamp 9 software suite (Molecular Devices). Statistical significance of the results was determined with paired (two-tailed) Students *t*-test. A *P* value of < 0.05 was considered statistically significant. All values are expressed as mean ± SEM. Kinetic analysis of NMDAR currents was performed on averaged traces. Decay kinetics were measured using a biexponential fit to calculate a weighted τ value (τ_w). No significant differences in decay kinetics or 10–90% rise times were observed between control and treatment in any of the experimental conditions ($p > 0.05$; **Table 1, Table 2, Table 3**).

4.5. Cell surface biotinylation assay and western blotting

Acute coronal hippocampal slices from mice were prepared, as described above, and the hippocampi from each slice were isolated, pooled, and allowed to recover. The hippocampi were then divided into six groups and incubated for 20 min at room temperature at pH 7.2, 6.8, or 7.6 in either the presence or absence of NAAG.

Table 1. Measurement of decay kinetics and 10–90% rise times of NMDAR currents following application of NAAG or 2-PMPA in hippocampal slices and HEK293 cells.

		Decay τ_w (ms)			
		Ctrl	**NAAG**	**Ctrl**	**2-PMPA**
Slice	Synaptic	105.4 ± 7.9	95 ± 5.9	117.5 ± 12.6	117.9 ± 15.9
	Extrasynaptic	193.7 ± 12.3	182.4 ± 10.4	190 ± 17.4	259.9 ± 48.7
HEK293	GluN2A	593.4 ± 6.4	623.2 ± 41.2	–	–
	GluN2B	3826.6 ± 941.8	3890.9 ± 792.4	–	–

		Rise time (ms)			
		Ctrl	**NAAG**	**Ctrl**	**2-PMPA**
Slice	Synaptic	16.7 ± 3.3	15.2 ± 2.3	11.6 ± 1.2	10.9 ± 0.7
	Extrasynaptic	26.9 ± 7.6	31.1 ± 7.2	29.3 ± 3	33.9 ± 2.9
HEK293	GluN2A	166.2 ± 18.5	142.7 ± 31.1	–	–
	GluN2B	137.5 ± 19.6	142.6 ± 18.2	–	–

Data are mean ± SEM of at least three cells. No significant differences were observed in all cases ($p > 0.05$).

Table 2. Measurement of decay kinetics and 10–90% rise times of NMDAR currents in hippocampal slices and HEK293 cells in different pH conditions.

		Decay τ_w (ms)					
		Ctrl	**pH 6.5**	**Ctrl**	**pH 6.8**	**Ctrl**	**pH 7.6**
Slice	Synaptic	127.7 ± 14	143.2 ± 3.6	106.6 ± 4.8	127.7 ± 5.3	96.8 ± 6.7	95.2 ± 7.5
	Extrasynaptic	215.3 ± 32.4	268.7 ± 12.9	178.2 ± 20.2	238.5 ± 29.7	323.7 ± 25.5	266.3 ± 22.7
HEK293	GluN2A	–	–	584.2 ± 132.1	422.7 ± 104.8	871.2 ± 261.9	1255.1 ± 349.6
	GluN2B	–	–	3262.2 ± 854.8	2890.9 ± 369.5	3336.7 ± 409.2	3426.3 ± 117.6
		Rise time (ms)					
		Ctrl	**pH 6.5**	**Ctrl**	**pH 6.8**	**Ctrl**	**pH 7.6**
Slice	Synaptic	14.7 ± 0.8	14.5 ± 1.8	14.6 ± 1.2	12.2 ± 0.8	11.5 ± 1	11.6 ± 0.8
	Extrasynaptic	24.1 ± 1.8	29.7 ± 4.5	21.2 ± 1.4	29.5 ± 5.7	35.4 ± 1.4	38.5 ± 2.9
HEK293	GluN2A	–	–	127.2 ± 26.4	108.5 ± 29.4	81.9 ± 29.8	86.7 ± 22.6
	GluN2B	–	–	205.4 ± 37.2	150.7 ± 38.9	254.1 ± 22.5	238.9 ± 25.4

Data are mean ± SEM of at least three cells. No significant differences were observed in all cases ($p > 0.05$).

Table 3. Measurement of decay kinetics and 10–90% rise times of NMDAR currents in hippocampal slices and HEK293 cells in different pH conditions following NAAG application.

		Decay τ_w (ms)					
		pH 6.5		pH 6.8		pH 7.6	
		Ctrl	NAAG	Ctrl	NAAG	Ctrl	NAAG
Slice	Synaptic	135.3 ± 10.2	140.2 ± 6.6	130.2 ± 10.1	148.4 ± 8.6	93.6 ± 10.8	84.6 ± 10.6
	Extrasynaptic	267.5 ± 13.9	289.4 ± 58.3	228.9 ± 26.2	264.5 ± 48.7	316.2 ± 59.8	219 ± 29.5
HEK293	GluN2A	–	–	265.1 ± 24.4	274.1 ± 30	468.9 ± 140.5	462.1 ± 135.5
	GluN2B	–	–	3646.2 ± 447.6	3846.8 ± 835.1	2976.9 ± 988.6	2718.6 ± 789.6
		Rise time (ms)					
		pH 6.5		pH 6.8		pH 7.6	
		Ctrl	NAAG	Ctrl	NAAG	Ctrl	NAAG
Slice	Synaptic	13 ± 1.9	14.2 ± 1.7	11.5 ± 0.9	13.2 ± 1.3	9.4 ± 0.9	11.2 ± 1.6
	Extrasynaptic	29.5 ± 4.5	34.4 ± 4.2	26.1 ± 4.5	32.8 ± 4.3	42.5 ± 3.9	41 ± 2.1
HEK293	GluN2A	–	–	92.8 ± 17.5	90.1 ± 18.6	80.3 ± 16.6	72.2 ± 11.5
	GluN2B	–	–	151.2 ± 21.1	138.3 ± 10	163.8 ± 46.4	161.9 ± 41.8

Data are mean ± SEM of at least three cells. No significant differences were observed in all cases ($p > 0.05$).

Biotinylation of surface proteins was performed following a previously published protocol (Pabba et al., 2014) with some modifications. To biotinylate surface proteins, the hippocampal slices (300 μm) were incubated for 20 min in ice cold (4°C), freshly made 0.5 mg/ml EZ-sulfo-NHS-SS-biotin (Pierce/Thermo Scientific) in phosphate-buffered saline (PBS, in mM: 137 NaCl, 2,7 KCl, 10 Na_2HPO_4, 1.8 KH_2PO_4, pH 7.4). Excess biotin was removed by washing the slices six times with cold supplemented Tris-buffered saline (TBS) (in mM: 20 Tris-HCl, 13.7 NaCl, and 0.5 KCl, pH 7.4). Slices were then homogenized in lysis buffer (in mM: 150 NaCl, 20 HEPES, 2 EDTA, 1×Protease Inhibitor, pH 7.4) using a Dounce homogenizer followed by sonication for 2×10 s. Cell debris was removed by centrifugation for 10 min at 14,000 rcf and the supernatants were incubated for 1 hour at 4°C with prewashed neutravidin beads (Pierce/Thermo Scientific) to capture biotinylated proteins. After washing six times with PBS supplemented with 0.05% SDS, the bound proteins were recovered from the beads with 400 μl of elution buffer (in mM: 50 Tris-HCl, 1 DTT; 2% SDS, pH 6.8) by boiling for 10 min. Protein concentrations were determined using DC assay (Bio-Rad) before Western blot.

Total membrane proteins (10 μg) were loaded and resolved as entire series on 8% SDS-PAGE and transferred to PVDF membranes. Primary antibodies used were anti-GluN1 (1:10,000; Synaptic Systems GmbH); anti-GluN2A and anti-GluN2B (both 1:750; LifeSpan Biosciences), and anti-Na^+/K^+-ATPase (Developmental Studies Hybridoma Bank). The blots were developed with Luminata Forte (Millipore) and visualized using the LI-COR Odyssey Fc System (LI-COR Biosciences). The band intensities were quantified using the Image Studio 2.0 software (LI-COR Biosciences) and normalized to

Na^+/K^+-ATPase, which remained unchanged with treatment. Statistics were done using one-way ANOVA and Tukey's post-hoc test with 95% confidence interval. All values are expressed as mean ± SEM.

5. *RESULTS*

5.1. NAAG differentially modulates synaptic and extrasynaptic NMDAR function in acute hippocampal slices

Using adult mice, we set out to investigate the role of NAAG in the regulation of NMDAR activity. The effect of NAAG on synaptic NMDAR activity was tested in the mouse hippocampus. Whole-cell currents from acute brain slices of CA1 pyramidal neurons were recorded and NMDAR EPSCs were isolated. For all experiments, control was established in the last 5 min of baseline recording before application of any treatment, and all data was thereafter normalized to this control (unless otherwise stated). Following a stable baseline recording, NAAG (20 μM) was perfused for 15 min followed by a 20 min washout. In the presence of NAAG, we observed a 44 ± 12.6% increase in NMDAR-mediated EPSC amplitude (n = 5 cells, $p < 0.05$; **Fig. 6A,B**). The effect of NAAG persisted even following washout, which has similarly been observed in other studies utilizing NAAG (Sanabria et al., 2004; Bergeron et al., 2007; Walder et al., 2013). Since no recovery was observed for 20 min in any of the experiments, only up to 10 min of washout is shown in all figures. Similar experiments were performed using the GCP-II inhibitor, 2-PMPA (10 μM), which endogenously increases the level of NAAG (Jackson et al., 1996; Slusher et al., 1999; Nagel et al., 2006). In agreement with the results obtained with exogenous application of NAAG, 2-PMPA significantly increased the amplitude of the NMDAR EPSC by 29 ± 6.1% (n = 6 cells, $p < 0.05$; **Fig. 6C,D**). To confirm that the effect of 2-PMPA was the result of its inhibitory effect on GCP-II and the consequent elevation of NAAG, we used 2-PMSA (10 μM), a structurally similar but inactive analogue of 2-PMPA (Jackson et al., 1996; Slusher et al., 1999). Our data shows

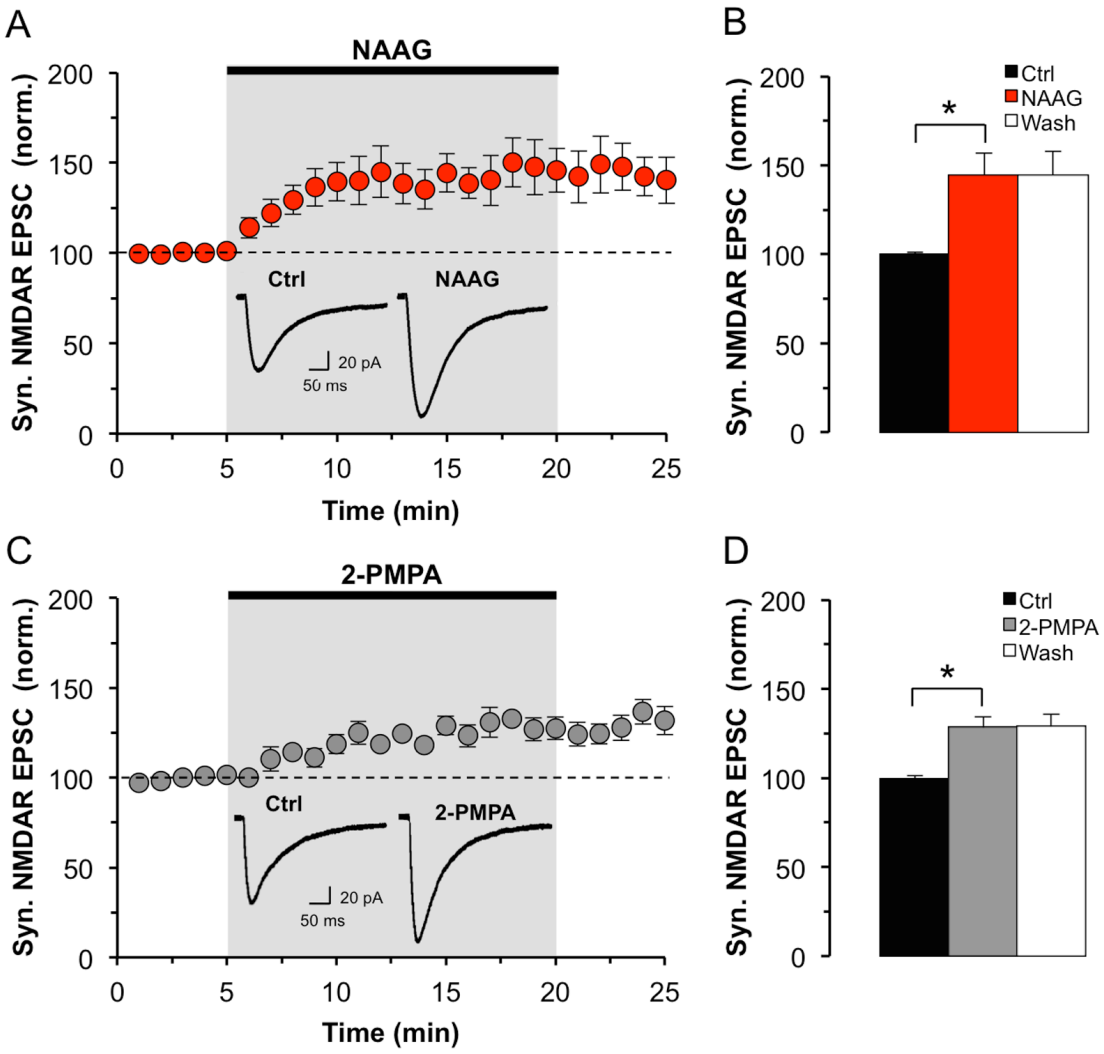

Figure 6. Endogenous and exogenous NAAG potentiate synaptic NMDAR EPSCs in acute hippocampal slices in physiological pH. (A) CA1 pyramidal neurons were recorded from hippocampal slices and the average amplitude of evoked synaptic NMDAR EPSCs were plotted during a 15 min exogenous NAAG application followed by washout and compared to control (represented by dotted line; n = 5 cells). Representative traces of synaptic NMDAR EPSCs of a control and NAAG-treated CA1 pyramidal neuron are also shown. (B) Representative bar graph from data in (A) showing average synaptic NMDAR EPSC amplitudes 5 min before NAAG application (Ctrl), during the last 5 min of NAAG treatment (NAAG), and during washout (Wash). (C) Average synaptic NMDAR EPSC amplitudes plotted during a 15 min 2-PMPA application followed by washout and compared to control (represented by dotted lines) (n = 6 cells). Representative traces of synaptic NMDAR EPSCs of a control and 2-PMPA-treated CA1 pyramidal neuron are also shown. (D) Representative bar graph from data in (C) showing average synaptic NMDAR EPSC amplitudes 5 min before 2-PMPA application (Ctrl), during the last 5 min of 2-PMPA treatment (2-PMPA), and during washout (Wash). The averages of the current amplitudes are normalized to the last 5 min of control in all cases. Data expressed as mean ± SEM. *, $p < 0.05$.

that 2-PMSA had no effect on NMDAR EPSCs (n = 4, $p > 0.05$; **Fig. 7A,B**).

To control for any influence that $mGluR_3$ may have had on these results, similar experiments were conducted in the presence of LY341495 (10 μM), a potent and selective group II mGluR antagonist. The effect of NAAG (n = 5) and 2-PMPA (n = 5) on NMDAR EPSCs was sustained throughout the application of LY341495 ($p < 0.05$; **Fig. 8A**), suggesting that the observed effect was not mediated by activation of $mGluR_3$. Furthermore, to demonstrate that the effects of NAAG and 2-PMPA are not mediated by presynaptic neurotransmitter release, we performed a paired pulse paradigm. No difference in the ratio of successive responses (amplitude 2/amplitude 1) was observed following application of either NAAG (n = 3 cells, $p > 0.05$) or 2-PMPA (n = 3 cells, $p > 0.05$; **Fig. 8C**). This is in agreement with a previous study also reporting no presynaptic effect of NAAG at CA1 synapses (Bergeron et al., 2005). These data suggest that the action of NAAG on the NMDAR EPSCs is mediated postsynaptically.

In the neonatal brain, GluN2B-containing NMDARs, characterized by slower decay kinetics, dominate at the synapse. Following postnatal development the subunit composition changes to be more GluN2A-containing at the synapse and GluN2B-containing extrasynaptically (Cull-Candy et al., 2001; Loftis and Janowsky, 2003; van Zundert et al., 2004; Sanz-Clemente et al., 2013). To investigate the influence of NAAG on NMDARs with different subunit compositions and subcellular localization, a previously established pharmacological paradigm (**Fig. 9A**) was used to block the activity of synaptic NMDARs, enabling us to specifically study the effect of NAAG on extrasynaptic NMDARs in adult mice (Hardingham et al., 2002; Carpenter-Hyland et al.,

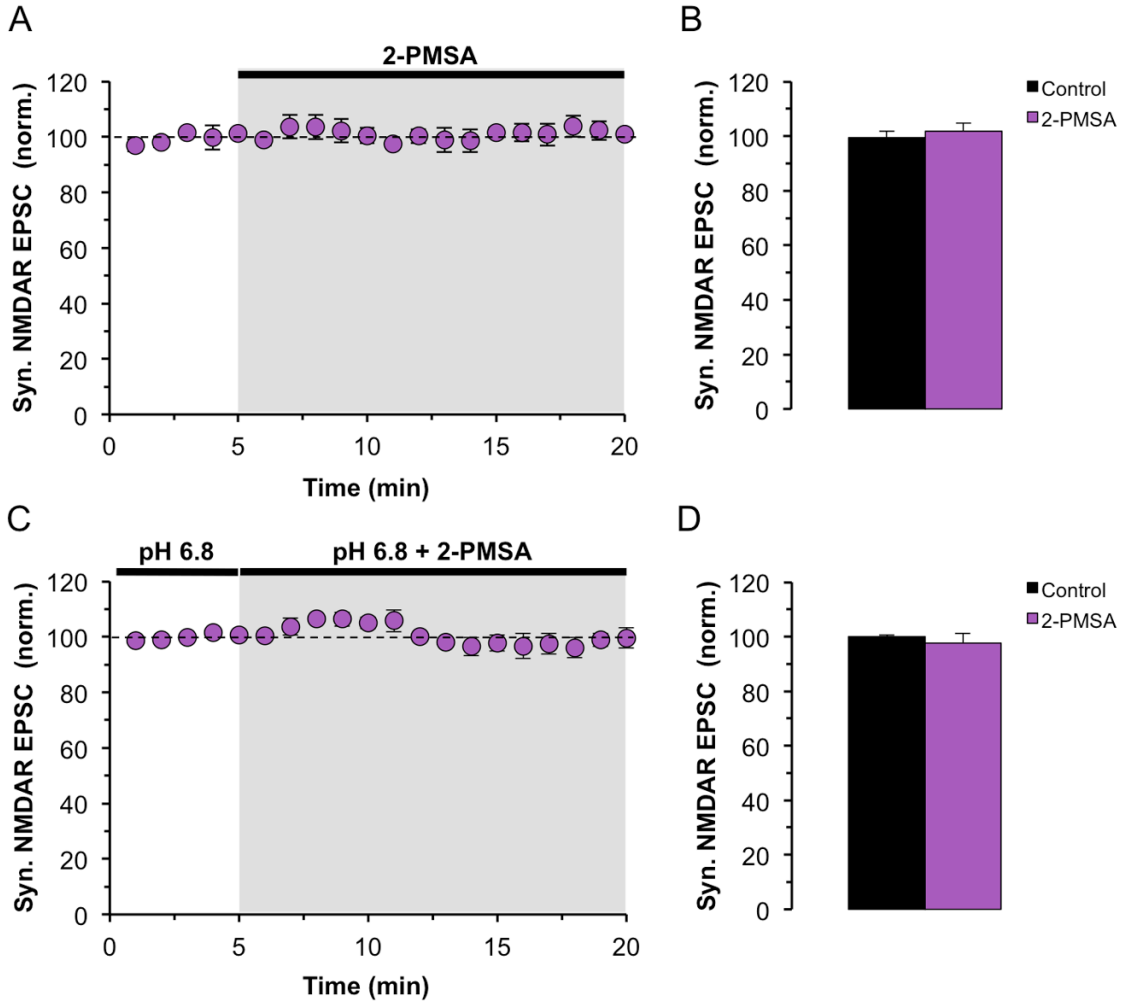

Figure 7. No effect of 2-PMSA, the inactive analogue of 2-PMPA, on synaptic NMDAR EPSCs in physiological and acidic pH. The effect of 2-PMSA on synaptic NMDAR-mediated EPSCs at pH 7.2 (n = 4) (A) and pH 6.8 (n = 3) (C) were measured and plotted. The average NMDAR amplitudes following 2-PMSA treatment and washout were normalized to their corresponding controls of pH change alone before application of 2-PMSA (control represented by dotted lines). (B) and (D) Representative bar graph of (A) and (C) showing normalized average of synaptic NMDAR EPSC amplitudes in pH 7.2 (B) and pH 6.8 (D) 5 min before 2-PMSA application (Ctrl), and the last 5 min of 2-PMSA treatment (2-PMSA). Data expressed as mean ± SEM.

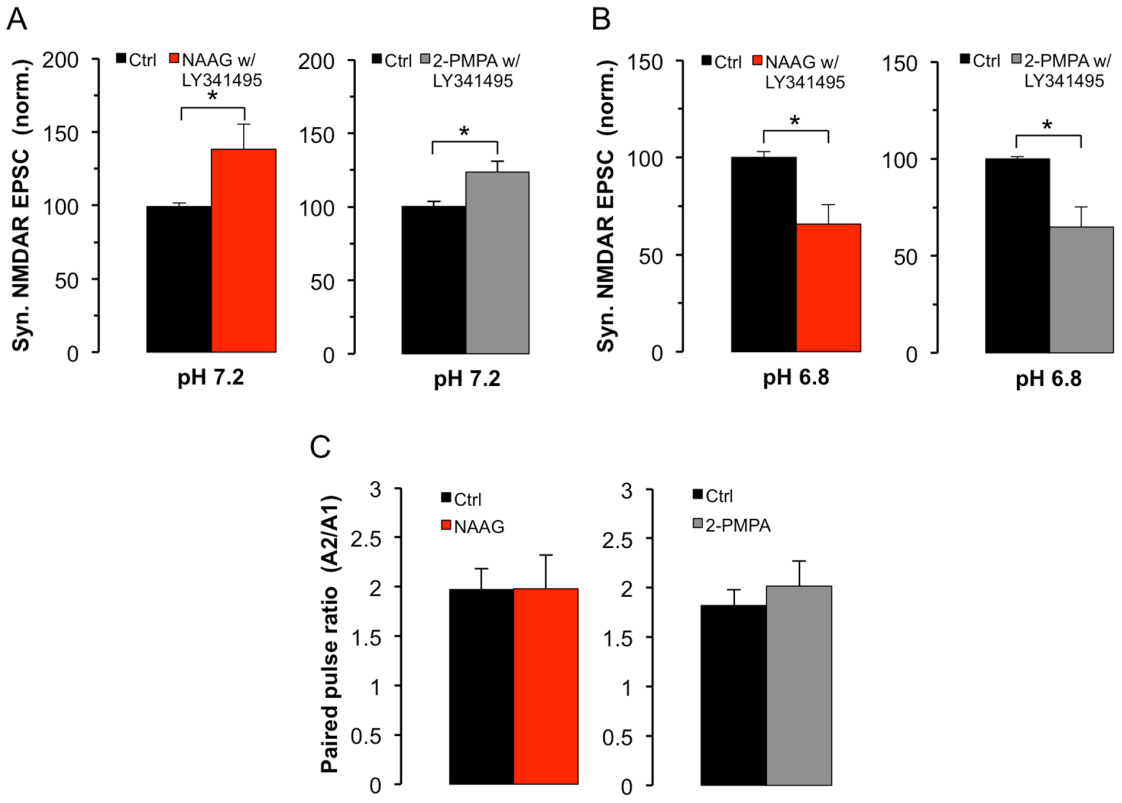

Figure 8. The effects of endogenous and exogenous NAAG on NMDARs are not mediated by mGluR$_3$ or by presynaptic neurotransmitter release. Representative bar graph showing average synaptic NMDAR EPSC amplitudes in the presence of the mGluR$_3$ antagonist, LY341494 in physiological pH (A) and acidic pH (B), 5 min before drug application (Ctrl), and during the last 5 min of treatment with either NAAG (n = 5 cells, pH 7.2; n = 4 cells, pH 6.8) or 2-PMPA (n = 5 cells, pH 7.2; n = 4, cells pH 6.8). The averages of the current amplitudes are normalized to the last 5 min of control. (C) Representative bar graph showing the effect of NAAG and 2-PMPA on paired pulse stimulation on pyramidal neurons in normal ACSF. Two pulses of identical intensity were delivered with an interval of 100 ms and the ratio between the amplitude of the second (A2) and the first (A1) evoked response was measured for control (Ctrl) and following treatment with either NAAG (n = 3 cells) or 2-PMPA (n = 3 cells). Data expressed as mean ± SEM. *, $p < 0.05$.

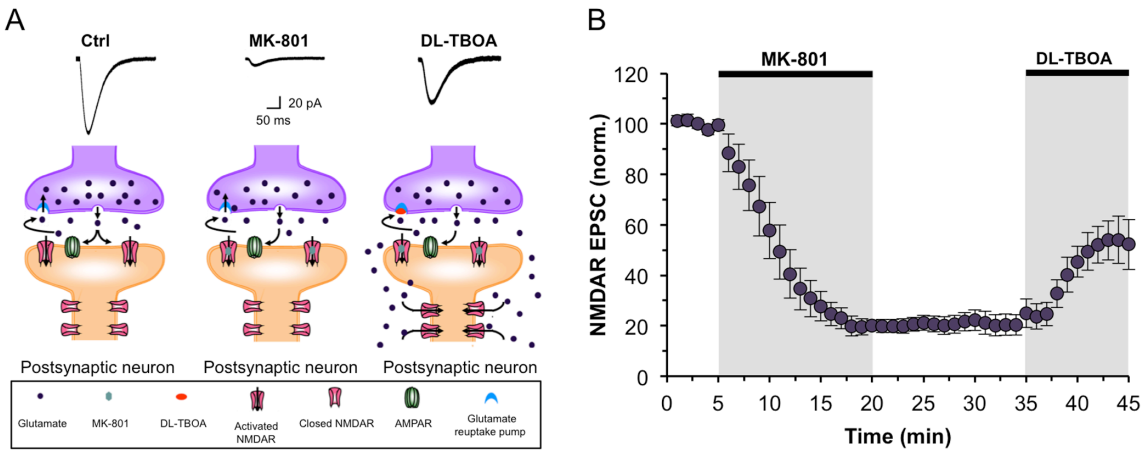

Figure 9. Pharmacological paradigm used to isolate extrasynaptic NMDARs. (A) MK-801, an irreversible use-dependent NMDAR antagonist, was bath applied to block synaptic NMDARs. Following washout of MK-801, the slice was treated with DL-TBOA, a glutamate reuptake inhibitor, in order to activate the extrasynaptic NMDAR population. (B) MK-801 effectively reduced the NMDAR EPSC, and the addition of DL-TBOA was able to partially recover the current by activating extrasynaptic NMDARs (n = 6 cells). The averages of the current amplitudes are normalized to the last 5 min of control. Data expressed as mean ± SEM. *, $p < 0.05$.

2004; Harney et al., 2008; Imamura et al., 2008; Okamoto et al., 2009; Hardingham and Bading, 2010; Xia et al., 2010; Li et al., 2011). MK-801 (30 μM), an irreversible use-dependent antagonist (Huettner and Bean, 1988), was used to block synaptic NMDARs. The glutamate reuptake inhibitor, DL-TBOA (30 μM), was then applied, allowing glutamate to diffuse away from the synapse and activate the extrasynaptic NMDAR population (**Fig. 9B**) (Clements et al., 1992).

Analysis of extrasynaptic NMDAR EPSCs indicates they are primarily GluN2B-containing due to their characteristically slow decay kinetics, as compared to the faster GluN2A-containing NMDARs (**Table 1**). In addition, there is ample evidence supporting the notion that GluN2B-containing NMDARs dominate extrasynaptic sites in mature animals, as reported by several studies utilizing the selective GluN2B inhibitor, ifenprodil (Tovar and Westbrook, 1999; Bellone and Nicoll, 2007; Mony et al., 2009b). To further verify NMDAR subunit distinction in our system we measured and demonstrated a difference in ifenprodil sensitivity on synaptic and extrasynaptic NMDARs. Following synaptic NMDAR isolation and a stable baseline recording, ifenprodil (3 μM) was bath applied for 15 min. We observed an 11 ± 3.2% increase in NMDAR-mediated EPSC amplitudes (n = 4 cells, $p < 0.05$; **Fig. 10A**). On the other hand, when ifenprodil was bath applied for 15 min following isolation of extrasynaptic NMDARs we observed a significant 49 ± 5.3% decrease in NMDAR-mediated EPSC amplitudes (n = 5 cells, $p < 0.05$; **Fig. 10B**). These findings clearly show an inhibition of extrasynaptic NMDARs by ifenprodil, however, no detectable sign of inhibition was observed on synaptic NMDARs. In addition, control experiments showing stable baseline recordings of NMDAR EPSCs

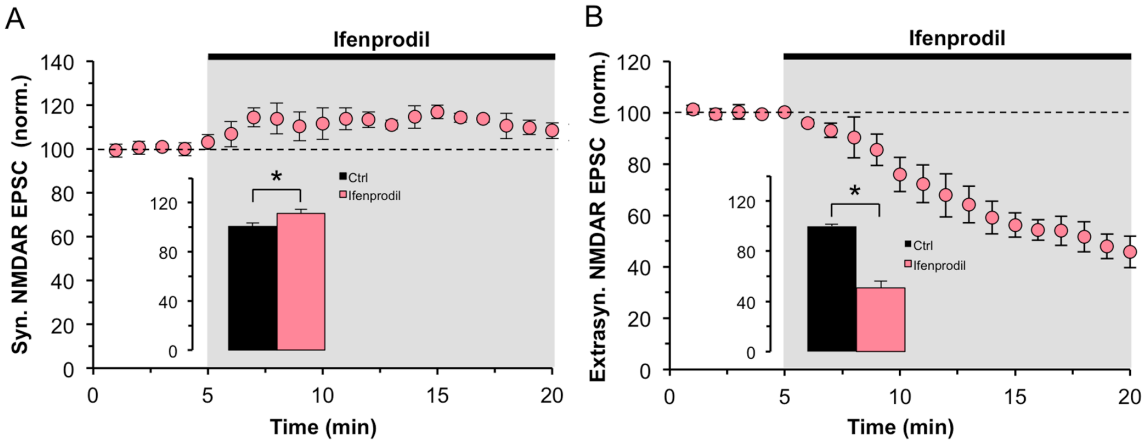

Figure 10. Ifenprodil sensitivity on synaptic and extrasynaptic NMDAR EPSCs in acute hippocampal slices in physiological pH. (A) Average synaptic NMDAR EPSC amplitudes plotted during a 15 min application of ifenprodil and compared to control (represented by dotted line; n = 4 cells). Representative bar graph showing average synaptic NMDAR EPSC amplitudes 5 min before ifenprodil application (Ctrl), and during the last 5 min of ifenprodil treatment (Ifenprodil). (B) Average extrasynaptic NMDAR EPSC amplitudes plotted during a 15 min application of ifenprodil and compared to control (represented by dotted line; n = 5 cells). Representative bar graph showing average extrasynaptic NMDAR EPSC amplitudes 5 min before ifenprodil application (Ctrl), and during the last 5 min of ifenprodil treatment (Ifenprodil). The averages of the current amplitudes are normalized to the last 5 min of control in all cases. Data expressed as mean ± SEM. *, $p < 0.05$.

over time in the absence of NAAG on both synaptic and extrasynaptic NMDARs are shown ($p > 0.05$; **Fig. 11A,B**). This demonstrates that NMDAR subunit composition is indeed different depending on the subcellular localization of the receptor, with GluN2A- and GluN2B-containing receptors dominating synaptic and extrasynaptic sites, respectively.

With the establishment of the extrasynaptic isolation paradigm, we next set out to determine the effect of NAAG on NMDARs that are located extrasynaptically. Following isolation of extrasynaptic NMDARs, NAAG or 2-PMPA was bath applied for 15 min, and we observed that both compounds significantly reduced the amplitude of the NMDAR EPSC. In the presence of NAAG, the decrease in amplitude was 27 ± 6.9% (n = 4 cells, $p < 0.05$; **Fig. 12A,B**) and in the presence of 2-PMPA it was 41 ± 4.7% (n = 8 cells, $p < 0.05$; **Fig. 12C,D**). This indicates that NAAG blocks NMDARs located extrasynaptically. Altogether, these results show that NAAG potentiates synaptic GluN2A-containing NMDAR EPSCs and inhibits extrasynaptic GluN2B-containing NMDAR EPSCs, suggesting that NAAG can evoke differential responses on NMDAR activity depending on its subunit composition and subcellular localization.

5.2. A subunit specific action of NAAG on GluN2A- and GluN2B-containing NMDARs in HEK293 cells

In native tissue, synaptic and extrasynaptic NMDAR populations are not homogenously GluN2A- or GluN2B-containing, but include both with one dominating (Suarez et al., 2010; Tovar et al., 2013). In order to validate that NAAG has distinctive effects on NMDARs with different subunit composition, we utilized an *in vitro* recombinant

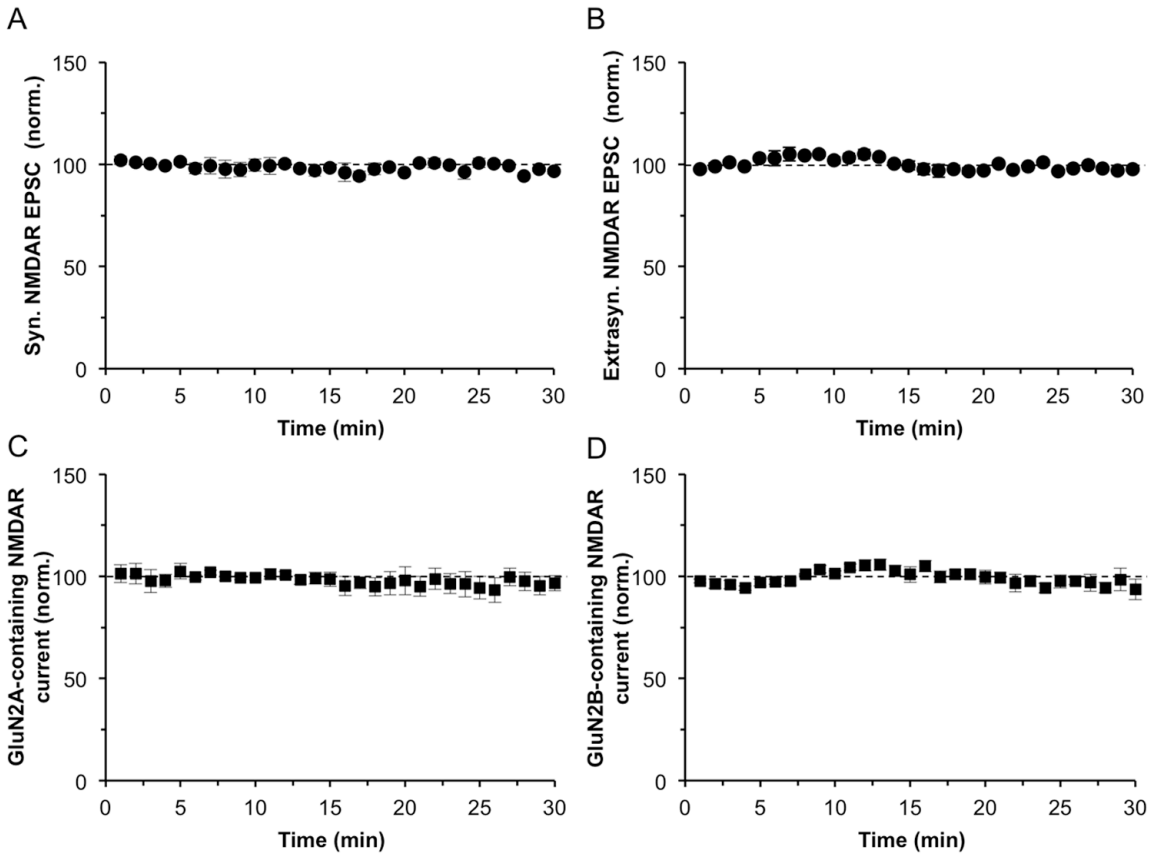

Figure 11. Stable baseline recordings. (A) Stable baseline recordings of average synaptic NMDAR EPSC amplitudes over a period of 30 min (n = 5 cells). (B) Stable baseline recordings of average extrasynaptic NMDAR EPSC amplitudes over a period of 30 min (n = 7 cells). (C) and (D) Stable baseline recordings of NMDAR currents over a period of 30 min in both GluN2A- (n = 5 cells) and GluN2B-containing (n = 4 cells) NMDARs, respectively.

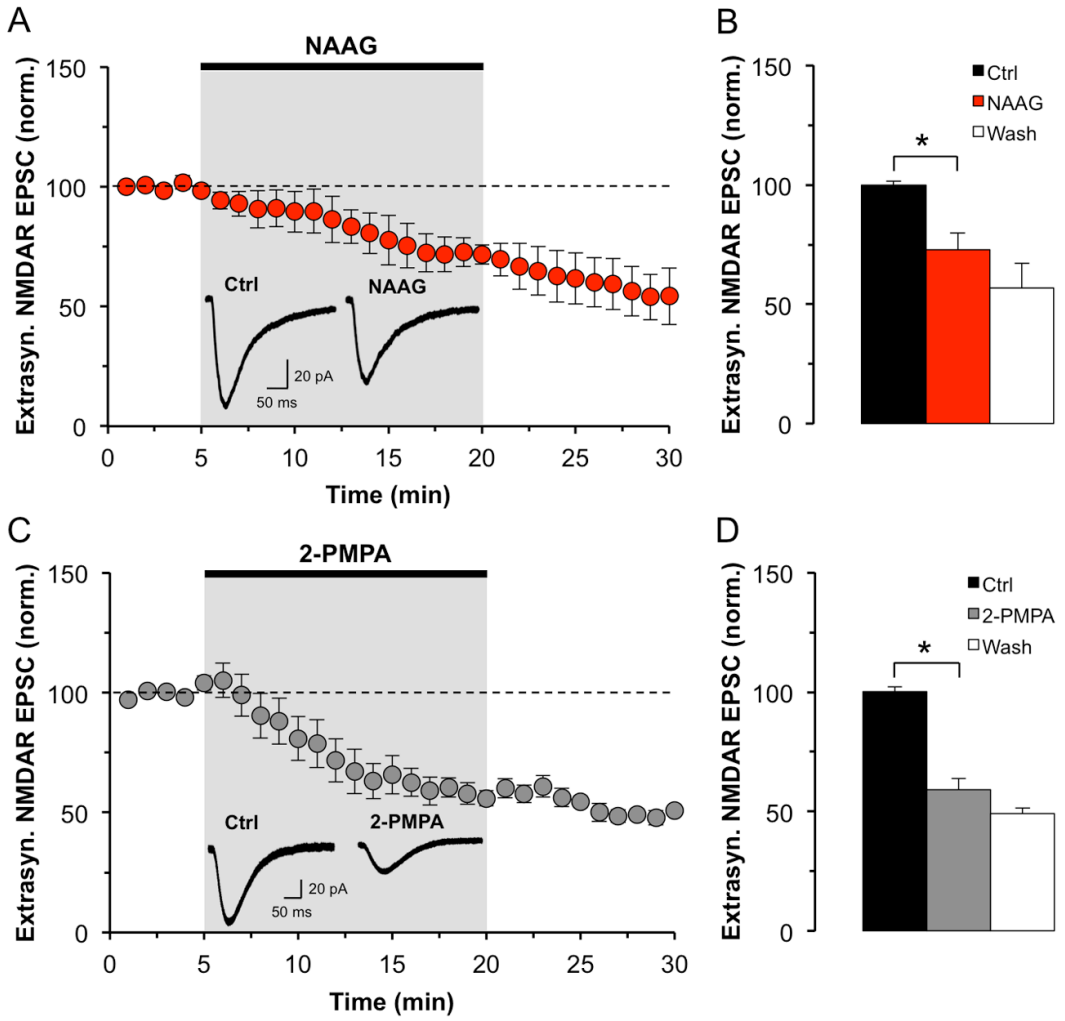

Figure 12. Endogenous and exogenous NAAG inhibit extrasynaptic NMDAR EPSCs in acute hippocampal slices in physiological pH. (A) Average extrasynaptic NMDAR EPSC amplitudes plotted during a 15 min exogenous NAAG application followed by washout and compared to control (represented by dotted line; n = 4 cells). Representative traces of extrasynaptic NMDAR EPSCs of a control and NAAG-treated CA1 pyramidal neuron are also shown. (B) Representative bar graph from data in (A) showing average extrasynaptic NMDAR EPSC amplitudes 5 min before NAAG application (Ctrl), during the last 5 min of NAAG treatment (NAAG), and during washout (Wash). (C) Average amplitude of extrasynaptic NMDAR EPSCs plotted during a 15 min 2-PMPA application followed by washout and compared to control (represented by a dotted line) (n = 8 cells). Representative traces of extrasynaptic NMDAR EPSCs of a control and 2-PMPA-treated CA1 pyramidal neuron are also shown. (D) Representative bar graph from data in (C) showing average extrasynaptic NMDAR EPSC amplitudes 5 min before 2-PMPA application (Ctrl), during the last 5 min of 2-PMPA treatment (2-PMPA), and during washout (Wash). The averages of the current amplitudes are normalized to the last 5 min of control in all cases. Data expressed as mean ± SEM. *, $p < 0.05$.

system. To establish cells containing a specified subunit makeup of NMDARs, HEK293 cells were transiently cotransfected with constructs encoding the GluN1 subunit in combination with either GluN2A or GluN2B subunits. Decay kinetics were measured for both GluN2A and GluN2B transfected HEK293 cells to ensure the correct subunit composition of the NMDARs. As expected, GluN2B-containing cells had slower kinetics than the GluN2A-containing cells (**Table 1**). Following application of NAAG on GluN2A-transfected HEK293 cells, there was a significant increase of 15 ± 4.4% in the NMDAR current amplitude (n = 7 cells, $p < 0.05$; **Fig. 13A,B**). However, in the GluN2B-transfected HEK293 cells, there was a significant decrease of 18 ± 9.1% in the NMDAR current amplitude in the presence of NAAG (n = 9 cells, $p < 0.05$; **Fig. 13C,D**). Furthermore, we performed control experiments showing stable baseline recordings of NMDAR currents over time in the absence of NAAG in both GluN2A- and GluN2B-containing NMDARs ($p > 0.05$; **Fig. 11C,D**). The results from our HEK293 recordings are in agreement with the data obtained from acute hippocampal slices and further support that NAAG potentiates GluN2A-containing NMDAR currents, while inhibiting GluN2B-containing NMDAR currents. Therefore, the data presented thus far demonstrate that NAAG has different effects on NMDAR activity depending on subunit composition.

5.3. Protons regulate the activity of NMDARs in acute hippocampal slices and HEK293 cells

In addition to subunit specificity, the effect of NAAG on NMDARs may also be pH dependent, whereby a higher potency in acidic ischemic conditions may underlie its

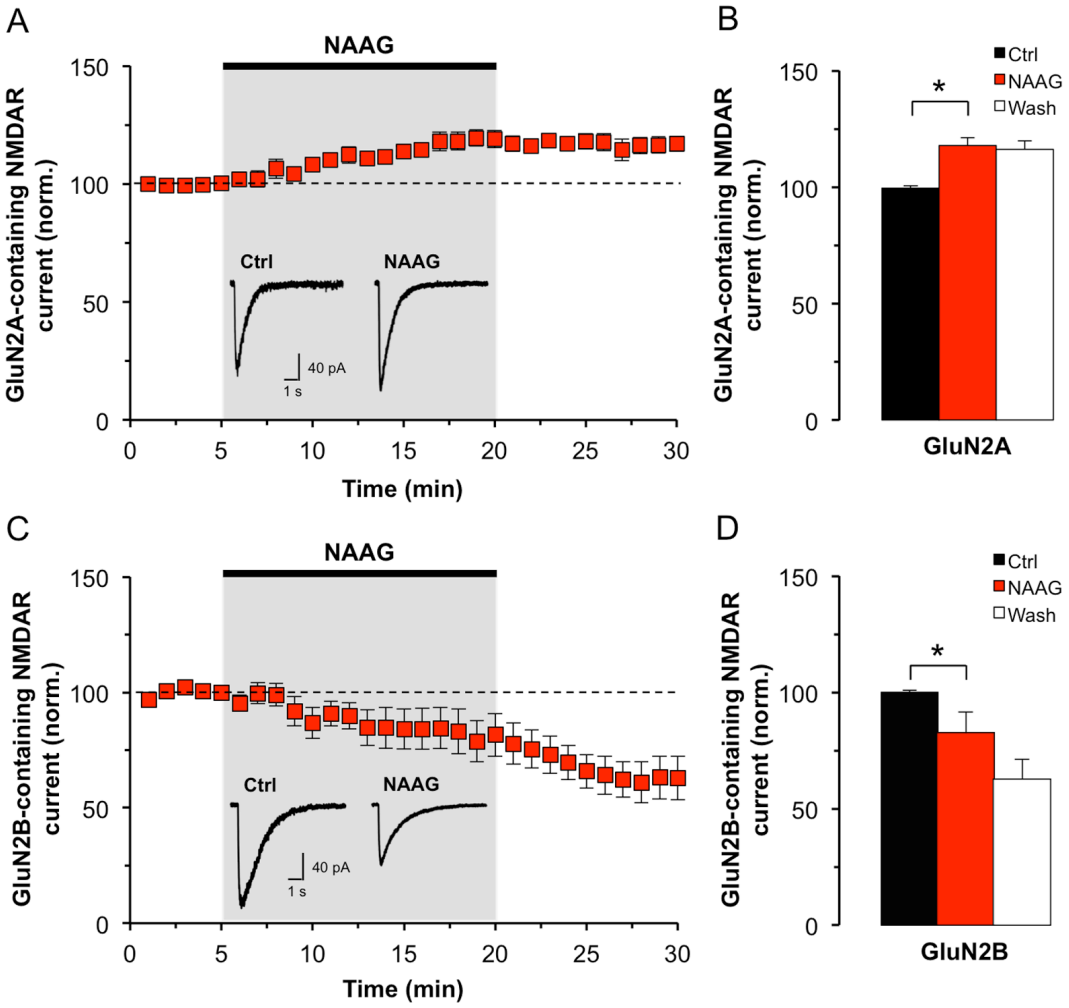

Figure 13. NAAG potentiates GluN2A-containing NMDAR currents and inhibits GluN2B-containing NMDAR currents in HEK293 cells in physiological pH. (A) GluN1/GluN2A-transfected HEK293 cells were recorded and the average NMDAR current amplitudes were plotted during a 15 min treatment with exogenous NAAG and compared to control (represented by a dotted line) (n = 7 cells). Representative traces of NMDAR currents of a control and NAAG-treated HEK293 cell are also shown. (B) Representative bar graph from data in (A) showing the average of GluN2A-containing NMDAR current amplitudes 5 min before NAAG application (Ctrl), during the last 5 min of NAAG treatment (NAAG) and during washout (Wash). (C) GluN1/GluN2B-transfected HEK293 cells were recorded and the average NMDAR current amplitudes were plotted during a 15 min treatment with exogenous NAAG and compared to control (represented by a dotted line) (n = 9 cells). Representative traces of NMDAR currents of a control and NAAG-treated HEK293 cell are also shown. (D) Representative bar graph from data in (C) showing the average of GluN2B-containing NMDAR current amplitudes 5 min before NAAG application (Ctrl), during the last 5 min of NAAG treatment (NAAG), and during washout (Wash). The averages of the current amplitudes are normalized to the last 5 min of control in all cases. Data expressed as mean ± SEM. *, $p < 0.05$.

neuroprotective mechanism (Shalaby et al., 1992; Pahk and Williams, 1997; Whittemore et al., 1997; Mott et al., 1998). We first established that the pH-dependent regulation of NMDARs occurs in our system. Synaptic and extrasynaptic NMDAR EPSCs were recorded in different pH conditions (6.5, 6.8, and 7.6) and normalized to baseline (pH 7.2). There was an 80 ± 3.2% reduction of the synaptic NMDAR EPSC amplitude at pH 6.5 (n = 10 cells, $p < 0.05$), and a 50 ± 3.9% reduction at pH 6.8 (n = 11 cells, $p < 0.05$). Additionally, changing the pH from 7.2 to 7.6 induced a 94 ± 21.1% increase in this NMDAR synaptic current (n = 10 cells, $p < 0.05$; **Fig. 14**). This change in pH also produced a very similar effect on extrasynaptic NMDARs. When the extracellular pH was decreased to 6.5, there was a 76 ± 4.9% reduction of the extrasynaptic NMDAR EPSC amplitude (n = 3 cells, $p < 0.05$), as well as a reduction of 51 ± 12.2% at pH 6.8 (n = 4 cells, $p < 0.05$). An increase in the extracellular pH to 7.6 resulted in a significant 34 ± 7.4% increase in the extrasynaptic NMDAR EPSC amplitude as compared to control (n = 4 cells, $p < 0.05$; **Fig. 15**).

The pH-dependent inhibitory effect was further validated in our *in vitro* system. Recording GluN2A-containing HEK293 cells at extracellular pH levels of 6.8 resulted in a 53 ± 7.6% decrease in the NMDAR current amplitude (n = 5 cells, $p < 0.05$), while at pH 7.6, there was a 45 ± 18.2% increase (n = 6 cells, $p < 0.05$; **Fig. 16A,B**). Similarly, when GluN2B-containing HEK293 cells were recorded at extracellular pH levels of 6.8 there was a 52 ± 5.6% decrease in the NMDAR current amplitude (n = 5 cells, $p < 0.05$), and a 44 ± 7.2% increase at pH 7.6 (n = 4 cells, $p < 0.05$; **Fig. 16C,D**). Our results are in

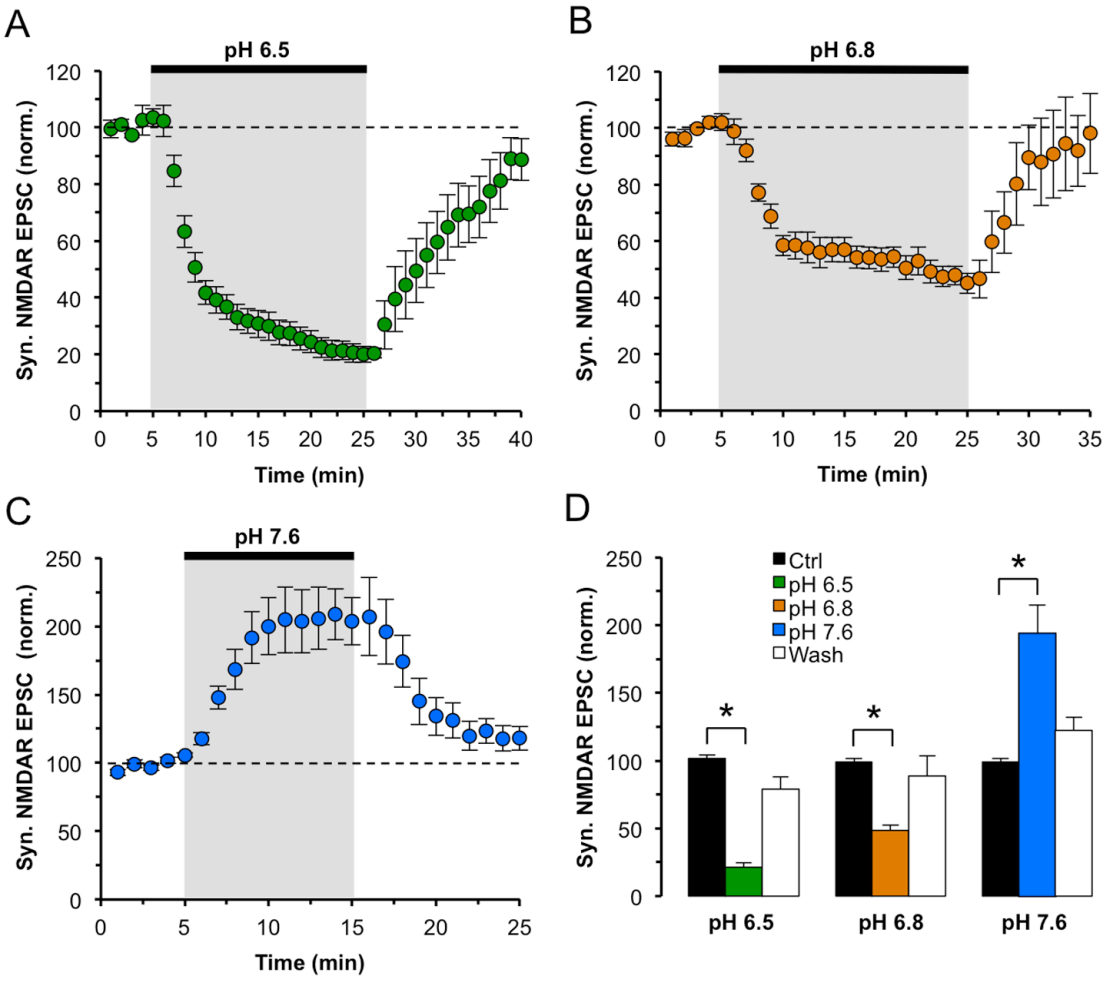

Figure 14. Protons modulate the activity of synaptic NMDARs in acute hippocampal slices. Synaptic NMDAR-mediated EPSC amplitudes were measured at pH 6.5 (n = 10 cells) (A), pH 6.8 (n = 11 cells) (B), and pH 7.6 (n = 10 cells) (C) and compared to control (pH 7.2 represented by dotted lines). (D) Representative bar graph from data in (A) – (C) showing average synaptic NMDAR EPSC amplitudes 5 min before pH change (Ctrl), during the last 5 min of pH treatment (pH 6.5, 6.8, or 7.6), and during washout (Wash). The averages of the current amplitudes are normalized to the last 5 min of control in all cases. Data expressed as mean ± SEM. *, $p < 0.05$.

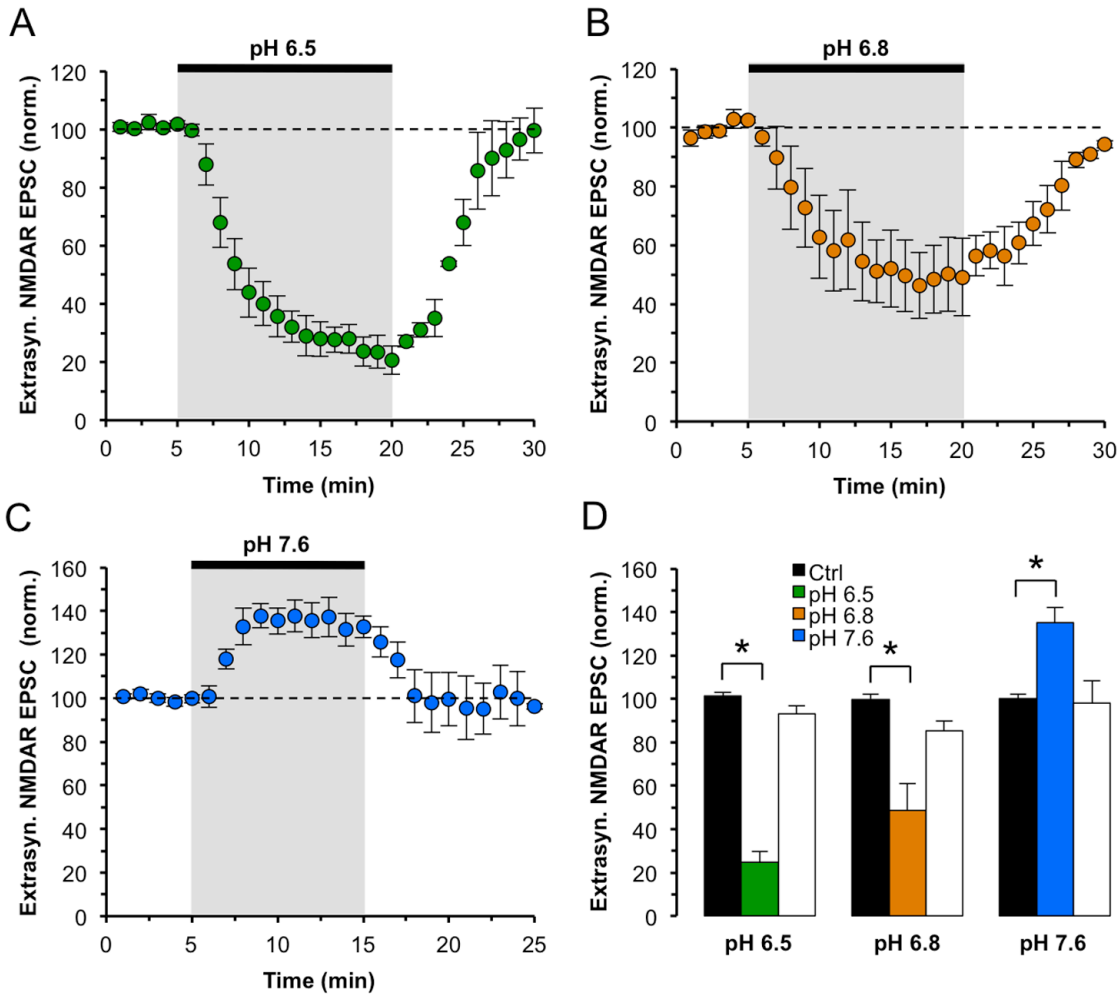

Figure 15. Protons modulate the activity of extrasynaptic NMDARs in acute hippocampal slices. Isolated extrasynaptic NMDAR-mediated EPSC amplitudes were measured at pH 6.5 (n = 3 cells) (A), pH 6.8 (n = 4 cells) (B) and pH 7.6 (n = 4 cells) (C) and compared to control (represented by a dotted line). (D) Representative bar graph from data in (A) – (C) showing the average extrasynaptic NMDAR EPSC amplitudes 5 min before pH change (Ctrl), during the last 5 min of pH treatment (pH 6.5, 6.8, or 7.6), and during washout (Wash). The averages of the current amplitudes are normalized to the last 5 min of control in all cases. Data expressed as mean ± SEM. *, $p < 0.05$.

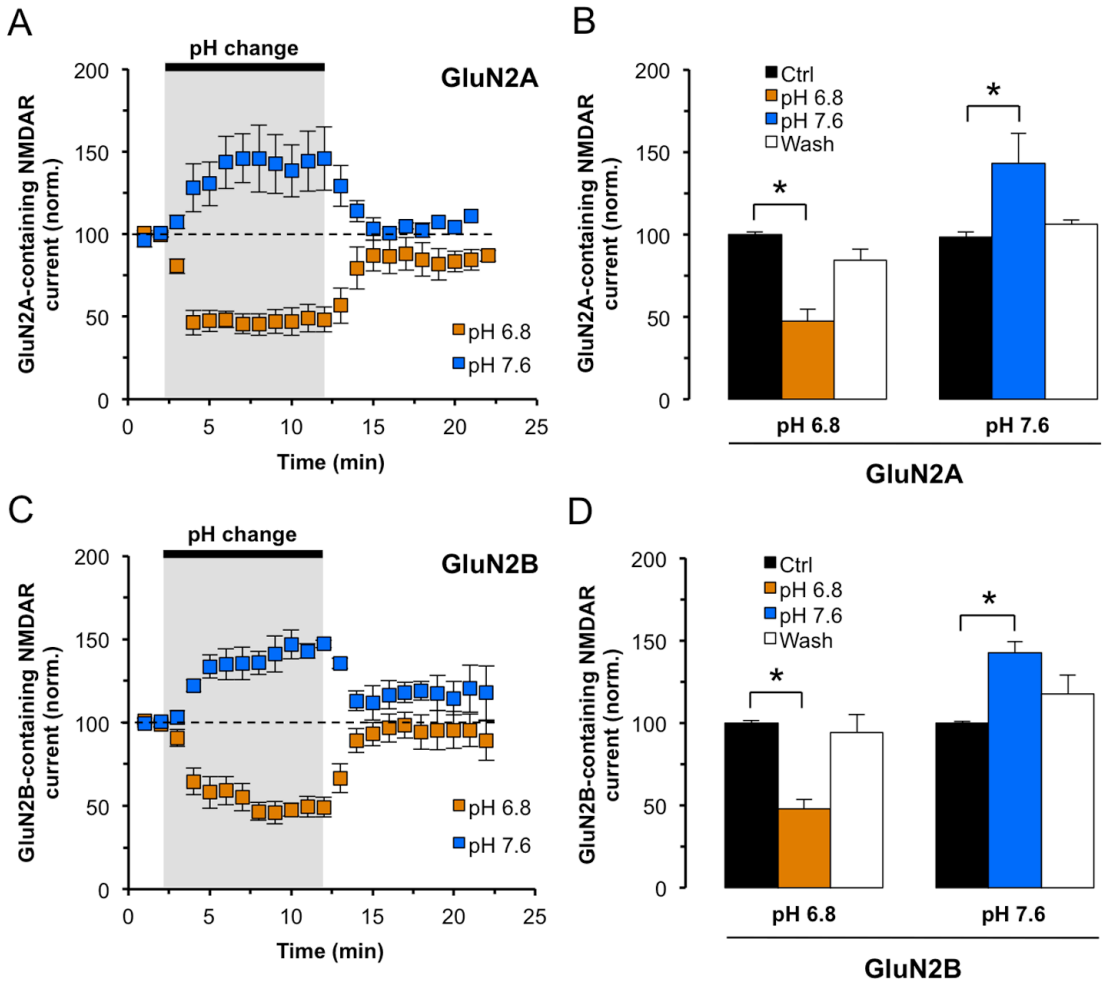

Figure 16. Protons modulate the activity of GluN2A- and GluN2B-containing NMDARs in HEK293 cells. (A) GluN1/GluN2A-transfected HEK293 cells were recorded before and during pH change and the average NMDAR current amplitudes for pH 6.8 (n = 5 cells) and pH 7.6 (n = 6 cells) were plotted and compared to control (pH 7.2 represented by dotted line). (B) Representative bar graph from data in (A) showing average GluN2A-containing NMDAR current amplitudes before pH change (Ctrl), during the last 5 min of pH treatment (pH 6.8 or pH 7.6), and during washout (Wash). (C) GluN1/GluN2B-transfected HEK293 cells were recorded before and during pH change and the average NMDAR current amplitudes for pH 6.8 (n = 5 cells) and pH 7.6 (n = 4 cells) were plotted and compared to control (pH 7.2 represented by dotted line). (D) Representative bar graphs from data in (C) showing average GluN2B-containing NMDAR amplitude before pH change (Ctrl), during the last 5 min of pH treatment (pH 6.8 or pH 7.6), and during washout (Wash). The averages of the current amplitudes are normalized to the last 2 min of control in all cases. Data expressed as mean ± SEM. *, $p < 0.05$.

agreement with previous studies (Tang et al., 1990; Traynelis and Cull-Candy, 1990; Vyklicky et al., 1990; Traynelis and Cull-Candy, 1991; Low et al., 2003; Dravid et al., 2007) and clearly demonstrate that protons modulate NMDAR function.

5.4. The effect of NAAG on NMDAR function is modulated by protons in acute hippocampal slices and HEK293 cells

The effect of NAAG on synaptic and extrasynaptic NMDAR activity under different pH conditions was investigated. NAAG was applied after establishing a stable baseline at pH 6.5, 6.8, or 7.6. In order to better visualize the effect of NAAG at different pH, the initial pH-induced NMDAR current was treated as a control and normalized to 100%. Interestingly, NAAG decreased the synaptic NMDAR EPSC amplitude by 53 ± 5.5% at pH 6.5 (n = 7 cells, $p < 0.05$; **Fig. 17A**), and by 27 ± 5.7% at pH 6.8 (n = 6 cells, $p < 0.05$; **Fig. 17B**). The effect of 2-PMPA on NMDAR EPSCs was also evaluated in low pH (6.8) and similarly a decrease of 37 ± 8.4% was observed (n = 5, $p < 0.05$; **Fig. 18**). To confirm that the effect of 2-PMPA was specific to GCP-II inhibition and mediated by an increase in NAAG, we tested the effect of 2-PMSA on NMDAR EPSCs in acidic pH. We found no significant change in the amplitude of the NMDAR EPSC (n = 3, $p > 0.05$; **Fig. 7C,D**). In contrast to what was observed at low pH, NAAG induced a 44 ± 12.6% increase in the synaptic NMDAR EPSC amplitude at physiological pH of 7.2 as shown in **Figure 6A,B**, as well as an 18 ± 16.5% increase at pH 7.6 (n = 5 cells, $p < 0.05$; **Fig. 17C**). These results are summarized in **Figure 17D**. To rule out any effect of $mGluR_3$ on our results, we repeated the study in acidic pH (6.8) with either NAAG (n = 4) or 2-

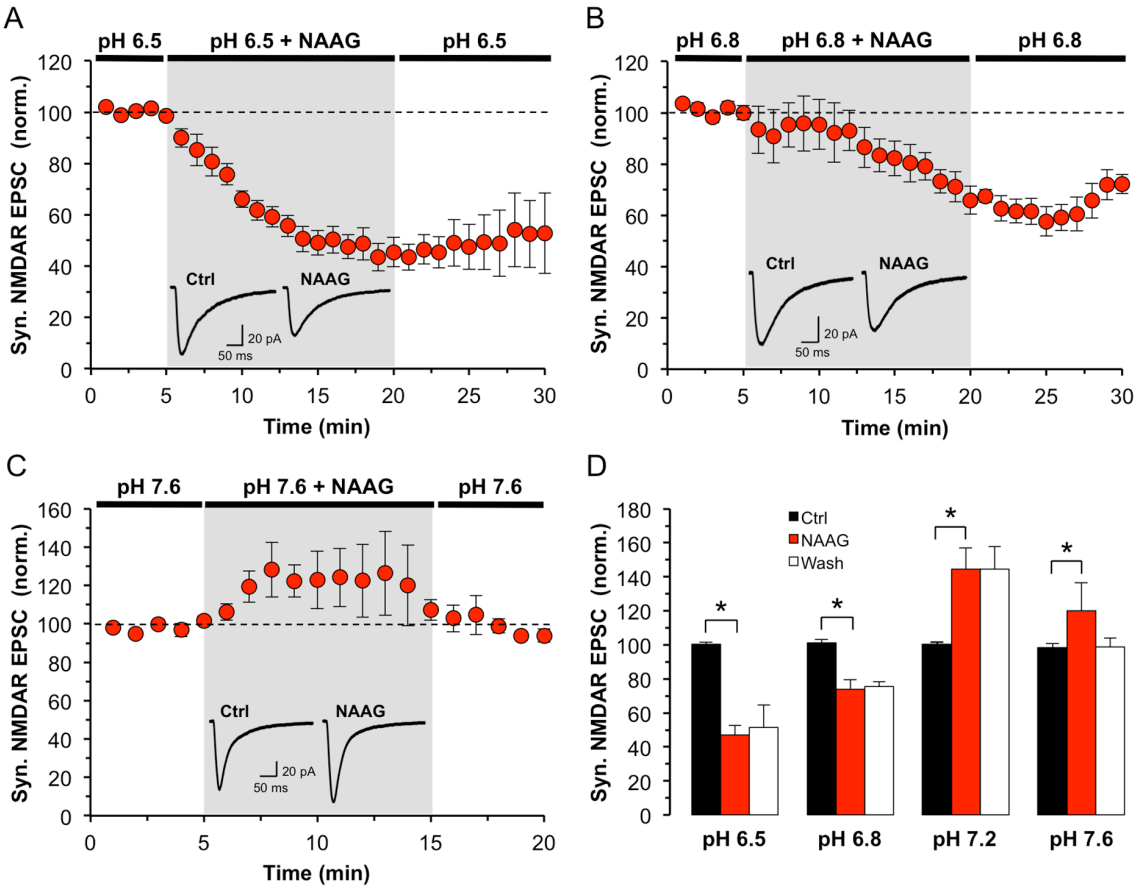

Figure 17. NAAG decreases the activity of synaptic NMDARs during acidic conditions in acute hippocampal slices. The effects of NAAG on synaptic NMDAR-mediated EPSCs at pH 6.5 (n = 7 cells) (A), pH 6.8 (n = 6 cells) (B), and pH 7.6 (n = 5 cells) (C) were measured and plotted. The average NMDAR amplitudes following NAAG treatment and washout were normalized to their corresponding controls of pH change alone before NAAG application (control represented by dotted lines). (D) Representative bar graph of (A)–(C) showing normalized average of synaptic NMDAR EPSC amplitudes in different pH conditions 5 min before NAAG application (Ctrl), the last 5 min of NAAG treatment (NAAG), and during washout (Wash). Data expressed as mean ± SEM. *, $p < 0.05$.

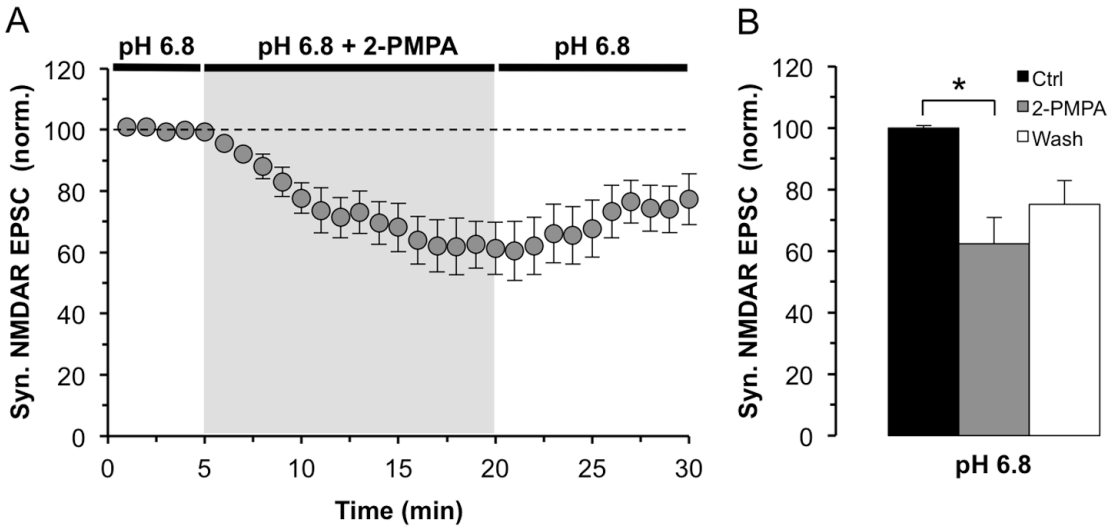

Figure 18. 2-PMPA decreases the activity of synaptic NMDARs in acidic conditions in acute hippocampal slices. (A) The effect of 2-PMPA on synaptic NMDAR-mediated EPSCs at pH 6.8 (n = 5 cells) was measured and plotted. The average NMDAR amplitudes following 2-PMPA treatment and washout were normalized to their corresponding controls of pH change alone before 2-PMPA application (control represented by dotted lines). (B) Representative bar graph of (A) showing normalized average of synaptic NMDAR EPSC amplitudes in acidic pH conditions 5 min before 2-PMPA application (Ctrl), the last 5 min of 2-PMPA treatment (2-PMPA), and during washout (Wash). Data expressed as mean ± SEM. *, $p < 0.05$.

PMPA (n = 4) in the presence of the LY341495 compound ($p < 0.05$; **Fig. 8B**). No detectable difference was observed upon inhibition of $mGluR_3$ with LY341495, confirming that $mGluR_3$ are not contributing to the effect of NAAG or 2-PMPA on NMDAR EPSCs.

We further examined whether a change in pH could amplify the inhibitory effect of NAAG in the extrasynaptic population of NMDARs as shown in **Figure 12A,B**. Following application of NAAG at a lower pH of 6.5 or 6.8, there was a further significant reduction of extrasynaptic NMDAR EPSC amplitude as compared to physiological pH levels ($p < 0.05$). An extracellular pH level of 6.5 induced a 53 ± 7.3% decrease in the extrasynaptic NMDAR EPSC amplitude (n = 3 cells, $p < 0.05$; **Fig. 19A**), while an extracellular pH of 6.8 decreased it by 47 ± 9% (n = 6 cells, $p < 0.05$; **Fig. 19B**). On the other hand, when extracellular pH was increased to 7.6 there was a non-significant 2 ± 16.8% change in the extrasynaptic NMDAR EPSC amplitude (n = 5 cells, $p > 0.05$; **Fig. 19C**). These results are summarized in **Figure 19D** and demonstrate that NAAG enhances the pH-dependent inhibitory effect on extrasynaptic NMDAR activity in hippocampal slices.

Recombinant experiments with the HEK293 cells were again utilized to verify that the potency of NAAG at NMDARs is pH-dependent. The effect of NAAG on the activity of GluN2A- or GluN2B-containing NMDARs was evaluated at different pH levels. When GluN2A-containing HEK293 cells were recorded at extracellular pH of 6.8 in the presence of NAAG, there was a 25 ± 7.3% decrease in the NMDAR amplitude (n = 6 cells, $p < 0.05$), while at pH 7.6, the presence of NAAG resulted in an increase of 28 ± 11.6% (n = 6 cells, $p < 0.05$; **Fig. 20A,B**). Application of NAAG on GluN2B-containing

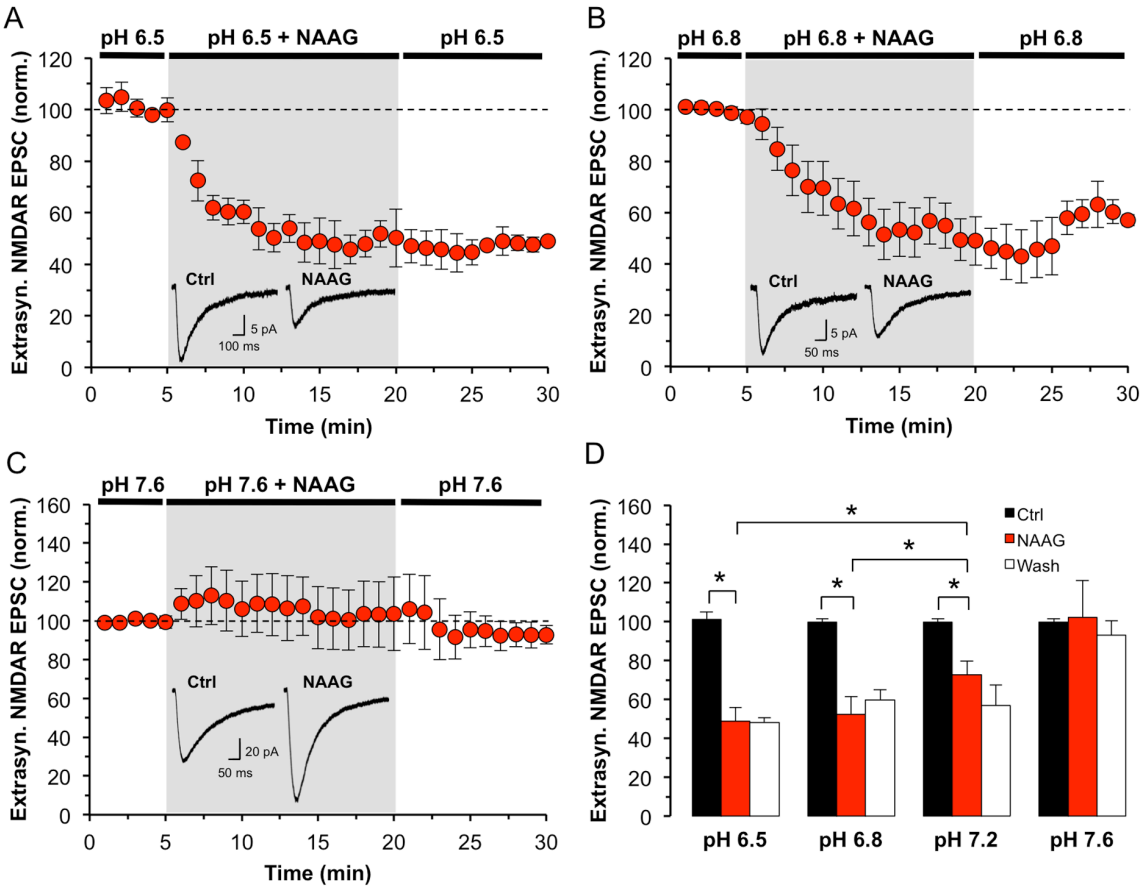

Figure 19. NAAG further inhibits extrasynaptic NMDARs during acidic conditions in acute hippocampal slices. The effects of NAAG on isolated extrasynaptic NMDAR-mediated EPSCs at pH 6.5 (n = 3 cells) (A), pH 6.8 (n = 6 cells) (B), and pH 7.6 (n = 5 cells) (C) were measured and plotted. The average NMDAR amplitudes following NAAG treatment and washout were normalized to their corresponding controls of pH change alone before NAAG application (control represented by dotted lines). (D) Representative bar graph of (A)–(C) showing normalized average of extrasynaptic NMDAR EPSC amplitudes in different pH conditions 5 min before NAAG application (Ctrl), the last 5 min of NAAG treatment (NAAG), and during washout (Wash). Data expressed as mean ± SEM. *, $p < 0.05$.

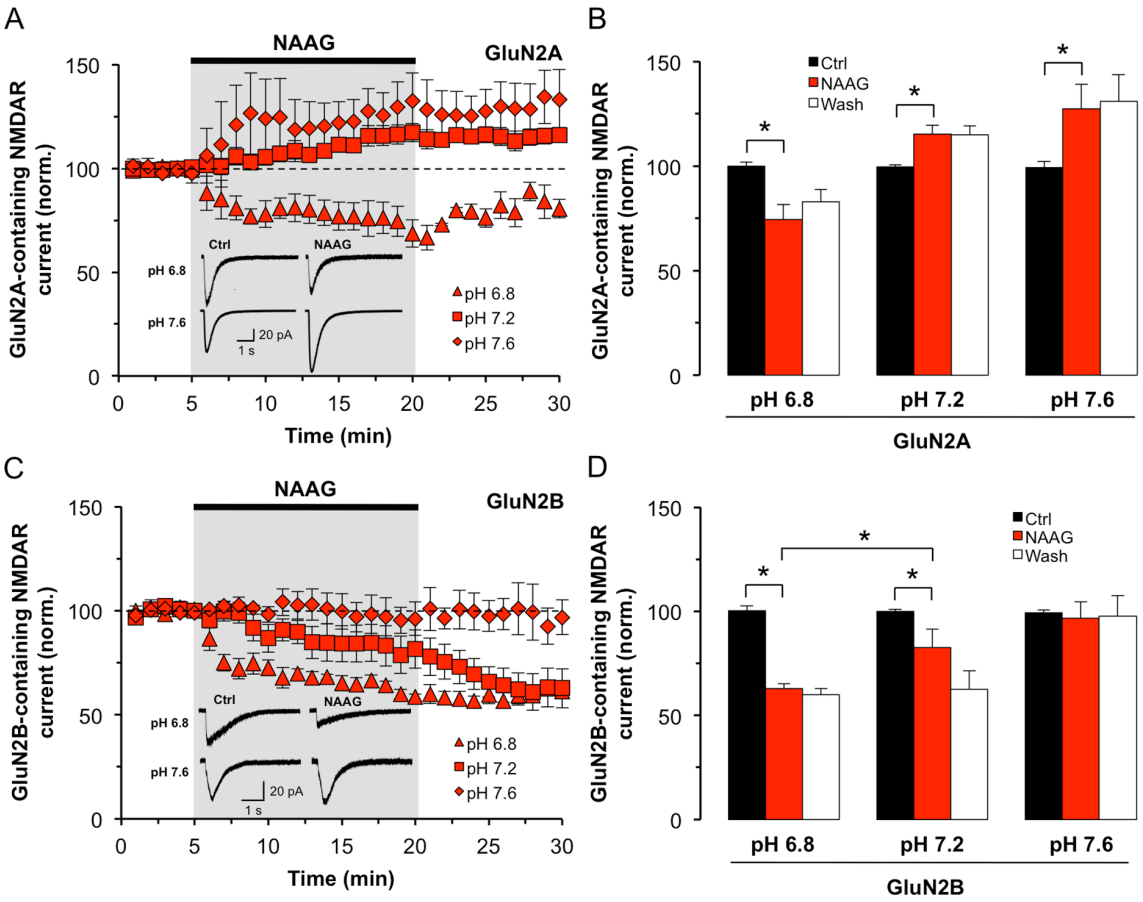

Figure 20. In acidic conditions NAAG decreases the activity of both GluN2A- and GluN2B-containing NMDARs in HEK293 cells. (A) GluN1/GluN2A-transfected HEK293 cells were recorded in different pH conditions in the presence of NAAG and average NMDAR current amplitudes were plotted (pH 6.8, n = 6 cells; pH 7.2, n = 7 cells; and pH 7.6, n = 6 cells). The average NMDAR amplitudes following NAAG treatment and washout were normalized to their corresponding controls of pH change alone before NAAG application (control represented by dotted lines). (B) Representative bar graph of (A) showing the normalized average of GluN2A-containing NMDAR current amplitudes in different pH conditions 5 min before NAAG application (Ctrl), the last 5 min of NAAG treatment (NAAG), and during washout (Wash). (C) GluN1/GluN2B-transfected HEK293 cells were recorded in different pH conditions in the presence of NAAG and the normalized average NMDAR current amplitudes were plotted (pH 6.8, n = 5 cells; pH 7.2, n = 9 cells; and pH 7.6, n = 3 cells). (D) Representative bar graph of (C) showing the normalized average of GluN2B-containing NMDAR current amplitudes in different pH conditions 5 min before NAAG application (Ctrl), the last 5 min of NAAG treatment (NAAG), and during washout (Wash). Data expressed as mean ± SEM. *, $p < 0.05$.

HEK293 cells at extracellular pH of 6.8 caused a further reduction in the NMDAR amplitude as compared to physiological pH levels ($p < 0.05$; **Fig. 20D**), and resulted in a 37 ± 2.3% decrease in the NMDAR current (n = 5 cells, $p < 0.05$) compared to baseline, while no change was observed at pH 7.6 (n = 3 cells, $p > 0.05$; **Fig. 20C,D**). Altogether, these results show that the effect of NAAG on NMDARs is pH-dependent on both synaptic and extrasynaptic NMDARs, and the data is further confirmed using our HEK293 cells recombinant system with GluN2A- and GluN2B-containing NMDARs. In acidic conditions, NAAG decreases the current amplitude of synaptic NMDARs (GluN2A-containing), and further inhibits the activity of extrasynaptic NMDARs (GluN2B-containing).

5.5. In acidic pH NAAG upregulates the surface expression of GluN2A- but not GluN2B-containing NMDARs in the hippocampus

The decrease in NMDAR EPSCs at low pH could potentially be attributed to a decrease in surface levels of the receptor. We therefore performed surface biotinylation experiments on mouse hippocampal slices to compare the levels of NMDAR subunits in different pH conditions in the presence or absence of NAAG. Analysis of surface expression of NMDAR subunits at pH 6.8, in the absence of NAAG, showed no significant alterations in the levels of GluN1, GluN2A, or GluN2B subunits (n = 4; $p > 0.05$), as well as no significant changes when the pH was increased to 7.6 (n = 4; $p > 0.05$; **Fig. 21A,B**). In addition, treatment with NAAG at physiological pH (7.2) did not cause a significant change in GluN1 (n = 4; $p > 0.05$), GluN2A (n = 4; $p > 0.05$), or GluN2B (n = 4; $p > 0.05$) surface expression compared to the untreated control (**Fig.**

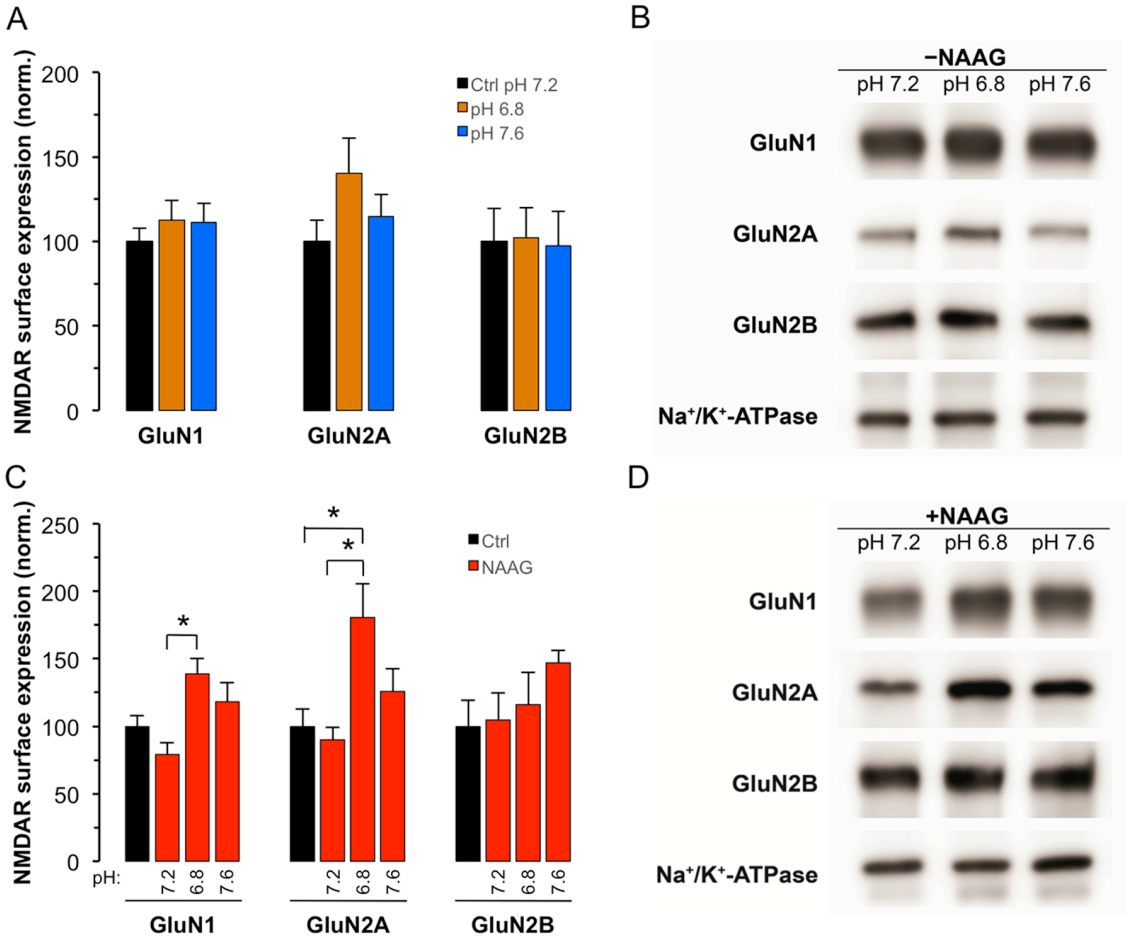

Figure 21. In low pH NAAG increases the surface expression of GluN2A-containing NMDARs in the hippocampus. Representative bar graph (A) and western blots (B) of biotinylated (surface) fractions from hippocampal tissue subjected to different pH conditions (6.8 and 7.6) and compared to control (pH 7.2). Representative bar graph (C) and western blots (D) of biotinylated (surface) fractions from hippocampal tissue subjected to different pH conditions (6.8 and 7.6) in the presence of NAAG and compared to control (pH 7.2 with and without NAAG). NMDAR subunits were visualized by GluN1, GluN2A, and GluN2B specific antibodies, and Na^+/K^+-ATPase was used as a loading control. Bar graphs are expressed as mean ± SEM of n = 4 animals. *, $p < 0.05$.

21C,D). Interestingly, when the pH was lowered to 6.8 in the presence of NAAG, there was a significant increase in the surface expression of GluN1 (60 ± 11.4%; n = 4; $p < 0.05$) and GluN2A (91 ± 24.6%; n = 4; $p < 0.05$) compared to physiological conditions with NAAG. These changes were unique to the GluN1 and GluN2A subunits since no significant differences in surface expression were detected for GluN2B (n = 4; $p > 0.05$; **Fig. 21C,D)**. Moreover, there were no significant differences in the expression of any of the subunits when the pH was increased to 7.6 in the presence of NAAG (n = 4, $p > 0.05$) compared to physiological conditions with NAAG (**Fig. 21C,D)**. These data serve to confirm that the inhibitory effect of NAAG on GluN2B-containing NMDARs does not result from changes in receptor levels, but is in fact due to actual alterations of the receptor activity. Furthermore, these results demonstrate that in conditions of low pH, NAAG increases the surface expression of GluN2A-containing NMDARs, and suggest a more complex role of NAAG in the regulation of NMDARs.

5.6. The activity of synaptic NMDARs is increased following low pH and NAAG application in acute hippocampal slices

To further validate our biotinylation results and to determine the functional significance of increased GluN2A surface expression, we performed electrophysiological experiments on mouse hippocampal slices using a similar sequence of events. Following isolation of the synaptic NMDAR EPSC, we acquired a 5 min baseline recording. We then lowered the pH to 6.8 in the presence of NAAG for 15 min. Subsequently, the pH was brought back to 7.2 without NAAG. The synaptic NMDAR EPSC was recorded and we measured a significant 210 ± 43.2% increase in the amplitude as compared to the 5 min baseline

recording (n = 5 cells, $p < 0.05$; **Fig. 22A,B**). Furthermore, we performed this protocol on extrasynaptic NMDARs and did not observe an increase in the EPSC following washout to pH 7.2 but rather a 74 ± 1.1% decrease (n = 3 cells, $p < 0.05$; **Fig. 22C,D**). To further analyze whether this increase in synaptic NMDAR EPSCs is truly an upregulation of the GluN2A subunit, we bath applied the GluN2B-selective inhibitor, ifenprodil, in place of NAAG, and detected no inhibitory effect but rather an 11 ± 3.1% increase in the synaptic NMDAR EPSC (n = 3 cells, $p < 0.05$; **Fig. 22E,F**). Altogether, these data suggest that NAAG causes an upregulation of GluN2A-containing NMDARs at low pH, and furthermore indicate that this upregulation is most likely occurring in the synaptic region. In addition, we provide evidence that the increased number of GluN2A-containing NMDARs are functional and contribute to an enhanced synaptic NMDAR activity following return to physiological pH conditions.

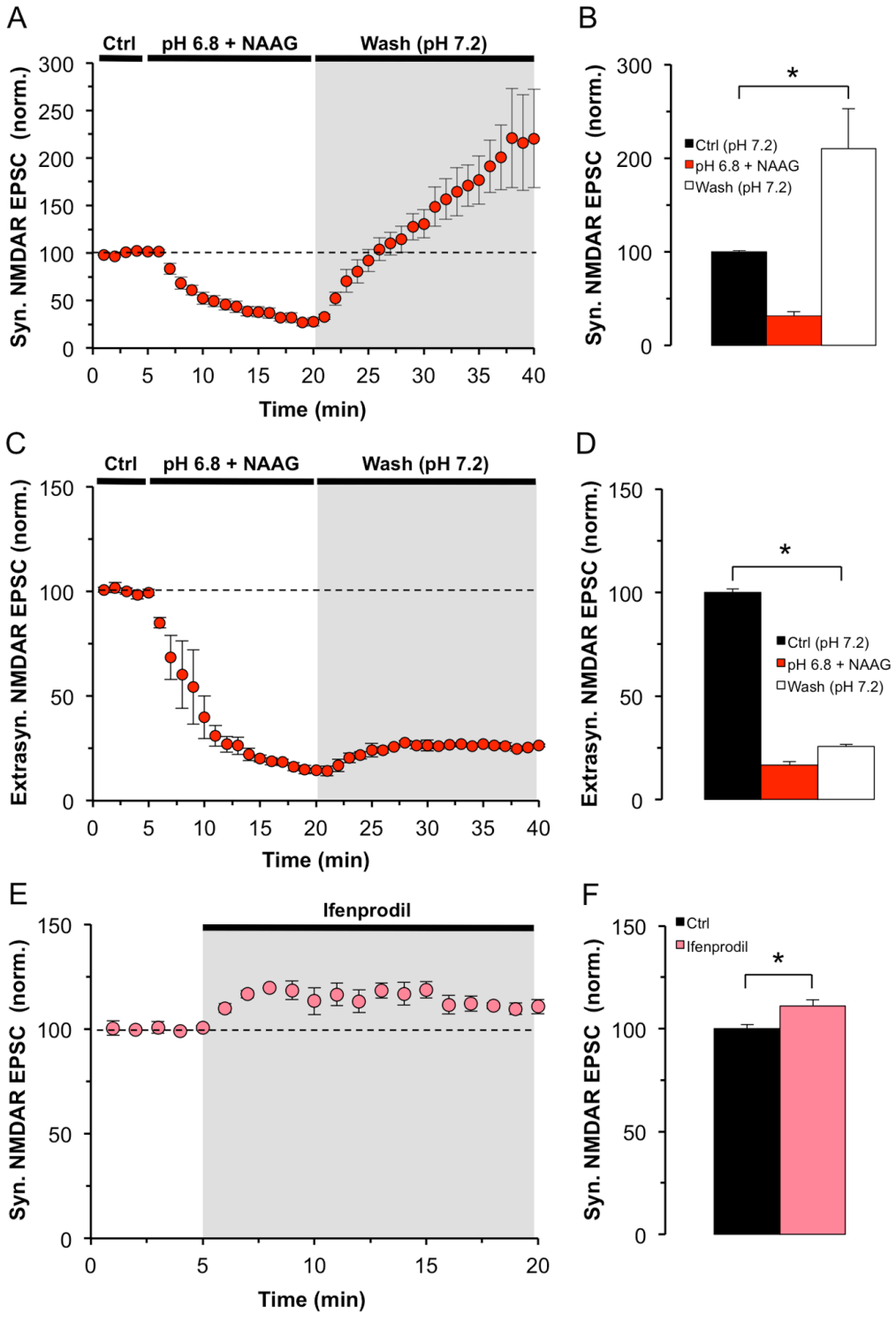
A
Ctrl
pH 6.8 + NAAG
Wash (pH 7.2)
Syn. NMDAR EPSC (norm.)
Time (min)
B
Ctrl (pH 7.2)
pH 6.8 + NAAG
Wash (pH 7.2)
C
Extrasyn. NMDAR EPSC (norm.)
D
E
Ifenprodil
F
Ctrl
Ifenprodil

Figure 22. The activity of synaptic NMDARs is increased following low pH and NAAG application in acute hippocampal slices. Average amplitudes of evoked synaptic (A) and extrasynaptic (C) NMDAR EPSCs were plotted following a 15 min treatment of low pH (6.8) in the presence of NAAG. The pH was subsequently brought back to 7.2 (without NAAG) and compared to the 5 min baseline recording (control at pH 7.2 represented by dotted line; n = 5 and 3 cells respectively). (B) Representative bar graph from data in (A) showing average synaptic NMDAR EPSC amplitudes 5 min before pH 6.8 and NAAG application (Ctrl (pH 7.2)), during the last 5 min of treatment (pH 6.8 + NAAG), and during washout back to pH 7.2 following pH 6.8 + NAAG (Wash (pH 7.2)). (D) Representative bar graph from data in (C) showing average extrasynaptic NMDAR EPSC amplitudes 5 min before pH 6.8 and NAAG application (Ctrl (pH 7.2)), during the last 5 min of treatment (pH 6.8 + NAAG), and during washout back to pH 7.2 following pH 6.8 + NAAG (Wash (pH 7.2)). (E) Average synaptic NMDAR EPSC amplitudes plotted during a 15 min application of ifenprodil and compared to the last 5 min of Wash (pH 7.2) depicted in (A) and (B) (control represented by dotted line; n = 3 cells). (F) Representative bar graph showing average synaptic NMDAR EPSC amplitudes 5 min before ifenprodil application (Ctrl), and during the last 5 min of ifenprodil treatment (Ifenprodil). The averages of the current amplitudes are normalized to the last 5 min of control in all cases. Data expressed as mean ± SEM. *, $p < 0.05$.

6. *DISCUSSION*

The data presented in this thesis (summarized in **Figure 23**) demonstrate that the endogenous neuropeptide NAAG differentially modulates NMDAR activity depending on its subunit composition. In addition, we provide evidence that this subunit selective function of NAAG is regulated by extracellular pH. Using whole-cell electrophysiological recordings from CA1 pyramidal neurons in acute brain slices, we show that in physiological pH, NAAG inhibits extrasynaptic GluN2B-containing NMDAR EPSCs, while potentiating synaptic GluN2A-containing NMDAR EPSCs. However, in low pH, NAAG inhibits both synaptic GluN2A- and extrasynaptic GluN2B-containing NMDAR EPSCs. We confirmed this subunit specificity and pH dependence of NAAG using the HEK293 cell recombinant system transfected with either GluN2A- or GluN2B-containing NMDARs. We also report, using cell surface biotinylation, that in acidic pH conditions NAAG increases the surface expression of GluN2A-containing NMDARs. Taken together, these results provide insight into the previously reported ambiguous effects of NAAG on NMDAR and its role in neuroprotection.

6.1. The differential effects of NAAG on NMDARs: An explanation to the controversy

The physiological role of NAAG in neurotransmission has been a topic of controversy for the last two decades. While it has been shown by several groups that NAAG is a potent agonist at $mGluR_3$ (Wroblewska et al., 1993; Wroblewska et al., 1997; Wroblewska et al., 1998; Sanabria et al., 2004; Neale, 2011), there has been controversy concerning the

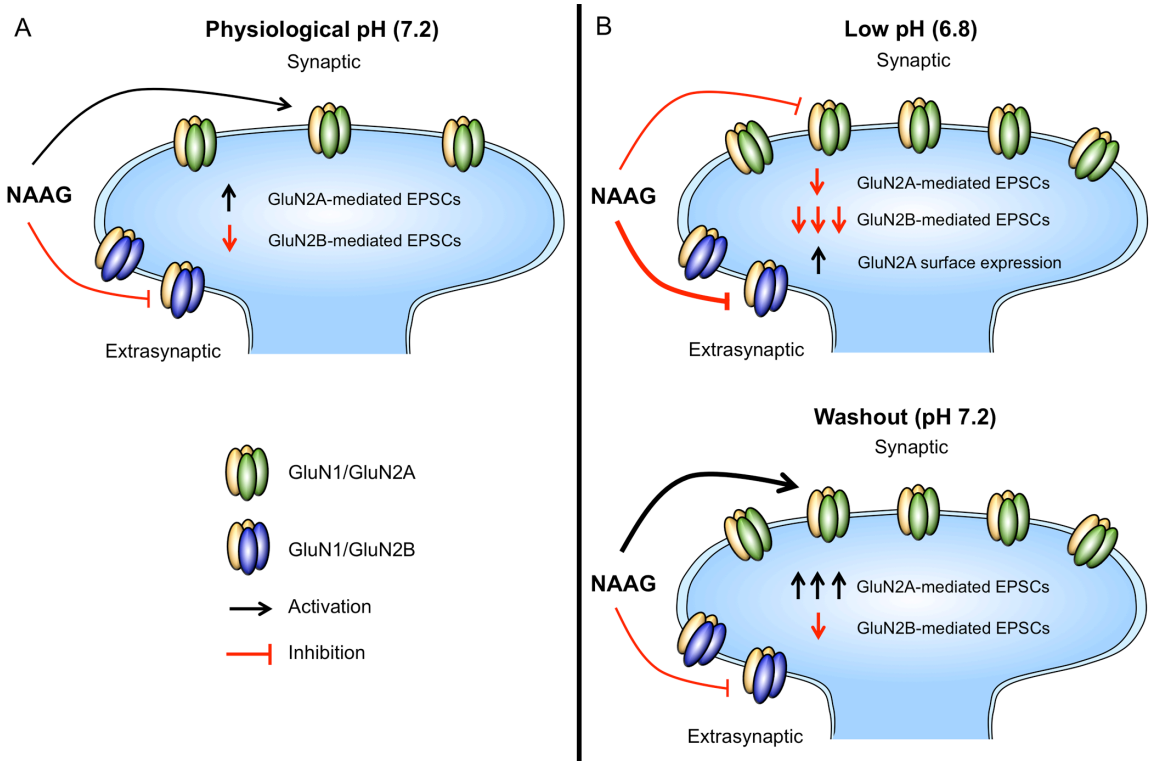

Figure 23. Schematic diagram summarizing the effect of NAAG on NMDARs in various conditions. (A) In physiological pH (7.2), NAAG increases the activity of synaptic GluN2A-containing NMDARs and inhibits extrasynaptic GluN2B-containing NMDARs. (B) In low pH (6.8), NAAG inhibits synaptic GluN2A-containing NMDARs, while further inhibiting extrasynaptic GluN2B-containing NMDARs. The presence of NAAG in low pH conditions also upregulates the surface expression of synaptic NMDARs. When the pH is brought back to 7.2 (washout) following a period of acidity, there is an increase in synaptic NMDAR EPSC as compared to control. In this setting, similar to a reperfusion scenario, NAAG would be capable of activating the upregulated synaptic GluN2A-containing NMDARs, while maintaining its inhibitory effect on extrasynaptic GluN2B-containing NMDARs.

role of NAAG on NMDARs. Some groups have reported that NAAG behaves as an antagonist (Sekiguchi et al., 1989; Puttfarcken et al., 1993; Grunze et al., 1996; Bergeron et al., 2005; Bergeron et al., 2007), while others have described an agonist-like effect on NMDARs (Westbrook et al., 1986; Sekiguchi et al., 1992; Valivullah et al., 1994; Kolodziejczyk et al., 2009). On the other hand, some have claimed no significant effect of NAAG on NMDARs (Lea et al., 2001; Losi et al., 2004; Fricker et al., 2009). The results of our investigation now provide insight and a possible explanation for these inconsistencies by demonstrating that NAAG can indeed have differential effects on NMDARs due to the intrinsic composition of the receptors, as well as the extracellular cues. We show that under physiological conditions, NAAG inhibits extrasynaptic GluN2B-containing NMDAR EPSCs, while potentiating synaptic GluN2A-containing NMDAR EPSCs. However, in low pH, NAAG inhibits both synaptic GluN2A- and extrasynaptic GluN2B-containing NMDAR EPSCs. Therefore, the previously described discrepancies related to the function of NAAG on NMDARs could be due to multiple factors, including NMDAR subunit composition, which changes depending on the developmental stage of the animal and subcellular localization of the receptor, as well as the cell type and brain region under investigation. The generation of conflicting results could also be attributed to the extracellular environment in which NAAG and NMDARs are studied, such as variations in extracellular pH.

By uncoupling the effect of NAAG on synaptic and extrasynaptic NMDARs in adult mice, and specifically studying its effect on GluN2A- and GluN2B-containing NMDARs, in various pH conditions, we reveal a better understanding of the function of NAAG on NMDARs, particularly as a neuroprotective agent. Several studies have shown

that increasing NAAG, through exogenous application (Lu et al., 2000; Cai et al., 2002) or by blocking its degradation (Slusher et al., 1999; Tortella et al., 2000), is neuroprotective during brain ischemia. Although it is well established that NAAG has neuroprotective properties during NMDAR-mediated neurotoxicity, its effect on NMDAR activity remains unclear (Slusher et al., 1999; Lu et al., 2000; Tortella et al., 2000; Cai et al., 2002). Our data showing the enhanced effect of NAAG inhibition on NMDARs under acidic conditions, such as that observed during stroke, may provide a mechanistic explanation for these convincing data. In addition, our results clarify why some studies have shown a specific neuroprotective effect of NAAG following ischemic (acidic) conditions, whereas others have shown no antagonistic effect of NAAG on NMDARs when studied under physiological pH conditions. Even though acidic pH conditions alone are not entirely representative of an ischemic event, we can nevertheless speculate on the possible mechanism underlying the neuroprotective qualities of NAAG based on its NMDAR subunit-selective and pH-dependent properties.

6.2. NAAG is a subunit-selective modulator of NMDAR activity

In order to gain a better understanding of the role of NAAG on NMDARs, we examined whether NAAG can differentially affect these receptors based on their localization and subunit composition. Using adult hippocampal slices, we uncovered that NAAG has differential modulatory functions on NMDARs depending on their synaptic versus extrasynaptic localization and consequently their subunit composition. Our data reveal that addition of exogenous NAAG or treatment with 2-PMPA, which increases

endogenous NAAG levels, results in a potentiation of synaptic NMDAR EPSCs, while inhibiting extrasynaptic NMDAR EPSCs (**Fig. 6 and Fig. 12**).

The ability to uncouple the effect of NAAG on synaptic and extrasynaptic NMDARs was based on an established pharmacological paradigm that allows for the isolation of extrasynaptic NMDARs (**Fig. 9**). Although these extrasynaptic NMDARs in the adult brain have been reported to be predominantly composed of GluN2B subunits, several approaches were used to confirm the prevalence of extrasynaptic GluN2B-containing NMDARs in our system. Analysis of extrasynaptic NMDAR EPSCs indicated that these receptors are primarily GluN2B-containing due to their characteristically slower decay kinetics, as compared to the faster GluN2A-containing NMDARs residing at the synapse (**Table 1**). However, although the decay times for synaptic and extrasynaptic recordings suggest different subunit populations, the conclusion that extrasynaptic NMDAR populations are largely GluN2B-containing cannot be drawn solely based on decay kinetics. The DL-TBOA-induced spillover of glutamate onto extrasynaptic NMDARs can also slow down decay kinetics due to their diffusion distance from the synapse regardless of the extrasynaptic NMDAR subunit composition (Arnth-Jensen et al., 2002; Diamond, 2002). For this reason, we utilized ifenprodil, a GluN2B-selective NMDAR inhibitor, to pharmacologically confirm the subunit composition of the isolated extrasynaptic NMDARs in our system (Tovar and Westbrook, 1999). We showed that extrasynaptic NMDAR EPSCs were highly sensitive to inhibition by ifenprodil, while this inhibition was undetectable in isolated synaptic NMDAR EPSCs (**Fig. 10**). Together, these results confirm that NMDAR subunit composition is indeed

different depending on the subcellular localization, with GluN2A- and GluN2B-containing receptors dominating synaptic and extrasynaptic sites, respectively.

The observed alteration in NMDAR activity as a specific effect of NAAG on NMDARs was also accounted for by controlling for several factors that may contribute to changes in EPSCs. The specificity of NAAG action on NMDARs in our experiments was taken into consideration by first confirming that the effect of NAAG or 2-PMPA on NMDARs was independent of the influence of $mGluR_3$, which has previously been shown to respond to the presence of NAAG. Using a potent and selective group II antagonist, LY341495, we show that NAAG maintains its effect on NMDARs despite the inhibition of $mGluR_3$ (**Fig. 8A,B**), confirming that in our conditions $mGluR_3$ are not contributing to the effect of NAAG on NMDARs. In addition, using a paired pulse paradigm, we show that the effects of NAAG and 2-PMPA on NMDARs are not mediated by presynaptic neurotransmitter release (**Fig. 8C**), which would indirectly alter the activity of NMDARs.

It was also taken into consideration that in native tissue, synaptic and extrasynaptic NMDAR populations are not homogenously GluN2A- or GluN2B-containing, but include both with one dominating (Suarez 2010; Tovar 2013). Additionally, triheteromeric NMDARs are present in adult hippocampal synapses (Gray et al., 2011; Rauner and Kohr, 2011; Tovar et al., 2013). Triheteromeric GluN1/GluN2A/GluN2B NMDARs have properties distinct from the GluN2A- and GluN2B-containing diheteromeric NMDARs, and differ in their pharmacological sensitivity to subunit-selective antagonists such as zinc and ifenprodil (the inhibitory effect is to a lesser extent) (Hatton and Paoletti, 2005; Neyton and Paoletti, 2006; Rauner

and Kohr, 2011). Triheteromeric NMDARs can also contain GluN3A subunits (Perez-Otano et al., 2001), which co-express with GluN1 and GluN2 and can exert inhibitory effects on NMDAR by reducing NMDAR-mediated Ca^{2+} influx and whole-cell currents (Sasaki et al., 2002; Tong et al., 2008; Kehoe et al., 2013). All these are potential factors that could influence or alter the effect of NAAG on NMDARs that is seen in our experiments. For this reason, we used an *in vitro* HEK293 recombinant system whereby a specified composition of NMDARs was established and the contribution of the other aforementioned factors can be negligible. Importantly, this *in vitro* recombinant system further validated our novel findings that NAAG does in fact regulate NMDAR activity and has distinctive effects on NMDARs depending on the subunit composition (**Fig. 13**). Thus our study has demonstrated, for the first time, that NAAG can simultaneously exhibit dual functions, and can evoke differential responses on NMDAR activity depending on its subunit composition.

6.3. The effect of NAAG on NMDARs is regulated in a pH-dependent manner

During ischemic conditions, pH in the extracellular space can drop by 0.2 to more than 1.0 pH units due to the accumulation of lactic acid (Doyle et al., 2008). It has been shown in numerous studies that protons modulate the activity of NMDAR (Tang et al., 1990; Traynelis and Cull-Candy, 1990; Vyklicky et al., 1990; Traynelis and Cull-Candy, 1991; Low et al., 2003; Dravid et al., 2007). Lower (acidic) pH induces an inhibitory effect on NMDARs, while more basic pH enhances NMDAR function, which we were able to reproduce in our study (**Fig. 14–16**). Moreover, some drugs have enhanced function in different pH conditions. For example, ifenprodil is neuroprotective in animal models of

stroke, not only by being selective for GluN2B-containing NMDARs, but also by increasing its sensitivity to inhibition by protons (Shalaby et al., 1992; Pahk and Williams, 1997; Whittemore et al., 1997; Mott et al., 1998). We have shown in our study that NAAG can exert a similar effect, in that it can also alter its function on GluN2A-containing synaptic and GluN2B-containing extrasynaptic NMDARs depending on the extracellular pH environment. At low pH conditions (6.5 and 6.8), in acute hippocampal slices, NAAG switches its function from being a differential regulator of NMDAR activity to a solely inhibitory role on both synaptic and extrasynaptic NMDARs (**Fig. 17 and Fig. 19**). Although NAAG already exhibited an inhibitory effect on extrasynaptic NMDARs at physiological pH, this effect was amplified in low pH conditions (**Fig. 19**). Additionally, in the HEK293 recombinant system we demonstrated that NAAG can alter the function of GluN2A- and GluN2B-containing NMDARs in parallel to the effect of NAAG on synaptic and extrasynaptic NMDARs in hippocampal slices, respectively (**Fig. 20**). These results indicate a novel pH-dependent interaction between NAAG and NMDARs. Furthermore, our data suggest that NAAG may regulate the NMDAR proton sensor, which is closely associated to the gating mechanism.

6.4. The rapid and long-lasting effect of NAAG on NMDARs

In our data, an effect on NMDAR EPSCs was induced after only 5 minutes following application of 2-PMPA. This rapid effect of 2-PMPA was confirmed to be due to an increase in endogenous NAAG, since addition of an inactive analogue of 2-PMPA, 2-PMSA, did not cause any detectable changes in NMDAR activity (**Fig. 7**). The ability of 2-PMPA to act rapidly in our experiments warrants some discussion particularly since

previous studies have shown that the increase in NAAG due to GCP-II inhibition is only observed hours following i.p. administration of 2-PMPA (Slusher et al., 1999; Nagel et al., 2006). 2-PMPA is highly hydrophilic, suggesting a potentially unfavourable blood-brain barrier penetration. Therefore, injection of 2-PMPA into the blood cavity would most likely take longer to reach the brain and inhibit GCP-II, as compared to acute application of 2-PMPA onto brain slices (as in our experimental conditions). Consistent with this idea, a recently published study (Rais et al., 2015) has reported a non-invasive route for delivery of GCP-II inhibitors to the brain via i.n. administration in rodents and non-human primates. Of the three structurally distinct GCP-II inhibitors that were evaluated, i.n. administration of 2-PMPA exhibited the highest level of brain penetration compared to i.p. administration (Rais et al., 2015). Therefore, the pharmacokinetic properties of 2-PMPA are likely affected by the method of administration, as well as the dose used. Therefore, the bioavailability of a one-time 2-PMPA injection *in vivo* would be significantly different compared to our *in vitro* model where we have a constant flow of 10 μM 2-PMPA perfusing onto the hippocampal slice.

In our experiments, the effect of NAAG on NMDARs also appears to be long-lasting. A sustained NAAG-dependent modulation of NMDAR activity persisted for as long as 40 minutes following washout. A number of studies have similarly demonstrated difficulty in washing out NAAG (Sanabria et al., 2004; Bergeron et al., 2007; Walder et al., 2013). For example, one study described that NAAG does not washout at neuromuscular junctions for at least 1 hour following its application. These results suggest that NAAG has a presynaptic effect, and decreases the quantal content of evoked acetylcholine release at the neuromuscular junction (Walder et al., 2013). However, in

our results, the lack of washout is likely not the result of altered presynaptic release, as there is no detectable change in paired pulse ratio following NAAG treatment, and no effect on $mGluR_3$ as shown in our results using LY341495 (**Fig. 8A,B**). Although the reason for the prolonged effect of NAAG in our study remains unclear, it is possible that NAAG binds directly to NMDARs and has a slow dissociation rate, or perhaps NAAG induces a long lasting conformational change in the receptor.

6.5. Possible mechanism of action of NAAG on NMDARs

NMDARs contain many sites capable of binding ligands, which act as agonists, co-agonists, competitive antagonists, channel blockers or allosteric modulators (Traynelis et al., 2010; Paoletti et al., 2013). The exact mechanism of action of NAAG on NMDARs remains unclear, however, given its subunit-specific modulation of NMDARs, as well as its pH-dependent effect, we speculate that NAAG may be an allosteric modulator (Mony et al., 2009a; Zhu and Paoletti, 2015). Allosteric modulators bind to a site distinct from that of the orthosteric agonist binding site, and indirectly influences NMDAR functions, usually by inducing a conformational change within the protein structure (Zhu and Paoletti, 2015). Recently, allosteric modulators have gained recognition as promising compounds for drug development and therapeutic interventions. This is mainly due to the several advantages that encompass the targeting of allosteric sites, as opposed to that of orthosteric or ion channel sites. One of these advantages is the subunit selectivity of allosteric modulators, which stems from their ability to interact with a target receptor at sites other than the agonist binding sites or channel pore (Kenakin, 2004). This subunit-selective nature of allosteric modulators likely contributes to the reduced side effects

observed with these compounds, and offers an important therapeutic advantage (Kalia et al., 2008; Mony et al., 2009a).

The NTDs of NMDARs, which play a key role in mediating functional diversity, are a major site for the allosteric modulation of NMDAR activity and can undergo large-scale conformational changes that impact downstream gating mechanisms. In addition, these regions play a key role in the pharmacological diversity of NMDARs and are a major locus for the binding of subunit-specific allosteric modulators (Gielen et al., 2009; Yuan et al., 2009). In particular, the NTD of the GluN2B subunit exhibits at least three distinct sites that confer interactions with negative and positive allosteric modulators (Mony et al., 2009a). In general, ligands that stabilize the NTDs in an open-cleft configuration act as positive allosteric modulators, while those that promote closure of the NTD cleft are considered allosteric inhibitors (Costa et al., 2010; Wyllie et al., 2013). Thus, through the NTDs, GluN2B-containing NMDARs have the ability to interact with a number of allosteric modulators such as ifenprodil (and related compounds), protons, zinc, and polyamines (Tang et al., 1990; Traynelis and Cull-Candy, 1990; Vyklicky et al., 1990; Williams, 1993; Paoletti et al., 1995; Traynelis et al., 1995; Gallagher et al., 1996; Kew et al., 1996; Perin-Dureau et al., 2002; Rachline et al., 2005; Karakas et al., 2009; Mony et al., 2009b; Karakas et al., 2011; Mony et al., 2011; Burger et al., 2012; Furukawa, 2012; Lee et al., 2014).

Interestingly, it has been shown that alterations in proton sensitivity is a common downstream mechanism of several NMDAR allosteric modulators (Traynelis et al., 1995; Mott et al., 1998; Choi and Lipton, 1999; Low et al., 2000). For example, ifenprodil and zinc, subunit-selective allosteric inhibitors of GluN2B- and GluN2A-containing

NMDARs respectively (Williams, 1993; Traynelis et al., 1995; Kew et al., 1996; Mott et al., 1998; Choi and Lipton, 1999; Yamakura and Shimoji, 1999; Low et al., 2000), modify proton sensitivity and alter NMDAR function by shifting the pKa of the proton sensor (Mott et al., 1998). Although several residues within the GluN1 and GluN2 subunits can regulate proton-dependent inhibition (Traynelis et al., 1998; Masuko et al., 1999; Low et al., 2000; Low et al., 2003), the precise location of the proton sensor remains unknown. Mutagenesis studies have demonstrated that residues which influence proton sensitivity most strongly cluster in two neighbouring regions (Low et al., 2003) closely associated with the activation gate of NMDARs (Chang and Kuo, 2008). This suggests that the proton sensor is likely tightly coupled to the gating mechanism of NMDARs (Tang et al., 1990; Low et al., 2003; Banke et al., 2005; Chang and Kuo, 2008). Furthermore, protons appear to prolong a shut-time component of GluN1/GluN2B receptors with little effect on channel open time (Banke et al., 2005), suggesting that protons mediate an inhibitory effect by stabilizing a closed state.

Our study indicates that the interaction between NAAG and NMDARs is subunit specific and likely linked to the proton sensor, therefore pointing to an allosteric mechanism. An allosteric mechanism would allow for subunit-specific modulation of NMDARs, as well as a pH-dependent effect on its function. There are a number of possible mechanisms by which NAAG can affect NMDARs in situations of altered pH. NAAG could potentially act by enhancing the NMDAR sensitivity to proton inhibition by inducing a conformational change within the receptor. However, we cannot exclude the possibility that protons may directly affect the binding site of NAAG on NMDARs, thereby modifying the coupling between binding of NAAG and inhibition of NMDAR

channel gating. These speculations of the possible interaction between NAAG and NMDARs are supported by our inability to washout the effect of NAAG in our experiments, possibly due to the long lasting effect of an NMDAR conformational change, or attributed to a slow dissociation rate. Identifying how pH and NMDAR subunit composition affects the regulation of NMDARs by NAAG is vital, not only from a physiological standpoint, but also from a pharmacological perspective.

6.6. Regulation of GluN2A surface expression by NAAG

The regulation of GluN2A- and GluN2B-containing NMDARs expression are regulated independently (Shipton and Paulsen, 2014). Interestingly, it has been shown that blocking NMDAR activity increases NMDAR levels on the cell surface, thereby altering the GluN2A/GluN2B ratio (Carmignoto and Vicini, 1992; Rao and Craig, 1997; Liao et al., 1999; Quinlan et al., 1999; Crump et al., 2001; Aoki et al., 2003; Fujisawa and Aoki, 2003; Chen and Bear, 2007). In one particular study, following NMDAR blockade, there was an upregulation of GluN2A-containing NMDARs, whereas GluN2B-containing NMDARs were not affected (von Engelhardt et al., 2009). This upregulation of GluN2A subunits is only seen when pan-NMDAR antagonists are used, such as APV, and is not observed when GluN2A- or GluN2B-containing receptors are blocked individually. Moreover, it was shown, using electrophysiological recordings of CA1 neurons in acute hippocampal slices, that these newly inserted GluN2A-containing NMDARs contribute to increased synaptic NMDAR EPSCs (von Engelhardt et al., 2009). Thus, NMDAR blockade results in the selective upregulation of synaptic GluN2A-containing NMDARs. In agreement with these studies, we show that the inhibitory effect of NAAG on

NMDARs in low pH (6.8) conditions results in an increase in surface expression of GluN2A- but not GluN2B-containing NMDARs (**Fig. 21**). Additionally, following upregulation of GluN2A and neutralization of the pH (7.2), we observe a significant increase in synaptic NMDAR EPSCs (**Fig. 22**), which is indicative of an increase in the number of synaptic receptors. Therefore, blocking NMDAR activity with NAAG in acidic conditions regulates the expression of GluN2A-containing NMDARs in the cell membrane. This represents an additional novel function of NAAG, whereby it not only modulates the activity of NMDARs, but can also influence receptor levels.

Different scenarios can account for the ability of NAAG to increase GluN2A-containing NMDAR surface expression, including, but not limited to, increased insertion, or decreased internalization of the receptors. It is possible that NAAG influences one of the different pathways involved with receptor insertion. The insertion of NMDARs at the cell surface is tightly regulated in response to synaptic activity. Regulation of NMDAR trafficking is mediated by activation of protein kinase A (PKA) and protein kinase C (PKC) downstream signaling (Scott et al., 2001; Scott et al., 2003). In addition, and relevant to our studies, it has been shown that activation of PKC results in rapid insertion of new receptors to the surface of hippocampal neurons (Lan et al., 2001b). This rapid channel insertion (within minutes) has been shown to occur through SNARE-dependent exocytosis (Lan et al., 2001b). This PKC-dependent insertion of NMDARs at the cell surface does not occur through direct subunit phosphorylation but involves a receptor anchoring and/or trafficking protein (Zheng et al., 1999). Also, the association of NMDARs with PSD-95 can enhance surface expression of these channels (Lin et al., 2006).

Internalization of NMDARs is also a process tightly regulated in a subunit-specific manner. The distal C-terminal region of GluN2A and GluN2B subunits contain distinct internalization motifs that regulate endocytosis at different rates (Lavezzari et al., 2004); for example, GluN2A receptor internalization appears to be quite slow (Lavezzari et al., 2004) when compared to GluN2B receptor internalization (Roche et al., 2001). Stabilization of GluN2A receptors at the cell surface is regulated by tyrosine phosphorylation (Vissel et al., 2001), whereby tyrosine dephosphorylation triggers NMDAR internalization. Receptor internalization is generally associated with an increase in activity of NMDARs. For example, repeated application of the NMDAR agonist glutamate promotes dephosphorylation of Tyr842 in the C-terminal tail of the GluN2A subunit and promotes receptor internalization (Vissel et al., 2001). Similarly, repetitive application of the co-agonist glycine primes NMDARs for internalization (Nong et al., 2003). Thus, overactivation of NMDARs by glutamate and glycine induces and primes the receptors for internalization, while blocking neuronal activity has been shown to upregulate synaptic NMDAR expression. Based on this information we can speculate that in our biotinylation experiments the increase in surface expression of GluN2A-containing NMDAR levels in the synapse is likely regulated by insertion of GluN2A-containing receptors into the membrane (Dunah and Standaert, 2001; Lan et al., 2001b; Lan et al., 2001a; Skeberdis et al., 2001), and not due to a decrease in the rate of internalization. Considering the short time frame that was set for our biotinylation and electrophysiological experimental conditions, it is not probable that the increased surface expression of NMDARs was a result of decreased internalization. The internalization rate for GluN2A-containing NMDARs is slow, while the insertion of NMDARs in the surface

seems to occur at a faster rate. The conditions we set to induce upregulation of GluN2A-containing NMDARs (exposure to low pH + NAAG) occurred over a period of 20 minutes. This is most likely not a sufficient amount of time for the detection of a change in receptor expression as a result of decreased internalization rate of GluN2A-containing NMDARs, given the slow rate of GluN2A internalization. However, with that being said, we cannot completely rule out the possibility of decreased receptor internalization (Vissel et al., 2001; Nong et al., 2003; Lau and Zukin, 2007).

Synaptic NMDAR levels are not only regulated by membrane insertion or internalization of NMDARs but also by lateral movement in the plasma membrane between synaptic and extrasynaptic sites in an activity- and phosphorylation-dependent manner (Tovar and Westbrook, 2002; Zhao et al., 2008). Lateral movement is very different for GluN2A and GluN2B subunits. Studies have shown that GluN2B-type receptors are highly mobile, whereas GluN2A-type receptors are fairly stable in the synapse (Wenthold et al., 2003; Groc et al., 2006). Furthermore, GluN2A-containing NMDARs diffuse laterally more slowly within the synapse than GluN2B-containing NMDARs (Groc et al., 2006). Our biotinylation experiments did not differentiate between extrasynaptic and synaptic NMDARs, but measured the total levels of NMDARs in the membrane. Therefore, lateral movement of NMDARs into the synapse, which would not change the total number of surface receptors, cannot account for the changes observed in these experiments. However, we cannot completely exclude that lateral diffusion contributed in some way to the observed electrophysiological changes.

In summary, our study showed, using surface biotinylation, an increase in GluN2A receptors in the cell membrane following NMDAR blockade in the presence of

NAAG in low pH conditions. The physiological relevance of these GluN2A-containing NMDARs and their integration into the synapse was addressed using electrophysiological measurements, which clearly showed a significant increase in the NMDAR EPSC amplitude. The increase in the expression of GluN2A subunits during NMDAR blockade indicates that the higher level of GluN2A-containing receptors in the membrane is likely due to increased insertion, with decreased internalization possibly contributing a minor role. This regulation of the synaptic levels and localization of NMDARs may define a novel mechanism by which NAAG can promote neuronal survival in certain conditions, such as an ischemic event.

6.7. Therapeutic advantages of the subunit-selectivity of NAAG and its ability to upregulate GluN2A-containing NMDARs in acidic conditions

During a brain ischemic episode, extracellular glutamate accumulates due to synaptic release and impairment or reversal of uptake mechanisms (Rossi et al., 2000; Camacho and Massieu, 2006). The consequent overactivation of NMDARs leads to neuronal damage and death (Choi, 1988). In the core region affected by stroke, cell death occurs rapidly via necrosis. Surrounding the lethally damaged ischemic core is the ischemic penumbral region, consisting of reversibly damaged tissue. Although it is believed that this tissue is salvageable, there is a limited time frame for positive outcomes. This is particularly due to the ongoing excitotoxicity following reperfusion, leading to post-ischemic inflammation and apoptosis. This window of opportunity to reverse the damage makes the penumbral area an important target for therapeutic interventions aiming to prevent further cell death and promote neuronal recovery following reperfusion (Dirnagl

et al., 1999; Doyle et al., 2008). NMDAR antagonists (competitive antagonists and channel blockers) have been shown to be very effective neuroprotective drugs that decrease damage in experimental animals (Lee et al., 1999). Although these agents proved to be therapeutically effective when tested both *in vitro* and in animal models of stroke, all clinical trials have failed when testing the same agents (Javitt and Zukin, 1991; ANS, 1992; RANTTAS, 1996; Albers et al., 2001; Sacco et al., 2001; Ikonomidou and Turski, 2002). There are a number of reasons why these drugs have failed, one of which includes the lack of NMDAR subunit selectivity, leading to high drug toxicity and intolerable side effects in human beings when given the same doses that were neuroprotective in rodents (Adams et al., 1995; Del Zoppo, 1995; Grotta, 1995; del Zoppo, 1998; Lee et al., 1999; Birmingham, 2002). The side effects such as psychotomimetic effects, memory impairment and neurotoxicity, which are usually exerted by NMDAR channel blockers and competitive antagonists, are not seen when drugs targeting specific subunits, such as ifenprodil, are used as neuroprotective agents. These reduced side effects may be ascribed to the GluN2B subunit specificity mediated by ifenprodil and related compounds (Gotti et al., 1988; McDonald and Johnston, 1990; Graham et al., 1992; Shalaby et al., 1992; Tamura et al., 1993; Baskaya et al., 1997; Geng et al., 1997; Yamakura and Shimoji, 1999; Picconi et al., 2006; Liu et al., 2007). Interestingly, both NAAG and 2-PMPA show robust neuroprotection without side effects when tested in stroke models, similar to other GluN2B-specific therapies (Slusher et al., 1999; Lu et al., 2000; Tortella et al., 2000; Cai et al., 2002). This is likely due to the subunit selectivity of NAAG that we have discovered in our study. Therefore, the reported differential effects of NAAG on GluN2A- and GluN2B-containing NMDARs

can be therapeutically advantageous, since NMDAR subunit composition and localization have been shown to have distinct downstream pathways.

6.8. A potential mechanism for NAAG-mediated neuroprotection

As previously mentioned, the NMDAR subunit composition has different effects on synaptic function depending on their regional and developmental expression, their subcellular location (synaptic or extrasynaptic) and their coupling to downstream signaling cascades. Specifically in the hippocampus, NMDAR subunit composition differs throughout development, from being predominantly GluN2B-containing to GluN2A-containing at maturation. In our experimental conditions we utilized acute hippocampal slices from adult mice. In this setting, it is generally recognized that, GluN2A-containing NMDARs are dominant at the synapse, while GluN2B-containing NMDARs are located extrasynaptically (Cull-Candy et al., 2001; van Zundert et al., 2004; Mony et al., 2009a; Sanz-Clemente et al., 2013). Indeed, this different localization of NMDARs was also observed in our experimental paradigms. The cytoplasmic CTDs of GluN2 subunits are involved in the targeting of these receptors to different locations and differentially associate with signaling molecules (Sprengel et al., 1998; Steigerwald et al., 2000; Ryan et al., 2008), thereby influencing the effect of Ca^{2+} influx through NMDARs (Martel et al., 2012). Thus, synaptic GluN2A-containing and extrasynaptic GluN2B-containing NMDARs mediate distinct physiological and pathological processes (Vanhoutte and Bading, 2003; Hardingham and Bading, 2010; Parsons and Raymond, 2014). Synaptic GluN2A-containing NMDARs are generally associated with neuronal survival, whereas activation of extrasynaptic GluN2B-containing NMDARs is coupled to

cell death pathways (Hardingham et al., 2002; Ivanov et al., 2006; Liu et al., 2007; Cross et al., 2010; Hardingham and Bading, 2010; Kaufman et al., 2012). Based on this premise, it can be hypothesized that the lack of efficacy of NMDAR channel blockers and competitive antagonists in clinical trials is likely attributed to the blockade of synaptic GluN2A-containing NMDARs, which has been shown to hinder neuronal survival by triggering apoptosis (Ikonomidou et al., 1999; Pohl et al., 1999). This concept is corroborated by findings that compounds which specifically block extrasynaptic GluN2B-containing NMDARs are found to be neuroprotective without debilitating side effects (Gotti et al., 1988; Shalaby et al., 1992).

Synaptic transmission mediated by NMDARs is essential for neuronal survival. Synaptic activation of NMDARs is neuroprotective and prevents spontaneous apoptosis in the hippocampus (Young et al., 1999). In contrast, therapeutic administration of NMDAR antagonists following traumatic brain injury or during neurodegenerative disorders worsens damage in the brain (Ikonomidou et al., 2000). This synaptic NMDAR-dependent neuroprotection is accompanied by activation of pro-survival transcription factors, such as CREB. It has been shown that Ca^{2+} influx through synaptic NMDARs activates ERK1/2, which prolongs CREB activation and enhances CREB-mediated induction of gene expression (Hardingham et al., 2002; Hardingham and Bading, 2010; Parsons and Raymond, 2014). CREB controls transcription of prosurvival genes such as BDNF and bcl-2 (Fink et al., 1991; Tao et al., 1998; Riccio et al., 1999; Wang et al., 1999). Thus, the survival-promoting properties of NMDAR-mediated synaptic activation could derive from the transcription of such pro-survival genes. Interestingly, it has been observed that surviving neurons within the ischemic penumbra

express high levels of BDNF, bcl-2 and activated CREB, suggesting maintained pro-survival signals (Chen et al., 1995; Tanaka et al., 1999; Tanaka et al., 2000; Walton and Dragunow, 2000). Synaptic NMDAR activation has also been implicated in the suppression of apoptosis (Lau and Bading, 2009; Leveille et al., 2010), decreased expression and/or activity of pro-death transcription factors (Papadia et al., 2008; Lau and Bading, 2009; Dick and Bading, 2010; Leveille et al., 2010), and enhanced antioxidant defence mechanisms (Papadia et al., 2008; Hardingham and Bading, 2010). Therefore, using non-selective NMDAR antagonists will block the pro-survival pathways induced by synaptic NMDARs and may facilitate neuronal death.

In contrast, extrasynaptic GluN2B-containing NMDARs are associated with the negative effects attributed to NMDAR overactivation. Ca^{2+} entry through extrasynaptic GluN2B-containing NMDARs inhibits the ERK1/2 pathway and shuts off CREB by rapid dephosphorylation (Sala et al., 2000; Hardingham et al., 2002). This in turn inhibits BDNF gene expression and initiates the cell death pathway (Hardingham et al., 2002; Kaufman et al., 2012). Extrasynaptic activation of NMDARs has been observed in several conditions that mimic aspects of an ischemic episode in cell culture, including oxygen-glucose deprivation (Hardingham et al., 2002) and increased glutamate levels by pharmacological reversal of glutamate transport (Gouix et al., 2009), resulting in decreased CREB phosphorylation and cell death. A recent study has demonstrated that extrasynaptic NMDAR activity, during ischemia, may be selectively enhanced by increased phosphorylation of GluN2B by the death-associated protein kinase 1 (DAPK1) (Tu et al., 2010). This effect is specific to GluN2B-containing NMDARs leading to selective enhancement of extrasynaptic currents. Moreover, preventing the interaction

between DAPK1 and NMDARs protected neurons against *in vitro* oxygen-glucose deprivation and *in vivo* ischemic injury (Tu et al., 2010). Generally, a significant reduction in infarct volume after ischemia is observed following specific blockade of GluN2B-containing NMDARs, deletion of DAPK1, or disruption of the DAPK1-GluN2B interaction (Gotti et al., 1988; Tu et al., 2010; Dong et al., 2013). More importantly, in another study, the peptide NR2B9c, which disrupts the interaction between GluN2B and PSD-95, was shown to reduce infarct volume when administered after an ischemic event in humans (Hill et al., 2012), as well as in rodents and nonhuman primates subjected to MCAO (Aarts et al., 2002; Sun et al., 2008; Bratane et al., 2011; Cook et al., 2012). Additionally, many intracellular signaling mechanisms implicated in ischemic cell death can be triggered by GluN2B and/or extrasynaptic NMDAR activation (Ning et al., 2004; Koumura et al., 2008; Taghibiglou et al., 2009; Dick and Bading, 2010; Hardingham and Bading, 2010; Lai et al., 2011; Zhang et al., 2013). Furthermore, not only do extrasynaptic NMDARs promote pro-death pathways, they also inhibit the pro-survival signaling of synaptic NMDARs (Hardingham and Bading, 2010). Taken together, these studies indicate that extrasynaptic NMDAR activity contributes to ischemic neuronal loss.

Based on this evidence, it can be concluded that a shift in balance resulting from a reduction of synaptic or enhancement of extrasynaptic NMDAR activity and signaling can be harmful to neurons. Evidence that synaptic NMDAR activity can exert a neuroprotective effect has led to suggestions that it may in fact promote recovery in the post-reperfusion phase, and prevent delayed neuronal loss in the penumbra (Albers et al., 2001; Ikonomidou and Turski, 2002). With that in mind, one can appreciate that although

treatment with NMDAR antagonists and channel blockers may reduce excitotoxic neuronal death following the initial insult, the continued block of synaptic NMDARs would in fact exacerbate secondary apoptosis which occurs following reperfusion, resulting in increased overall death (Pohl et al., 1999). Therefore, NMDAR antagonists may be protective in early stages of the insult progression, however, may contribute to neuronal injury in the long-term. For this reason, an ideal neuroprotective strategy should aim to disrupt extrasynaptic NMDAR-dependent death signaling, while simultaneously enhancing the activity or number of synaptic NMDARs in order to promote protection during the ischemic event and the reperfusion phase (Lipton, 2007). According to our data, NAAG appears to have the pharmacological properties suited for such an effective pathological therapy. The ability of NAAG to change its function depending on the extracellular environment may promote neuroprotection on multiple levels; 1) decreasing extrasynaptic GluN2B-containing NMDAR activity, 2) increasing synaptic GluN2A-containing NMDAR activity, and 3) upregulating synaptic GluN2A surface expression in acidic conditions, which would be most clinically relevant during the reperfusion and recovery phase following an ischemic event. These newly discovered properties of NAAG, identified in our studies, provide a novel approach in mediating neuroprotection.

Our overall findings provide insight into the dual role of NAAG on NMDARs following an ischemic event, in which it can inhibit extrasynaptic GluN2B-containing NMDAR-dependent death signaling, while up-regulating GluN2A receptors and enhancing their activity. Our results show that in physiological conditions (pH 7.2), NAAG only blocks GluN2B-containing NMDARs and activate GluN2A-containing NMDARs. However, in acidic conditions (pH 6.5 and 6.8) NAAG blocks both GluN2A-

and GluN2B-containing NMDARs. Consequently, this blockade by NAAG in low pH conditions allows for the upregulation of GluN2A-containing NMDARs. Although this population of increased GluN2A-containing NMDARs remains inactive at low pH, as shown in our results, we propose that they may contribute, at least in part, to the neuroprotective effect of NAAG following reperfusion. During a brain ischemic event, ATP levels and intracellular pH decrease as a result of anaerobic metabolism and lactate accumulation. Reperfusion restores the delivery of oxygen and substrates required for aerobic ATP generation and normalize extracellular pH by washing out accumulated H^+ (Fellman and Raivio, 1997; White et al., 2000; Kalogeris et al., 2012). In a scenario involving NAAG, reperfusion of the ischemic region and return to a physiological extracellular environment (pH 7.2) would allow NAAG to release its inhibitory effect on the now upregulated synaptic GluN2A-containing NMDARs, while continuing to inhibit the extrasynaptic GluN2B-containing NMDARs. As previously discussed, synaptic GluN2A-containing NMDARs mediate pro-survival signaling (Hardingham et al., 2002; Parsons and Raymond, 2014), and may therefore promote neuronal recovery in the post-reperfusion phase and prevent neuronal loss in the penumbra. Thus, the increased numbers of NMDARs at the synapse, along with the ability of NAAG to activate GluN2A-containing NMDARs in physiological conditions, are both ways by which pro-survival synaptic signaling could be enhanced in order to promote recovery following excitotoxic conditions. Simultaneously, NAAG would be preferentially blocking the extrasynaptic pro-death GluN2B-containing NMDARs following reperfusion. Normally, the activation of this pathway inhibits the pro-survival signaling of synaptic NMDARs; therefore, this is another possible mechanism by which NAAG is neuroprotective. The

ability of NAAG to upregulate and activate synaptic GluN2A-containing NMDARs to mediate pro-survival signals, while maintaining its inhibitory effect on the extrasynaptic pro-death GluN2B-containing NMDARs, suggests a clinically relevant therapeutic advantage of NAAG in the treatment of ischemic events.

7. *CONCLUDING REMARKS AND SIGNIFICANCE*

To address the challenges of stroke prevention or treatment, it would be beneficial to identify a prophylactic drug for those at risk, since early drug administration has been shown to be neuroprotective in animal models of ischemia. Demonstrating that the potency of some compounds, such as NAAG, is increased at lower pH provides an interesting pharmacological avenue. The new information provided here can be used for future studies aimed at the synthesis of GCP-II inhibitors that are inactive at physiological pH but become therapeutically effective in the acidic environment that arises in pathological conditions. The results of this study reveal a modulatory effect of NAAG on NMDARs depending on protons as well as NMDAR subunit composition and localization, and highlight a novel aspect of the function of NAAG. Given that rodents and humans share similar NMDAR expression patterns, as well as pH regulation (Law et al., 2003; Casey et al., 2010; Orlowski et al., 2011), it is plausible that NAAG can induce comparable effects in both. Altogether, these findings suggest NAAG as a valuable therapeutic agent in the treatment of ischemic events.

8. *REFERENCES*

Aarts M, Liu Y, Liu L, Besshoh S, Arundine M, Gurd JW, Wang YT, Salter MW, Tymianski M (2002) Treatment of ischemic brain damage by perturbing NMDA receptor- PSD-95 protein interactions. Science 298:846-850.

Abramov AY, Scorziello A, Duchen MR (2007) Three distinct mechanisms generate oxygen free radicals in neurons and contribute to cell death during anoxia and reoxygenation. J Neurosci 27:1129-1138.

Adams RJ, Fisher M, Furlan AJ, del Zoppo G (1995) Acute stroke treatment trials in the United States. Rethinking strategies for success. Stroke 26:2216-2218.

Adedoyin MO, Vicini S, Neale JH (2010) Endogenous N-acetylaspartylglutamate (NAAG) inhibits synaptic plasticity/transmission in the amygdala in a mouse inflammatory pain model. Mol Pain 6:60.

Aggarwal A, Aggarwal P, Khatak M, Khatak S (2010) Cerebral ischemic stroke: Sequels of cascade. International Journal of Pharma and Bio Sciences 1:1-24.

Akazawa C, Shigemoto R, Bessho Y, Nakanishi S, Mizuno N (1994) Differential expression of five N-methyl-D-aspartate receptor subunit mRNAs in the cerebellum of developing and adult rats. J Comp Neurol 347:150-160.

Albers GW, Goldstein LB, Hall D, Lesko LM, Aptiganel Acute Stroke I (2001) Aptiganel hydrochloride in acute ischemic stroke: a randomized controlled trial. JAMA 286:2673-2682.

Anderson KJ, Monaghan DT, Cangro CB, Namboodiri MA, Neale JH, Cotman CW (1986) Localization of N-acetylaspartylglutamate-like immunoreactivity in selected areas of the rat brain. Neurosci Lett 72:14-20.

ANS (1992) Clinical trial of nimodipine in acute ischemic stroke. The American Nimodipine Study Group. Stroke 23:3-8.

Aoki C, Fujisawa S, Mahadomrongkul V, Shah PJ, Nader K, Erisir A (2003) NMDA receptor blockade in intact adult cortex increases trafficking of NR2A subunits into spines, postsynaptic densities, and axon terminals. Brain Res 963:139-149.

Arnth-Jensen N, Jabaudon D, Scanziani M (2002) Cooperation between independent hippocampal synapses is controlled by glutamate uptake. Nat Neurosci 5:325-331.

Arundine M, Tymianski M (2003) Molecular mechanisms of calcium-dependent neurodegeneration in excitotoxicity. Cell Calcium 34:325-337.

Arundine M, Tymianski M (2004) Molecular mechanisms of glutamate-dependent neurodegeneration in ischemia and traumatic brain injury. Cell Mol Life Sci 61:657-668.

Bacich DJ, Wozniak KM, Lu XC, O'Keefe DS, Callizot N, Heston WD, Slusher BS (2005) Mice lacking glutamate carboxypeptidase II are protected from peripheral neuropathy and ischemic brain injury. J Neurochem 95:314-323.

Bacich DJ, Ramadan E, O'Keefe DS, Bukhari N, Wegorzewska I, Ojeifo O, Olszewski R, Wrenn CC, Bzdega T, Wroblewska B, Heston WD, Neale JH (2002) Deletion of the glutamate carboxypeptidase II gene in mice reveals a second enzyme activity that hydrolyzes N-acetylaspartylglutamate. J Neurochem 83:20-29.

Banke TG, Dravid SM, Traynelis SF (2005) Protons trap NR1/NR2B NMDA receptors in a nonconducting state. J Neurosci 25:42-51.

Barinka C, Rojas C, Slusher B, Pomper M (2012) Glutamate carboxypeptidase II in diagnosis and treatment of neurologic disorders and prostate cancer. Curr Med Chem 19:856-870.

Barinka C, Byun Y, Dusich CL, Banerjee SR, Chen Y, Castanares M, Kozikowski AP, Mease RC, Pomper MG, Lubkowski J (2008) Interactions between human glutamate carboxypeptidase II and urea-based inhibitors: structural characterization. J Med Chem 51:7737-7743.

Baskaya MK, Rao AM, Donaldson D, Prasad MR, Dempsey RJ (1997) Protective effects of ifenprodil on ischemic injury size, blood-brain barrier breakdown, and edema formation in focal cerebral ischemia. Neurosurgery 40:364-370; discussion 370-361.

Baslow MH (2010) Evidence that the tri-cellular metabolism of N-acetylaspartate functions as the brain's "operating system": how NAA metabolism supports meaningful intercellular frequency-encoded communications. Amino Acids 39:1139-1145.

Becker I, Lodder J, Gieselmann V, Eckhardt M (2010) Molecular characterization of N-acetylaspartylglutamate synthetase. J Biol Chem 285:29156-29164.

Beckman JS, Crow JP (1993) Pathological implications of nitric oxide, superoxide and peroxynitrite formation. Biochem Soc Trans 21:330-334.

Beckman JS, Koppenol WH (1996) Nitric oxide, superoxide, and peroxynitrite: the good, the bad, and ugly. Am J Physiol 271:C1424-1437.

Bellone C, Nicoll RA (2007) Rapid bidirectional switching of synaptic NMDA receptors. Neuron 55:779-785.

Berger UV, Carter RE, McKee M, Coyle JT (1995) N-acetylated alpha-linked acidic dipeptidase is expressed by non-myelinating Schwann cells in the peripheral nervous system. J Neurocytol 24:99-109.

Bergeron R, Coyle JT (2012) NAAG, NMDA receptor and psychosis. Curr Med Chem 19:1360-1364.

Bergeron R, Coyle JT, Tsai G, Greene RW (2005) NAAG reduces NMDA receptor current in CA1 hippocampal pyramidal neurons of acute slices and dissociated neurons. Neuropsychopharmacology 30:7-16.

Bergeron R, Imamura Y, Frangioni JV, Greene RW, Coyle JT (2007) Endogenous N-acetylaspartylglutamate reduced NMDA receptor-dependent current neurotransmission in the CA1 area of the hippocampus. J Neurochem 100:346-357.

Bernstein J, Fisher RS, Zaczek R, Coyle J (1985) Dipeptides of glutamate and aspartate may be endogenous neuroexcitants in the rat hippocampal slice. J Neurosci 5:1429-1433.

Birmingham K (2002) Future of neuroprotective drugs in doubt. Nat Med 8:5.

Bischofberger J, Schild D (1996) Glutamate and N-acetylaspartylglutamate block HVA calcium currents in frog olfactory bulb interneurons via an mGluR2/3-like receptor. J Neurophysiol 76:2089-2092.

Blakely RD, Robinson MB, Thompson RC, Coyle JT (1988a) Hydrolysis of the brain dipeptide N-acetyl-L-aspartyl-L-glutamate: subcellular and regional distribution, ontogeny, and the effect of lesions on N-acetylated-alpha-linked acidic dipeptidase activity. J Neurochem 50:1200-1209.

Blakely RD, Robinson MB, Guarda AS, Coyle JT (1988b) A re-examination of the interaction of N-acetyl-L-aspartyl-L-glutamate with a subpopulation of rat brain membrane L-[3H]glutamate binding sites. Eur J Pharmacol 151:419-426.

Bonita R, Beaglehole R (1988) Recovery of motor function after stroke. Stroke 19:1497-1500.

Bratane BT, Cui H, Cook DJ, Bouley J, Tymianski M, Fisher M (2011) Neuroprotection by freezing ischemic penumbra evolution without cerebral blood flow augmentation with a postsynaptic density-95 protein inhibitor. Stroke 42:3265-3270.

Bruno V, Battaglia G, Casabona G, Copani A, Caciagli F, Nicoletti F (1998) Neuroprotection by glial metabotropic glutamate receptors is mediated by transforming growth factor-beta. J Neurosci 18:9594-9600.

Burger PB, Yuan H, Karakas E, Geballe M, Furukawa H, Liotta DC, Snyder JP, Traynelis SF (2012) Mapping the binding of GluN2B-selective N-methyl-D-aspartate receptor negative allosteric modulators. Mol Pharmacol 82:344-359.

Bzdega T, Crowe SL, Ramadan ER, Sciarretta KH, Olszewski RT, Ojeifo OA, Rafalski VA, Wroblewska B, Neale JH (2004) The cloning and characterization of a second brain enzyme with NAAG peptidase activity. J Neurochem 89:627-635.

Cai Z, Lin S, Rhodes PG (2002) Neuroprotective effects of N-acetylaspartylglutamate in a neonatal rat model of hypoxia-ischemia. Eur J Pharmacol 437:139-145.

Camacho A, Massieu L (2006) Role of glutamate transporters in the clearance and release of glutamate during ischemia and its relation to neuronal death. Arch Med Res 37:11-18.

Cangro CB, Namboodiri MA, Sklar LA, Corigliano-Murphy A, Neale JH (1987) Immunohistochemistry and biosynthesis of N-acetylaspartylglutamate in spinal sensory ganglia. J Neurochem 49:1579-1588.

Carmignoto G, Vicini S (1992) Activity-dependent decrease in NMDA receptor responses during development of the visual cortex. Science 258:1007-1011.

Carpenter-Hyland EP, Woodward JJ, Chandler LJ (2004) Chronic ethanol induces synaptic but not extrasynaptic targeting of NMDA receptors. J Neurosci 24:7859-7868.

Cartmell J, Schoepp DD (2000) Regulation of neurotransmitter release by metabotropic glutamate receptors. J Neurochem 75:889-907.

Casey JR, Grinstein S, Orlowski J (2010) Sensors and regulators of intracellular pH. Nat Rev Mol Cell Biol 11:50-61.

Cassidy M, Neale JH (1993) N-acetylaspartylglutamate catabolism is achieved by an enzyme on the cell surface of neurons and glia. Neuropeptides 24:271-278.

Celsi F, Pizzo P, Brini M, Leo S, Fotino C, Pinton P, Rizzuto R (2009) Mitochondria, calcium and cell death: a deadly triad in neurodegeneration. Biochim Biophys Acta 1787:335-344.

Chang HR, Kuo CC (2008) The activation gate and gating mechanism of the NMDA receptor. J Neurosci 28:1546-1556.

Chen J, Graham SH, Chan PH, Lan J, Zhou RL, Simon RP (1995) bcl-2 is expressed in neurons that survive focal ischemia in the rat. Neuroreport 6:394-398.

Chen N, Luo T, Raymond LA (1999) Subtype-dependence of NMDA receptor channel open probability. J Neurosci 19:6844-6854.

Chen WS, Bear MF (2007) Activity-dependent regulation of NR2B translation contributes to metaplasticity in mouse visual cortex. Neuropharmacology 52:200-214.

Choi DW (1987) Ionic dependence of glutamate neurotoxicity. J Neurosci 7:369-379.

Choi DW (1988) Calcium-mediated neurotoxicity: relationship to specific channel types and role in ischemic damage. Trends Neurosci 11:465-469.

Choi DW, Rothman SM (1990) The role of glutamate neurotoxicity in hypoxic-ischemic neuronal death. Annu Rev Neurosci 13:171-182.

Choi DW, Koh JY, Peters S (1988) Pharmacology of glutamate neurotoxicity in cortical cell culture: attenuation by NMDA antagonists. J Neurosci 8:185-196.

Choi YB, Lipton SA (1999) Identification and mechanism of action of two histidine residues underlying high-affinity Zn2+ inhibition of the NMDA receptor. Neuron 23:171-180.

Chopra M, Yao Y, Blake TJ, Hampson DR, Johnson EC (2009) The neuroactive peptide N-acetylaspartylglutamate is not an agonist at the metabotropic glutamate receptor subtype 3 of metabotropic glutamate receptor. J Pharmacol Exp Ther 330:212-219.

Choy CJ, Fulton MD, Davis AL, Hopkins M, Choi JK, Anderson MO, Berkman CE (2013) Rationally designed sulfamides as glutamate carboxypeptidase II inhibitors. Chem Biol Drug Des 82:612-619.

Ciccarelli R, Di Iorio P, Bruno V, Battaglia G, D'Alimonte I, D'Onofrio M, Nicoletti F, Caciagli F (1999) Activation of A(1) adenosine or mGlu3 metabotropic glutamate

receptors enhances the release of nerve growth factor and S-100beta protein from cultured astrocytes. Glia 27:275-281.

Clements JD, Lester RA, Tong G, Jahr CE, Westbrook GL (1992) The time course of glutamate in the synaptic cleft. Science 258:1498-1501.

Collard F, Stroobant V, Lamosa P, Kapanda CN, Lambert DM, Muccioli GG, Poupaert JH, Opperdoes F, Van Schaftingen E (2010) Molecular identification of N-acetylaspartylglutamate synthase and beta-citrylglutamate synthase. J Biol Chem 285:29826-29833.

Collingridge GL, Isaac JT, Wang YT (2004) Receptor trafficking and synaptic plasticity. Nat Rev Neurosci 5:952-962.

Conti F, Weinberg RJ (1999) Shaping excitation at glutamatergic synapses. Trends Neurosci 22:451-458.

Cook DJ, Teves L, Tymianski M (2012) Treatment of stroke with a PSD-95 inhibitor in the gyrencephalic primate brain. Nature 483:213-217.

Costa BM, Irvine MW, Fang G, Eaves RJ, Mayo-Martin MB, Skifter DA, Jane DE, Monaghan DT (2010) A novel family of negative and positive allosteric modulators of NMDA receptors. J Pharmacol Exp Ther 335:614-621.

Cross JL, Meloni BP, Bakker AJ, Lee S, Knuckey NW (2010) Modes of Neuronal Calcium Entry and Homeostasis following Cerebral Ischemia. Stroke Res Treat 2010:316862.

Crump FT, Dillman KS, Craig AM (2001) cAMP-dependent protein kinase mediates activity-regulated synaptic targeting of NMDA receptors. J Neurosci 21:5079-5088.

Cui H, Hayashi A, Sun HS, Belmares MP, Cobey C, Phan T, Schweizer J, Salter MW, Wang YT, Tasker RA, Garman D, Rabinowitz J, Lu PS, Tymianski M (2007) PDZ protein interactions underlying NMDA receptor-mediated excitotoxicity and neuroprotection by PSD-95 inhibitors. J Neurosci 27:9901-9915.

Cull-Candy S, Brickley S, Farrant M (2001) NMDA receptor subunits: diversity, development and disease. Curr Opin Neurobiol 11:327-335.

Cull-Candy SG, Leszkiewicz DN (2004) Role of distinct NMDA receptor subtypes at central synapses. Sci STKE 2004:re16.

Curatolo A, D AP, Lino A, Brancati A (1965) Distribution of N-Acetyl-Aspartic and N-Acetyl-Aspartyl-Glutamic Acids in Nervous Tissue. J Neurochem 12:339-342.

Del Zoppo GJ (1995) Why do all drugs work in animals but none in stroke patients? 1. Drugs promoting cerebral blood flow. J Intern Med 237:79-88.

del Zoppo GJ (1998) Clinical trials in acute stroke: why have they not been successful? Neurology 51:S59-61.

Diamond JS (2002) A broad view of glutamate spillover. Nat Neurosci 5:291-292.

Dick O, Bading H (2010) Synaptic activity and nuclear calcium signaling protect hippocampal neurons from death signal-associated nuclear translocation of FoxO3a induced by extrasynaptic N-methyl-D-aspartate receptors. J Biol Chem 285:19354-19361.

Dingledine R, Borges K, Bowie D, Traynelis SF (1999) The glutamate receptor ion channels. Pharmacol Rev 51:7-61.

Dirnagl U, Iadecola C, Moskowitz MA (1999) Pathobiology of ischaemic stroke: an integrated view. Trends Neurosci 22:391-397.

Dong QP, He JQ, Chai Z (2013) Astrocytic Ca(2+) waves mediate activation of extrasynaptic NMDA receptors in hippocampal neurons to aggravate brain damage during ischemia. Neurobiol Dis 58:68-75.

Doroshenko P, Renaud LP (2009) Acid-sensitive TASK-like K+ conductances contribute to resting membrane potential and to orexin-induced membrane depolarization in rat thalamic paraventricular nucleus neurons. Neuroscience 158:1560-1570.

Doyle KP, Simon RP, Stenzel-Poore MP (2008) Mechanisms of ischemic brain damage. Neuropharmacology 55:310-318.

Dravid SM, Erreger K, Yuan H, Nicholson K, Le P, Lyuboslavsky P, Almonte A, Murray E, Mosely C, Barber J, French A, Balster R, Murray TF, Traynelis SF (2007) Subunit-specific mechanisms and proton sensitivity of NMDA receptor channel block. J Physiol 581:107-128.

Dudek SM, Bear MF (1992) Homosynaptic long-term depression in area CA1 of hippocampus and effects of N-methyl-D-aspartate receptor blockade. Proc Natl Acad Sci U S A 89:4363-4367.

Dunah AW, Standaert DG (2001) Dopamine D1 receptor-dependent trafficking of striatal NMDA glutamate receptors to the postsynaptic membrane. J Neurosci 21:5546-5558.

Durand D, Carniglia L, Caruso C, Lasaga M (2013) mGlu3 receptor and astrocytes: partners in neuroprotection. Neuropharmacology 66:1-11.

Erreger K, Dravid SM, Banke TG, Wyllie DJ, Traynelis SF (2005) Subunit-specific gating controls rat NR1/NR2A and NR1/NR2B NMDA channel kinetics and synaptic signalling profiles. J Physiol 563:345-358.

Fagg G, Foster A, Ganong A (1986) Excitatory amino acid synaptic mechanisms and neurological function. Trends Pharmacol Sci 7:357-363.

Fellin T, Pascual O, Gobbo S, Pozzan T, Haydon PG, Carmignoto G (2004) Neuronal synchrony mediated by astrocytic glutamate through activation of extrasynaptic NMDA receptors. Neuron 43:729-743.

Fellman V, Raivio KO (1997) Reperfusion injury as the mechanism of brain damage after perinatal asphyxia. Pediatr Res 41:599-606.

Ffrench-Mullen JM, Koller K, Zaczek R, Coyle JT, Hori N, Carpenter DO (1985) N-Acetylaspartylglutamate: possible role as the neurotransmitter of the lateral olfactory tract. Proc Natl Acad Sci U S A 82:3897-3900.

Fink JS, Verhave M, Walton K, Mandel G, Goodman RH (1991) Cyclic AMP- and phorbol ester-induced transcriptional activation are mediated by the same enhancer element in the human vasoactive intestinal peptide gene. J Biol Chem 266:3882-3887.

Finkbeiner S, Stevens CF (1988) Applications of quantitative measurements for assessing glutamate neurotoxicity. Proc Natl Acad Sci U S A 85:4071-4074.

Fisher M, Feuerstein G, Howells DW, Hurn PD, Kent TA, Savitz SI, Lo EH, Group S (2009) Update of the stroke therapy academic industry roundtable preclinical recommendations. Stroke 40:2244-2250.

Flint AC, Maisch US, Weishaupt JH, Kriegstein AR, Monyer H (1997) NR2A subunit expression shortens NMDA receptor synaptic currents in developing neocortex. J Neurosci 17:2469-2476.

Forloni G, Grzanna R, Blakely RD, Coyle JT (1987) Co-localization of N-acetyl-aspartyl-glutamate in central cholinergic, noradrenergic, and serotonergic neurons. Synapse 1:455-460.

Fricker AC, Mok MH, de la Flor R, Shah AJ, Woolley M, Dawson LA, Kew JN (2009) Effects of N-acetylaspartylglutamate (NAAG) at group II mGluRs and NMDAR. Neuropharmacology 56:1060-1067.

Fuhrman S, Palkovits M, Cassidy M, Neale JH (1994) The regional distribution of N-acetylaspartylglutamate (NAAG) and peptidase activity against NAAG in the rat nervous system. J Neurochem 62:275-281.

Fujisawa S, Aoki C (2003) In vivo blockade of N-methyl-D-aspartate receptors induces rapid trafficking of NR2B subunits away from synapses and out of spines and terminals in adult cortex. Neuroscience 121:51-63.

Furukawa H (2012) Structure and function of glutamate receptor amino terminal domains. J Physiol 590:63-72.

Gallagher MJ, Huang H, Pritchett DB, Lynch DR (1996) Interactions between ifenprodil and the NR2B subunit of the N-methyl-D-aspartate receptor. J Biol Chem 271:9603-9611.

Gehl LM, Saab OH, Bzdega T, Wroblewska B, Neale JH (2004) Biosynthesis of NAAG by an enzyme-mediated process in rat central nervous system neurons and glia. J Neurochem 90:989-997.

Geng MY, Saito H, Nishiyama N (1997) Protective effect of ifenprodil against glucose deprivation-induced damage in cultured rat hippocampal neurons. Jpn J Pharmacol 73:97-100.

Ghose S, Wroblewska B, Corsi L, Grayson DR, De Blas AL, Vicini S, Neale JH (1997) N-acetylaspartylglutamate stimulates metabotropic glutamate receptor 3 to regulate expression of the GABA(A) alpha6 subunit in cerebellar granule cells. J Neurochem 69:2326-2335.

Gielen M, Siegler Retchless B, Mony L, Johnson JW, Paoletti P (2009) Mechanism of differential control of NMDA receptor activity by NR2 subunits. Nature 459:703-707.

Gielen M, Le Goff A, Stroebel D, Johnson JW, Neyton J, Paoletti P (2008) Structural rearrangements of NR1/NR2A NMDA receptors during allosteric inhibition. Neuron 57:80-93.

Ginsberg MD (2008) Neuroprotection for ischemic stroke: past, present and future. Neuropharmacology 55:363-389.

Gotti B, Benavides J, MacKenzie ET, Scatton B (1990) The pharmacotherapy of focal cortical ischaemia in the mouse. Brain Res 522:290-307.

Gotti B, Duverger D, Bertin J, Carter C, Dupont R, Frost J, Gaudilliere B, MacKenzie ET, Rousseau J, Scatton B, et al. (1988) Ifenprodil and SL 82.0715 as cerebral anti-ischemic agents. I. Evidence for efficacy in models of focal cerebral ischemia. J Pharmacol Exp Ther 247:1211-1221.

Gouix E, Leveille F, Nicole O, Melon C, Had-Aissouni L, Buisson A (2009) Reverse glial glutamate uptake triggers neuronal cell death through extrasynaptic NMDA receptor activation. Mol Cell Neurosci 40:463-473.

Graham D, Darles G, Langer SZ (1992) The neuroprotective properties of ifenprodil, a novel NMDA receptor antagonist, in neuronal cell culture toxicity studies. Eur J Pharmacol 226:373-376.

Gray JA, Shi Y, Usui H, During MJ, Sakimura K, Nicoll RA (2011) Distinct modes of AMPA receptor suppression at developing synapses by GluN2A and GluN2B: single-cell NMDA receptor subunit deletion in vivo. Neuron 71:1085-1101.

Green AR, Shuaib A (2006) Therapeutic strategies for the treatment of stroke. Drug Discov Today 11:681-693.

Gresham GE, Alexander D, Bishop DS, Giuliani C, Goldberg G, Holland A, Kelly-Hayes M, Linn RT, Roth EJ, Stason WB, Trombly CA (1997) American Heart Association Prevention Conference. IV. Prevention and Rehabilitation of Stroke. Rehabilitation. Stroke 28:1522-1526.

Groc L, Heine M, Cousins SL, Stephenson FA, Lounis B, Cognet L, Choquet D (2006) NMDA receptor surface mobility depends on NR2A-2B subunits. Proc Natl Acad Sci U S A 103:18769-18774.

Grotta J (1995) Why do all drugs work in animals but none in stroke patients? 2. Neuroprotective therapy. J Intern Med 237:89-94.

Grunze HC, Rainnie DG, Hasselmo ME, Barkai E, Hearn EF, McCarley RW, Greene RW (1996) NMDA-dependent modulation of CA1 local circuit inhibition. J Neurosci 16:2034-2043.

Hardingham GE, Bading H (2010) Synaptic versus extrasynaptic NMDA receptor signalling: implications for neurodegenerative disorders. Nat Rev Neurosci 11:682-696.

Hardingham GE, Fukunaga Y, Bading H (2002) Extrasynaptic NMDARs oppose synaptic NMDARs by triggering CREB shut-off and cell death pathways. Nat Neurosci 5:405-414.

Harney SC, Jane DE, Anwyl R (2008) Extrasynaptic NR2D-containing NMDARs are recruited to the synapse during LTP of NMDAR-EPSCs. J Neurosci 28:11685-11694.

Harris AZ, Pettit DL (2007) Extrasynaptic and synaptic NMDA receptors form stable and uniform pools in rat hippocampal slices. J Physiol 584:509-519.

Hatton CJ, Paoletti P (2005) Modulation of triheteromeric NMDA receptors by N-terminal domain ligands. Neuron 46:261-274.

Heart&Stroke (2015) Heart and Stroke Foundation of Canada. Retrieved from http://www.heartandstroke.com/site/c.ikIQLcMWJtE/b.3483991/k.34A8/Statistics.htm - stroke.

Hess S, Pasieczny R, Rao S, Jachec C, Varney M, Johnson E (1999) Activity of N-acetylaspartylglutamate at human recombinant glutamate receptors. 29th Annual Meeting, Society for Neuroscience, Miami Beach, FL: p 975.

Hestrin S (1992) Developmental regulation of NMDA receptor-mediated synaptic currents at a central synapse. Nature 357:686-689.

Hill MD et al. (2012) Safety and efficacy of NA-1 in patients with iatrogenic stroke after endovascular aneurysm repair (ENACT): a phase 2, randomised, double-blind, placebo-controlled trial. Lancet Neurol 11:942-950.

Hlouchova K, Barinka C, Klusak V, Sacha P, Mlcochova P, Majer P, Rulisek L, Konvalinka J (2007) Biochemical characterization of human glutamate carboxypeptidase III. J Neurochem 101:682-696.

Hollmann M, Heinemann S (1994) Cloned glutamate receptors. Annu Rev Neurosci 17:31-108.

Hollmann M, O'Shea-Greenfield A, Rogers SW, Heinemann S (1989) Cloning by functional expression of a member of the glutamate receptor family. Nature 342:643-648.

Huettner JE, Bean BP (1988) Block of N-methyl-D-aspartate-activated current by the anticonvulsant MK-801: selective binding to open channels. Proc Natl Acad Sci U S A 85:1307-1311.

Iadecola C (1997) Bright and dark sides of nitric oxide in ischemic brain injury. Trends Neurosci 20:132-139.

Ikonomidou C, Turski L (2002) Why did NMDA receptor antagonists fail clinical trials for stroke and traumatic brain injury? Lancet Neurol 1:383-386.

Ikonomidou C, Stefovska V, Turski L (2000) Neuronal death enhanced by N-methyl-D-aspartate antagonists. Proc Natl Acad Sci U S A 97:12885-12890.

Ikonomidou C, Bosch F, Miksa M, Bittigau P, Vockler J, Dikranian K, Tenkova TI, Stefovska V, Turski L, Olney JW (1999) Blockade of NMDA receptors and apoptotic neurodegeneration in the developing brain. Science 283:70-74.

Imamura Y, Ma CL, Pabba M, Bergeron R (2008) Sustained saturating level of glycine induces changes in NR2B-containing-NMDA receptor localization in the CA1 region of the hippocampus. J Neurochem 105:2454-2465.

Ivanov A, Pellegrino C, Rama S, Dumalska I, Salyha Y, Ben-Ari Y, Medina I (2006) Opposing role of synaptic and extrasynaptic NMDA receptors in regulation of the extracellular signal-regulated kinases (ERK) activity in cultured rat hippocampal neurons. J Physiol 572:789-798.

Jackson PF, Slusher BS (2001) Design of NAALADase inhibitors: a novel neuroprotective strategy. Curr Med Chem 8:949-957.

Jackson PF, Cole DC, Slusher BS, Stetz SL, Ross LE, Donzanti BA, Trainor DA (1996) Design, synthesis, and biological activity of a potent inhibitor of the neuropeptidase N-acetylated alpha-linked acidic dipeptidase. J Med Chem 39:619-622.

Javitt DC, Zukin SR (1991) Recent advances in the phencyclidine model of schizophrenia. Am J Psychiatry 148:1301-1308.

Johnson JW, Ascher P (1987) Glycine potentiates the NMDA response in cultured mouse brain neurons. Nature 325:529-531.

Jones HE, Sillito AM (1992) The action of the putative neurotransmitters N-acetylaspartylglutamate and L-homocysteate in cat dorsal lateral geniculate nucleus. J Neurophysiol 68:663-672.

Kaku DA, Giffard RG, Choi DW (1993) Neuroprotective effects of glutamate antagonists and extracellular acidity. Science 260:1516-1518.

Kalia LV, Kalia SK, Salter MW (2008) NMDA receptors in clinical neurology: excitatory times ahead. Lancet Neurol 7:742-755.

Kalogeris T, Baines CP, Krenz M, Korthuis RJ (2012) Cell biology of ischemia/reperfusion injury. Int Rev Cell Mol Biol 298:229-317.

Karakas E, Simorowski N, Furukawa H (2009) Structure of the zinc-bound amino-terminal domain of the NMDA receptor NR2B subunit. EMBO J 28:3910-3920.

Karakas E, Simorowski N, Furukawa H (2011) Subunit arrangement and phenylethanolamine binding in GluN1/GluN2B NMDA receptors. Nature 475:249-253.

Kashiwagi K, Pahk AJ, Masuko T, Igarashi K, Williams K (1997) Block and modulation of N-methyl-D-aspartate receptors by polyamines and protons: role of amino acid residues in the transmembrane and pore-forming regions of NR1 and NR2 subunits. Mol Pharmacol 52:701-713.

Kaufman AM, Milnerwood AJ, Sepers MD, Coquinco A, She K, Wang L, Lee H, Craig AM, Cynader M, Raymond LA (2012) Opposing roles of synaptic and extrasynaptic NMDA receptor signaling in cocultured striatal and cortical neurons. J Neurosci 32:3992-4003.

Kaufmann AM, Firlik AD, Fukui MB, Wechsler LR, Jungries CA, Yonas H (1999) Ischemic core and penumbra in human stroke. Stroke 30:93-99.

Kehoe LA, Bernardinelli Y, Muller D (2013) GluN3A: an NMDA receptor subunit with exquisite properties and functions. Neural Plast 2013:145387.

Keinanen K, Wisden W, Sommer B, Werner P, Herb A, Verdoorn TA, Sakmann B, Seeburg PH (1990) A family of AMPA-selective glutamate receptors. Science 249:556-560.

Kenakin T (2004) Allosteric modulators: the new generation of receptor antagonist. Mol Interv 4:222-229.

Kew JN, Trube G, Kemp JA (1996) A novel mechanism of activity-dependent NMDA receptor antagonism describes the effect of ifenprodil in rat cultured cortical neurones. J Physiol 497 (Pt 3):761-772.

Kim E, Sheng M (2004) PDZ domain proteins of synapses. Nat Rev Neurosci 5:771-781.

Kleckner NW, Dingledine R (1988) Requirement for glycine in activation of NMDA-receptors expressed in Xenopus oocytes. Science 241:835-837.

Kohr G (2006) NMDA receptor function: subunit composition versus spatial distribution. Cell Tissue Res 326:439-446.

Koller KJ, Coyle JT (1984) Characterization of the interactions of N-acetyl-aspartyl-glutamate with [3H]L-glutamate receptors. Eur J Pharmacol 98:193-199.

Koller KJ, Zaczek R, Coyle JT (1984) N-acetyl-aspartyl-glutamate: regional levels in rat brain and the effects of brain lesions as determined by a new HPLC method. J Neurochem 43:1136-1142.

Kolodziejczyk K, Hamilton NB, Wade A, Karadottir R, Attwell D (2009) The effect of N-acetyl-aspartyl-glutamate and N-acetyl-aspartate on white matter oligodendrocytes. Brain 132:1496-1508.

Kornau HC, Schenker LT, Kennedy MB, Seeburg PH (1995) Domain interaction between NMDA receptor subunits and the postsynaptic density protein PSD-95. Science 269:1737-1740.

Koumura A, Nonaka Y, Hyakkoku K, Oka T, Shimazawa M, Hozumi I, Inuzuka T, Hara H (2008) A novel calpain inhibitor, ((1S)-1((((1S)-1-benzyl-3-cyclopropylamino-2,3-di-oxopropyl)amino)carbonyl)-3-met hylbutyl) carbamic acid 5-methoxy-3-

oxapentyl ester, protects neuronal cells from cerebral ischemia-induced damage in mice. Neuroscience 157:309-318.

Kozikowski AP, Zhang J, Nan F, Petukhov PA, Grajkowska E, Wroblewski JT, Yamamoto T, Bzdega T, Wroblewska B, Neale JH (2004) Synthesis of urea-based inhibitors as active site probes of glutamate carboxypeptidase II: efficacy as analgesic agents. J Med Chem 47:1729-1738.

Kullmann DM (1999) Excitatory synapses. Neither too loud nor too quiet. Nature 399:111-112.

Kuryatov A, Laube B, Betz H, Kuhse J (1994) Mutational analysis of the glycine-binding site of the NMDA receptor: structural similarity with bacterial amino acid-binding proteins. Neuron 12:1291-1300.

Lai TW, Shyu WC, Wang YT (2011) Stroke intervention pathways: NMDA receptors and beyond. Trends Mol Med 17:266-275.

Lan JY, Skeberdis VA, Jover T, Zheng X, Bennett MV, Zukin RS (2001a) Activation of metabotropic glutamate receptor 1 accelerates NMDA receptor trafficking. J Neurosci 21:6058-6068.

Lan JY, Skeberdis VA, Jover T, Grooms SY, Lin Y, Araneda RC, Zheng X, Bennett MV, Zukin RS (2001b) Protein kinase C modulates NMDA receptor trafficking and gating. Nat Neurosci 4:382-390.

Lau CG, Zukin RS (2007) NMDA receptor trafficking in synaptic plasticity and neuropsychiatric disorders. Nat Rev Neurosci 8:413-426.

Lau D, Bading H (2009) Synaptic activity-mediated suppression of p53 and induction of nuclear calcium-regulated neuroprotective genes promote survival through inhibition of mitochondrial permeability transition. J Neurosci 29:4420-4429.

Laube B, Hirai H, Sturgess M, Betz H, Kuhse J (1997) Molecular determinants of agonist discrimination by NMDA receptor subunits: analysis of the glutamate binding site on the NR2B subunit. Neuron 18:493-503.

Lavezzari G, McCallum J, Dewey CM, Roche KW (2004) Subunit-specific regulation of NMDA receptor endocytosis. J Neurosci 24:6383-6391.

Law AJ, Weickert CS, Webster MJ, Herman MM, Kleinman JE, Harrison PJ (2003) Expression of NMDA receptor NR1, NR2A and NR2B subunit mRNAs during development of the human hippocampal formation. Eur J Neurosci 18:1197-1205.

Lea PMt, Wroblewska B, Sarvey JM, Neale JH (2001) beta-NAAG rescues LTP from blockade by NAAG in rat dentate gyrus via the type 3 metabotropic glutamate receptor. J Neurophysiol 85:1097-1106.

Lee CH, Lu W, Michel JC, Goehring A, Du J, Song X, Gouaux E (2014) NMDA receptor structures reveal subunit arrangement and pore architecture. Nature 511:191-197.

Lee JM, Zipfel GJ, Choi DW (1999) The changing landscape of ischaemic brain injury mechanisms. Nature 399:A7-14.

Lees KR (1997) Cerestat and other NMDA antagonists in ischemic stroke. Neurology 49:S66-69.

Leveille F, Papadia S, Fricker M, Bell KF, Soriano FX, Martel MA, Puddifoot C, Habel M, Wyllie DJ, Ikonomidou C, Tolkovsky AM, Hardingham GE (2010)

Suppression of the intrinsic apoptosis pathway by synaptic activity. J Neurosci 30:2623-2635.

Li S, Jin M, Koeglsperger T, Shepardson NE, Shankar GM, Selkoe DJ (2011) Soluble Abeta oligomers inhibit long-term potentiation through a mechanism involving excessive activation of extrasynaptic NR2B-containing NMDA receptors. J Neurosci 31:6627-6638.

Liao D, Zhang X, O'Brien R, Ehlers MD, Huganir RL (1999) Regulation of morphological postsynaptic silent synapses in developing hippocampal neurons. Nat Neurosci 2:37-43.

Lin Y, Jover-Mengual T, Wong J, Bennett MV, Zukin RS (2006) PSD-95 and PKC converge in regulating NMDA receptor trafficking and gating. Proc Natl Acad Sci U S A 103:19902-19907.

Lipton SA (2007) Pathologically activated therapeutics for neuroprotection. Nat Rev Neurosci 8:803-808.

Liu L, Wong TP, Pozza MF, Lingenhoehl K, Wang Y, Sheng M, Auberson YP, Wang YT (2004) Role of NMDA receptor subtypes in governing the direction of hippocampal synaptic plasticity. Science 304:1021-1024.

Liu Y, Wong TP, Aarts M, Rooyakkers A, Liu L, Lai TW, Wu DC, Lu J, Tymianski M, Craig AM, Wang YT (2007) NMDA receptor subunits have differential roles in mediating excitotoxic neuronal death both in vitro and in vivo. J Neurosci 27:2846-2857.

Liu Z, Stafstrom CE, Sarkisian M, Tandon P, Yang Y, Hori A, Holmes GL (1996) Age-dependent effects of glutamate toxicity in the hippocampus. Brain Res Dev Brain Res 97:178-184.

Lodder-Gadaczek J, Becker I, Gieselmann V, Wang-Eckhardt L, Eckhardt M (2011) N-acetylaspartylglutamate synthetase II synthesizes N-acetylaspartylglutamylglutamate. J Biol Chem 286:16693-16706.

Loftis JM, Janowsky A (2003) The N-methyl-D-aspartate receptor subunit NR2B: localization, functional properties, regulation, and clinical implications. Pharmacol Ther 97:55-85.

Losi G, Vicini S, Neale J (2004) NAAG fails to antagonize synaptic and extrasynaptic NMDA receptors in cerebellar granule neurons. Neuropharmacology 46:490-496.

Low CM, Zheng F, Lyuboslavsky P, Traynelis SF (2000) Molecular determinants of coordinated proton and zinc inhibition of N-methyl-D-aspartate NR1/NR2A receptors. Proc Natl Acad Sci U S A 97:11062-11067.

Low CM, Lyuboslavsky P, French A, Le P, Wyatte K, Thiel WH, Marchan EM, Igarashi K, Kashiwagi K, Gernert K, Williams K, Traynelis SF, Zheng F (2003) Molecular determinants of proton-sensitive N-methyl-D-aspartate receptor gating. Mol Pharmacol 63:1212-1222.

Lu XM, Tang Z, Liu W, Lin Q, Slusher BS (2000) N-acetylaspartylglutamate protects against transient focal cerebral ischemia in rats. Eur J Pharmacol 408:233-239.

Lujan B, Liu X, Wan Q (2012) Differential roles of GluN2A- and GluN2B-containing NMDA receptors in neuronal survival and death. Int J Physiol Pathophysiol Pharmacol 4:211-218.

Lynch G, Larson J, Kelso S, Barrionuevo G, Schottler F (1983) Intracellular injections of EGTA block induction of hippocampal long-term potentiation. Nature 305:719-721.

Majer P, Jackson PF, Delahanty G, Grella BS, Ko YS, Li W, Liu Q, Maclin KM, Polakova J, Shaffer KA, Stoermer D, Vitharana D, Wang EY, Zakrzewski A, Rojas C, Slusher BS, Wozniak KM, Burak E, Limsakun T, Tsukamoto T (2003) Synthesis and biological evaluation of thiol-based inhibitors of glutamate carboxypeptidase II: discovery of an orally active GCP II inhibitor. J Med Chem 46:1989-1996.

Martel MA, Wyllie DJ, Hardingham GE (2009) In developing hippocampal neurons, NR2B-containing N-methyl-D-aspartate receptors (NMDARs) can mediate signaling to neuronal survival and synaptic potentiation, as well as neuronal death. Neuroscience 158:334-343.

Martel MA, Ryan TJ, Bell KF, Fowler JH, McMahon A, Al-Mubarak B, Komiyama NH, Horsburgh K, Kind PC, Grant SG, Wyllie DJ, Hardingham GE (2012) The subtype of GluN2 C-terminal domain determines the response to excitotoxic insults. Neuron 74:543-556.

Martin RL, Lloyd HG, Cowan AI (1994) The early events of oxygen and glucose deprivation: setting the scene for neuronal death? Trends Neurosci 17:251-257.

Masuko T, Kashiwagi K, Kuno T, Nguyen ND, Pahk AJ, Fukuchi J, Igarashi K, Williams K (1999) A regulatory domain (R1-R2) in the amino terminus of the N-methyl-D-aspartate receptor: effects of spermine, protons, and ifenprodil, and structural

similarity to bacterial leucine/isoleucine/valine binding protein. Mol Pharmacol 55:957-969.

Matsuo Y, Kihara T, Ikeda M, Ninomiya M, Onodera H, Kogure K (1995) Role of neutrophils in radical production during ischemia and reperfusion of the rat brain: effect of neutrophil depletion on extracellular ascorbyl radical formation. J Cereb Blood Flow Metab 15:941-947.

Maung J, Mallari JP, Girtsman TA, Wu LY, Rowley JA, Santiago NM, Brunelle AN, Berkman CE (2004) Probing for a hydrophobic a binding register in prostate-specific membrane antigen with phenylalkylphosphonamidates. Bioorg Med Chem 12:4969-4979.

Mayer ML (2006) Glutamate receptors at atomic resolution. Nature 440:456-462.

Mayer ML, Westbrook GL (1987) Permeation and block of N-methyl-D-aspartic acid receptor channels by divalent cations in mouse cultured central neurones. J Physiol 394:501-527.

Mayer ML, Westbrook GL, Guthrie PB (1984) Voltage-dependent block by Mg2+ of NMDA responses in spinal cord neurones. Nature 309:261-263.

McDonald JW, Johnston MV (1990) Pharmacology of N-methyl-D-aspartate-induced brain injury in an in vivo perinatal rat model. Synapse 6:179-188.

Meldrum BS (2000) Glutamate as a neurotransmitter in the brain: review of physiology and pathology. J Nutr 130:1007S-1015S.

Meyer FB, Anderson RE, Sundt TM, Jr., Yaksh TL (1986) Intracellular brain pH, indicator tissue perfusion, electroencephalography, and histology in severe and

moderate focal cortical ischemia in the rabbit. J Cereb Blood Flow Metab 6:71-78.

Mitani A, Tanaka K (2003) Functional changes of glial glutamate transporter GLT-1 during ischemia: an in vivo study in the hippocampal CA1 of normal mice and mutant mice lacking GLT-1. J Neurosci 23:7176-7182.

Miyake M, Kakimoto Y, Sorimachi M (1981) A gas chromatographic method for the determination of N-acetyl-L-aspartic acid, N-acetyl-alpha-aspartylglutamic acid and beta-citryl-L-glutamic acid and their distributions in the brain and other organs of various species of animals. J Neurochem 36:804-810.

Miyamoto E, Kakimoto Y, Sano I (1966) Identification of N-acetyl-alpha-aspartylglutamic acid in the bovine brain. J Neurochem 13:999-1003.

Moffett JR, Namboodiri MA (1995) Differential distribution of N-acetylaspartylglutamate and N-acetylaspartate immunoreactivities in rat forebrain. J Neurocytol 24:409-433.

Moffett JR, Palkovits M, Namboodiri A, Neale JH (1994) Comparative distribution of N-acetylaspartylglutamate and GAD67 in the cerebellum and precerebellar nuclei of the rat utilizing enhanced carbodiimide fixation and immunohistochemistry. J Comp Neurol 347:598-618.

Mony L, Kew JN, Gunthorpe MJ, Paoletti P (2009a) Allosteric modulators of NR2B-containing NMDA receptors: molecular mechanisms and therapeutic potential. Br J Pharmacol 157:1301-1317.

Mony L, Zhu S, Carvalho S, Paoletti P (2011) Molecular basis of positive allosteric modulation of GluN2B NMDA receptors by polyamines. EMBO J 30:3134-3146.

Mony L, Krzaczkowski L, Leonetti M, Le Goff A, Alarcon K, Neyton J, Bertrand HO, Acher F, Paoletti P (2009b) Structural basis of NR2B-selective antagonist recognition by N-methyl-D-aspartate receptors. Mol Pharmacol 75:60-74.

Monyer H, Burnashev N, Laurie DJ, Sakmann B, Seeburg PH (1994) Developmental and regional expression in the rat brain and functional properties of four NMDA receptors. Neuron 12:529-540.

Mori T, Asano T, Matsui T, Muramatsu H, Ueda M, Kamiya T, Katayama Y, Abe T (1999) Intraluminal increase of superoxide anion following transient focal cerebral ischemia in rats. Brain Res 816:350-357.

Morimoto T, Globus MY, Busto R, Martinez E, Ginsberg MD (1996) Simultaneous measurement of salicylate hydroxylation and glutamate release in the penumbral cortex following transient middle cerebral artery occlusion in rats. J Cereb Blood Flow Metab 16:92-99.

Mothet JP, Parent AT, Wolosker H, Brady RO, Jr., Linden DJ, Ferris CD, Rogawski MA, Snyder SH (2000) D-serine is an endogenous ligand for the glycine site of the N-methyl-D-aspartate receptor. Proc Natl Acad Sci U S A 97:4926-4931.

Mott DD, Doherty JJ, Zhang S, Washburn MS, Fendley MJ, Lyuboslavsky P, Traynelis SF, Dingledine R (1998) Phenylethanolamines inhibit NMDA receptors by enhancing proton inhibition. Nat Neurosci 1:659-667.

Murphy SN, Thayer SA, Miller RJ (1987) The effects of excitatory amino acids on intracellular calcium in single mouse striatal neurons in vitro. J Neurosci 7:4145-4158.

Nagel J, Belozertseva I, Greco S, Kashkin V, Malyshkin A, Jirgensons A, Shekunova E, Eilbacher B, Bespalov A, Danysz W (2006) Effects of NAAG peptidase inhibitor 2-PMPA in model chronic pain - relation to brain concentration. Neuropharmacology 51:1163-1171.

Neale JH (2011) N-acetylaspartylglutamate is an agonist at mGluR(3) in vivo and in vitro. J Neurochem 119:891-895.

Neale JH, Bzdega T, Wroblewska B (2000) N-Acetylaspartylglutamate: the most abundant peptide neurotransmitter in the mammalian central nervous system. J Neurochem 75:443-452.

Neale JH, Olszewski RT, Gehl LM, Wroblewska B, Bzdega T (2005) The neurotransmitter N-acetylaspartylglutamate in models of pain, ALS, diabetic neuropathy, CNS injury and schizophrenia. Trends Pharmacol Sci 26:477-484.

Neale JH, Olszewski RT, Zuo D, Janczura KJ, Profaci CP, Lavin KM, Madore JC, Bzdega T (2011) Advances in understanding the peptide neurotransmitter NAAG and appearance of a new member of the NAAG neuropeptide family. J Neurochem 118:490-498.

Neyton J, Paoletti P (2006) Relating NMDA receptor function to receptor subunit composition: limitations of the pharmacological approach. J Neurosci 26:1331-1333.

NINDS (1995) The National Institute of Neurological Disorders and Stroke, rt-PA stroke study group, Tissue plasminogen activator for acute ischemic stroke. New Engl J Med 333:1581-1587.

Ning K, Pei L, Liao M, Liu B, Zhang Y, Jiang W, Mielke JG, Li L, Chen Y, El-Hayek YH, Fehlings MG, Zhang X, Liu F, Eubanks J, Wan Q (2004) Dual neuroprotective signaling mediated by downregulating two distinct phosphatase activities of PTEN. J Neurosci 24:4052-4060.

Nong Y, Huang YQ, Ju W, Kalia LV, Ahmadian G, Wang YT, Salter MW (2003) Glycine binding primes NMDA receptor internalization. Nature 422:302-307.

Nour M, Scalzo F, Liebeskind DS (2013) Ischemia-reperfusion injury in stroke. Interv Neurol 1:185-199.

O'Connor RE, McGraw P, Edelsohn L (1999) Thrombolytic therapy for acute ischemic stroke: why the majority of patients remain ineligible for treatment. Ann Emerg Med 33:9-14.

Obrenovitch TP (1995) The ischaemic penumbra: twenty years on. Cerebrovasc Brain Metab Rev 7:297-323.

Okamoto S, Pouladi MA, Talantova M, Yao D, Xia P, Ehrnhoefer DE, Zaidi R, Clemente A, Kaul M, Graham RK, Zhang D, Vincent Chen HS, Tong G, Hayden MR, Lipton SA (2009) Balance between synaptic versus extrasynaptic NMDA receptor activity influences inclusions and neurotoxicity of mutant huntingtin. Nat Med 15:1407-1413.

Oliver AJ, Wiest O, Helquist P, Miller MJ, Tenniswood M (2003) Conformational and SAR analysis of NAALADase and PSMA inhibitors. Bioorg Med Chem 11:4455-4461.

Olney JW, de Gubareff T (1978) Glutamate neurotoxicity and Huntington's chorea. Nature 271:557-559.

Orlowski P, Chappell M, Park CS, Grau V, Payne S (2011) Modelling of pH dynamics in brain cells after stroke. Interface Focus 1:408-416.

Pabba M, Wong AY, Ahlskog N, Hristova E, Biscaro D, Nassrallah W, Ngsee JK, Snyder M, Beique JC, Bergeron R (2014) NMDA receptors are upregulated and trafficked to the plasma membrane after sigma-1 receptor activation in the rat hippocampus. J Neurosci 34:11325-11338.

Pahk AJ, Williams K (1997) Influence of extracellular pH on inhibition by ifenprodil at N-methyl-D-aspartate receptors in Xenopus oocytes. Neurosci Lett 225:29-32.

Paoletti P, Neyton J, Ascher P (1995) Glycine-independent and subunit-specific potentiation of NMDA responses by extracellular Mg2+. Neuron 15:1109-1120.

Paoletti P, Bellone C, Zhou Q (2013) NMDA receptor subunit diversity: impact on receptor properties, synaptic plasticity and disease. Nat Rev Neurosci 14:383-400.

Papadia S, Soriano FX, Leveille F, Martel MA, Dakin KA, Hansen HH, Kaindl A, Sifringer M, Fowler J, Stefovska V, McKenzie G, Craigon M, Corriveau R, Ghazal P, Horsburgh K, Yankner BA, Wyllie DJ, Ikonomidou C, Hardingham GE (2008) Synaptic NMDA receptor activity boosts intrinsic antioxidant defenses. Nat Neurosci 11:476-487.

Papouin T, Ladepeche L, Ruel J, Sacchi S, Labasque M, Hanini M, Groc L, Pollegioni L, Mothet JP, Oliet SH (2012) Synaptic and extrasynaptic NMDA receptors are gated by different endogenous coagonists. Cell 150:633-646.

Park CK, Nehls DG, Teasdale GM, McCulloch J (1989) Effect of the NMDA antagonist MK-801 on local cerebral blood flow in focal cerebral ischaemia in the rat. J Cereb Blood Flow Metab 9:617-622.

Parsons MP, Raymond LA (2014) Extrasynaptic NMDA receptor involvement in central nervous system disorders. Neuron 82:279-293.

Passani LA, Vonsattel JP, Coyle JT (1997) Distribution of N-acetylaspartylglutamate immunoreactivity in human brain and its alteration in neurodegenerative disease. Brain Res 772:9-22.

Perez-Otano I, Schulteis CT, Contractor A, Lipton SA, Trimmer JS, Sucher NJ, Heinemann SF (2001) Assembly with the NR1 subunit is required for surface expression of NR3A-containing NMDA receptors. J Neurosci 21:1228-1237.

Perin-Dureau F, Rachline J, Neyton J, Paoletti P (2002) Mapping the binding site of the neuroprotectant ifenprodil on NMDA receptors. J Neurosci 22:5955-5965.

Petralia RS, Wang YX, Hua F, Yi Z, Zhou A, Ge L, Stephenson FA, Wenthold RJ (2010) Organization of NMDA receptors at extrasynaptic locations. Neuroscience 167:68-87.

PHAC (2009) Public Health Agency of Canada, Tracking Heart Disease and Stroke in Canada. Retrieved from: http://www.phac-aspc.gc.ca/publicat/2009/cvd-avc/pdf/cvd-avs-2009-eng.pdf.

Phillis JW, Ren J, O'Regan MH (2000) Transporter reversal as a mechanism of glutamate release from the ischemic rat cerebral cortex: studies with DL-threo-beta-benzyloxyaspartate. Brain Res 868:105-112.

Picconi B, Tortiglione A, Barone I, Centonze D, Gardoni F, Gubellini P, Bonsi P, Pisani A, Bernardi G, Di Luca M, Calabresi P (2006) NR2B subunit exerts a critical role in postischemic synaptic plasticity. Stroke 37:1895-1901.

Pittaluga A, Barbeito L, Serval V, Godeheu G, Artaud F, Glowinski J, Cheramy A (1988) Depolarization-evoked release of N-acetyl-L-aspartyl-L-glutamate from rat brain synaptosomes. Eur J Pharmacol 158:263-266.

Pohl D, Bittigau P, Ishimaru MJ, Stadthaus D, Hubner C, Olney JW, Turski L, Ikonomidou C (1999) N-Methyl-D-aspartate antagonists and apoptotic cell death triggered by head trauma in developing rat brain. Proc Natl Acad Sci U S A 96:2508-2513.

Portera-Cailliau C, Price DL, Martin LJ (1996) N-methyl-D-aspartate receptor proteins NR2A and NR2B are differentially distributed in the developing rat central nervous system as revealed by subunit-specific antibodies. J Neurochem 66:692-700.

Prass K, Dirnagl U (1998) Glutamate antagonists in therapy of stroke. Restor Neurol Neurosci 13:3-10.

Prybylowski K, Chang K, Sans N, Kan L, Vicini S, Wenthold RJ (2005) The synaptic localization of NR2B-containing NMDA receptors is controlled by interactions with PDZ proteins and AP-2. Neuron 47:845-857.

Puttfarcken PS, Handen JS, Montgomery DT, Coyle JT, Werling LL (1993) N-acetyl-aspartylglutamate modulation of N-methyl-D-aspartate-stimulated [3H]norepinephrine release from rat hippocampal slices. J Pharmacol Exp Ther 266:796-803.

Quaba O, Robertson CE (2002) Thrombolysis and its implications in the management of stroke in the accident and emergency department. Scott Med J 47:57-59.

Quinlan EM, Philpot BD, Huganir RL, Bear MF (1999) Rapid, experience-dependent expression of synaptic NMDA receptors in visual cortex in vivo. Nat Neurosci 2:352-357.

Rachline J, Perin-Dureau F, Le Goff A, Neyton J, Paoletti P (2005) The micromolar zinc-binding domain on the NMDA receptor subunit NR2B. J Neurosci 25:308-317.

Rais R, Wozniak K, Wu Y, Niwa M, Stathis M, Alt J, Giroux M, Sawa A, Rojas C, Slusher BS (2015) Selective CNS Uptake of the GCP-II Inhibitor 2-PMPA following Intranasal Administration. PLoS One 10:e0131861.

RANTTAS (1996) A randomized trial of Tirilazed Mesylate in patients with acute stroke (RANTTAS). The RANTTAS Investigators. Stroke 27:1453-1458.

Rao A, Craig AM (1997) Activity regulates the synaptic localization of the NMDA receptor in hippocampal neurons. Neuron 19:801-812.

Rauner C, Kohr G (2011) Triheteromeric NR1/NR2A/NR2B receptors constitute the major N-methyl-D-aspartate receptor population in adult hippocampal synapses. J Biol Chem 286:7558-7566.

Renno WM, Lee JH, Beitz AJ (1997) Light and electron microscopic immunohistochemical localization of N-acetylaspartylglutamate (NAAG) in the olivocerebellar pathway of the rat. Synapse 26:140-154.

Riccio A, Ahn S, Davenport CM, Blendy JA, Ginty DD (1999) Mediation by a CREB family transcription factor of NGF-dependent survival of sympathetic neurons. Science 286:2358-2361.

Riveros N, Orrego F (1984) A study of possible excitatory effects of N-acetylaspartylglutamate in different in vivo and in vitro brain preparations. Brain Res 299:393-395.

Robinson MB, Blakely RD, Couto R, Coyle JT (1987) Hydrolysis of the brain dipeptide N-acetyl-L-aspartyl-L-glutamate. Identification and characterization of a novel N-acetylated alpha-linked acidic dipeptidase activity from rat brain. J Biol Chem 262:14498-14506.

Roche KW, Standley S, McCallum J, Dune Ly C, Ehlers MD, Wenthold RJ (2001) Molecular determinants of NMDA receptor internalization. Nat Neurosci 4:794-802.

Rossi DJ, Oshima T, Attwell D (2000) Glutamate release in severe brain ischaemia is mainly by reversed uptake. Nature 403:316-321.

Rothman SM (1983) Synaptic activity mediates death of hypoxic neurons. Science 220:536-537.

Ryan TJ, Emes RD, Grant SG, Komiyama NH (2008) Evolution of NMDA receptor cytoplasmic interaction domains: implications for organisation of synaptic signalling complexes. BMC Neurosci 9:6.

Sacco RL, DeRosa JT, Haley EC, Jr., Levin B, Ordronneau P, Phillips SJ, Rundek T, Snipes RG, Thompson JL, Glycine Antagonist in Neuroprotection Americas I (2001) Glycine antagonist in neuroprotection for patients with acute stroke: GAIN Americas: a randomized controlled trial. JAMA 285:1719-1728.

Sacha P, Zamecnik J, Barinka C, Hlouchova K, Vicha A, Mlcochova P, Hilgert I, Eckschlager T, Konvalinka J (2007) Expression of glutamate carboxypeptidase II in human brain. Neuroscience 144:1361-1372.

Sala C, Rudolph-Correia S, Sheng M (2000) Developmentally regulated NMDA receptor-dependent dephosphorylation of cAMP response element-binding protein (CREB) in hippocampal neurons. J Neurosci 20:3529-3536.

Sanabria ER, Wozniak KM, Slusher BS, Keller A (2004) GCP II (NAALADase) inhibition suppresses mossy fiber-CA3 synaptic neurotransmission by a presynaptic mechanism. J Neurophysiol 91:182-193.

Sans N, Petralia RS, Wang YX, Blahos J, 2nd, Hell JW, Wenthold RJ (2000) A developmental change in NMDA receptor-associated proteins at hippocampal synapses. J Neurosci 20:1260-1271.

Sanz-Clemente A, Nicoll RA, Roche KW (2013) Diversity in NMDA receptor composition: many regulators, many consequences. Neuroscientist 19:62-75.

Sasaki YF, Rothe T, Premkumar LS, Das S, Cui J, Talantova MV, Wong HK, Gong X, Chan SF, Zhang D, Nakanishi N, Sucher NJ, Lipton SA (2002) Characterization and comparison of the NR3A subunit of the NMDA receptor in recombinant systems and primary cortical neurons. J Neurophysiol 87:2052-2063.

Sattler R, Tymianski M (2000) Molecular mechanisms of calcium-dependent excitotoxicity. J Mol Med (Berl) 78:3-13.

Sattler R, Tymianski M (2001) Molecular mechanisms of glutamate receptor-mediated excitotoxic neuronal cell death. Mol Neurobiol 24:107-129.

Sattler R, Charlton MP, Hafner M, Tymianski M (1998) Distinct influx pathways, not calcium load, determine neuronal vulnerability to calcium neurotoxicity. J Neurochem 71:2349-2364.

Sattler R, Xiong Z, Lu WY, MacDonald JF, Tymianski M (2000) Distinct roles of synaptic and extrasynaptic NMDA receptors in excitotoxicity. J Neurosci 20:22-33.

Sattler R, Xiong Z, Lu WY, Hafner M, MacDonald JF, Tymianski M (1999) Specific coupling of NMDA receptor activation to nitric oxide neurotoxicity by PSD-95 protein. Science 284:1845-1848.

Scatton B (1994) Excitatory amino acid receptor antagonists: a novel treatment for ischemic cerebrovascular diseases. Life Sci 55:2115-2124.

Schell MJ, Molliver ME, Snyder SH (1995) D-serine, an endogenous synaptic modulator: localization to astrocytes and glutamate-stimulated release. Proc Natl Acad Sci U S A 92:3948-3952.

Schinder AF, Olson EC, Spitzer NC, Montal M (1996) Mitochondrial dysfunction is a primary event in glutamate neurotoxicity. J Neurosci 16:6125-6133.

Schneggenburger R, Zhou Z, Konnerth A, Neher E (1993) Fractional contribution of calcium to the cation current through glutamate receptor channels. Neuron 11:133-143.

Schwarze SR, Ho A, Vocero-Akbani A, Dowdy SF (1999) In vivo protein transduction: delivery of a biologically active protein into the mouse. Science 285:1569-1572.

Scimemi A, Fine A, Kullmann DM, Rusakov DA (2004) NR2B-containing receptors mediate cross talk among hippocampal synapses. J Neurosci 24:4767-4777.

Scott DB, Blanpied TA, Ehlers MD (2003) Coordinated PKA and PKC phosphorylation suppresses RXR-mediated ER retention and regulates the surface delivery of NMDA receptors. Neuropharmacology 45:755-767.

Scott DB, Blanpied TA, Swanson GT, Zhang C, Ehlers MD (2001) An NMDA receptor ER retention signal regulated by phosphorylation and alternative splicing. J Neurosci 21:3063-3072.

Sekiguchi M, Okamoto K, Sakai Y (1989) Low-concentration N-acetylaspartylglutamate suppresses the climbing fiber response of Purkinje cells in guinea pig cerebellar slices and the responses to excitatory amino acids of Xenopus laevis oocytes injected with cerebellar mRNA. Brain Res 482:87-96.

Sekiguchi M, Wada K, Wenthold RJ (1992) N-acetylaspartylglutamate acts as an agonist upon homomeric NMDA receptor (NMDAR1) expressed in Xenopus oocytes. FEBS Lett 311:285-289.

Serval V, Barbeito L, Pittaluga A, Cheramy A, Lavielle S, Glowinski J (1990) Competitive inhibition of N-acetylated-alpha-linked acidic dipeptidase activity by N-acetyl-L-aspartyl-beta-linked L-glutamate. J Neurochem 55:39-46.

Shalaby IA, Chenard BL, Prochniak MA, Butler TW (1992) Neuroprotective effects of the N-methyl-D-aspartate receptor antagonists ifenprodil and SL-82,0715 on hippocampal cells in culture. J Pharmacol Exp Ther 260:925-932.

Shaywitz AJ, Greenberg ME (1999) CREB: a stimulus-induced transcription factor activated by a diverse array of extracellular signals. Annu Rev Biochem 68:821-861.

Shi J, Aamodt SM, Constantine-Paton M (1997) Temporal correlations between functional and molecular changes in NMDA receptors and GABA neurotransmission in the superior colliculus. J Neurosci 17:6264-6276.

Shi J, Townsend M, Constantine-Paton M (2000) Activity-dependent induction of tonic calcineurin activity mediates a rapid developmental downregulation of NMDA receptor currents. Neuron 28:103-114.

Shipton OA, Paulsen O (2014) GluN2A and GluN2B subunit-containing NMDA receptors in hippocampal plasticity. Philos Trans R Soc Lond B Biol Sci 369:20130163.

Siemkowicz E, Hansen AJ (1981) Brain extracellular ion composition and EEG activity following 10 minutes ischemia in normo- and hyperglycemic rats. Stroke 12:236-240.

Skeberdis VA, Lan J, Zheng X, Zukin RS, Bennett MV (2001) Insulin promotes rapid delivery of N-methyl-D- aspartate receptors to the cell surface by exocytosis. Proc Natl Acad Sci U S A 98:3561-3566.

Slusher BS, Vornov JJ, Thomas AG, Hurn PD, Harukuni I, Bhardwaj A, Traystman RJ, Robinson MB, Britton P, Lu XC, Tortella FC, Wozniak KM, Yudkoff M, Potter BM, Jackson PF (1999) Selective inhibition of NAALADase, which converts NAAG to glutamate, reduces ischemic brain injury. Nat Med 5:1396-1402.

Sprengel R, Suchanek B, Amico C, Brusa R, Burnashev N, Rozov A, Hvalby O, Jensen V, Paulsen O, Andersen P, Kim JJ, Thompson RF, Sun W, Webster LC, Grant SG, Eilers J, Konnerth A, Li J, McNamara JO, Seeburg PH (1998) Importance of

the intracellular domain of NR2 subunits for NMDA receptor function in vivo. Cell 92:279-289.

Statcan (2011) Statistics Canada, Table 102-0561, Leading causes of death, total population, by age group and sex, Canada, annual, CANSIM (database): http://www5.statcan.gc.ca/cansim/a26?lang=eng&id=1020561.

Steigerwald F, Schulz TW, Schenker LT, Kennedy MB, Seeburg PH, Kohr G (2000) C-Terminal truncation of NR2A subunits impairs synaptic but not extrasynaptic localization of NMDA receptors. J Neurosci 20:4573-4581.

Stroke Therapy Academic Industry R (1999) Recommendations for standards regarding preclinical neuroprotective and restorative drug development. Stroke 30:2752-2758.

Suarez F, Zhao Q, Monaghan DT, Jane DE, Jones S, Gibb AJ (2010) Functional heterogeneity of NMDA receptors in rat substantia nigra pars compacta and reticulata neurones. Eur J Neurosci 32:359-367.

Sun HS, Doucette TA, Liu Y, Fang Y, Teves L, Aarts M, Ryan CL, Bernard PB, Lau A, Forder JP, Salter MW, Wang YT, Tasker RA, Tymianski M (2008) Effectiveness of PSD95 inhibitors in permanent and transient focal ischemia in the rat. Stroke 39:2544-2553.

Taghibiglou C, Martin HG, Lai TW, Cho T, Prasad S, Kojic L, Lu J, Liu Y, Lo E, Zhang S, Wu JZ, Li YP, Wen YH, Imm JH, Cynader MS, Wang YT (2009) Role of NMDA receptor-dependent activation of SREBP1 in excitotoxic and ischemic neuronal injuries. Nat Med 15:1399-1406.

Tamura Y, Sato Y, Yokota T, Akaike A, Sasa M, Takaori S (1993) Ifenprodil prevents glutamate cytotoxicity via polyamine modulatory sites of N-methyl-D-aspartate receptors in cultured cortical neurons. J Pharmacol Exp Ther 265:1017-1025.

Tanaka K, Nagata E, Suzuki S, Dembo T, Nogawa S, Fukuuchi Y (1999) Immunohistochemical analysis of cyclic AMP response element binding protein phosphorylation in focal cerebral ischemia in rats. Brain Res 818:520-526.

Tanaka K, Nogawa S, Ito D, Suzuki S, Dembo T, Kosakai A, Fukuuchi Y (2000) Activated phosphorylation of cyclic AMP response element binding protein is associated with preservation of striatal neurons after focal cerebral ischemia in the rat. Neuroscience 100:345-354.

Tang CM, Dichter M, Morad M (1990) Modulation of the N-methyl-D-aspartate channel by extracellular H+. Proc Natl Acad Sci U S A 87:6445-6449.

Tao X, Finkbeiner S, Arnold DB, Shaywitz AJ, Greenberg ME (1998) Ca2+ influx regulates BDNF transcription by a CREB family transcription factor-dependent mechanism. Neuron 20:709-726.

Thomas CG, Miller AJ, Westbrook GL (2006) Synaptic and extrasynaptic NMDA receptor NR2 subunits in cultured hippocampal neurons. J Neurophysiol 95:1727-1734.

Tieman SB, Butler K, Neale JH (1988) N-acetylaspartylglutamate. A neuropeptide in the human visual system. JAMA 259:2020.

Tieman SB, Neale JH, Tieman DG (1991) N-acetylaspartylglutamate immunoreactivity in neurons of the monkey's visual pathway. J Comp Neurol 313:45-64.

Tong G, Takahashi H, Tu S, Shin Y, Talantova M, Zago W, Xia P, Nie Z, Goetz T, Zhang D, Lipton SA, Nakanishi N (2008) Modulation of NMDA receptor properties and synaptic transmission by the NR3A subunit in mouse hippocampal and cerebrocortical neurons. J Neurophysiol 99:122-132.

Tortella FC, Lin Y, Ved H, Slusher BS, Dave JR (2000) Neuroprotection produced by the NAALADase inhibitor 2-PMPA in rat cerebellar neurons. Eur J Pharmacol 402:31-37.

Tovar KR, Westbrook GL (1999) The incorporation of NMDA receptors with a distinct subunit composition at nascent hippocampal synapses in vitro. J Neurosci 19:4180-4188.

Tovar KR, Westbrook GL (2002) Mobile NMDA receptors at hippocampal synapses. Neuron 34:255-264.

Tovar KR, McGinley MJ, Westbrook GL (2013) Triheteromeric NMDA receptors at hippocampal synapses. J Neurosci 33:9150-9160.

Townsend M, Yoshii A, Mishina M, Constantine-Paton M (2003) Developmental loss of miniature N-methyl-D-aspartate receptor currents in NR2A knockout mice. Proc Natl Acad Sci U S A 100:1340-1345.

Traynelis SF, Cull-Candy SG (1990) Proton inhibition of N-methyl-D-aspartate receptors in cerebellar neurons. Nature 345:347-350.

Traynelis SF, Cull-Candy SG (1991) Pharmacological properties and H+ sensitivity of excitatory amino acid receptor channels in rat cerebellar granule neurones. J Physiol 433:727-763.

Traynelis SF, Hartley M, Heinemann SF (1995) Control of proton sensitivity of the NMDA receptor by RNA splicing and polyamines. Science 268:873-876.

Traynelis SF, Burgess MF, Zheng F, Lyuboslavsky P, Powers JL (1998) Control of voltage-independent zinc inhibition of NMDA receptors by the NR1 subunit. J Neurosci 18:6163-6175.

Traynelis SF, Wollmuth LP, McBain CJ, Menniti FS, Vance KM, Ogden KK, Hansen KB, Yuan H, Myers SJ, Dingledine R (2010) Glutamate receptor ion channels: structure, regulation, and function. Pharmacol Rev 62:405-496.

Trombley PQ, Westbrook GL (1990) Excitatory synaptic transmission in cultures of rat olfactory bulb. J Neurophysiol 64:598-606.

Tsai G, Slusher BS, Sim L, Coyle JT (1993) Immunocytochemical distribution of N-acetylaspartylglutamate in the rat forebrain and glutamatergic pathways. J Chem Neuroanat 6:277-292.

Tsai G, Forloni G, Robinson MB, Stauch BL, Coyle JT (1988) Calcium-dependent evoked release of N-[3H]acetylaspartylglutamate from the optic pathway. J Neurochem 51:1956-1959.

Tsai G, Stauch BL, Vornov JJ, Deshpande JK, Coyle JT (1990) Selective release of N-acetylaspartylglutamate from rat optic nerve terminals in vivo. Brain Res 518:313-316.

Tsukamoto T, Wozniak KM, Slusher BS (2007) Progress in the discovery and development of glutamate carboxypeptidase II inhibitors. Drug Discov Today 12:767-776.

Tsukamoto T, Flanary JM, Rojas C, Slusher BS, Valiaeva N, Coward JK (2002) Phosphonate and phosphinate analogues of N-acylated gamma-glutamylglutamate. potent inhibitors of glutamate carboxypeptidase II. Bioorg Med Chem Lett 12:2189-2192.

Tu W, Xu X, Peng L, Zhong X, Zhang W, Soundarapandian MM, Balel C, Wang M, Jia N, Lew F, Chan SL, Chen Y, Lu Y (2010) DAPK1 interaction with NMDA receptor NR2B subunits mediates brain damage in stroke. Cell 140:222-234.

Tymianski M (1996) Cytosolic calcium concentrations and cell death in vitro. Adv Neurol 71:85-105.

Tymianski M, Tator CH (1996) Normal and abnormal calcium homeostasis in neurons: a basis for the pathophysiology of traumatic and ischemic central nervous system injury. Neurosurgery 38:1176-1195.

Tymianski M, Charlton MP, Carlen PL, Tator CH (1993) Source specificity of early calcium neurotoxicity in cultured embryonic spinal neurons. J Neurosci 13:2085-2104.

Valivullah HM, Lancaster J, Sweetnam PM, Neale JH (1994) Interactions between N-acetylaspartylglutamate and AMPA, kainate, and NMDA binding sites. J Neurochem 63:1714-1719.

van der Post JP, de Visser SJ, de Kam ML, Woelfler M, Hilt DC, Vornov J, Burak ES, Bortey E, Slusher BS, Limsakun T, Cohen AF, van Gerven JM (2005) The central nervous system effects, pharmacokinetics and safety of the NAALADase-inhibitor GPI 5693. Br J Clin Pharmacol 60:128-136.

van Zundert B, Yoshii A, Constantine-Paton M (2004) Receptor compartmentalization and trafficking at glutamate synapses: a developmental proposal. Trends Neurosci 27:428-437.

Vanhoutte P, Bading H (2003) Opposing roles of synaptic and extrasynaptic NMDA receptors in neuronal calcium signalling and BDNF gene regulation. Curr Opin Neurobiol 13:366-371.

Vergun O, Keelan J, Khodorov BI, Duchen MR (1999) Glutamate-induced mitochondrial depolarisation and perturbation of calcium homeostasis in cultured rat hippocampal neurones. J Physiol 519 Pt 2:451-466.

Vicini S, Wang JF, Li JH, Zhu WJ, Wang YH, Luo JH, Wolfe BB, Grayson DR (1998) Functional and pharmacological differences between recombinant N-methyl-D-aspartate receptors. J Neurophysiol 79:555-566.

Vissel B, Krupp JJ, Heinemann SF, Westbrook GL (2001) A use-dependent tyrosine dephosphorylation of NMDA receptors is independent of ion flux. Nat Neurosci 4:587-596.

Vizi ES, Kisfali M, Lorincz T (2013) Role of nonsynaptic GluN2B-containing NMDA receptors in excitotoxicity: evidence that fluoxetine selectively inhibits these receptors and may have neuroprotective effects. Brain Res Bull 93:32-38.

von Engelhardt J, Doganci B, Seeburg PH, Monyer H (2009) Synaptic NR2A- but not NR2B-Containing NMDA Receptors Increase with Blockade of Ionotropic Glutamate Receptors. Front Mol Neurosci 2:19.

Vornov JJ, Wozniak K, Lu M, Jackson P, Tsukamoto T, Wang E, Slusher B (1999) Blockade of NAALADase: a novel neuroprotective strategy based on limiting glutamate and elevating NAAG. Ann N Y Acad Sci 890:400-405.

Vyklicky L, Jr., Vlachova V, Krusek J (1990) The effect of external pH changes on responses to excitatory amino acids in mouse hippocampal neurones. J Physiol 430:497-517.

Walder KK, Ryan SB, Bzdega T, Olszewski RT, Neale JH, Lindgren CA (2013) Immunohistological and electrophysiological evidence that N-acetylaspartylglutamate is a co-transmitter at the vertebrate neuromuscular junction. Eur J Neurosci 37:118-129.

Walton MR, Dragunow I (2000) Is CREB a key to neuronal survival? Trends Neurosci 23:48-53.

Wang JM, Chao JR, Chen W, Kuo ML, Yen JJ, Yang-Yen HF (1999) The antiapoptotic gene mcl-1 is up-regulated by the phosphatidylinositol 3-kinase/Akt signaling pathway through a transcription factor complex containing CREB. Mol Cell Biol 19:6195-6206.

Wardlaw JM, Warlow CP, Counsell C (1997) Systematic review of evidence on thrombolytic therapy for acute ischaemic stroke. Lancet 350:607-614.

Watanabe M, Inoue Y, Sakimura K, Mishina M (1992) Developmental changes in distribution of NMDA receptor channel subunit mRNAs. Neuroreport 3:1138-1140.

Watanabe M, Inoue Y, Sakimura K, Mishina M (1993) Distinct distributions of five N-methyl-D-aspartate receptor channel subunit mRNAs in the forebrain. J Comp Neurol 338:377-390.

Waxman EA, Lynch DR (2005) N-methyl-D-aspartate receptor subtypes: multiple roles in excitotoxicity and neurological disease. Neuroscientist 11:37-49.

Wenthold RJ, Prybylowski K, Standley S, Sans N, Petralia RS (2003) Trafficking of NMDA receptors. Annu Rev Pharmacol Toxicol 43:335-358.

Westbrook GL, Mayer ML, Namboodiri MA, Neale JH (1986) High concentrations of N-acetylaspartylglutamate (NAAG) selectively activate NMDA receptors on mouse spinal cord neurons in cell culture. J Neurosci 6:3385-3392.

White BC, Sullivan JM, DeGracia DJ, O'Neil BJ, Neumar RW, Grossman LI, Rafols JA, Krause GS (2000) Brain ischemia and reperfusion: molecular mechanisms of neuronal injury. J Neurol Sci 179:1-33.

Whittemore ER, Koerner JF (1989) An explanation for the purported excitation of piriform cortical neurons by N-acetyl-L-aspartyl-L-glutamic acid (NAAG). Proc Natl Acad Sci U S A 86:9602-9605.

Whittemore ER, Ilyin VI, Woodward RM (1997) Antagonism of N-methyl-D-aspartate receptors by sigma site ligands: potency, subtype-selectivity and mechanisms of inhibition. J Pharmacol Exp Ther 282:326-338.

Williams AJ, Lu XM, Slusher B, Tortella FC (2001) Electroencephalogram analysis and neuroprotective profile of the N-acetylated-alpha-linked acidic dipeptidase inhibitor, GPI5232, in normal and brain-injured rats. J Pharmacol Exp Ther 299:48-57.

Williams K (1993) Ifenprodil discriminates subtypes of the N-methyl-D-aspartate receptor: selectivity and mechanisms at recombinant heteromeric receptors. Mol Pharmacol 44:851-859.

Williams K, Russell SL, Shen YM, Molinoff PB (1993) Developmental switch in the expression of NMDA receptors occurs in vivo and in vitro. Neuron 10:267-278.

Williamson LC, Neale JH (1988) Ultrastructural localization of N-acetylaspartylglutamate in synaptic vesicles of retinal neurons. Brain Res 456:375-381.

Williamson LC, Neale JH (1992) Uptake, metabolism, and release of N-[3H]acetylaspartylglutamate by the avian retina. J Neurochem 58:2191-2199.

Williamson LC, Eagles DA, Brady MJ, Moffett JR, Namboodiri MA, Neale JH (1991) Localization and Synaptic Release of N-acetylaspartylglutamate in the Chick Retina and Optic Tectum. Eur J Neurosci 3:441-451.

Wroblewska B, Santi MR, Neale JH (1998) N-acetylaspartylglutamate activates cyclic AMP-coupled metabotropic glutamate receptors in cerebellar astrocytes. Glia 24:172-179.

Wroblewska B, Wroblewski JT, Saab OH, Neale JH (1993) N-acetylaspartylglutamate inhibits forskolin-stimulated cyclic AMP levels via a metabotropic glutamate receptor in cultured cerebellar granule cells. J Neurochem 61:943-948.

Wroblewska B, Wegorzewska IN, Bzdega T, Olszewski RT, Neale JH (2006) Differential negative coupling of type 3 metabotropic glutamate receptor to cyclic GMP levels in neurons and astrocytes. J Neurochem 96:1071-1077.

Wroblewska B, Wroblewski JT, Pshenichkin S, Surin A, Sullivan SE, Neale JH (1997) N-acetylaspartylglutamate selectively activates mGluR3 receptors in transfected cells. J Neurochem 69:174-181.

Wyllie DJ, Livesey MR, Hardingham GE (2013) Influence of GluN2 subunit identity on NMDA receptor function. Neuropharmacology 74:4-17.

Xia P, Chen HS, Zhang D, Lipton SA (2010) Memantine preferentially blocks extrasynaptic over synaptic NMDA receptor currents in hippocampal autapses. J Neurosci 30:11246-11250.

Yamakura T, Shimoji K (1999) Subunit- and site-specific pharmacology of the NMDA receptor channel. Prog Neurobiol 59:279-298.

Yoshii A, Sheng MH, Constantine-Paton M (2003) Eye opening induces a rapid dendritic localization of PSD-95 in central visual neurons. Proc Natl Acad Sci U S A 100:1334-1339.

Young D, Lawlor PA, Leone P, Dragunow M, During MJ (1999) Environmental enrichment inhibits spontaneous apoptosis, prevents seizures and is neuroprotective. Nat Med 5:448-453.

Yuan H, Hansen KB, Vance KM, Ogden KK, Traynelis SF (2009) Control of NMDA receptor function by the NR2 subunit amino-terminal domain. J Neurosci 29:12045-12058.

Yuan H, Myers SJ, Wells G, Nicholson KL, Swanger SA, Lyuboslavsky P, Tahirovic YA, Menaldino DS, Ganesh T, Wilson LJ, Liotta DC, Snyder JP, Traynelis SF (2015) Context-dependent GluN2B-selective inhibitors of NMDA receptor function are neuroprotective with minimal side effects. Neuron 85:1305-1318.

Zaczek R, Koller K, Cotter R, Heller D, Coyle JT (1983) N-acetylaspartylglutamate: an endogenous peptide with high affinity for a brain "glutamate" receptor. Proc Natl Acad Sci U S A 80:1116-1119.

Zhang S, Taghibiglou C, Girling K, Dong Z, Lin SZ, Lee W, Shyu WC, Wang YT (2013) Critical role of increased PTEN nuclear translocation in excitotoxic and ischemic neuronal injuries. J Neurosci 33:7997-8008.

Zhao J, Peng Y, Xu Z, Chen RQ, Gu QH, Chen Z, Lu W (2008) Synaptic metaplasticity through NMDA receptor lateral diffusion. J Neurosci 28:3060-3070.

Zheng F, Erreger K, Low CM, Banke T, Lee CJ, Conn PJ, Traynelis SF (2001) Allosteric interaction between the amino terminal domain and the ligand binding domain of NR2A. Nat Neurosci 4:894-901.

Zheng X, Zhang L, Wang AP, Bennett MV, Zukin RS (1999) Protein kinase C potentiation of N-methyl-D-aspartate receptor activity is not mediated by phosphorylation of N-methyl-D-aspartate receptor subunits. Proc Natl Acad Sci U S A 96:15262-15267.

Zhong C, Luo Q, Jiang J (2014) Blockade of N-acetylaspartylglutamate peptidases: a novel protective strategy for brain injuries and neurological disorders. Int J Neurosci 124:867-873.

Zhong C, Zhao X, Sarva J, Kozikowski A, Neale JH, Lyeth BG (2005) NAAG peptidase inhibitor reduces acute neuronal degeneration and astrocyte damage following lateral fluid percussion TBI in rats. J Neurotrauma 22:266-276.

Zhong C, Zhao X, Van KC, Bzdega T, Smyth A, Zhou J, Kozikowski AP, Jiang J, O'Connor WT, Berman RF, Neale JH, Lyeth BG (2006) NAAG peptidase

inhibitor increases dialysate NAAG and reduces glutamate, aspartate and GABA levels in the dorsal hippocampus following fluid percussion injury in the rat. J Neurochem 97:1015-1025.

Zhong J, Russell SL, Pritchett DB, Molinoff PB, Williams K (1994) Expression of mRNAs encoding subunits of the N-methyl-D-aspartate receptor in cultured cortical neurons. Mol Pharmacol 45:846-853.

Zhou J, Neale JH, Pomper MG, Kozikowski AP (2005) NAAG peptidase inhibitors and their potential for diagnosis and therapy. Nat Rev Drug Discov 4:1015-1026.

Zhu S, Paoletti P (2015) Allosteric modulators of NMDA receptors: multiple sites and mechanisms. Curr Opin Pharmacol 20:14-23.

Zollinger M, Amsler U, Do KQ, Streit P, Cuenod M (1988) Release of N-acetylaspartylglutamate on depolarization of rat brain slices. J Neurochem 51:1919-1923.

Zollinger M, Brauchli-Theotokis J, Gutteck-Amsler U, Do KQ, Streit P, Cuenod M (1994) Release of N-acetylaspartylglutamate from slices of rat cerebellum, striatum, and spinal cord, and the effect of climbing fiber deprivation. J Neurochem 63:1133-1142.

APPENDIX - Publications

Neurobiology of Disease 82 (2015) 580–592

Contents lists available at ScienceDirect

Neurobiology of Disease

journal homepage: www.elsevier.com/locate/ynbdi

Differential effects of *N*-acetyl-aspartyl-glutamate on synaptic and extrasynaptic NMDA receptors are subunit- and pH-dependent in the CA1 region of the mouse hippocampus

Pamela Khacho [a], Boyang Wang [a], Nina Ahlskog [a], Elitza Hristova [a], Richard Bergeron [a,b,c,*]

[a] Department of Cellular and Molecular Medicine, University of Ottawa, Ottawa, ON K1H 8M5, Canada
[b] Department of Psychiatry, University of Ottawa, Ottawa, ON K1Z 7K4, Canada
[c] Neuroscience Program, Ottawa Hospital Research Institute, Ottawa, ON K1Y 4E9, Canada

ARTICLE INFO

Article history:
Received 16 April 2015
Revised 13 August 2015
Accepted 17 August 2015
Available online 22 August 2015

Keywords:
N-acetyl-aspartyl-glutamate (NAAG)
2-PMPA
NMDA receptors
Protons
Hippocampus
Electrophysiology
Biotinylation
Neuroprotection

ABSTRACT

Ischemic strokes cause excessive release of glutamate, leading to overactivation of *N*-methyl-D-aspartate receptors (NMDARs) and excitotoxicity-induced neuronal death. For this reason, inhibition of NMDARs has been a central focus in identifying mechanisms to avert this extensive neuronal damage. *N*-acetyl-aspartyl-glutamate (NAAG), the most abundant neuropeptide in the brain, is neuroprotective in ischemic conditions *in vivo*. Despite this evidence, the exact mechanism underlying its neuroprotection, and more specifically its effect on NMDARs, is currently unknown due to conflicting results in the literature. Here, we uncover a pH-dependent subunit-specific action of NAAG on NMDARs. Using whole-cell electrophysiological recordings on acute hippocampal slices from adult mice and on HEK293 cells, we found that NAAG increases synaptic GluN2A-containing NMDAR EPSCs, while effectively decreasing extrasynaptic GluN2B-containing NMDAR EPSCs in physiological pH. Intriguingly, the results of our study further show that in low pH, which is a physiological occurrence during ischemia, NAAG depresses GluN2A-containing NMDAR EPSCs and amplifies its inhibitory effect on GluN2B-containing NMDAR EPSCs, as well as upregulates the surface expression of the GluN2A subunit. Altogether, our data demonstrate that NAAG has differential effects on NMDAR function based on subunit composition and pH. These findings suggest that the role of NAAG as a neuroprotective agent during an ischemic stroke is likely mediated by its ability to reduce NMDAR excitation. The inhibitory effect of NAAG on NMDARs and its enhanced function in acidic conditions make NAAG a prime therapeutic agent for the treatment of ischemic events.

1. Introduction

Stroke is one of the leading causes of death and disability worldwide (Truelsen et al., 2003). During an ischemic event, such as stroke, there is excessive release of the neurotransmitter glutamate, leading to Ca^{2+}-induced excitotoxic neuronal death due to overactivation of *N*-methyl-D-aspartate receptors (NMDARs) (Weilinger et al., 2013). NMDAR antagonists have been shown to protect against excitotoxicity in ischemic models, however, none of these agents are currently approved for clinical use due to lack of efficacy or intolerable side effects (Ikonomidou and Turski, 2002; Gardoni and Di Luca, 2006).

N-acetyl-aspartyl-glutamate (NAAG), the most abundant neuropeptide in the mammalian brain, modulates the glutamatergic system and is thought to play a key role in neuroprotection (Neale et al., 2005). NAAG is stored in synaptic vesicles and released upon Ca^{2+}-dependent depolarization, and is degraded by the astrocytic glycoprotein glutamate carboxypeptidase II (GCP-II) into *N*-acetylaspartate and glutamate (Neale et al., 2011). The levels of NAAG can be increased endogenously through the use of GCP-II inhibitors, such as 2-(phosphonomethyl)pentanedioic acid (2-PMPA) (Jackson et al., 1996). Numerous studies have shown that an increase in NAAG, either by exogenous or endogenous manipulation, is neuroprotective against NMDAR-mediated neurotoxicity without adverse side effects (Slusher et al., 1999; Lu et al., 2000; Tortella et al., 2000; Cai et al., 2002). Although it is well established that NAAG has neuroprotective properties, the literature to date has reported conflicting results regarding its effect on NMDARs (Westbrook et al., 1986; Sekiguchi et al., 1989, 1992; Losi et al., 2004; Bergeron et al., 2005, 2007; Fricker et al., 2009; Bergeron and Coyle, 2012). Therefore, it remains unclear whether this

Abbreviations: 2-PMPA, 2-(phosphonomethyl)pentanedioic acid; 2-PMSA, 2-(phosphonomethyl)succinic acid; ACSF, artificial cerebrospinal fluid; BDNF, brain-derived neurotrophic factor; CREB, cAMP response element binding protein; EPSC, excitatory postsynaptic current; GCP-II, glutamate carboxypeptidase type II; $mGluR_3$, metabotropic glutamate receptor 3; NAAG, *N*-acetyl-aspartyl-glutamate; NMDAR, *N*-methyl-D-aspartate receptor.

* Corresponding author at: 451 Smyth Road, Roger Guindon Building, Room 3501N, Ottawa, Ontario K1H 8M5, Canada. Tel. +1 613 729 2068; fax. +1 613 729 1266
E-mail address: rbergeron@ohri.ca (R. Bergeron).
Available online on ScienceDirect (www.sciencedirect.com).

http://dx.doi.org/10.1016/j.nbd.2015.08.017
0969-9961/

neuroprotection is mediated through the modification of NMDAR activity, which could depend on the subunit composition of the receptor, as well as extracellular conditions.

NMDARs are heterotetramers composed of two obligatory GluN1 and two GluN2 (A–D) subunits. A third family of NMDAR subunits, GluN3, has also been described, which includes subtypes GluN3A and GluN3B. In the adult mouse hippocampus GluN2A and GluN2B subunits are prominent in CA1 pyramidal neurons and are located on both synaptic and extrasynaptic sites. The expression of GluN1/GluN2 subunit composition in the brain changes throughout development and conveys different pharmacological and kinetic properties on functional NMDARs. In the neonatal brain, GluN2B-containing NMDARs, characterized by slower decay kinetics, dominate at the synapse. Following postnatal development the subunit composition changes to be more GluN2A-containing at the synapse and GluN2B-containing extrasynaptically (Cull-Candy et al., 2001; Loftis and Janowsky, 2003; van Zundert et al., 2004; Paoletti et al., 2013; Sanz-Clemente et al., 2013). There is ample evidence supporting the notion that GluN2B-containing NMDARs dominate extrasynaptic sites in mature animals, as reported by several studies utilizing the selective GluN2B antagonist, ifenprodil (Tovar and Westbrook, 1999; Bellone and Nicoll, 2007; Mony et al., 2009b).

Alterations in NMDAR function can result from changes in subunit composition of the receptor, as well as pH conditions. Lower pH (6.3–6.8) induces an inhibitory effect on NMDARs, while more basic pH enhances NMDAR activity (Tang et al., 1990; Traynelis and Cull-Candy, 1990, 1991; Vyklicky et al., 1990; Low et al., 2003; Dravid et al., 2007). During ischemic conditions, pH in the extracellular space can drop by 0.2 to more than 1.0 pH units due to the accumulation of lactic acid (Doyle et al., 2008). Interestingly, some drugs have enhanced function in different pH conditions. For example, ifenprodil is neuroprotective in animal models of stroke, not only by being selective for GluN2B-containing NMDARs, but also by increasing the receptor's sensitivity to inhibition by protons (Shalaby et al., 1992; Pahk and Williams, 1997; Whittemore et al., 1997; Mott et al., 1998). Perhaps the discrepancies observed in previous studies of the effect of NAAG on NMDARs arise from differences in subunit composition as well as variations in pH, whereby NAAG could be neuroprotective in ischemic models (acidic pH), but show no effect on NMDARs when studied in a physiological pH environment.

Here we show, using mouse acute hippocampal slices and a HEK293 recombinant system, a subunit-specific action of NAAG on NMDARs. We found that NAAG increases synaptic GluN2A-containing NMDAR excitatory postsynaptic currents (EPSCs), while effectively decreasing extrasynaptic GluN2B-containing NMDAR EPSCs in physiological conditions. We also show that in acidic pH, NAAG inhibits both GluN2A- and GluN2B-containing NMDAR EPSCs, as well as upregulates the surface expression of the GluN2A subunit. These novel findings suggest that NAAG differentially modulates NMDAR function during physiological and pathological conditions. Given that NMDAR subunit development and pH are similarly regulated in mice and humans (Law et al., 2003; Casey et al., 2010; Orlowski et al., 2011), our results suggest a potential therapeutic relevance in neurological conditions, such as stroke.

2. Materials and Methods

2.1. Slice Preparation

Acute coronal hippocampal brain slices (300 μm thick) were obtained from wild type Swiss mice of either sex (8–12 weeks old). Prior to decapitation, animals were anesthetized by isoflurane inhalation, in agreement with the guidelines of the Canadian Council of Animal Care and approved by the University of Ottawa Animal Care Committee. The brain was removed and placed in oxygenated (95% O_2/5% CO_2) artificial cerebrospinal fluid (ACSF) at 4°C containing (in mM): 126 NaCl, 2.5 KCl, 2 $CaCl_2$, 1 $MgCl_2$, 1.25 NaH_2PO_4, 26 $NaHCO_3$, and 10 glucose (300 mOsm, pH 7.2). Slices were cut with a vibrating microtome (Leica VT 1000S) and incubated for 1 h in oxygenated ACSF at room temperature before they were used for experiments.

2.2. Whole-cell Electrophysiology on Hippocampal Slices

Whole-cell voltage-clamp recordings were performed on CA1 pyramidal neurons from acute hippocampal slices using differential interference contrast optics and infrared video microscopy (IR-DIC; Leica DMLFSA). All experiments were performed at room temperature in ACSF and cells were voltage-clamped at −65 mV. A stable baseline recording was first obtained in normal ACSF. To isolate synaptic NMDAR-mediated EPSCs, ACSF with a low concentration of Mg^{2+} (0.1 mM) was used containing (in μM): 5 NBQX, 50 picrotoxin, 10 bicuculline, and 0.5 strychnine (all purchased from Tocris Bioscience). To isolate for extrasynaptic NMDAR-mediated EPSCs, 30 μM MK-801 (purchased from Abcam) and 30 μM DL-TBOA (purchased from Tocris Bioscience) were included in the low Mg^{2+} ACSF as previously described (Hardingham et al., 2002; Carpenter-Hyland et al., 2004; Harney et al., 2008; Imamura et al., 2008; Okamoto et al., 2009; Hardingham and Bading, 2010; Xia et al., 2010; Li et al., 2011). When required, additional drugs were bath applied (in μM): 20 NAAG, 10 2-PMPA, 3 ifenprodil, 10 LY341495 (all purchased from Tocris Bioscience), and 10 2-(phosphonomethyl)succinic acid (2-PMSA; a generous gift from Dr. Barbara Slusher, Brain Science Institute, Johns Hopkins School of Medicine, Baltimore, MD). Extracellular solutions with modified pH values were prepared by replacing $NaHCO_3$ in the ACSF with one of two different pH buffers (depending on their pH ranges), PIPES (20 mM) or HEPES (20 mM), and the pH was adjusted to either 6.5, 6.8, or 7.6 with NaOH (Doroshenko and Renaud, 2009). For voltage-clamp recordings, borosilicate glass electrodes were filled with an internal solution containing (in mM): 128 Cs-methanesulfonate, 10 tetraethylammonium-Cl, 10 HEPES, 0.6 EGTA, 2 $MgCl_2$, 2 Mg-ATP, 0.5 Na-GTP (all purchased from Sigma-Aldrich), and 5 QX-314 (purchased from Abcam), and the pH was adjusted to 7.2 (280–290 mOsm). The recording electrodes had a resistance of 4–6 MΩ. The series resistance was continuously monitored throughout the experiment by delivering a 5 mV hyperpolarizing step at the onset of every electrophysiological sweep. Recordings with series resistance higher than 25 MΩ were excluded. EPSCs were evoked by electrical stimulation of the Schaffer collaterals in the CA3 region of the hippocampus with a bipolar stimulating electrode. The single stimulation protocol consisted of 100 μs current pulses (10–200 μA) evoked every 12 s. To facilitate the blocking of synaptic NMDAR currents by MK-801 throughout the extrasynaptic NMDAR isolation protocol, the interval of stimulation was changed from 12 to 6 s during MK-801 application only. The intensity of the stimulation was adjusted to obtain evoked postsynaptic currents in the amplitude range of 100–150 pA.

2.3. HEK293 Cells Maintenance and Whole-cell Electrophysiology

HEK293 cells were maintained in minimal essential media supplemented with 10% fetal bovine serum, 100 U/ml penicillin/streptomycin, 100 μM neomycin, and 1× glutaMAX™ (all purchased from Life Technologies) and grown in a humidified 37°C, 5% CO_2 incubator. Twenty-four hours prior to transfection, approximately 0.18×10^6 cells were plated on Thermanox plastic coverslips (15 mm diameter, thickness 0.2 mm; Thermo Scientific) in 12-well plates. The cells were then transiently transfected with GluN1 together with either GluN2A or GluN2B cDNAs using the TransIT-2020 transfection reagent (Mirus). For visualization purposes, mCherry fluorescent protein was used as co-transfectant. The total amount of cDNA added for these triple transfections was approximately 1 μg per well at a cDNA molar ratio of 1:2:0.5 (GluN1:GluN2A:mCherry or GluN1:GluN2B:mCherry). Following transfection, the cells were grown in the presence of 100 mM DL-APV (selective NMDAR antagonist; purchased from Tocris Bioscience) to prevent overactivation of expressed receptors and subsequently cell

death. Cells were used for electrophysiological recordings 48–72 h after transfection. Individually transfected HEK293 cells were then identified for whole-cell recordings and currents were evoked using pressure ejection (10 psi) from a picospritzer micropipette filled with glutamate (100 μM) and glycine (10 μM; both purchased from Sigma-Aldrich) for a duration of 5–30 ms every 20 s. For HEK293 cell electrophysiological recordings, the external solution contained (in mM): 150 NaCl, 10 HEPES, 3 KCl and 2 $CaCl_2$. The pH was adjusted accordingly using 5 M NaOH and the osmolality to 290 mOsm using sucrose. The borosilicate electrodes were filled with internal solution containing (in mM): 115 NaCl, 10 NaF, 5 HEPES, 5 Na_4-BAPTA, 0.5 $CaCl_2$, 1 $MgCl_2$ and 10 Na_2-ATP (all purchased from Sigma-Aldrich), and the pH was adjusted to 7.2 (280–290 mOsm).

2.4. Analysis

Data were collected using a Multiclamp 700A amplifier (Axon Instruments), filtered at 2 kHz and digitized at 10 kHz by a Digidata 1322A digitizer (Molecular Devices). Recordings were analyzed using the pClamp 9 software suite (Molecular Devices). Statistical significance of the results was determined with paired (two-tailed) Student's *t*-test. A p value of < 0.05 was considered statistically significant. All values are expressed as mean ± SEM. Kinetic analysis of NMDAR currents was performed on averaged traces. Decay kinetics were measured using a biexponential fit to calculate a weighted τ value (τ_w). No significant differences in decay kinetics or 10–90% rise times were observed between control and treatment in any of the experimental conditions ($p > 0.05$; Tables S1–S3).

2.5. Cell Surface Biotinylation Assay and Western Blotting

Acute coronal hippocampal slices from mice were prepared as described above and the hippocampi from each slice were isolated, pooled, and allowed to recover. The hippocampi were then divided into six groups and incubated for 20 min at room temperature at pH 7.2, 6.8, or 7.6 in either the presence or absence of NAAG. Biotinylation of surface proteins was thereafter performed as previously described (Pabba et al., 2014). In short, the hippocampal slices were incubated for 20 min in ice-cold 0.5 mg/ml EZ-sulfo-NHS-SS-biotin (Pierce/Thermo Scientific) in phosphate-buffered saline (PBS, in mM: 137 NaCl, 2.7 KCl, 10 Na_2HPO_4, 1.8 KH_2PO_4, pH 7.4). After washing and homogenization, the lysates were incubated with neutravidin beads (Pierce/Thermo Scientific). The bound proteins were recovered from the beads with 400 μl of elution buffer (in mM: 50 Tris–HCl, 1 DTT; 2% SDS, pH 6.8) by boiling for 10 min. Protein concentrations were determined using DC assay (Bio-Rad) before Western blot.

Total membrane proteins (10 μg) were loaded and resolved as entire series on 8% SDS-PAGE and transferred to PVDF membranes. Primary

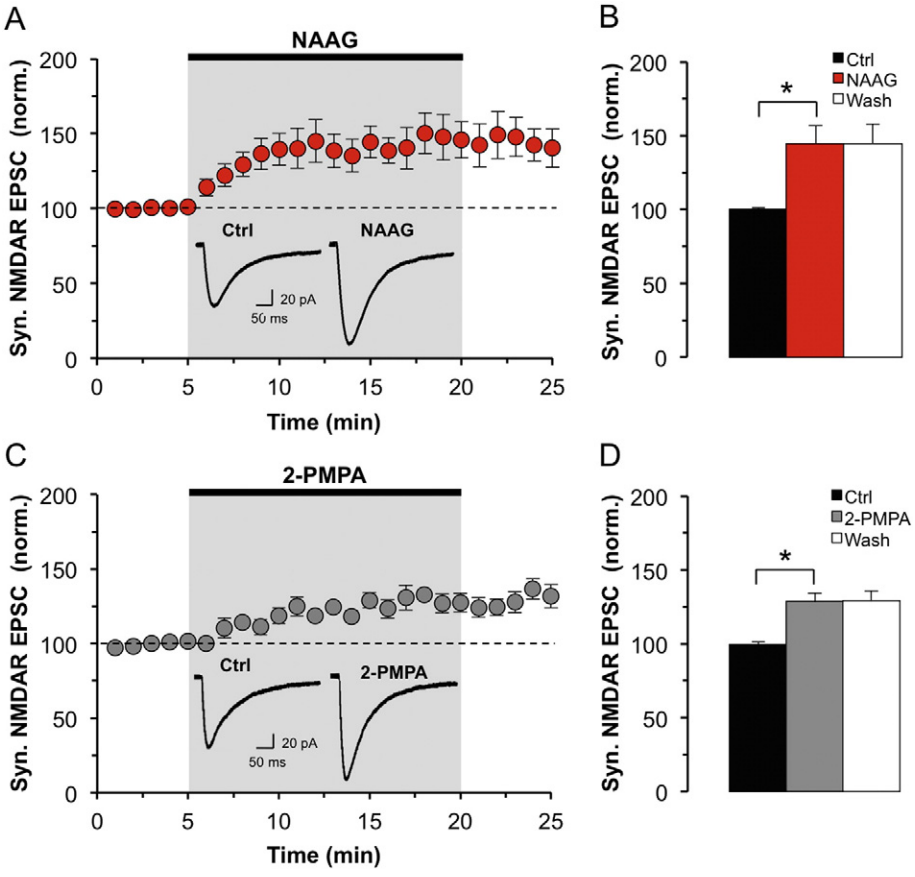

Fig. 1. Endogenous and exogenous NAAG potentiate synaptic NMDAR EPSCs in acute hippocampal slices in physiological pH. (A) CA1 pyramidal neurons were recorded from hippocampal slices and the average amplitude of evoked synaptic NMDAR EPSCs was plotted during a 15 min exogenous NAAG application followed by washout and compared to control (represented by a dotted line; n = 5 cells). Representative traces of synaptic NMDAR EPSCs of a control and NAAG-treated CA1 pyramidal neuron are also shown. (B) Representative bar graph from data in (A) showing the average synaptic NMDAR EPSC amplitudes 5 min before NAAG application (Ctrl), during the last 5 min of NAAG treatment (NAAG), and during washout (Wash). (C) Average synaptic NMDAR EPSC amplitudes plotted during a 15 min 2-PMPA application followed by washout and compared to control (represented by a dotted line) (n = 6 cells). Representative traces of synaptic NMDAR EPSCs of a control and 2-PMPA-treated CA1 pyramidal neuron are also shown. (D) Representative bar graph from data in (C) showing the average synaptic NMDAR EPSC amplitudes 5 min before 2-PMPA application (Ctrl), during the last 5 min of 2-PMPA treatment (2-PMPA), and during washout (Wash). The averages of the current amplitudes are normalized to the last 5 min of control in all cases. Data expressed as mean ± SEM. *, $p < 0.05$.

antibodies used were anti-GluN1 (1:10,000; Synaptic Systems GmbH); anti-GluN2A and anti-GluN2B (both 1:750; LifeSpan Biosciences), and anti-Na^+/K^+-ATPase (Developmental Studies Hybridoma Bank). The blots were developed with Luminata Forte (Millipore) and visualized using the LI-COR Odyssey Fc System (LI-COR Biosciences). The band intensities were quantified using the Image Studio 2.0 software (LI-COR Biosciences) and normalized to Na^+/K^+-ATPase, which remained unchanged with treatment. Statistics were done using one-way ANOVA and Tukey's post-hoc test with 95% confidence interval. All values are expressed as mean ± SEM.

3. Results

3.1. NAAG Differentially Modulates Synaptic and Extrasynaptic NMDAR Function in Acute Hippocampal Slices

Using adult mice, we set out to investigate the role of NAAG in the regulation of NMDAR activity. The effect of NAAG on synaptic NMDARs was tested in the mouse hippocampus. Whole-cell currents from acute brain slices of CA1 pyramidal neurons were recorded and NMDAR EPSCs were isolated. For all experiments, control was established in the last 5 min of baseline recording before application of any treatment, and all data was thereafter normalized to this control (unless otherwise stated). Following a stable baseline recording, NAAG (20 μM) was perfused for 15 min followed by a 20 min washout. In the presence of NAAG, we observed a 44 ± 12.6% increase in the synaptic NMDAR-mediated EPSC amplitude (n = 5 cells, $p < 0.05$; Fig. 1A, B). The effect of NAAG persisted even following washout. Since no recovery was observed for 20 min in any of the experiments, only up to 10 min of washout is shown in all figures. Similar experiments were performed using the GCP-II inhibitor, 2-PMPA (10 μM), which endogenously increases the level of NAAG (Jackson et al., 1996; Slusher et al., 1999; Nagel et al., 2006). In agreement with the results obtained with exogenous application of NAAG, 2-PMPA significantly increased the amplitude of the synaptic NMDAR EPSC by 29 ± 6.1% (n = 6 cells, $p < 0.05$; Fig. 1C, D). To confirm that the effect of 2-PMPA was the result of its inhibitory effect on GCP-II and the consequent elevation of NAAG, we used 2-PMSA (10 μM), a structurally similar but inactive analogue of 2-PMPA (Jackson et al., 1996; Slusher et al., 1999). Our data shows that 2-PMSA has no effect on NMDAR EPSCs (n = 4, $p > 0.05$; Fig. S1A).

To control for any influence that $mGluR_3$ may have had on these results, similar experiments were conducted in the presence of LY341495 (10 μM), a potent and selective group II mGluR antagonist. The effect of NAAG (n = 5) and 2-PMPA (n = 5) on NMDAR EPSCs was sustained throughout the application of LY341495 ($p < 0.05$; Fig. S2A), suggesting that the observed effect was not mediated by activation of $mGluR_3$. Furthermore, to demonstrate that the effects of NAAG and 2-PMPA are not mediated by presynaptic neurotransmitter release, we performed a paired-pulse paradigm. No difference in the ratio of successive responses (amplitude 2/amplitude 1) was observed following application of either NAAG (n = 3 cells, $p > 0.05$) or 2-PMPA (n = 3 cells, $p > 0.05$; Fig. S2C).

To investigate the influence of NAAG on NMDARs with different subunit compositions and subcellular localization, a previously established pharmacological paradigm (Fig. S3A) was used to block the activity of synaptic NMDARs, enabling us to specifically study the effect of NAAG

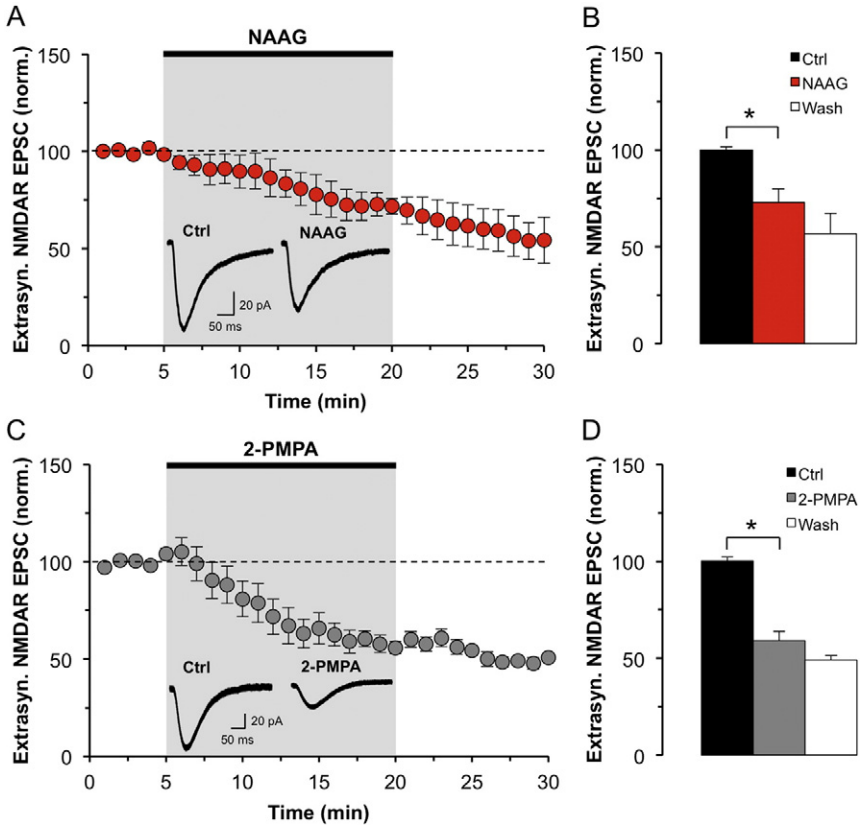

Fig. 2. Endogenous and exogenous NAAG inhibit extrasynaptic NMDAR EPSCs in acute hippocampal slices in physiological pH. (A) Average extrasynaptic NMDAR EPSC amplitudes plotted during a 15 min exogenous NAAG application followed by washout and compared to control (represented by a dotted line; n = 4 cells). Representative traces of extrasynaptic NMDAR EPSCs of a control and NAAG-treated CA1 pyramidal neuron are also shown. (B) Representative bar graph from data in (A) showing the average extrasynaptic NMDAR EPSC amplitudes 5 min before NAAG application (Ctrl), during the last 5 min of NAAG treatment (NAAG), and during washout (Wash). (C) Average amplitude of extrasynaptic NMDAR EPSCs plotted during a 15 min 2-PMPA application followed by washout and compared to control (represented by a dotted line) (n = 8 cells). Representative traces of extrasynaptic NMDAR EPSCs of a control and 2-PMPA-treated CA1 pyramidal neuron are also shown. (D) Representative bar graph from data in (C) showing the average extrasynaptic NMDAR EPSC amplitudes 5 min before 2-PMPA application (Ctrl), during the last 5 min of 2-PMPA treatment (2-PMPA), and during washout (Wash). The averages of the current amplitudes are normalized to the last 5 min of control in all cases. Data expressed as mean ± SEM. *, $p < 0.05$.

on extrasynaptic NMDARs in adult mice (Hardingham et al., 2002; Carpenter-Hyland et al., 2004; Harney et al., 2008; Imamura et al., 2008; Okamoto et al., 2009; Hardingham and Bading, 2010; Xia et al., 2010; Li et al., 2011). MK-801 (30 μM), an irreversible use-dependent NMDAR antagonist (Huettner and Bean, 1988), was used to block synaptic NMDARs. The glutamate reuptake inhibitor, DL-TBOA (30 μM), was then applied, allowing glutamate to diffuse away from the synapse and activate the extrasynaptic NMDAR population (Fig. S3B) (Clements et al., 1992). Analysis of extrasynaptic NMDAR EPSCs indicates that they are primarily GluN2B-containing due to their characteristically slow decay kinetics, as compared to the faster GluN2A-containing NMDARs (Table S1). To further verify NMDAR subunit distinction in our system we measured and demonstrated a difference in ifenprodil sensitivity on synaptic and extrasynaptic NMDARs. Following synaptic NMDAR isolation and a stable baseline recording, ifenprodil (3 μM) was bath applied for 15 min. We observed a significant 11 ± 3.2% increase in NMDAR-mediated EPSC amplitudes (n = 4 cells, $p < 0.05$; Fig. S3C). On the other hand, when ifenprodil was bath applied for 15 min following isolation of extrasynaptic NMDARs we observed a significant 49 ± 5.3% decrease in NMDAR-mediated EPSC amplitudes (n = 5 cells, $p < 0.05$; Fig. S3D). These findings clearly show an inhibition of extrasynaptic NMDARs by ifenprodil, however, no sign of inhibition of synaptic NMDARs. This demonstrates that NMDAR subunit composition is indeed different depending on the subcellular localization, with GluN2A- and GluN2B-containing receptors dominating synaptic and extrasynaptic sites, respectively. In addition, control experiments showing stable baseline recordings of NMDAR EPSCs over time in the absence of NAAG on both synaptic and extrasynaptic NMDARs are shown ($p > 0.05$; Fig. S4A, B). Following isolation of extrasynaptic NMDARs, NAAG or 2-PMPA was bath applied for 15 min, and we observed that both compounds significantly reduced the amplitude of the extrasynaptic NMDAR EPSC. In the presence of NAAG, the decrease in amplitude was 27 ± 6.9% (n = 4 cells, $p < 0.05$; Fig. 2A, B) and in the presence of 2-PMPA it was 41 ± 4.7% (n = 8 cells, $p < 0.05$; Fig. 2C, D). These data show that NAAG potentiates synaptic GluN2A-containing NMDAR EPSCs and inhibits extrasynaptic GluN2B-containing NMDAR EPSCs.

3.2. A Subunit-Specific Action of NAAG on GluN2A- and GluN2B-containing NMDARs in HEK293 Cells

In native tissue, synaptic and extrasynaptic NMDAR populations are not homogenously GluN2A- or GluN2B-containing, but include both with one dominating (Suarez et al., 2010; Tovar et al., 2013). In order to validate that NAAG has distinctive effects on NMDARs with different subunit compositions, we utilized an *in vitro* recombinant system. To establish cells containing a specified subunit makeup of NMDARs, HEK293 cells were transiently transfected with GluN1 in combination with either GluN2A or GluN2B subunits. Decay kinetics were measured for both GluN2A and GluN2B transfected HEK293 cells to ensure the correct subunit composition of the NMDARs. As expected, GluN2B-containing cells had slower kinetics than the GluN2A-containing cells (Table S1). Following application of NAAG on GluN2A-transfected HEK293 cells, there was a significant increase of 18 ± 3.4% in the NMDAR current

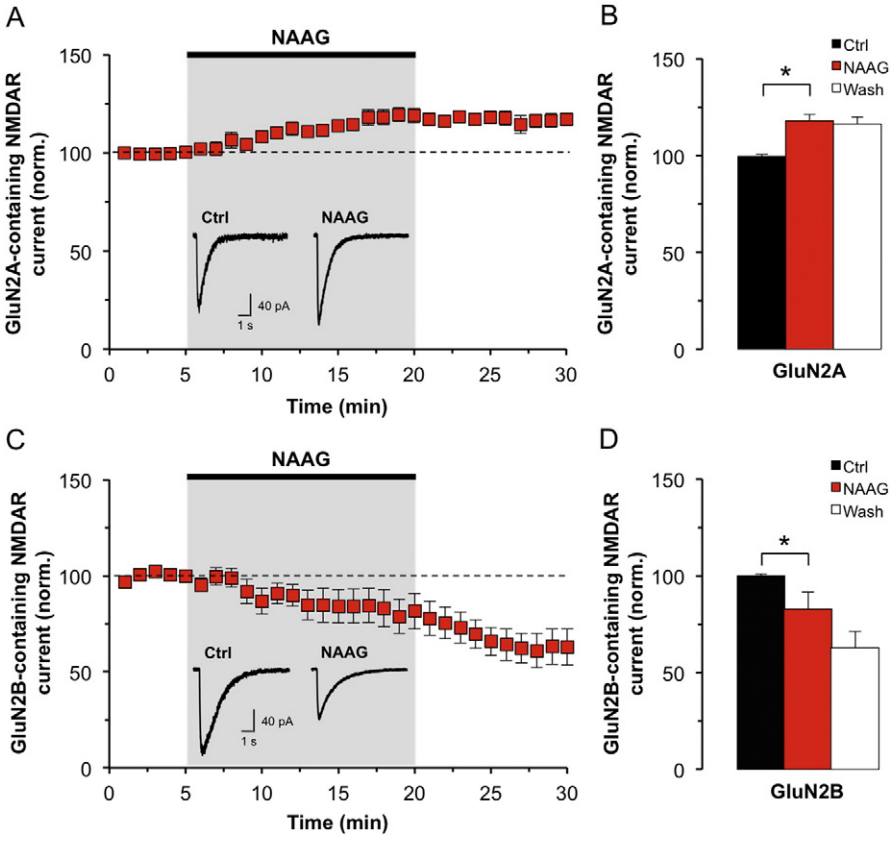

Fig. 3. NAAG potentiates GluN2A-containing NMDAR currents and inhibits GluN2B-containing NMDAR currents in HEK293 cells in physiological pH. (A) GluN1/GluN2A-transfected HEK293 cells were recorded and the average NMDAR current amplitudes were plotted during a 15 min treatment with exogenous NAAG and compared to control (represented by a dotted line) (n = 7 cells). Representative traces of NMDAR currents of a control and NAAG-treated HEK293 cell are also shown. (B) Representative bar graph from data in (A) showing the average of GluN2A-containing NMDAR current amplitudes 5 min before NAAG application (Ctrl), during the last 5 min of NAAG treatment (NAAG) and during washout (Wash). (C) GluN1/GluN2B-transfected HEK293 cells were recorded and the average NMDAR current amplitudes were plotted during a 15 min treatment with exogenous NAAG and compared to control (represented by a dotted line) (n = 9 cells). Representative traces of NMDAR currents of a control and NAAG-treated HEK293 cell are also shown. (D) Representative bar graph from data in (C) showing the average of GluN2B-containing NMDAR current amplitudes 5 min before NAAG application (Ctrl), during the last 5 min of NAAG treatment (NAAG), and during washout (Wash). The averages of the current amplitudes are normalized to the last 5 min of control in all cases. Data expressed as mean ± SEM. *, $p < 0.05$.

amplitude (n = 7 cells, $p < 0.05$; Fig. 3A, B). However, in the GluN2B-transfected HEK293 cells, there was a significant decrease of 18 ± 9.1% in the NMDAR current amplitude in the presence of NAAG (n = 9 cells, $p < 0.05$; Fig. 3C, D). Furthermore, we performed control experiments showing stable baseline recordings of NMDAR currents over time in the absence of NAAG in both GluN2A- and GluN2B-containing NMDARs ($p > 0.05$; Fig. S4C, D). The results from our HEK293 recordings are in agreement with the data obtained from acute hippocampal slices and further support that NAAG potentiates GluN2A-containing NMDAR currents, while inhibiting GluN2B-containing NMDAR currents.

3.3. The Effect of NAAG on NMDAR Function is Modulated by Protons in Acute Hippocampal Slices and HEK293 Cells

In addition to subunit specificity, the effect of NAAG on NMDARs could also be pH-dependent, whereby a higher potency in acidic ischemic conditions may underlie its neuroprotective mechanism (Shalaby et al., 1992; Pahk and Williams, 1997; Whittemore et al., 1997; Mott et al., 1998). We first established that the pH-dependent regulation of NMDARs occurs in our system. Synaptic and extrasynaptic NMDAR EPSCs were recorded in different pH conditions (6.5, 6.8, and 7.6) and normalized to baseline (pH 7.2). There was an 80 ± 3.2% reduction of the synaptic NMDAR EPSC amplitude at pH 6.5 (n = 10 cells, $p < 0.05$), and a 50 ± 3.9% reduction at pH 6.8 (n = 11 cells, $p < 0.05$). Additionally, changing the pH from 7.2 to 7.6 induced a 94 ± 21.1% increase in this NMDAR synaptic current (n = 10 cells, $p < 0.05$; Fig. S5). This change in pH also produced a very similar effect on extrasynaptic NMDARs. When the extracellular pH was decreased to 6.5, there was a 76 ± 4.9% reduction of the extrasynaptic NMDAR EPSC amplitude (n = 3 cells, $p < 0.05$), as well as a reduction of 51 ± 12.2% at pH 6.8 (n = 4 cells, $p < 0.05$). An increase in the extracellular pH to 7.6 resulted in a significant 34 ± 7.4% increase in the extrasynaptic NMDAR EPSC amplitude as compared to control (n = 4 cells, $p < 0.05$; Fig. S6).

The pH-dependent inhibitory effect was further validated in our *in vitro* system. Recording GluN2A-containing HEK293 cells at extracellular pH levels of 6.8 resulted in a 53 ± 7.6% decrease in the NMDAR current amplitude (n = 5 cells, $p < 0.05$), while at pH 7.6, there was a 45 ± 18.2% increase (n = 6 cells, $p < 0.05$; Fig. S7A, B). Similarly, when GluN2B-containing HEK293 cells were recorded at extracellular pH levels of 6.8 there was a 52 ± 5.6% decrease in the NMDAR current amplitude (n = 5 cells, $p < 0.05$), and a 44 ± 7.2% increase at pH 7.6 (n = 4 cells, $p < 0.05$; Fig. S7C, D). Our results show that protons modulate NMDAR function.

Next, the effect of NAAG on synaptic and extrasynaptic NMDAR activity under different pH conditions was investigated. NAAG was applied after establishing a stable baseline at pH 6.5, 6.8, or 7.6. In order to better visualize the effect of NAAG in different pH conditions, the initial pH-induced NMDAR current was treated as a control and normalized to 100%. Interestingly, NAAG decreased the synaptic NMDAR EPSC amplitude by 53 ± 5.5% at pH 6.5 (n = 7 cells, $p < 0.05$; Fig. 4A), and by 27 ± 5.7% at pH 6.8 (n = 6 cells, $p < 0.05$; Fig. 4B). The effect of 2-PMPA on NMDAR EPSCs was also evaluated in low pH (6.8) and similarly a decrease of 37 ± 8.4% was observed (n = 5, $p < 0.05$; Fig. S8). To confirm that the effect of 2-PMPA was specific to GCP-II inhibition and mediated by an increase in NAAG, we tested the effect of 2-PMSA on NMDAR EPSCs in acidic pH. We found no significant change

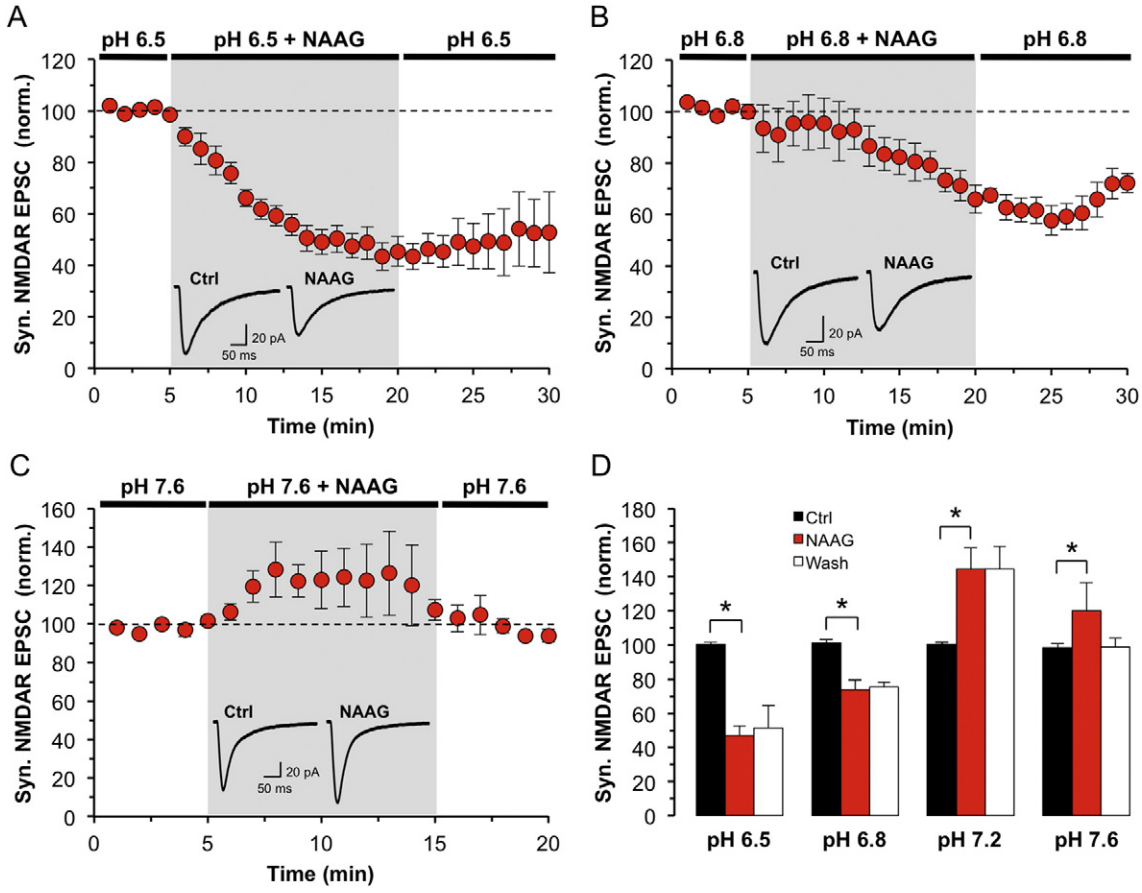

Fig. 4. NAAG decreases the activity of synaptic NMDARs during acidic conditions in acute hippocampal slices. The effects of NAAG on synaptic NMDAR-mediated EPSCs at pH 6.5 (n = 7 cells) (A), pH 6.8 (n = 6 cells) (B), and pH 7.6 (n = 5 cells) (C) were measured and plotted. The average NMDAR amplitudes following NAAG treatment and washout were normalized to their corresponding controls of pH change alone before NAAG application (control represented by dotted lines). (D) Representative bar graph of (A)–(C) showing the normalized average of synaptic NMDAR EPSC amplitudes in different pH conditions 5 min before NAAG application (Ctrl), the last 5 min of NAAG treatment (NAAG), and during washout (Wash). Data expressed as mean ± SEM. *, $p < 0.05$.

in the amplitude of the NMDAR EPSC (n = 3, $p > 0.05$; Fig. S1B). In contrast to what was observed in low pH (6.8), NAAG-induced a 44 ± 12.6% increase in the synaptic NMDAR EPSC amplitude at physiological pH of 7.2 as shown in Fig. 1A–B, as well as an 18 ± 16.5% increase at pH 7.6 (n = 5 cells, $p < 0.05$; Fig. 4C). These results are summarized in Fig. 4D. To rule out any effect of $mGluR_3$, we repeated the study in acidic pH (6.8) with either NAAG (n = 4) or 2-PMPA (n = 4) in the presence of the LY341495 compound ($p < 0.05$; Fig. S2B).

We further examined whether a change in pH could amplify the inhibitory effect of NAAG in the extrasynaptic population of NMDARs as shown in Fig. 2. Following application of NAAG at a lower pH of 6.5 or 6.8, there was a further significant reduction of extrasynaptic NMDAR EPSC amplitude as compared to physiological pH levels ($p < 0.05$). An extracellular pH level of 6.5 induced a 53 ± 7.3% decrease in the extrasynaptic NMDAR EPSC amplitude (n = 3 cells, $p < 0.05$; Fig. 5A), while an extracellular pH of 6.8 decreased it by 47 ± 9% (n = 6 cells, $p < 0.05$; Fig. 5B). On the other hand, when extracellular pH was increased to 7.6 there was a non-significant 2 ± 16.8% change in the extrasynaptic NMDAR EPSC amplitude (n = 5 cells, $p > 0.05$; Fig. 5C). These results are summarized in Fig. 5D.

Recombinant experiments with the HEK293 cells were again utilized to verify that the potency of NAAG at NMDARs is pH-dependent. The effect of NAAG on the activity of GluN2A- or GluN2B-containing NMDARs was evaluated at different pH levels. When GluN2A-containing HEK293 cells were recorded at extracellular pH of 6.8 in the presence of NAAG, there was a 25 ± 7.3% decrease in the NMDAR amplitude (n = 6 cells, $p < 0.05$), while at pH 7.6, the presence of NAAG resulted in an increase of 28 ± 11.6% (n = 6 cells, $p < 0.05$; Fig. 6A, B). Application of NAAG on GluN2B-containing HEK293 cells at extracellular pH of 6.8 caused a further reduction in the NMDAR amplitude as compared to physiological pH levels ($p < 0.05$; Fig. 6D), and resulted in a 37 ± 2.3% decrease in the NMDAR current (n = 5 cells, $p < 0.05$) compared to baseline, while no change was observed at pH 7.6 (n = 3 cells, $p > 0.05$; Fig. 6C, D). Altogether, these results show that the effect of NAAG on NMDARs is pH-dependent on both synaptic and extrasynaptic NMDARs, and the data is further confirmed using our HEK293 cells recombinant system with GluN2A- and GluN2B-containing NMDARs. In acidic conditions, NAAG decreases the current amplitude of synaptic NMDARs (GluN2A-containing), and further inhibits the activity of extrasynaptic NMDARs (GluN2B-containing).

3.4. In Acidic pH NAAG Upregulates the Surface Expression of GluN2A- but not GluN2B-containing NMDARs in the Hippocampus

The decrease in NMDAR EPSCs observed at low pH could potentially be attributed to a decrease in surface levels of the receptor. We therefore performed cell surface biotinylation on mouse hippocampal slices to compare the levels of NMDAR subunits in different pH conditions in the presence or absence of exogenous NAAG. Analysis of surface expression of NMDAR subunits at pH 6.8 showed no significant alterations (n = 4; $p > 0.05$), as well as no significant changes when the pH was increased to 7.6 (n = 4; $p > 0.05$; Fig. 7A, B). In addition, treatment with NAAG at physiological pH did not cause a significant change in GluN1 (n = 4; $p > 0.05$), GluN2A (n = 4; $p > 0.05$), or GluN2B (n = 4; $p > 0.05$) surface expression compared to the untreated control (Fig. 7C, D). Interestingly, when the pH was lowered to 6.8 in the

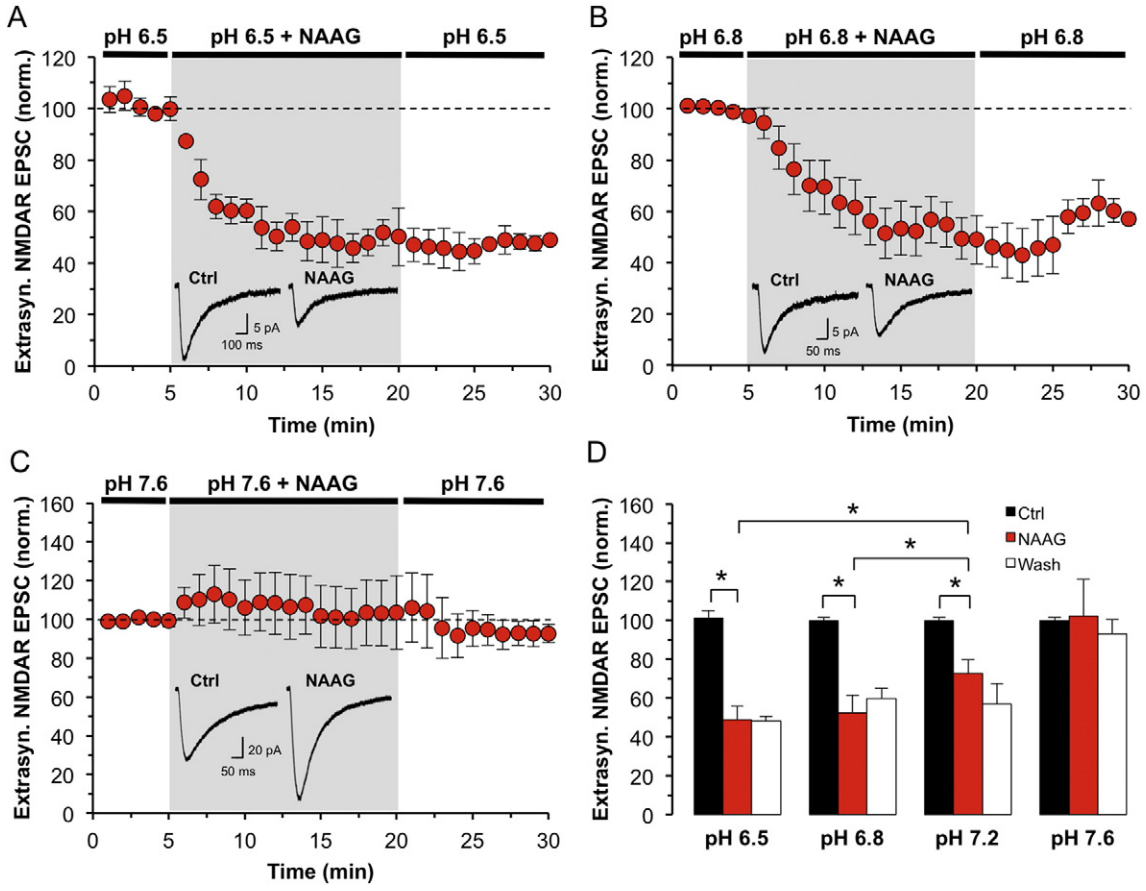

Fig. 5. NAAG further inhibits extrasynaptic NMDARs during acidic conditions in acute hippocampal slices. The effects of NAAG on isolated extrasynaptic NMDAR-mediated EPSCs at pH 6.5 (n = 3 cells) (A), pH 6.8 (n = 6 cells) (B), and pH 7.6 (n = 5 cells) (C) were measured and plotted. The average NMDAR amplitudes following NAAG treatment and washout were normalized to their corresponding controls of pH change alone before NAAG application (control represented by dotted lines). (D) Representative bar graph of (A)–(C) showing the normalized average of extrasynaptic NMDAR EPSC amplitudes in different pH conditions 5 min before NAAG application (Ctrl), the last 5 min of NAAG treatment (NAAG), and during washout (Wash). Data expressed as mean ± SEM. *, $p < 0.05$.

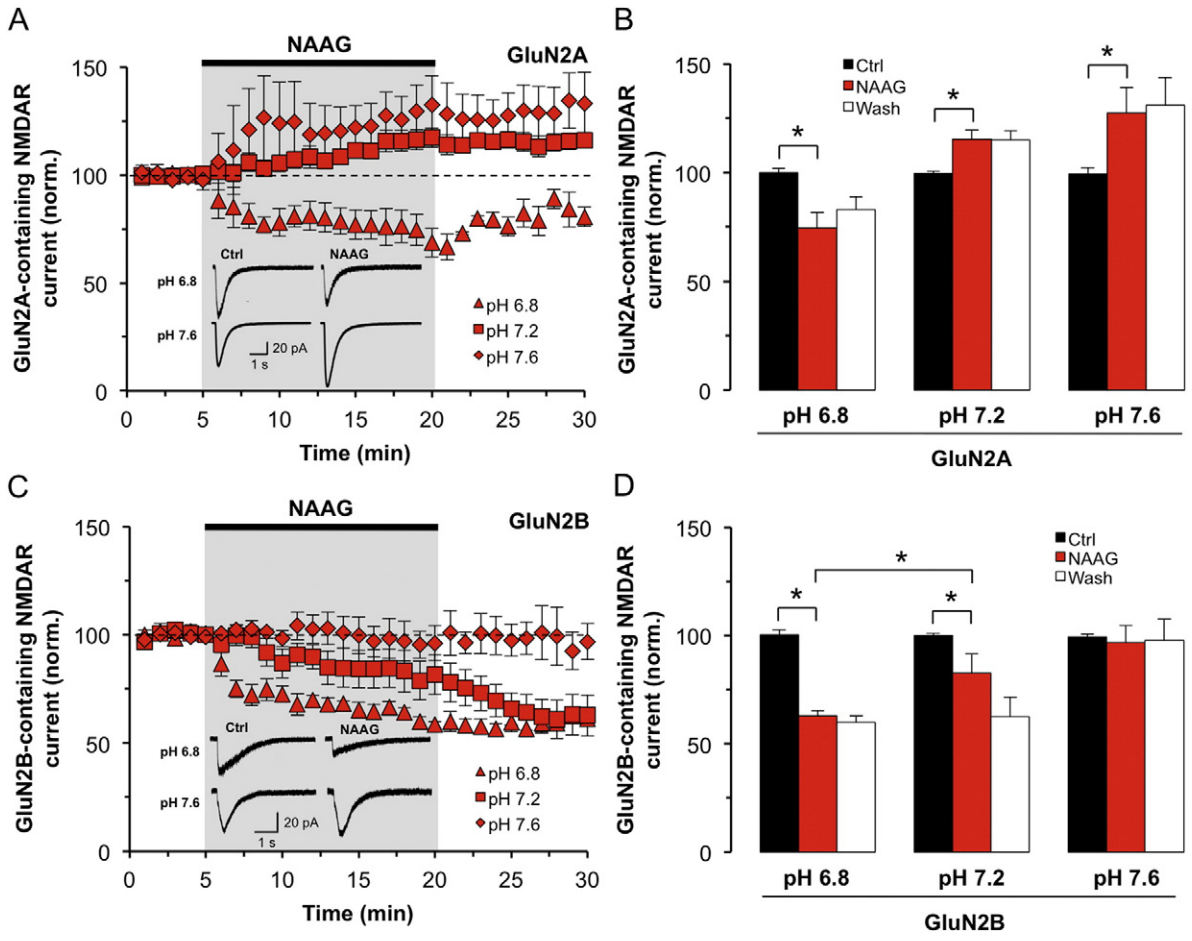

Fig. 6. In acidic conditions NAAG decreases the activity of both GluN2A- and GluN2B-containing NMDARs in HEK293 cells. (A) GluN1/GluN2A-transfected HEK293 cells were recorded in different pH conditions in the presence of NAAG and average NMDAR current amplitudes were plotted (pH 6.8, n = 6 cells; pH 7.2, n = 7 cells; and pH 7.6, n = 6 cells). The average NMDAR amplitudes following NAAG treatment and washout were normalized to their corresponding controls of pH change alone before NAAG application (control represented by a dotted line). (B) Representative bar graph of (A) showing the normalized average of GluN2A-containing NMDAR current amplitudes in different pH conditions 5 min before NAAG application (Ctrl), the last 5 min of NAAG treatment (NAAG), and during washout (Wash). (C) GluN1/GluN2B-transfected HEK293 cells were recorded in different pH conditions in the presence of NAAG and the normalized average NMDAR current amplitudes were plotted (pH 6.8, n = 5 cells; pH 7.2, n = 9 cells; and pH 7.6, n = 3 cells; control represented by a dotted line). (D) Representative bar graph of (C) showing the normalized average of GluN2B-containing NMDAR current amplitudes in different pH conditions 5 min before NAAG application (Ctrl), the last 5 min of NAAG treatment (NAAG), and during washout (Wash). Data expressed as mean ± SEM. *, $p < 0.05$.

presence of NAAG, there was a significant increase in the surface expression of GluN1 (60 ± 11.4%; n = 4; $p < 0.05$) and GluN2A (91 ± 24.6%; n = 4; $p < 0.05$) compared to physiological conditions with NAAG. These changes were unique to the GluN1 and GluN2A subunits since no significant differences in surface expression were detected for GluN2B (n = 4; $p > 0.05$; Fig. 7C, D). Moreover, there were no significant differences in the expression of any of the subunits when the pH was increased to 7.6 in the presence of NAAG (n = 4, $p > 0.05$) compared to physiological conditions with NAAG (Fig. 7C, D). These data show that the inhibitory effect of NAAG on GluN2B-containing NMDARs is not due to changes in receptor levels. Furthermore, in low pH conditions, NAAG increases the surface expression of GluN2A-containing NMDARs.

To further validate these results, we performed electrophysiological experiments on mouse hippocampal slices using a similar sequence of events. Following isolation of the synaptic NMDAR EPSC, we acquired a 5 min baseline recording. We then lowered the pH to 6.8 in the presence of NAAG for 15 min. Subsequently, the pH was brought back to 7.2 without NAAG. The synaptic NMDAR EPSC was recorded and we measured a significant 210 ± 43.2% increase in the amplitude as compared to the 5 min baseline recording (n = 5 cells, $p < 0.05$; Fig. 8A, B). Furthermore, we performed this protocol on extrasynaptic NMDARs and did not observe an increase in the EPSC following washout to pH 7.2, but rather a 74 ± 1.1% decrease (n = 3 cells, $p < 0.05$; Fig. 8C, D). To further investigate whether this increase in synaptic NMDAR EPSCs is truly an upregulation of the GluN2A subunit, we washed on ifenprodil, in place of NAAG, and detected no inhibitory effect but rather an 11 ± 3.1% increase in the synaptic NMDAR EPSC (n = 3 cells, $p < 0.05$; Fig. 8E, F). Altogether, these data show that, in acidic conditions, NAAG causes an upregulation of synaptic GluN2A-containing NMDARs.

4. Discussion

The data presented in this study (summarized in Fig. 9) demonstrate that the endogenous neuropeptide NAAG modulates NMDAR activity depending on its subunit composition and this effect is regulated by extracellular pH. Using whole-cell electrophysiological recordings from CA1 pyramidal neurons in acute brain slices and from HEK293 cells, we show that in physiological pH, NAAG inhibits GluN2B-containing NMDAR EPSCs, while potentiating GluN2A-containing NMDAR EPSCs. However, in low pH, NAAG inhibits both GluN2A- and GluN2B-containing NMDAR EPSCs. We also report, using cell surface biotinylation, that in acidic pH conditions NAAG increases the surface expression of GluN2A-containing NMDARs. Taken together, these results provide insight into the previously reported ambiguous effects of NAAG on NMDAR-mediated neuroprotection.

The physiological role of NAAG in neurotransmission has been a topic of controversy for the last two decades. While it has been shown

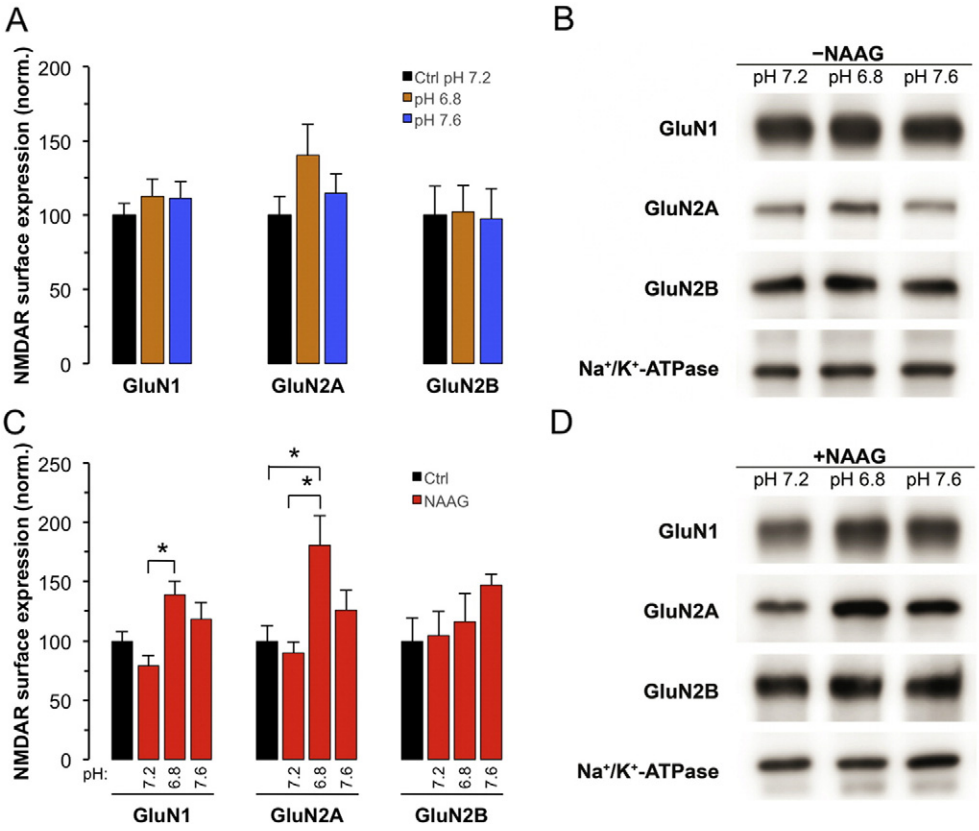

Fig. 7. In low pH NAAG increases the surface expression of GluN2A-containing NMDARs in the hippocampus. Representative bar graph (A) and Western blots (B) of biotinylated (surface) fractions from hippocampal tissue subjected to different pH conditions (6.8 and 7.6) and compared to control (pH 7.2). Representative bar graph (C) and Western blots (D) of biotinylated (surface) fractions from hippocampal tissue subjected to different pH conditions (6.8 and 7.6) in the presence of NAAG and compared to control (pH 7.2 with and without NAAG). NMDAR subunits were visualized by GluN1, GluN2A, and GluN2B specific antibodies, and Na^+/K^+-ATPase was used as a loading control. Bar graphs are expressed as mean ± SEM of n = 4 animals. *, $p < 0.05$.

by several groups that NAAG is a potent agonist at $mGluR_3$ (Wroblewska et al., 1993, 1997, 1998; Sanabria et al., 2004; Neale, 2011), there is controversy concerning the role of NAAG on NMDARs. Some groups have reported that NAAG behaves as an antagonist (Sekiguchi et al., 1989; Puttfarcken et al., 1993; Grunze et al., 1996; Bergeron et al., 2005, 2007), while others have described an agonist-like effect on NMDARs (Westbrook et al., 1986; Sekiguchi et al., 1992; Valivullah et al., 1994; Kolodziejczyk et al., 2009). On the other hand, some have claimed no significant effect of NAAG on NMDARs (Lea et al., 2001; Losi et al., 2004; Fricker et al., 2009). These discrepancies could be due to multiple factors, including differences in NMDAR subunit composition, which depends on the developmental stage of the animal and subcellular localization of the receptor, as well as the cell type and brain region under investigation. The generation of conflicting results could also be attributed to the experimental conditions in which NAAG and NMDARs are studied, such as variations in extracellular pH. The results of our investigation now provide some insight for these inconsistencies by demonstrating that NAAG can indeed have differential effects on NMDARs due to the intrinsic composition of the receptors, as well as the extracellular cues.

Synaptic and extrasynaptic NMDARs are known to mediate distinct physiological and pathological processes (Hardingham and Bading, 2010). NMDAR subunit compositions have different effects on synaptic function depending on their regional and developmental expression, their subcellular location (synaptic or extrasynaptic) and their coupling to downstream signaling cascades. NMDAR subunit composition differs throughout development, from being predominantly GluN2B-containing to GluN2A-containing at maturation. In the adult hippocampus, GluN2A-containing NMDARs are dominant at the synapse, while GluN2B-containing NMDARs are located extrasynaptically (Cull-Candy et al., 2001; van Zundert et al., 2004; Mony et al., 2009a; Sanz-Clemente et al., 2013). By uncoupling the effect of NAAG on synaptic and extrasynaptic NMDARs in older animals, and specifically studying its effect on GluN2A- and GluN2B-containing NMDARs, we revealed that NAAG has dual functions. Furthermore, several studies have shown that increasing NAAG, through exogenous application (Lu et al., 2000; Cai et al., 2002) or blocking its degradation (Slusher et al., 1999; Tortella et al., 2000), is neuroprotective during brain ischemia. Indeed, the enhanced effect of NAAG inhibition on NMDARs under acidic conditions, such as that observed during stroke, may provide an explanation for these convincing data. In addition, our data clarifies why some studies have shown a specific neuroprotective effect of NAAG under ischemic conditions, whereas others have shown no antagonistic effect of NAAG on NMDARs when studied in physiological pH conditions.

The differential effect of NAAG on GluN2A- and GluN2B-containing NMDARs can have therapeutic advantages since NMDARs with different subunit composition and localization have been shown to have different downstream effects. Synaptic GluN2A-containing NMDARs are generally associated with neuronal survival, whereas activation of extrasynaptic GluN2B-containing NMDARs is coupled to cell death pathways. Synaptic and extrasynaptic NMDARs have opposing effects on the function of cAMP response element binding protein (CREB), gene regulation and cell fate (Vanhoutte and Bading, 2003; Hardingham and Bading, 2010; Parsons and Raymond, 2014). The transcription factor CREB is responsible for regulating the expression of many proteins, including the brain-derived neurotrophic factor (BDNF), which is important for neuronal survival (Shaywitz and Greenberg, 1999; West et al., 2001). The entry of Ca^{2+} through synaptic GluN2A-containing NMDARs induces CREB activity and BDNF gene expression, which initiates pro-survival programs by reducing the expression of pro-apoptotic factors. In contrast, Ca^{2+} entry though extrasynaptic GluN2B-containing NMDARs activates the CREB

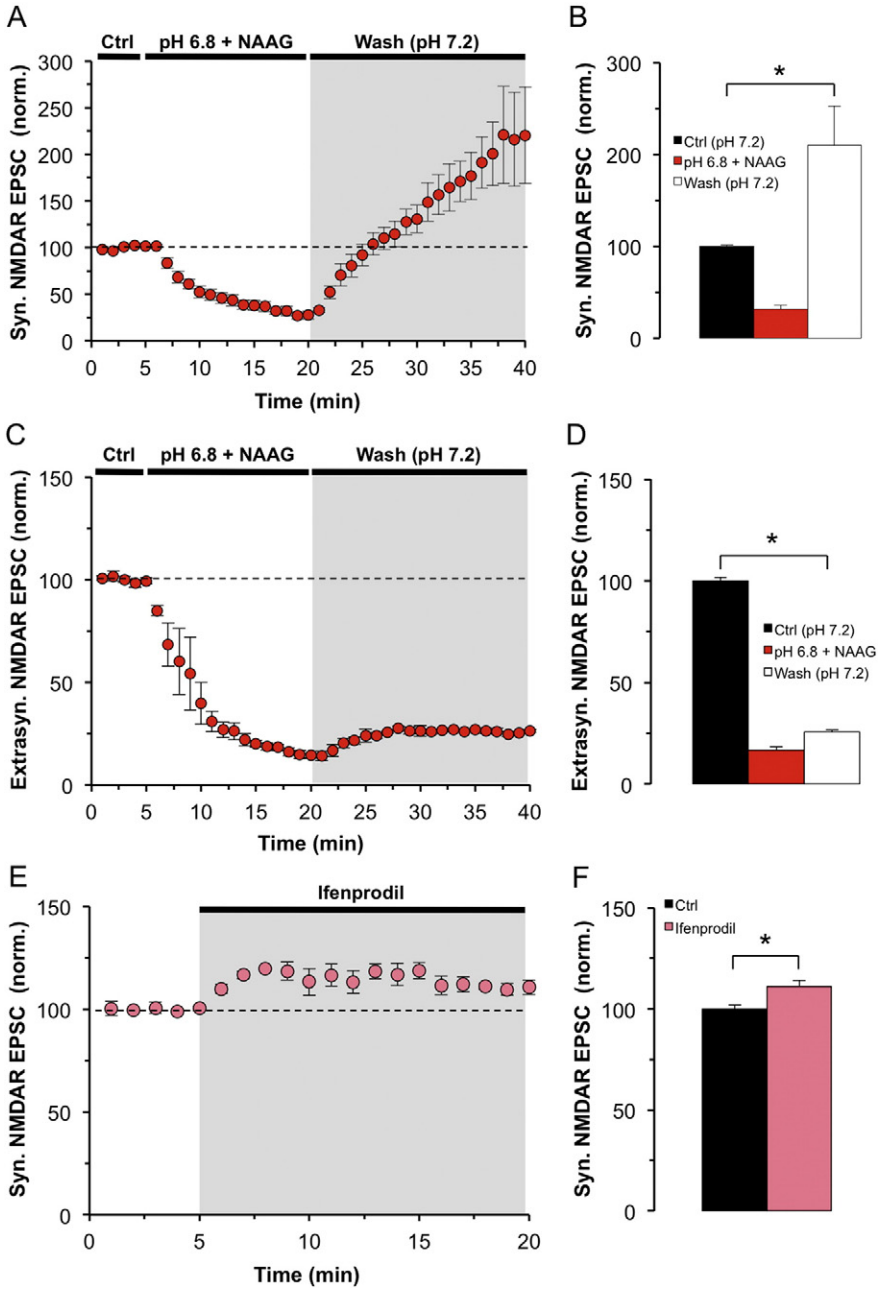

Fig. 8. The activity of synaptic NMDARs increases following low pH and NAAG application in acute hippocampal slices. Average amplitudes of evoked synaptic (A) and extrasynaptic (C) NMDAR EPSCs were plotted following a 15 min treatment of low pH (6.8) in the presence of NAAG. The pH was subsequently brought back to 7.2 (without NAAG) and compared to the 5 min baseline recording (control at pH 7.2 represented by a dotted line; n = 5 and 3 cells respectively). (B) Representative bar graph from data in (A) showing the average synaptic NMDAR EPSC amplitudes 5 min before pH 6.8 and NAAG application (Ctrl (pH 7.2)), during the last 5 min of treatment (pH 6.8 + NAAG), and during washout back to pH 7.2 following pH 6.8 + NAAG (Wash (pH 7.2)). (D) Representative bar graph from data in (C) showing the average extrasynaptic NMDAR EPSC amplitudes 5 min before pH 6.8 and NAAG application (Ctrl (pH 7.2)), during the last 5 min of treatment (pH 6.8 + NAAG), and during washout back to pH 7.2 following pH 6.8 + NAAG (Wash (pH 7.2)). (E) Average synaptic NMDAR EPSC amplitudes plotted during a 15 min application of ifenprodil and compared to the last 5 min of wash (pH 7.2) depicted in (A) and (B) (control represented by a dotted line; n = 3 cells). (F) Representative bar graph showing the average synaptic NMDAR EPSC amplitudes 5 min before ifenprodil application (Ctrl) and during the last 5 min of ifenprodil treatment (Ifenprodil). The averages of the current amplitudes are normalized to the last 5 min of control in all cases. Data expressed as mean ± SEM. *, $p < 0.05$.

shut-off pathway, which inhibits BDNF gene expression and initiates the cell death pathway causing loss of mitochondrial membrane potential, an early marker for glutamate-mediated neuronal damage (Hardingham et al., 2002; Kaufman et al., 2012). There is evidence suggesting that increased activation of GluN2B-containing extrasynaptic NMDARs contributes, at least in part, to the toxicity seen in neurodegenerative disorders such as Huntington's and Alzheimer's disease (Parsons and Raymond, 2014). It has also been reported that the levels of NAAG in these diseases are altered, and the brains of affected individuals show evidence of widespread loss of NAAG-positive neurons (Jaarsma et al., 1994; Passani et al., 1997). Hence, NAAG may not only be therapeutically beneficial in the treatment of ischemic events, but may also play an important role in neurodegenerative disorders by decreasing the activity of GluN2B-containing extrasynaptic NMDARs. Therefore, neuroprotective therapies should aim to both enhance the effect of synaptic activity and disrupt extrasynaptic NMDAR-dependent death signaling.

The mechanism of action of NAAG on NMDARs remains unclear, however, its effect may be allosterically modulated. An allosteric mechanism would allow for subunit-specific modulation of NMDARs, as well as a pH-dependent effect on its function (Mony et al., 2009a; Zhu and

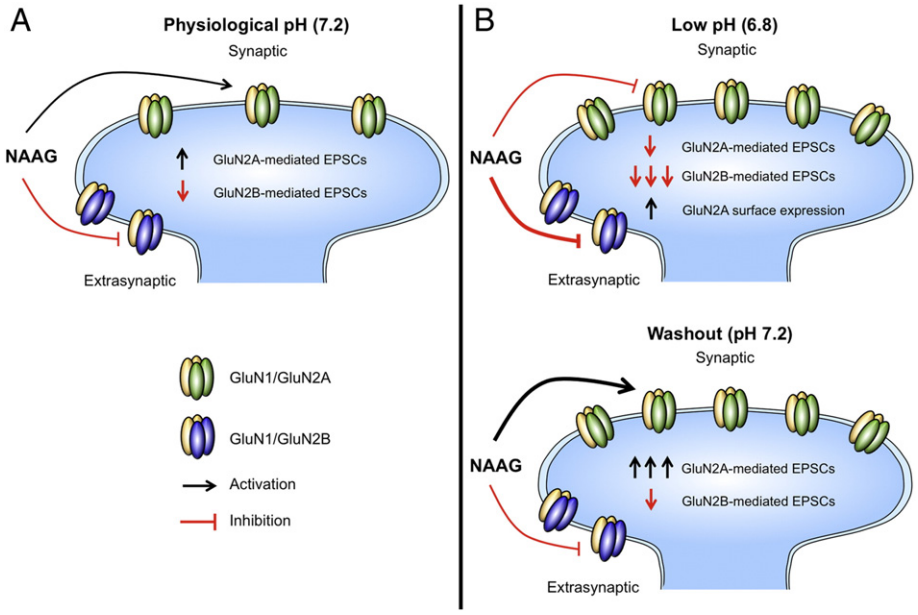

Fig. 9. Schematic diagram summarizing the effect of NAAG on NMDARs in various conditions. (A) In physiological pH (7.2), NAAG increases the activity of synaptic GluN2A-containing NMDARs and inhibits extrasynaptic GluN2B-containing NMDARs. (B) In low pH (6.8), NAAG inhibits synaptic GluN2A-containing NMDAR EPSCs, while further inhibiting extrasynaptic GluN2B-containing NMDAR EPSCs. The presence of NAAG in low pH conditions also upregulates the surface expression of synaptic NMDARs. When the pH is brought back to 7.2 (washout) following a period of acidity, there is an increase in synaptic NMDAR EPSC as compared to control. In this setting, similar to a reperfusion scenario, NAAG would be capable of overactivating the upregulated synaptic GluN2A-containing NMDARs, while maintaining its inhibitory effect on extrasynaptic GluN2B-containing NMDARs.

Paoletti, 2015). Ifenprodil is a subunit-selective allosteric inhibitor of GluN2B-containing NMDARs (Williams, 1993). Additionally, ifenprodil modifies proton sensitivity and alters NMDAR function by shifting the pKa of the proton sensor (Mott et al., 1998). The proton sensor is closely associated to the gating mechanism of NMDARs (Tang et al., 1990; Low et al., 2003; Banke et al., 2005; Chang and Kuo, 2008) and a change in its sensitivity to protons is a common downstream mechanism of several NMDAR allosteric modulators (Traynelis et al., 1995; Mott et al., 1998; Choi and Lipton, 1999; Low et al., 2000). Our study indicates that the interaction between NAAG and NMDARs is subunit-specific and likely linked to the proton sensor, therefore pointing to an allosteric mechanism. There are a number of possible mechanisms by which NAAG can affect NMDARs in situations of altered pH. NAAG could potentially act by enhancing the NMDAR sensitivity to proton inhibition by inducing a conformational change within the receptor. This speculation of the possible interaction between NAAG and NMDARs is supported by our inability to washout the effect of NAAG in our experiments, possibly due to a long lasting effect. This lack of washout has similarly been observed in other studies utilizing NAAG (Sanabria et al., 2004; Bergeron et al., 2007; Walder et al., 2013). However, we cannot exclude the possibility that protons may directly affect the binding site of NAAG on NMDARs, thereby modifying the coupling between binding of NAAG and inhibition of NMDAR channel gating. In this case, if NAAG were directly binding to NMDARs, the lack of washout could be attributed to a slow dissociation rate. Identifying how pH and NMDAR subunit composition affects the regulation of NMDARs by NAAG is vital, not only from a physiological standpoint, but also from a pharmacological perspective.

GluN2A- and GluN2B-containing NMDARs are regulated independently depending on synaptic activity (Shipton and Paulsen, 2014). Interestingly, it has been shown that blocking NMDARs upregulates GluN2A-containing NMDARs, whereas GluN2B-containing NMDARs are not affected (von Engelhardt et al., 2009). In agreement with this study, we show that the inhibitory effect of NAAG at low pH results in a drastic increase in surface expression of GluN2A- but not GluN2B-containing NMDARs, suggesting a more complex role of NAAG in the regulation of NMDARs. Our findings provide insight into the dual role of NAAG on NMDARs during an ischemic event in which it can inhibit extrasynaptic GluN2B-containing NMDAR-dependent death signaling, while up-regulating GluN2A receptors and enhancing their activity. Although this population of increased GluN2A-containing NMDARs would remain inactive at low pH as shown in our results, we propose that they may contribute to the neuroprotective effect of NAAG following reperfusion. In this scenario, reperfusion of the ischemic region and return to a physiological extracellular environment (pH 7.2) would allow NAAG to activate the upregulated GluN2A-containing NMDARs to mediate pro-survival signals, while maintaining its inhibitory effect on the pro-death GluN2B-containing NMDARs (Fellman and Raivio, 1997; White et al., 2000).

To address the challenges of stroke prevention or treatment, it would be beneficial to identify a prophylactic drug for those at risk, since early drug administration has been shown to be neuroprotective in animal models of ischemia. Demonstrating that the potency of some compounds, such as NAAG or 2-PMPA, is increased at lower pH, provides an interesting pharmacological avenue. The new information provided here can be used for future studies aimed at the synthesis of GCP-II inhibitors that are inactive at physiological pH but become therapeutically effective in the acidic environment that arise in pathological conditions. The results of this study reveal a modulatory effect of NAAG on NMDARs depending on protons as well as NMDAR subunit composition and localization, and highlight a novel aspect of the function of NAAG. Since rodents and humans share similar NMDAR expression patterns, as well as pH regulation (Law et al., 2003; Casey et al., 2010; Orlowski et al., 2011), it is plausible that NAAG can induce comparable effects in both. Altogether, these findings suggest NAAG as a valuable therapeutic agent in the treatment of ischemic events.

Acknowledgments

The authors thank Dr. Barbara Slusher from the Johns Hopkins University School of Medicine for providing 2-PMSA, Dr. Jean-Claude Béïque from the University of Ottawa for offering helpful insight and discussion, and Dr. Mireille Khacho from the University of Ottawa for assistance in writing and proof reading. The work was supported by operating grants from the Canadian Institutes of Health Research

(CIHR MOP-79360) awarded to R.B. The authors declare no conflicts of interest.

Appendix A. Supplementary data

Supplementary data to this article can be found online at http://dx.doi.org/10.1016/j.nbd.2015.08.017.

References

Banke, T.G., Dravid, S.M., Traynelis, S.F., 2005. Protons trap NR1/NR2B NMDA receptors in a nonconducting state. J. Neurosci. 25, 42–51.

Bellone, C., Nicoll, R.A., 2007. Rapid bidirectional switching of synaptic NMDA receptors. Neuron 55, 779–785.

Bergeron, R., Coyle, J.T., 2012. NAAG, NMDA receptor and psychosis. Curr. Med. Chem. 19, 1360–1364.

Bergeron, R., Coyle, J.T., Tsai, G., Greene, R.W., 2005. NAAG reduces NMDA receptor current in CA1 hippocampal pyramidal neurons of acute slices and dissociated neurons. Neuropsychopharmacology 30, 7–16.

Bergeron, R., Imamura, Y., Frangioni, J.V., Greene, R.W., Coyle, J.T., 2007. Endogenous N-acetylaspartylglutamate reduced NMDA receptor-dependent current neurotransmission in the CA1 area of the hippocampus. J. Neurochem. 100, 346–357.

Cai, Z., Lin, S., Rhodes, P.G., 2002. Neuroprotective effects of N-acetylaspartylglutamate in a neonatal rat model of hypoxia–ischemia. Eur. J. Pharmacol. 437, 139–145.

Carpenter-Hyland, E.P., Woodward, J.J., Chandler, L.J., 2004. Chronic ethanol induces synaptic but not extrasynaptic targeting of NMDA receptors. J. Neurosci. 24, 7859–7868.

Casey, J.R., Grinstein, S., Orlowski, J., 2010. Sensors and regulators of intracellular pH. Nat. Rev. Mol. Cell Biol. 11, 50–61.

Chang, H.R., Kuo, C.C., 2008. The activation gate and gating mechanism of the NMDA receptor. J. Neurosci. 28, 1546–1556.

Choi, Y.B., Lipton, S.A., 1999. Identification and mechanism of action of two histidine residues underlying high-affinity Zn^{2+} inhibition of the NMDA receptor. Neuron 23, 171–180.

Clements, J.D., Lester, R.A., Tong, G., Jahr, C.E., Westbrook, G.L., 1992. The time course of glutamate in the synaptic cleft. Science 258, 1498–1501.

Cull-Candy, S., Brickley, S., Farrant, M., 2001. NMDA receptor subunits: diversity, development and disease. Curr. Opin. Neurobiol. 11, 327–335.

Doroshenko, P., Renaud, L.P., 2009. Acid-sensitive TASK-like K^+ conductances contribute to resting membrane potential and to orexin-induced membrane depolarization in rat thalamic paraventricular nucleus neurons. Neuroscience 158, 1560–1570.

Doyle, K.P., Simon, R.P., Stenzel-Poore, M.P., 2008. Mechanisms of ischemic brain damage. Neuropharmacology 55, 310–318.

Dravid, S.M., Erreger, K., Yuan, H., Nicholson, K., Le, P., Lyuboslavsky, P., Almonte, A., Murray, E., Mosely, C., Barber, J., French, A., Balster, R., Murray, T.F., Traynelis, S.F., 2007. Subunit-specific mechanisms and proton sensitivity of NMDA receptor channel block. J. Physiol. 581, 107–128.

Fellman, V., Raivio, K.O., 1997. Reperfusion injury as the mechanism of brain damage after perinatal asphyxia. Pediatr. Res. 41, 599–606.

Fricker, A.C., Mok, M.H., de la Flor, R., Shah, A.J., Woolley, M., Dawson, L.A., Kew, J.N., 2009. Effects of N-acetylaspartylglutamate (NAAG) at group II mGluRs and NMDAR. Neuropharmacology 56, 1060–1067.

Gardoni, F., Di Luca, M., 2006. New targets for pharmacological intervention in the glutamatergic synapse. Eur. J. Pharmacol. 545, 2–10.

Grunze, H.C., Rainnie, D.G., Hasselmo, M.E., Barkai, E., Hearn, E.F., McCarley, R.W., Greene, R.W., 1996. NMDA-dependent modulation of CA1 local circuit inhibition. J. Neurosci. 16, 2034–2043.

Hardingham, G.E., Bading, H., 2010. Synaptic versus extrasynaptic NMDA receptor signalling: implications for neurodegenerative disorders. Nat. Rev. Neurosci. 11, 682–696.

Hardingham, G.E., Fukunaga, Y., Bading, H., 2002. Extrasynaptic NMDARs oppose synaptic NMDARs by triggering CREB shut-off and cell death pathways. Nat. Neurosci. 5, 405–414.

Harney, S.C., Jane, D.E., Anwyl, R., 2008. Extrasynaptic NR2D-containing NMDARs are recruited to the synapse during LTP of NMDAR-EPSCs. J. Neurosci. 28, 11685–11694.

Huettner, J.E., Bean, B.P., 1988. Block of N-methyl-D-aspartate-activated current by the anticonvulsant MK-801: selective binding to open channels. Proc. Natl. Acad. Sci. U. S. A. 85, 1307–1311.

Ikonomidou, C., Turski, L., 2002. Why did NMDA receptor antagonists fail clinical trials for stroke and traumatic brain injury? Lancet Neurol. 1, 383–386.

Imamura, Y., Ma, C.L., Pabba, M., Bergeron, R., 2008. Sustained saturating level of glycine induces changes in NR2B-containing-NMDA receptor localization in the CA1 region of the hippocampus. J. Neurochem. 105, 2454–2465.

Jaarsma, D., Veenma-van der Duin, L., Korf, J., 1994. N-acetylaspartate and N-acetylaspartylglutamate levels in Alzheimer's disease post-mortem brain tissue. J. Neurol. Sci. 127, 230–233.

Jackson, P.F., Cole, D.C., Slusher, B.S., Stetz, S.L., Ross, L.E., Donzanti, B.A., Trainor, D.A., 1996. Design, synthesis, and biological activity of a potent inhibitor of the neuropeptidase N-acetylated alpha-linked acidic dipeptidase. J. Med. Chem. 39, 619–622.

Kaufman, A.M., Milnerwood, A.J., Sepers, M.D., Coquinco, A., She, K., Wang, L., Lee, H., Craig, A.M., Cynader, M., Raymond, L.A., 2012. Opposing roles of synaptic and extrasynaptic NMDA receptor signaling in cocultured striatal and cortical neurons. J. Neurosci. 32, 3992–4003.

Kolodziejczyk, K., Hamilton, N.B., Wade, A., Karadottir, R., Attwell, D., 2009. The effect of N-acetyl-aspartyl-glutamate and N-acetyl-aspartate on white matter oligodendrocytes. Brain 132, 1496–1508.

Law, A.J., Weickert, C.S., Webster, M.J., Herman, M.M., Kleinman, J.E., Harrison, P.J., 2003. Expression of NMDA receptor NR1, NR2A and NR2B subunit mRNAs during development of the human hippocampal formation. Eur. J. Neurosci. 18, 1197–1205.

Lea, PMt, Wroblewska, B., Sarvey, J.M., Neale, J.H., 2001. beta-NAAG rescues LTP from blockade by NAAG in rat dentate gyrus via the type 3 metabotropic glutamate receptor. J. Neurophysiol. 85, 1097–1106.

Li, S., Jin, M., Koeglsperger, T., Shepardson, N.E., Shankar, G.M., Selkoe, D.J., 2011. Soluble Abeta oligomers inhibit long-term potentiation through a mechanism involving excessive activation of extrasynaptic NR2B-containing NMDA receptors. J. Neurosci. 31, 6627–6638.

Loftis, J.M., Janowsky, A., 2003. The N-methyl-D-aspartate receptor subunit NR2B: localization, functional properties, regulation, and clinical implications. Pharmacol. Ther. 97, 55–85.

Losi, G., Vicini, S., Neale, J., 2004. NAAG fails to antagonize synaptic and extrasynaptic NMDA receptors in cerebellar granule neurons. Neuropharmacology 46, 490–496.

Low, C.M., Zheng, F., Lyuboslavsky, P., Traynelis, S.F., 2000. Molecular determinants of coordinated proton and zinc inhibition of N-methyl-D-aspartate NR1/NR2A receptors. Proc. Natl. Acad. Sci. U. S. A. 97, 11062–11067.

Low, C.M., Lyuboslavsky, P., French, A., Le, P., Wyatte, K., Thiel, W.H., Marchan, E.M., Igarashi, K., Kashiwagi, K., Gernert, K., Williams, K., Traynelis, S.F., Zheng, F., 2003. Molecular determinants of proton-sensitive N-methyl-D-aspartate receptor gating. Mol. Pharmacol. 63, 1212–1222.

Lu, X.M., Tang, Z., Liu, W., Lin, Q., Slusher, B.S., 2000. N-acetylaspartylglutamate protects against transient focal cerebral ischemia in rats. Eur. J. Pharmacol. 408, 233–239.

Mony, L., Kew, J.N., Gunthorpe, M.J., Paoletti, P., 2009a. Allosteric modulators of NR2B-containing NMDA receptors: molecular mechanisms and therapeutic potential. Br. J. Pharmacol. 157, 1301–1317.

Mony, L., Krzaczkowski, L., Leonetti, M., Le Goff, A., Alarcon, K., Neyton, J., Bertrand, H.O., Acher, F., Paoletti, P., 2009b. Structural basis of NR2B-selective antagonist recognition by N-methyl-D-aspartate receptors. Mol. Pharmacol. 75, 60–74.

Mott, D.D., Doherty, J.J., Zhang, S., Washburn, M.S., Fendley, M.J., Lyuboslavsky, P., Traynelis, S.F., Dingledine, R., 1998. Phenylethanolamines inhibit NMDA receptors by enhancing proton inhibition. Nat. Neurosci. 1, 659–667.

Nagel, J., Belozertseva, I., Greco, S., Kashkin, V., Malyshkin, A., Jirgensons, A., Shekunova, E., Eilbacher, B., Bespalov, A., Danysz, W., 2006. Effects of NAAG peptidase inhibitor 2-PMPA in model chronic pain — relation to brain concentration. Neuropharmacology 51, 1163–1171.

Neale, J.H., 2011. N-acetylaspartylglutamate is an agonist at mGluR(3) in vivo and in vitro. J. Neurochem. 119, 891–895.

Neale, J.H., Olszewski, R.T., Gehl, L.M., Wroblewska, B., Bzdega, T., 2005. The neurotransmitter N-acetylaspartylglutamate in models of pain, ALS, diabetic neuropathy, CNS injury and schizophrenia. Trends Pharmacol. Sci. 26, 477–484.

Neale, J.H., Olszewski, R.T., Zuo, D., Janczura, K.J., Profaci, C.P., Lavin, K.M., Madore, J.C., Bzdega, T., 2011. Advances in understanding the peptide neurotransmitter NAAG and appearance of a new member of the NAAG neuropeptide family. J. Neurochem. 118, 490–498.

Okamoto, S., Pouladi, M.A., Talantova, M., Yao, D., Xia, P., Ehrnhoefer, D.E., Zaidi, R., Clemente, A., Kaul, M., Graham, R.K., Zhang, D., Vincent Chen, H.S., Tong, G., Hayden, M.R., Lipton, S.A., 2009. Balance between synaptic versus extrasynaptic NMDA receptor activity influences inclusions and neurotoxicity of mutant huntingtin. Nat. Med. 15, 1407–1413.

Orlowski, P., Chappell, M., Park, C.S., Grau, V., Payne, S., 2011. Modelling of pH dynamics in brain cells after stroke. Interface Focus 1, 408–416.

Pabba, M., Wong, A.Y., Ahlskog, N., Hristova, E., Biscaro, D., Nassrallah, W., Ngsee, J.K., Snyder, M., Beique, J.C., Bergeron, R., 2014. NMDA receptors are upregulated and trafficked to the plasma membrane after sigma-1 receptor activation in the rat hippocampus. J. Neurosci. 34, 11325–11338.

Pahk, A.J., Williams, K., 1997. Influence of extracellular pH on inhibition by ifenprodil at N-methyl-D-aspartate receptors in *Xenopus* oocytes. Neurosci. Lett. 225, 29–32.

Paoletti, P., Bellone, C., Zhou, Q., 2013. NMDA receptor subunit diversity: impact on receptor properties, synaptic plasticity and disease. Nat. Rev. Neurosci. 14, 383–400.

Parsons, M.P., Raymond, L.A., 2014. Extrasynaptic NMDA receptor involvement in central nervous system disorders. Neuron 82, 279–293.

Passani, L.A., Vonsattel, J.P., Carter, R.E., Coyle, J.T., 1997. N-acetylaspartylglutamate, N-acetylaspartate, and N-acetylated alpha-linked acidic dipeptidase in human brain and their alterations in Huntington and Alzheimer's diseases. Mol. Chem. Neuropathol. 31, 97–118.

Puttfarcken, P.S., Handen, J.S., Montgomery, D.T., Coyle, J.T., Werling, L.L., 1993. N-acetylaspartylglutamate modulation of N-methyl-D-aspartate-stimulated [^{3}H]norepinephrine release from rat hippocampal slices. J. Pharmacol. Exp. Ther. 266, 796–803.

Sanabria, E.R., Wozniak, K.M., Slusher, B.S., Keller, A., 2004. GCP II (NAALADase) inhibition suppresses mossy fiber-CA3 synaptic neurotransmission by a presynaptic mechanism. J. Neurophysiol. 91, 182–193.

Sanz-Clemente, A., Nicoll, R.A., Roche, K.W., 2013. Diversity in NMDA receptor composition: many regulators, many consequences. Neuroscientist 19, 62–75.

Sekiguchi, M., Okamoto, K., Sakai, Y., 1989. Low-concentration N-acetylaspartylglutamate suppresses the climbing fiber response of Purkinje cells in guinea pig cerebellar slices and the responses to excitatory amino acids of *Xenopus laevis* oocytes injected with cerebellar mRNA. Brain Res. 482, 87–96.

Sekiguchi, M., Wada, K., Wenthold, R.J., 1992. N-acetylaspartylglutamate acts as an agonist upon homomeric NMDA receptor (NMDAR1) expressed in *Xenopus* oocytes. FEBS Lett. 311, 285–289.

Shalaby, I.A., Chenard, B.L., Prochniak, M.A., Butler, T.W., 1992. Neuroprotective effects of the N-methyl-D-aspartate receptor antagonists ifenprodil and SL-82,0715 on hippocampal cells in culture. J. Pharmacol. Exp. Ther. 260, 925–932.
Shaywitz, A.J., Greenberg, M.E., 1999. CREB: a stimulus-induced transcription factor activated by a diverse array of extracellular signals. Annu. Rev. Biochem. 68, 821–861.
Shipton, O.A., Paulsen, O., 2014. GluN2A and GluN2B subunit-containing NMDA receptors in hippocampal plasticity. Philos. Trans. R. Soc. Lond. B Biol. Sci. 369, 20130163.
Slusher, B.S., Vornov, J.J., Thomas, A.G., Hurn, P.D., Harukuni, I., Bhardwaj, A., Traystman, R.J., Robinson, M.B., Britton, P., Lu, X.C., Tortella, F.C., Wozniak, K.M., Yudkoff, M., Potter, B.M., Jackson, P.F., 1999. Selective inhibition of NAALADase, which converts NAAG to glutamate, reduces ischemic brain injury. Nat. Med. 5, 1396–1402.
Suarez, F., Zhao, Q., Monaghan, D.T., Jane, D.E., Jones, S., Gibb, A.J., 2010. Functional heterogeneity of NMDA receptors in rat substantia nigra pars compacta and reticulata neurones. Eur. J. Neurosci. 32, 359–367.
Tang, C.M., Dichter, M., Morad, M., 1990. Modulation of the N-methyl-D-aspartate channel by extracellular H^+. Proc. Natl. Acad. Sci. U. S. A. 87, 6445–6449.
Tortella, F.C., Lin, Y., Ved, H., Slusher, B.S., Dave, J.R., 2000. Neuroprotection produced by the NAALADase inhibitor 2-PMPA in rat cerebellar neurons. Eur. J. Pharmacol. 402, 31–37.
Tovar, K.R., Westbrook, G.L., 1999. The incorporation of NMDA receptors with a distinct subunit composition at nascent hippocampal synapses in vitro. J. Neurosci. 19, 4180–4188.
Tovar, K.R., McGinley, M.J., Westbrook, G.L., 2013. Triheteromeric NMDA receptors at hippocampal synapses. J. Neurosci. 33, 9150–9160.
Traynelis, S.F., Cull-Candy, S.G., 1990. Proton inhibition of N-methyl-D-aspartate receptors in cerebellar neurons. Nature 345, 347–350.
Traynelis, S.F., Cull-Candy, S.G., 1991. Pharmacological properties and H^+ sensitivity of excitatory amino acid receptor channels in rat cerebellar granule neurones. J. Physiol. 433, 727–763.
Traynelis, S.F., Hartley, M., Heinemann, S.F., 1995. Control of proton sensitivity of the NMDA receptor by RNA splicing and polyamines. Science 268, 873–876.
Truelsen, T., Mahonen, M., Tolonen, H., Asplund, K., Bonita, R., Vanuzzo, D., Project, W.M., 2003. Trends in stroke and coronary heart disease in the WHO MONICA Project. Stroke 34, 1346–1352.
Valivullah, H.M., Lancaster, J., Sweetnam, P.M., Neale, J.H., 1994. Interactions between N-acetylaspartylglutamate and AMPA, kainate, and NMDA binding sites. J. Neurochem. 63, 1714–1719.
van Zundert, B., Yoshii, A., Constantine-Paton, M., 2004. Receptor compartmentalization and trafficking at glutamate synapses: a developmental proposal. Trends Neurosci. 27, 428–437.
Vanhoutte, P., Bading, H., 2003. Opposing roles of synaptic and extrasynaptic NMDA receptors in neuronal calcium signalling and BDNF gene regulation. Curr. Opin. Neurobiol. 13, 366–371.
von Engelhardt, J., Doganci, B., Seeburg, P.H., Monyer, H., 2009. Synaptic NR2A- but not NR2B-containing NMDA receptors increase with blockade of ionotropic glutamate receptors. Front. Mol. Neurosci. 2, 19.
Vyklicky Jr., L., Vlachova, V., Krusek, J., 1990. The effect of external pH changes on responses to excitatory amino acids in mouse hippocampal neurones. J. Physiol. 430, 497–517.
Walder, K.K., Ryan, S.B., Bzdega, T., Olszewski, R.T., Neale, J.H., Lindgren, C.A., 2013. Immunohistological and electrophysiological evidence that N-acetylaspartylglutamate is a co-transmitter at the vertebrate neuromuscular junction. Eur. J. Neurosci. 37, 118–129.
Weilinger, N.L., Maslieieva, V., Bialecki, J., Sridharan, S.S., Tang, P.L., Thompson, R.J., 2013. Ionotropic receptors and ion channels in ischemic neuronal death and dysfunction. Acta Pharmacol. Sin. 34, 39–48.
West, A.E., Chen, W.G., Dalva, M.B., Dolmetsch, R.E., Kornhauser, J.M., Shaywitz, A.J., Takasu, M.A., Tao, X., Greenberg, M.E., 2001. Calcium regulation of neuronal gene expression. Proc. Natl. Acad. Sci. U. S. A. 98, 11024–11031.
Westbrook, G.L., Mayer, M.L., Namboodiri, M.A., Neale, J.H., 1986. High concentrations of N-acetylaspartylglutamate (NAAG) selectively activate NMDA receptors on mouse spinal cord neurons in cell culture. J. Neurosci. 6, 3385–3392.
White, B.C., Sullivan, J.M., DeGracia, D.J., O'Neil, B.J., Neumar, R.W., Grossman, L.I., Rafols, J.A., Krause, G.S., 2000. Brain ischemia and reperfusion: molecular mechanisms of neuronal injury. J. Neurol. Sci. 179, 1–33.
Whittemore, E.R., Ilyin, V.I., Woodward, R.M., 1997. Antagonism of N-methyl-D-aspartate receptors by sigma site ligands: potency, subtype-selectivity and mechanisms of inhibition. J. Pharmacol. Exp. Ther. 282, 326–338.
Williams, K., 1993. Ifenprodil discriminates subtypes of the N-methyl-D-aspartate receptor: selectivity and mechanisms at recombinant heteromeric receptors. Mol. Pharmacol. 44, 851–859.
Wroblewska, B., Wroblewski, J.T., Saab, O.H., Neale, J.H., 1993. N-acetylaspartylglutamate inhibits forskolin-stimulated cyclic AMP levels via a metabotropic glutamate receptor in cultured cerebellar granule cells. J. Neurochem. 61, 943–948.
Wroblewska, B., Wroblewski, J.T., Pshenichkin, S., Surin, A., Sullivan, S.E., Neale, J.H., 1997. N-acetylaspartylglutamate selectively activates mGluR3 receptors in transfected cells. J. Neurochem. 69, 174–181.
Wroblewska, B., Santi, M.R., Neale, J.H., 1998. N-acetylaspartylglutamate activates cyclic AMP-coupled metabotropic glutamate receptors in cerebellar astrocytes. Glia 24, 172–179.
Xia, P., Chen, H.S., Zhang, D., Lipton, S.A., 2010. Memantine preferentially blocks extrasynaptic over synaptic NMDA receptor currents in hippocampal autapses. J. Neurosci. 30, 11246–11250.
Zhu, S., Paoletti, P., 2015. Allosteric modulators of NMDA receptors: multiple sites and mechanisms. Curr. Opin. Pharmacol. 20, 14–23.

nature COMMUNICATIONS

ARTICLE

Received 28 Dec 2013 | Accepted 5 Mar 2014 | Published 1 Apr 2014

DOI: 10.1038/ncomms4550 OPEN

Acidosis overrides oxygen deprivation to maintain mitochondrial function and cell survival

Mireille Khacho[1], Michelle Tarabay[1], David Patten[1,*], Pamela Khacho[1,*], Jason G. MacLaurin[1], Jennifer Guadagno[2], Richard Bergeron[1,3], Sean P. Cregan[2], Mary-Ellen Harper[4], David S. Park[1] & Ruth S. Slack[1]

Sustained cellular function and viability of high-energy demanding post-mitotic cells rely on the continuous supply of ATP. The utilization of mitochondrial oxidative phosphorylation for efficient ATP generation is a function of oxygen levels. As such, oxygen deprivation, in physiological or pathological settings, has profound effects on cell metabolism and survival. Here we show that mild extracellular acidosis, a physiological consequence of anaerobic metabolism, can reprogramme the mitochondrial metabolic pathway to preserve efficient ATP production regardless of oxygen levels. Acidosis initiates a rapid and reversible homeostatic programme that restructures mitochondria, by regulating mitochondrial dynamics and cristae architecture, to reconfigure mitochondrial efficiency, maintain mitochondrial function and cell survival. Preventing mitochondrial remodelling results in mitochondrial dysfunction, fragmentation and cell death. Our findings challenge the notion that oxygen availability is a key limiting factor in oxidative metabolism and brings forth the concept that mitochondrial morphology can dictate the bioenergetic status of post-mitotic cells.

[1] Department of Cellular and Molecular Medicine, Faculty of Medicine, University of Ottawa, Ottawa, Ontario K1H 8M5, Canada. [2] Department of Physiology and Pharmacology, J. Allyn Taylor Centre for Cell Biology, Robarts Research Institute, The University of Western Ontario, London, Ontario N6A 5B7, Canada. [3] Ottawa Hospital Research Institute, Ottawa, Ontario K1H 8M5, Canada. [4] Department of Biochemistry, Microbiology and Immunology, University of Ottawa, Ottawa, Ontario K1H 8M5, Canada. * These authors contributed equally to this work. Correspondence and requests for materials should be addressed to R.S.S. (email: rslack@uottawa.ca).

Long-term survival of post-mitotic cells, which have a limited regenerative capacity, is essential to ensure continued biological function of an organism. In recent years, it has become apparent that the decline of post-mitotic cells, during aging, neurodegenerative diseases and ischemic disorders, is generally associated with mitochondrial dysfunction[1,2]. Mitochondria are essential organelles for energy production, regulation of signalling cascades and cell death[3]. These organelles form a dynamic interconnecting network through continuous cycles of fission and fusion events[4]. The regulation of mitochondrial morphology is closely coupled to cell survival and metabolic adaptation during stress[5–7]. For example, aberrant mitochondrial fission has been observed in many disease and injury models and considered a key contributor to mitochondrial dysfunction and cell death[8–10]. In these settings, inhibition of mitochondrial fission or enhancing mitochondrial fusion restores cell viability[11–14]. These observations highlight the importance in the regulation of mitochondrial dynamics as a strategy to promote cellular survival.

A common characteristic of high-energy-demanding post-mitotic cells, such as neurons, muscle and cardiomyocytes, is their dependence on a continuous supply of energy for sustained cellular function and viability. For this reason, contemporary eukaryotic cells are highly dependent on oxygen and functional mitochondria for the efficient generation of ATP through oxidative phosphorylation[15,16]. In this context, it can be appreciated how limitations in oxygen availability, or hypoxia, have profound physiological effects. Low oxygen levels cause major changes in mitochondrial structure and dynamics, ultimately leading to defective mitochondrial function, reduced ATP supply and activation of cell death pathways[17–19]. Importantly, a defective mitochondrial function induced by hypoxic stress is observed in diverse complex disorders such as type-2 diabetes mellitus, Alzheimer's disease, cardiac and brain ischemia/reperfusion injury and tissue inflammation[17]. The fate of post-mitotic cells subjected to physiological or pathological settings of hypoxia is thus entirely reliant on their ability to respond and adapt to changing environments and stress conditions. Consequently, understanding oxygen sensing and response mechanisms in cells and tissues has been at the forefront of research for many years with the aim of exploiting adaptive strategies to promote cell survival.

An essential and often neglected aspect of hypoxia is the accumulation of lactic acid as the end product of glycolysis. Excess H^+ ions resulting from an increased glycolytic rate are pumped outside the cell, inevitably causing acidification of the extracellular milieu. Physiological levels of acidosis in regions subjected to limited oxygen availability, such as the ischemic penumbra following a stroke, can range within the pH values of 6.0–6.5 depending on the severity of the insult[20–22]. A long-standing debate in biology is the effect of acidosis on cell survival. Although extracellular acidosis is historically viewed as a mere toxic byproduct of fermentation that is detrimental to cells, it is now clinically recognized as a protective agent when present at mild levels (pH 6.5 and above)[21,23–35]. In this regard, although several reports have clearly demonstrated the protective nature of mild acidosis, the underlying molecular mechanisms are still poorly understood. Furthermore, the role of mitochondria, being central to cell survival and death, has surprisingly never been addressed in this perspective. Here we show the unexpected observation that mild acidosis triggers massive morphological reorganization of mitochondria in post-mitotic cells, triggered by a dual programme that both activates fusion and cristae remodelling while inhibiting mitochondrial fragmentation. Activation of this reversible homeostatic programme reconfigures mitochondrial bioenergetics to allow for the persistence of efficient ATP production through oxidative phosphorylation despite oxygen limitations. Our work reveals a novel and physiological mechanism that can control the metabolic status of cells and protect mitochondrial-reliant post-mitotic cells following a hypoxic insult, by reprogramming mitochondrial morphology and functional efficiency.

Results

Acidosis triggers mitochondrial elongation during hypoxia. As mitochondria are central in the cell death that is instigated during hypoxic stress, we investigated mitochondrial morphology in this setting. Cortical neurons were chosen for these experiments since they are a major population affected by hypoxic stress and thus represent a biologically relevant system for the study of adaptive mechanisms in post-mitotic cells. For our studies, we developed an *in vitro* model that mimics the physiological microenvironment found under hypoxic conditions, such as the penumbral region following an ischemic brain injury. This model recapitulates the low oxygen/glucose environment and takes into account that ischemic tissues or hypoxic cells normally acidify their extracellular milieu as a physiological consequence of anaerobic glycolysis. For this, a low glucose media was buffered in a manner to accommodate physiological acidification of the extracellular milieu when neurons are incubated at 1% O_2 (termed acidosis-permissive media (AP)). The control condition utilizes a low glucose media that maintains a stable neutral pH (pH 7.2) throughout experimentation (termed standard media (SD)). Mitochondria from cultured cortical neurons subjected to hypoxic conditions in a neutral pH environment had severely fragmented mitochondria as observed through immunofluorescence staining of the outer mitochondrial membrane protein Tom20 (Fig. 1a and quantified in Fig. 1b). Mitochondrial fragmentation was observed before signs of cell death or changes in neuronal morphology (Supplementary Fig. 1). Unexpectedly, neurons subjected to hypoxia but allowed to undergo physiological extracellular acidification (measured pH post experiment was 6.5) exhibited massive mitochondrial elongation compared with control (Fig. 1a and quantified in Fig. 1b). Elongated mitochondria were observed in the cell body of cortical neurons and spanned along the axons (Fig. 1c). Mitochondrial elongation was also observed in cultured cerebellar granular neurons (CGNs; Fig. 1d,e) and *in vivo* hippocampal slice preparations (Fig. 1f,g), as well as in differentiated C2C12 myotubes (Supplementary Fig. 2), suggesting that this is a general phenomenon. Interestingly, acidosis-mediated mitochondrial elongation was not observed in proliferative cells, such as primary and transformed mouse embryonic fibroblast cells (MEF), C2C12 myoblasts, Cos7, HeLa and several cancer cell lines, including MCF-7, A549 and P19, suggesting that this response is unique to post-mitotic cells (Supplementary Fig. 2).

The acidosis-dependent alteration in mitochondrial morphology is pH-specific and elongation of mitochondria was only observed at a pH threshold value between 6.65 and 6.45 (Fig. 2a,b and Supplementary Fig. 3), representing mildly acidic conditions as observed in physiological settings of hypoxic stress. In contrast, cells within a neutral (pH 7.2–6.8) or severely acidic (pH 6.0) extracellular environment during hypoxia exhibited significant mitochondrial fragmentation (Fig. 2a,b and Supplementary Fig. 3). Acidosis-mediated mitochondrial elongation is a rapid process whereby the onset of elongation occurred at about 3-h post-treatment (Fig. 2c,d and Supplementary Fig. 4). This opposed the hypoxia-mediated mitochondrial fragmentation that occurs in neutral conditions beginning 3 h following treatment (Fig. 2c and Supplementary Fig. 4). In addition, although acidosis generally occurs as a consequence of increased glycolysis

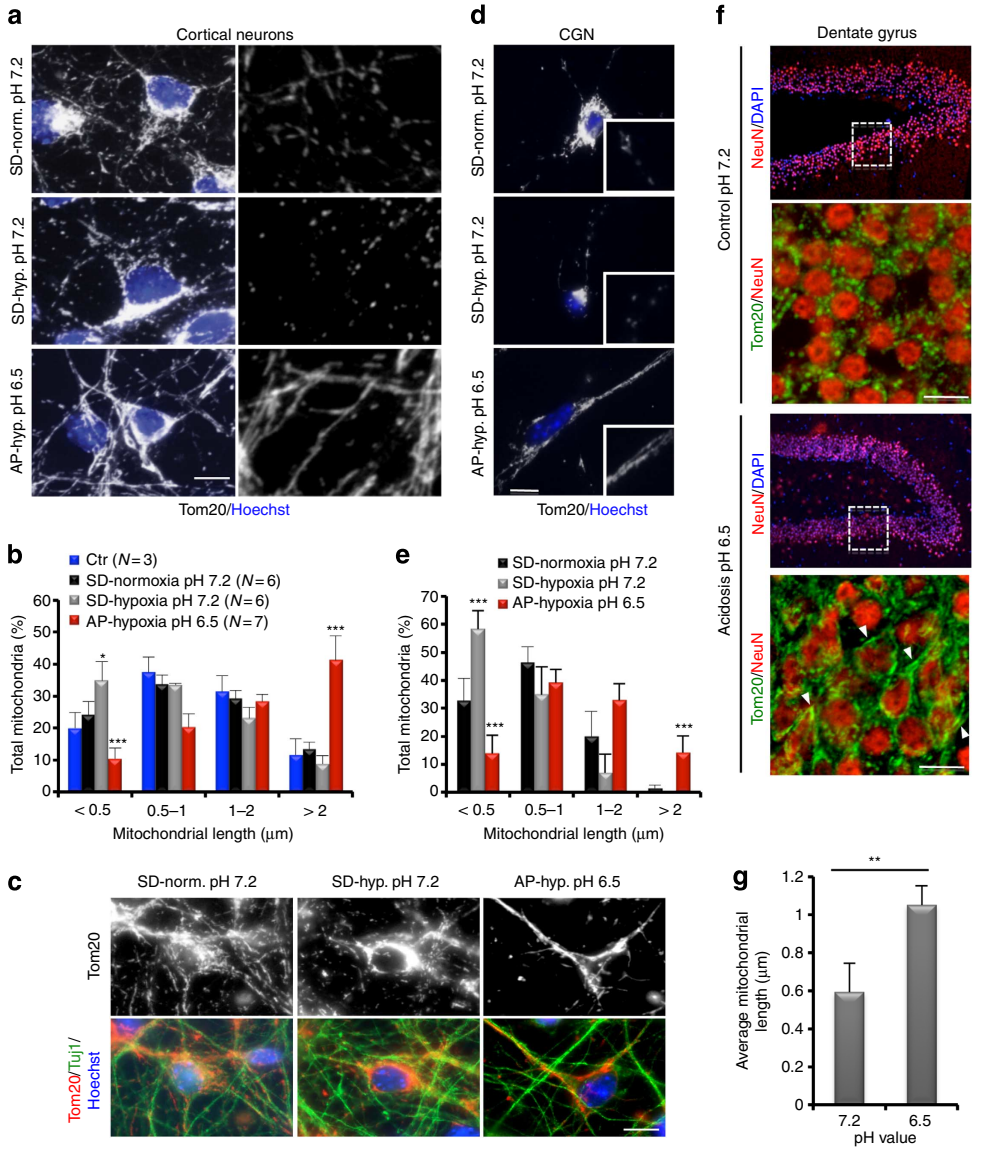

Figure 1 | Extracellular acidification restructures mitochondria in post-mitotic cells. (**a**) Representative confocal images of mitochondrial morphology in cultured cortical neurons following 18-h incubation at normoxic (Norm.) or hypoxic (Hyp.) conditions in SD or AP media. Mitochondria were visualized by Tom20 immunofluorescence. Panels on the right represent zoomed views of the mitochondria. (**b**) Mitochondrial length from (**a**) was quantified and binned into different length categories. Represented as mean and s.d. (*n* values indicated on graph). Ctr = control; represents neurons incubated in neurobasal media. (**c**) Representative images of mitochondrial morphology, revealed by Tom20 staining, in Tuj1+ cortical neurons at the indicated conditions. (**d** and **e**) Mitochondrial morphology in cultured CGN after 18-h incubation at the indicated conditions. Insets in (**d**) are zoomed views of mitochondria. (**e**) Mean and s.d. ($n = 3$) of mitochondrial length data in (**d**). (**f** and **g**) Mitochondrial morphology in *ex vivo* hippocampal slice preparations incubated in normoxia for 4 h at the indicated conditions. Neurons were immunostained with NeuN (neuronal-specific nuclear protein) and Tom20 (mitochondria). Panels showing Tom20/NeuN staining are zoomed views of the boxed area within the hippocampus. Arrowheads indicate elongated mitochondria. (**g**) Average mitochondrial length and s.d. were plotted for the indicated conditions. $^{*}P<0.05$; $^{**}P<0.01$; $^{***}P<0.001$ (Student's *t*-test). For all images scale = 10 μm.

during limited oxygen availability, its effect on mitochondrial morphology was in fact independent of oxygen. Incubation of cortical neurons in media set to pH 6.5 in the presence of oxygen (normoxia) resulted in a significant increase in mitochondrial length compared with control (Fig. 2e). To further confirm the direct affect of acidosis on mitochondrial length, the contribution of low glucose levels in the experimental paradigm, which represents a more physiologically relevant setting, was assessed. The effect of acidosis on mitochondrial length was not a consequence of decreased glucose availability since mitochondrial elongation persisted in the presence of high glucose levels (Fig. 2f and Supplementary Fig. 5). Thus, mitochondrial elongation in these settings is directly mediated by acidosis and is not a consequence of an induced starvation response. This is supported by the observation that the limited glucose availability in these experiments was not sufficient to activate autophagy (Supplementary Fig. 6) such as that observed during complete glucose starvation, where there is a marked increase in LC3II, degradation of p62 and loss of outer membrane Tom20 due to mitophagy (Supplementary Fig. 6). These results demonstrate that acidosis alone is sufficient to promote mitochondrial elongation. Acidosis-driven elongation is also a reversible process. Mitochondria remain elongated regardless of oxygen levels, confirming that this process is oxygen-independent (Fig. 2g,h

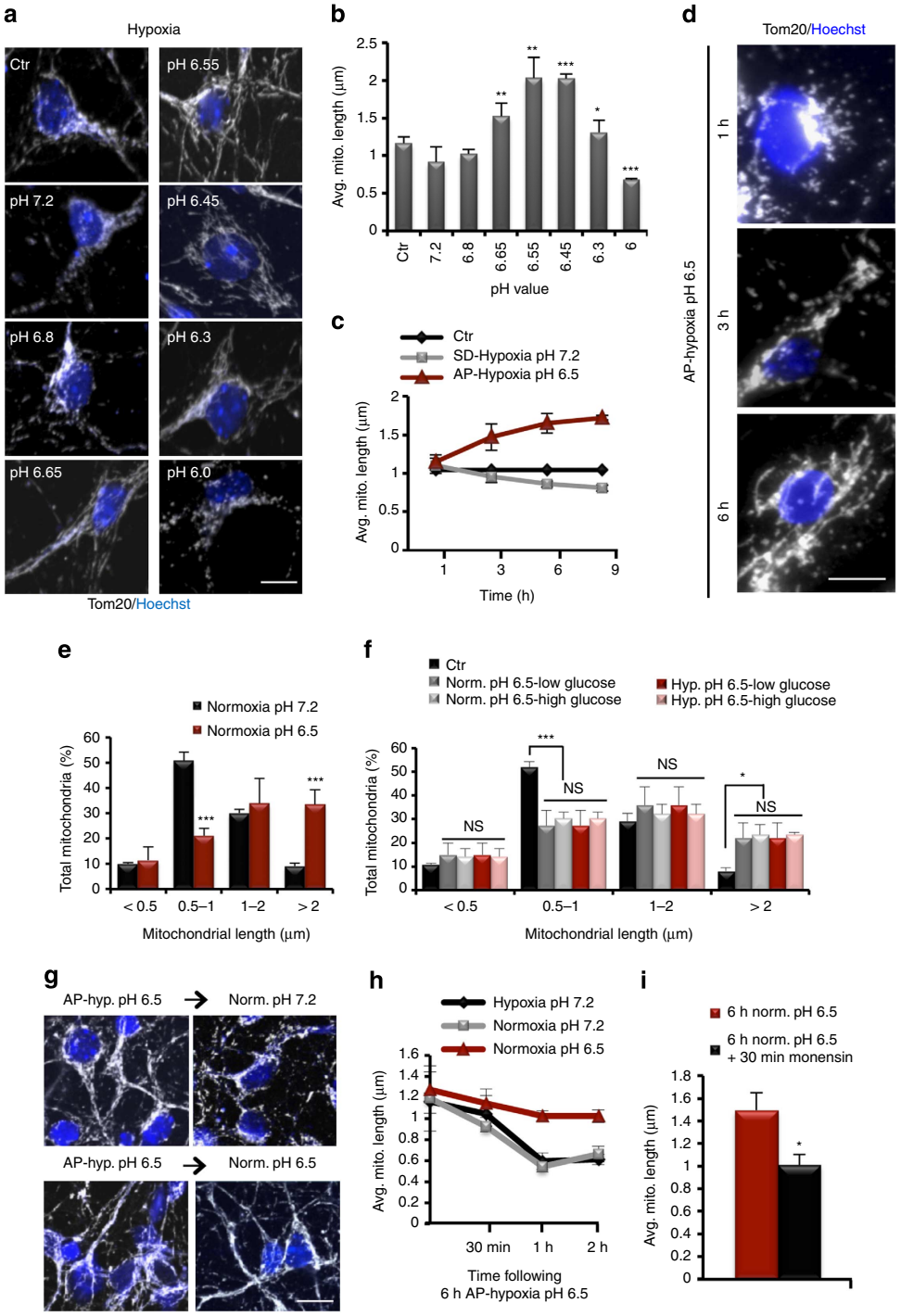

Figure 2 | Acidosis-mediated mitochondrial elongation is pH-specific, rapid, reversible and O_2- and glucose-independent. (**a**) Representative confocal images of mitochondrial morphology in cultured cortical neurons following incubation at fixed pH values in hypoxia. Ctr = control; represents neurons incubated in neurobasal media. (**b**) Average mitochondrial length and s.d. ($n = 3$) were plotted for the indicated pH values. (**c**) Average mitochondrial length and s.d. ($n = 3$) over time at indicated conditions. (**d**) Immunofluorescence of Tom20 (mitochondria) showing the change in mitochondrial length in cortical neurons by physiological acidosis at the indicated times. (**e**) Mean and s.d. ($n = 3$) of mitochondrial length distribution during normoxic conditions at indicated pH values for 6 h. (**f**) Mean and s.d. ($n = 3$) of mitochondrial length distribution during normoxic or hypoxic conditions in the presence of low (5.5 mM) or high (25 mM) glucose levels for 6 h. (**g** and **h**) Analysis of mitochondrial morphology after 6-h incubation in AP-Hypoxia pH 6.5 and following reoxygenation at the indicated pH values. (**h**) Graph of the change in average mitochondrial length (s.d., $n = 3$) at the indicated conditions following a 6-h incubation in AP-Hypoxia pH 6.5. (**i**) Average mitochondrial length and s.d. ($n = 3$) were plotted for the indicated conditions. ns = not significant, $^*P < 0.05$; $^{**}P < 0.01$; $^{***}P < 0.001$ (Student's *t*-test). For all images scale = 10 µm.

and Supplementary Fig. 7). However, mitochondria revert back to a fragmented phenotype following neutralization of the extracellular pH both under hypoxic or reoxygenation conditions (Fig. 2g,h and Supplementary Fig. 7). In fact, the level of fragmentation following reoxygenation in a neutral context was very rapid (within 30 min) and was quite severe (Fig. 2h

and Supplementary Fig. 7). In order to gain insight as to how extracellular acidosis can relay an intracellular signal to modify mitochondrial morphology, pH changes within the intracellular environment were examined. Analysis of intracellular pH changes using the ratiometric fluorescent indicator BCECF-AM (Supplementary Fig. 8a) showed that a decrease in extracellular pH as used in our studies (pH 6.5) was sufficient to cause a reduction in intracellular pH (Supplementary Fig. 8b) and is consistent with previous reports showing that intracellular pH can be modified by the extracellular milieu[36,37]. Furthermore, neutralization of the intracellular pH using the Na+/H+ exchanger Monensin (Supplementary Fig. 8c) rapidly reverses the mitochondrial elongation phenotype that was instigated by extracellular acidosis (Fig. 2i and Supplementary Fig. 8d,e). Together, these results demonstrate a pH-dependent regulation of mitochondrial morphology that is oxygen- and glucose-independent and is reversible.

Acidosis inhibits DRP1-mediated mitochondrial fission. Mitochondrial fragmentation is a prominent phenotype during hypoxic stress conditions as observed here (Figs 1a,b and 2c) and in previous studies[19,38,39]. However, physiological acidification appears to prevent hypoxia-induced mitochondrial fragmentation. An essential component of the mitochondrial fission machinery, the dynamin protein DRP1, is a cytosolic factor that is recruited to mitochondria upon activation[40]. As expected, localization analysis of endogenous DRP1 showed a pronounced increase in mitochondrial-specific DRP1 foci during hypoxia-neutral conditions that correlate with the observed increase in fragmentation (Fig. 3a,b). Interestingly, a decrease in the number of DRP1 foci per unit length of mitochondria was observed during acidosis (Fig. 3a,b). A decline in mitochondrial DRP1 during acidosis was not due to changes in total cellular protein expression of DRP1 (Fig. 3c) but was reminiscent of the decreased number of mitochondrial DRP1 foci observed in the presence of the selective inhibitor of DRP1-mediated mitochondrial fission, Mdivi-1(ref. 41; Fig. 3d). Analysis of DRP1 protein interactions revealed that in cultured cortical neurons DRP1 associates with Fis1 but not Mff, two previously identified DRP1-binding proteins (Supplementary Fig. 9a)[42]. Furthermore, immunoprecipitation of endogenous DRP1 at the onset of mitochondrial elongation by acidosis revealed a decreased level of interaction between DRP1 and Fis1, a mitochondrial DRP1-binding protein important for DRP1 recruitment and fission[42,43]. The decrease in DRP1–Fis1 interaction was similar to what is observed following treatment with forskolin, an inhibitor of fission through its activation of PKA-mediated phosphorylation and inhibition of DRP1 recruitment to mitochondria (Fig. 3e and Supplementary Fig. 9b,d). These data suggest that acidosis inhibits DRP1-mediated fission during hypoxia. Although PKA-dependent phosphorylation at Ser637 represents a major regulatory sight for DRP1 activation[44], we did not observe a change in the phosphorylation status of DRP1 at Ser637. Moreover, inhibition of the PKA pathway did not affect acidosis-mediated mitochondrial elongation nor did activation of this pathway affects mitochondrial morphology during hypoxia (Supplementary Fig. 9b,d). Furthermore, the phosphorylation status of DRP1 at Ser616, a common target of DRP1 regulation during oxidative stress[45], was not altered at the time point where mitochondrial elongation is observed (Supplementary Fig. 9c). Thus, mild acidosis prevents mitochondrial fragmentation under hypoxic conditions through the PKA and CDK1/PKCδ-independent regulation of DRP1 activation and recruitment to mitochondria.

Mitochondrial fusion by acidosis depends on the SIMH pathway. The degree and rate of elongation observed during acidosis suggested the possibility of a pH-dependent enhancement in mitochondrial fusion activity, in addition to suppression of the fission pathway. This was tested in live neurons, infected

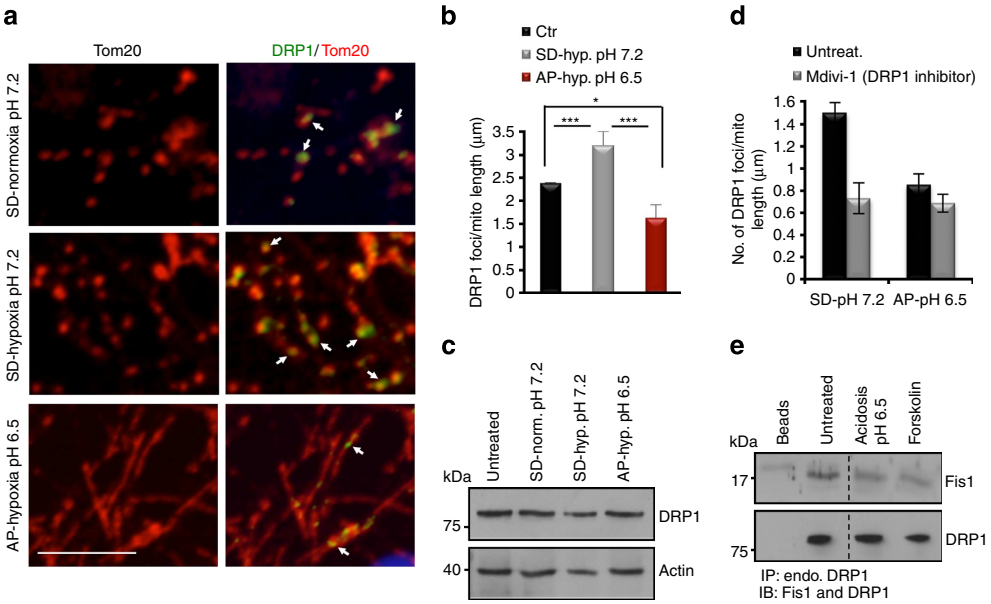

Figure 3 | Mild acidosis inhibits DRP1-mediated mitochondrial fission. (**a**) Colocalization of DRP1 foci at mitochondria by immunofluorescence of DRP1 and Tom20 in cortical neurons using confocal imaging. Arrows show DRP1 foci localized at mitochondria. Scale = 5 µm. (**b**) Quantification of the number of DRP1 foci colocalized to mitochondria and represented as mean and s.d. ($n = 3$). (**c**) Western blot of the indicated proteins from whole cell lysates of cultured cortical neurons following 6-h incubation at the indicated conditions. (**d**) Quantification of the number of DRP1 foci colocalized to mitochondria following 6-h hypoxic incubation in SD or AP media in the presence or absence of the fission inhibitor Mdivi-1. (**e**) Western blot of indicated proteins following incubation for 3 h at the indicated conditions and immunoprecipitation of endogenous (endo.) DRP1 using anti-DRP1 antibody.

with a mitochondrial matrix targeted photo-activatable green-fluorescent protein (GFP) lentivirus (PA-Oct-GFP), following 3 h of incubation at pH 7.2 or 6.5 under normoxic conditions, representing the onset of elongation in the absence of hypoxia-induced fission. The rate of dilution and spread of the photo-converted GFP molecules are used as a measure of fusion activity. Time-lapse imaging of the activated mitochondrial GFP signal demonstrated an increase in mitochondrial fusion in neurons subjected to mild acidosis (Fig. 4a,b and Supplementary Fig. 10). Examination of mitochondrial mass further confirmed that mitochondrial elongation during acidosis is a result of enhanced fusion activity rather than increased mitochondrial biogenesis

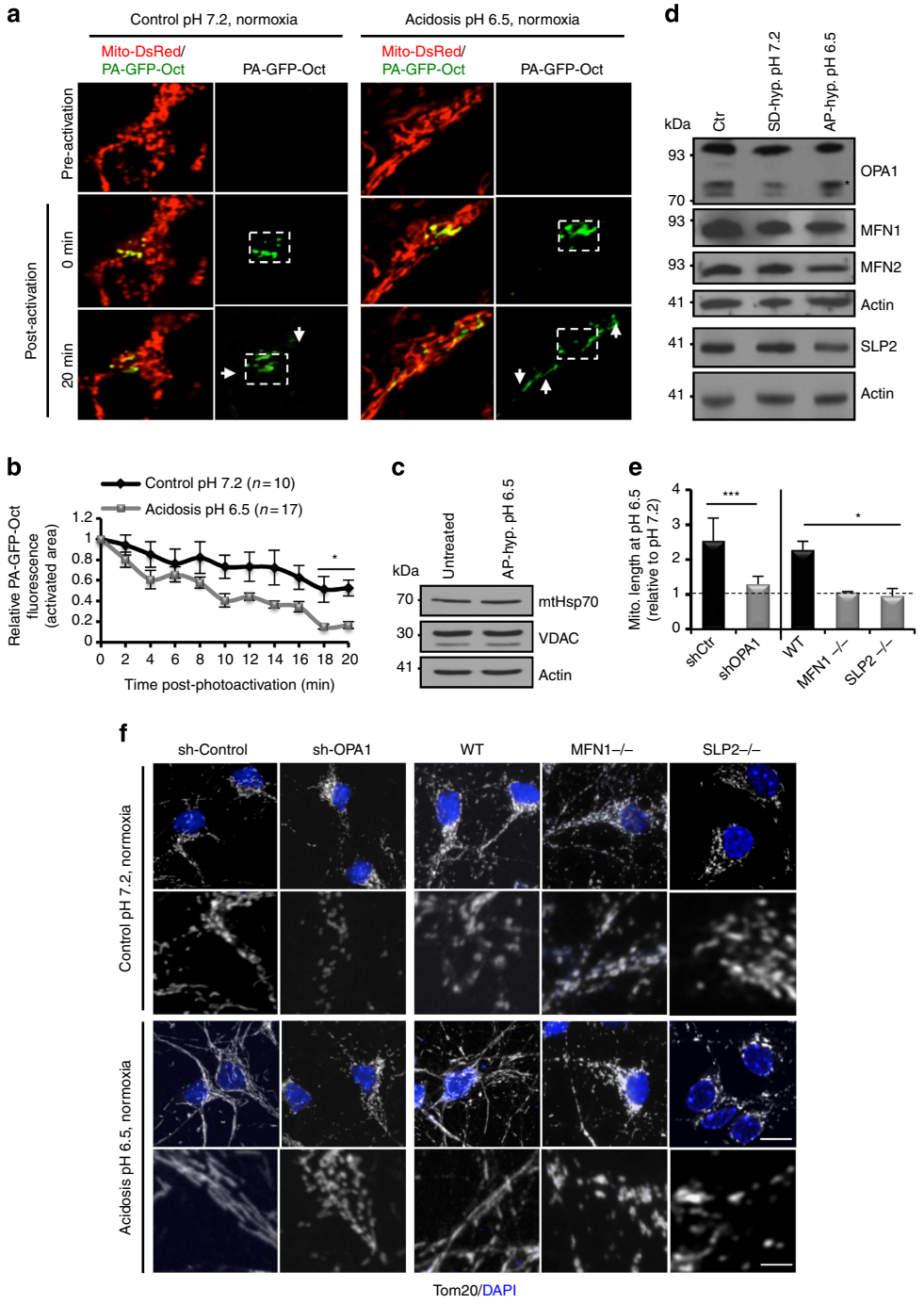

Figure 4 | Mild acidosis regulates mitochondrial dynamics. (**a**) Representative images of mitochondrial fusion over time (indicated in minutes) following activation of exogenously expressed PA-GFP-Oct. Boxes indicate photo-activated regions and arrows indicate spread of the GFP signal within mitochondria (revealed by exogenous expression of Mito-DsRed). (**b**) Quantification of mitochondrial fusion in cortical neurons as a loss of GFP fluorescence in the activated region. Data represent the mean and s.d. of $n=10$ (control) and $n=17$ (experimental) from three independent experiments. (**c** and **d**) Western blot of the indicated proteins from whole-cell lysates of cortical neurons incubated for 6 h at the indicated conditions. Asterisk indicates s-OPA1. (**e**) Mean and s.d. ($n=3$) of mitochondrial length during acidosis, of the indicated genotypes, relative to control conditions. (**f**) Representative images of mitochondrial morphology from cortical neurons of the indicated genotypes following 6-h incubation in MES-buffered media at the indicated conditions. Bottom panel of each condition is a zoom view of mitochondria. Scale = 10 μm. $^{*}P<0.05$; $^{***}P<0.001$ (Student's *t*-test).

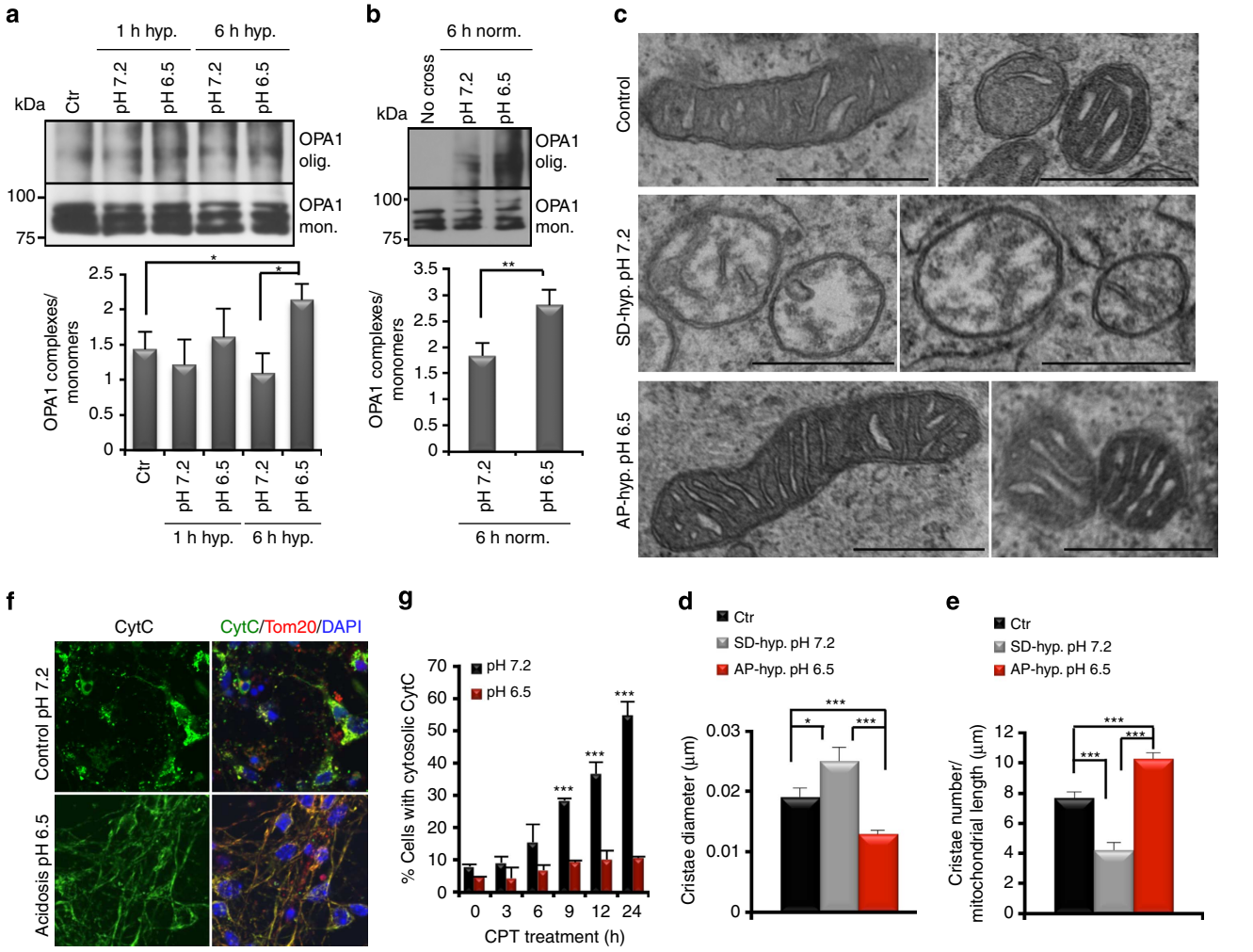

Figure 5 | Mild acidosis regulates cristae architecture. (**a**,**b**) Western blot of OPA1 oligomers and monomers from lysates of BMH crosslinking in live cortical neurons at the indicated conditions. OPA1 western blot has been spliced to better clarify where monomeric and oligomerized Opa1 appear. Graphs represent the mean and s.d. ($n=3$) quantification of OPA1 oligomer:monomer ratio. (**c**–**e**) Representative EM images of mitochondrial ultrastructure following 6-h incubation at the indicated conditions. Scale = 500 nm. Graphs in (**d**,**e**) represent mean and s.e.m ($n=10$) for quantification of cristae diameter and cristae number. Ctr = control represents neurons incubated in neurobasal media. (**f**,**g**) Representative images and quantification (mean and s.d., $n=4$) of CytC localization following CPT treatment in MES-buffered media at pH 7.2 or 6.5 in normoxia. $^{*}P<0.05$; $^{**}P<0.01$; $^{***}P<0.001$ (Student's *t*-test).

since the levels of resident mitochondrial proteins HSP70 and VDAC were unchanged (Fig. 4c). Mitochondrial elongation during acidosis does not appear to be activated through increased expression levels of core fusion proteins OPA1 and MFN1/2 (refs 46–48; Fig. 4d). Moreover, addition of the protein synthesis inhibitor cycloheximide did not prevent acidosis-mediated mitochondrial elongation or significantly alter mitochondrial length during control conditions, suggesting that acidosis may regulate mitochondrial dynamics at the post-translational level (Supplementary Fig. 11). To further decipher the molecular mechanism enabling enhanced fusion activity, we examined the possibility that acidosis activates the stress-induced mitochondrial hyperfusion (SIMH) pathway[7]. We found that removal of the key molecular components of the mitochondrial fusion machinery and the SIMH pathway, OPA1, MFN1 and SLP2, rendered neurons unresponsive to acidosis-induced mitochondrial elongation in normoxia (Fig. 4e,f). Together, these data demonstrate that mild acidosis enhances mitochondrial fusion, requires an intact fusion machinery and suggests a specific role for the SIMH pathway in the hyperfusion observed by mild acidosis during hypoxic stress.

Acidosis regulates cristae remodelling during stress. The internal structures of mitochondria, the cristae, are also dynamic and can undergo OPA1-dependent remodelling during stress conditions[49,50]. OPA1 oligomeric complexes, consisting of both membrane-bound long (l-OPA1) and soluble short forms (s-OPA1) of OPA1 in the intermembrane space, have been associated with inner membrane morphology, tightness of the cristae junctions, as well as sequestration of Cytochrome *c* (CytC) within the cristae[46,49,51,52]. We found that the relative amount of s-OPA1 was altered following 6 h of hypoxic treatment (Fig. 4d) and OPA1-specific oligomeric complexes were disrupted as early as 1 h after treatment (Fig. 5a and Supplementary Fig. 12). However, a mild decrease in the extracellular pH during hypoxia rescued both the levels of s-OPA1 and OPA1 oligomeric complexes (Figs 4d and 5a). Acidosis also increased OPA1 oligomeric complexes under normoxic conditions (Fig. 5b). This suggested that acidosis not only changes mitochondrial length but it may also alter cristae morphology. Examination of mitochondrial ultrastructure using transmission electron microscopy (TEM) revealed that mitochondrial ultrastructure, which is severely disrupted during hypoxia, was preserved by

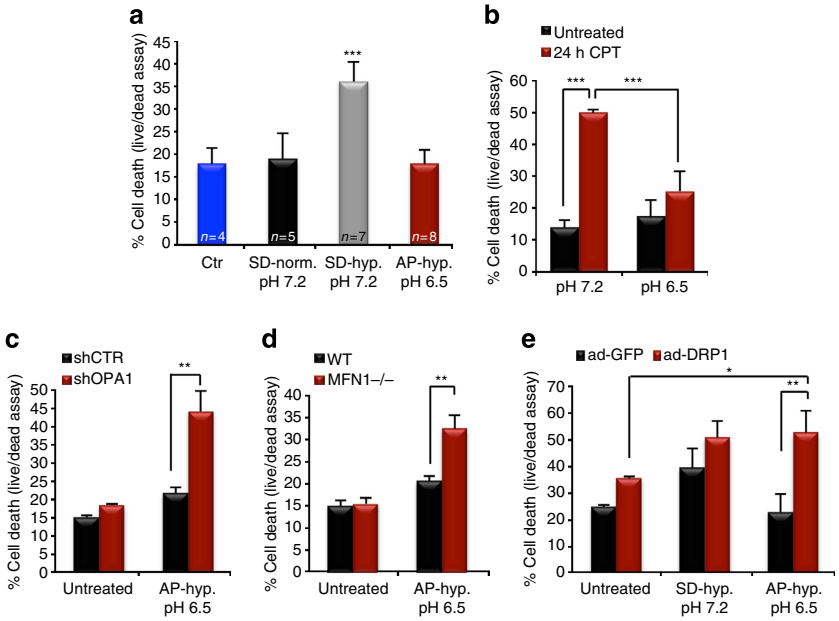

Figure 6 | Acidosis-mediated mitochondrial remodelling protects neurons from cell death during hypoxic stress. (**a**) Quantification of cell death of cortical neurons as mean and s.d. (*n* values indicate independent experiments) following 30-h incubation in SD or AP media at the indicated conditions. (**b**) Mean and s.d. ($n=3$) of neuronal cell death analysis following 24-h treatment with CPT in MES-buffered media at pH 7.2 or 6.5 in normoxia. (**c**) Quantification of cell death in neurons infected with lentivirus encoding a scrambled (shCTR) or OPA1-specific (shOPA1) shRNA following 30 h in SD or AP media at the indicated conditions (mean and s.d., $n=3$). (**d**) Mean and s.d. ($n=4$) of cell death quantification in WT (wild-type) or MFN1-deficient (MFN1 $-/-$) cortical neurons following 30-h incubation in SD or AP media at the indicated conditions. (**e**) Quantification of cell death in neurons infected with adenovirus-encoding GFP or DRP1-YFP following 30-h incubation in SD or AP media at the indicated conditions (mean and s.d., $n=3$). $^{*}P<0.05$; $^{**}P<0.01$; $^{***}P<0.001$ (Student's *t*-test).

acidosis (Fig. 5c–e). During hypoxia-neutral conditions, where aberrant mitochondrial fragmentation is observed, there is a severe disruption of mitochondrial ultrastructure leading to a significant increase in cristae diameter as well as a reduction in cristae number (Fig. 5c–e). More importantly, a mild decrease in the pH during hypoxia not only rescued this defect but also resulted in a significant tightness of the cristae diameter and increased cristae number, relative to control (Fig. 5c–e). These data suggest a role for acidosis in cristae maintenance and remodelling. This was further confirmed through an indirect examination of cristae remodelling by measuring the degree of CytC release following an apoptotic stimulus, which can provide information related to the tightness of the cristae junctions[49,53]. Treatment of neurons with Camptothecin (CPT), a DNA-damaging agent that triggers the apoptotic cell death pathway, revealed that mitochondrial restructuring by acidosis renders cells resistant to CytC release (Fig. 5f,g), in the presence of apoptosis signalling as indicated by BAX activation (Supplementary Fig. 13). Together, these data demonstrate that mild acidosis modulates mitochondrial dynamics as well as cristae architecture. Furthermore, these data suggest that acidosis prevents the intramitochondrial remodelling, as a result of OPA1 oligomer destabilization, that is associated with mitochondrial fragmentation and cell death signalling.

Mitochondrial restructuring protects cells in hypoxia. Several studies have demonstrated the protective effect of mild acidosis during ischemic conditions. Importantly, this observation was recapitulated in our model of ischemia. A significant increase in cell death is observed in hypoxia under neutral conditions; however, a physiological decrease in the extracellular pH (pH 6.5) protects neurons from death (Fig. 6a). Interestingly, acidosis rendered neurons resistant to other damaging agents such as CPT (Fig. 6b), suggesting that cells subjected to mild changes in extracellular pH can sustain survival under different modes of stress. The observation that mild acidosis in our system also promotes mitochondrial remodelling suggests that this may be the underlying mechanism of cellular protection previously observed at similar pH levels. To confirm this hypothesis, we tested neuronal survival during hypoxia–acidosis where we prevented the impact of acidosis on mitochondrial dynamics. The protective effect of acidosis was reversed in the absence of the essential fusion machinery. Acute RNA interference-mediated loss of OPA1 expression or genetic ablation of MFN1 prevented acidosis-mediated mitochondrial elongation (Fig. 4e,f) and was sufficient to increase cell death during hypoxia even in the presence of acidosis (Fig. 6c,d). Moreover, overexpression of the mitochondrial fission protein DRP1, in wild-type neurons, resulted in a significant increase in cell death during hypoxia–acidosis (Fig. 6e). These data demonstrate that the restructuring of mitochondria during stress is a major player in the protective effect of mild acidosis.

Reprogrammed mitochondria maintain ATP production in hypoxia. A prominent response to cellular hypoxic stress is mitochondrial fragmentation, and loss of mitochondrial membrane potential and dysfunction[17,19]. Since acidosis prevents hypoxia-induced mitochondrial fragmentation and cell death, we wanted to investigate the status of mitochondrial integrity and function. We found that mild acidosis maintains mitochondrial membrane potential during hypoxia (Fig. 7a, and Supplementary Fig. 14). Maintenance of mitochondrial membrane potential requires a protonmotive force that is generated by the electron transport chain through respiration or, in pathological situations, by ATP hydrolysis via the F_1F_0-ATPase (ATP synthase). A highly polarized membrane potential suggests that either mitochondrial

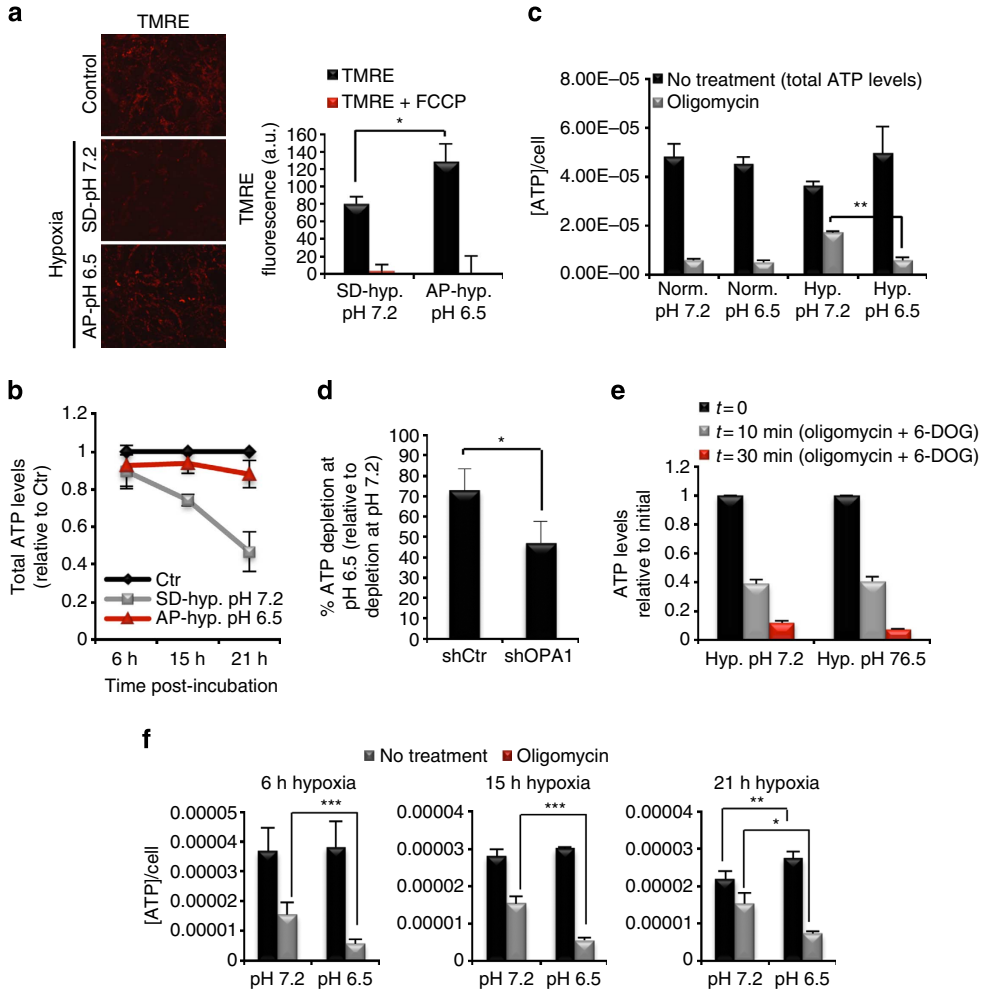

Figure 7 | Acidosis maintains mitochondrial function during hypoxic stress. (**a**) TMRE staining and quantification of fluorescence intensity following 18-h incubation in SD or AP media in hypoxia. Mean and s.d. ($n=3$ from three independent experiments). The uncoupler FCCP, which dissipates the membrane potential, is used to show specificity of the measured TMRE fluorescence. (**b**) Total ATP levels relative to normoxic control (in black). Mean and s.d. ($n=5$). (**c**) Total ATP concentration per cell at steady state (black) and after 1-h oligomycin treatment (grey) following 6 h of treatment at the indicated conditions. Mean and s.d. ($n=3$ replicates from six independent experiments). (**d**) Quantification of the amount of ATP depletion following 1-h oligomycin treatment in cortical neurons infected with lentivirus encoding a scrambled control (shCtr) or OPA1-specific shRNA (shOPA1). Mean and s.d. ($n=3$ replicates from three independent experiments). (**e**) ATP levels per cell relative to initial values (black) following oligomycin and 6-DOG treatment. Mean and s.d. ($n=3$ replicates from three independent experiments). (**f**) Total ATP levels per cell at steady state (black) and after 1-h oligomycin treatment (grey). Graphs represent mean and s.d. of $n=3$ replicates from six independent experiments. $^{*}P<0.05$; $^{**}P<0.01$; $^{***}P<0.001$ (Student's *t*-test).

respiratory function was preserved by mild acidosis or that the membrane potential was maintained by the reversal of the ATP synthase, which would result in ATP consumption. Interestingly, total ATP levels were sustained for an extended period in hypoxia if cells underwent physiological acidification (Fig. 7b), suggesting that ATP hydrolysis by the ATP synthase was not a central contributing factor in maintaining membrane potential.

It is well established that mitochondrial function and the generation of ATP through oxidative phosphorylation (OXPHOS) is impaired during hypoxic conditions, causing cells to shift to anaerobic glycolysis[54]. Although this shift in metabolism is important for cell survival during acute hypoxic stress, glycolysis represents a much less efficient mode of ATP production, and over the long run it is reasonable to conceive how this can pose an energy deficit in high-energy-demanding cells such as neurons. The remodelling of mitochondria, as well as maintained membrane potential and ATP levels by acidosis, led us to postulate that acidosis may also preserve mitochondrial function during hypoxic conditions. Intriguingly, we found that addition of oligomycin, an ATP synthase inhibitor that blocks mitochondrial ATP production, resulted in a significant depletion, of ~90%, in total ATP levels during hypoxia–acidosis conditions, to the same extent as that observed during normoxia (at pH 7.2 and 6.5; Fig. 7c). This is in contrast to what is observed under hypoxia-neutral conditions whereby oligomycin treatment following short-term hypoxia (6 h) results in only about 50% decrease in ATP levels, suggesting the use of a non-mitochondrial ATP production pathway (that is, glycolysis). Preventing mitochondrial fusion and disrupting cristae structure during acidosis, through acute loss of OPA1 expression, resulted in decreased oligomycin-sensitive ATP depletion at pH 6.5 (Fig. 7d). The increased level of ATP depletion in wild-type neurons, observed in the presence of oligomycin during acidosis, was not due to an elevation in ATP utilization since arrest of both ATP production pathways using 6-deoxyglucose (6-DOG; glycolysis inhibitor) and oligomycin showed a similar rate of ATP consumption over time during hypoxia at pH 7.2 and 6.5 (Fig. 7e). Given that an increase in consumption cannot account

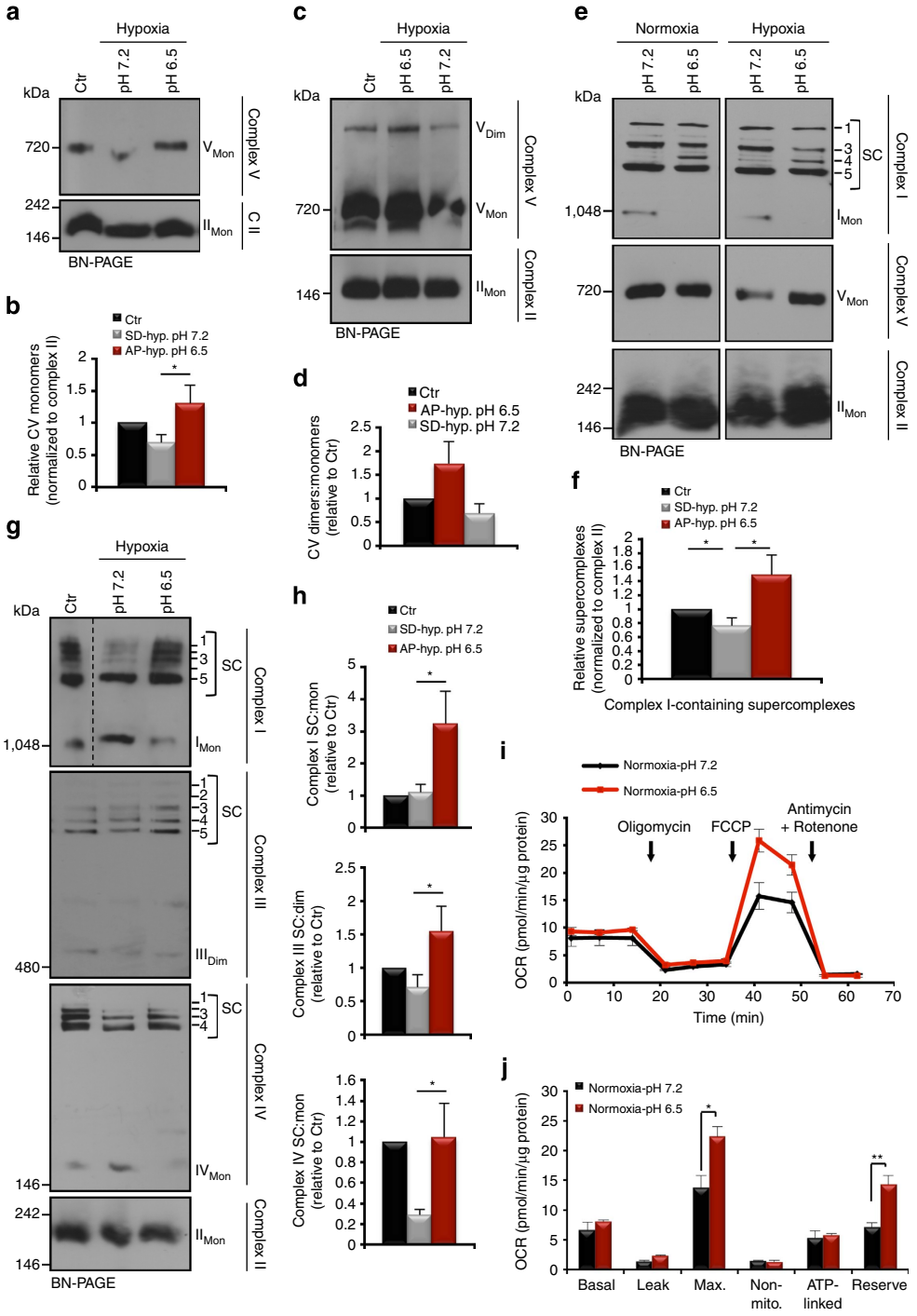

Figure 8 | Acidosis instigates an adaptive reprogramming of mitochondrial respiratory efficiency. (**a**–**d**) Representative BN-PAGE of Complex V (ATP synthase) (**a**) monomers (whole cells) and (**c**) dimers (isolated mitochondria) in cortical neurons following 6-h treatment in the indicated conditions. In (**c**), longer exposure of the membrane was required to visualize the dimeric Complex V. Graphs represent mean and s.e.m of (**b**) $n=5$ and (**d**) $n=3$ independent experiments. Mon = monomers, Dim = dimers, and CV = Complex V. (**e**) Representative BN-PAGE of the indicated respiratory complexes using anti-NDUFA9 (Complex-I), anti-ATP5a (Complex-V) and anti-Core2 (Complex-II). Cortical neurons were treated for 6 h in the indicated conditions. SC 1–5 = supercomplex assembly. (**f**) Quantification of relative assembly of supercomplexes visualized using anti-NDUFA9 (Complex-I). Mean and s.e.m of $n=4$ independent experiments. (**g**,**h**) Representative BN-PAGE of the indicated respiratory complexes using anti-NDUFA9 (Complex-I), anti-UQCRC2 (Complex-III), anti-Complex IV subunit 1 (Complex-IV) and anti-Core2 (Complex-II) following 6 h in the indicated conditions. Graphs in (**h**) are mean and s.e.m of $n=6$ (Complex-I), $n=4$ (Complex-III) and $n=3$ (Complex-IV) independent experiments. (**i**,**j**) OCR in cortical neurons using a Seahorse XF24 Extracellular Flux Analyzer. Mean and s.d. ($n=4$ replicates from three independent experiments). $^{*}P<0.05$; $^{**}P<0.01$; $^{***}P<0.001$ (Student's *t*-test).

for the significant depletion of ATP in the presence of oligomycin, this suggests that cells in acidosis rely less on the glycolytic ATP generation pathway and supports the idea that acidosis preserves mitochondrial function and sustains OXPHOS during hypoxia. This observation was quite surprising considering that oxygen availability is historically viewed as a limiting factor

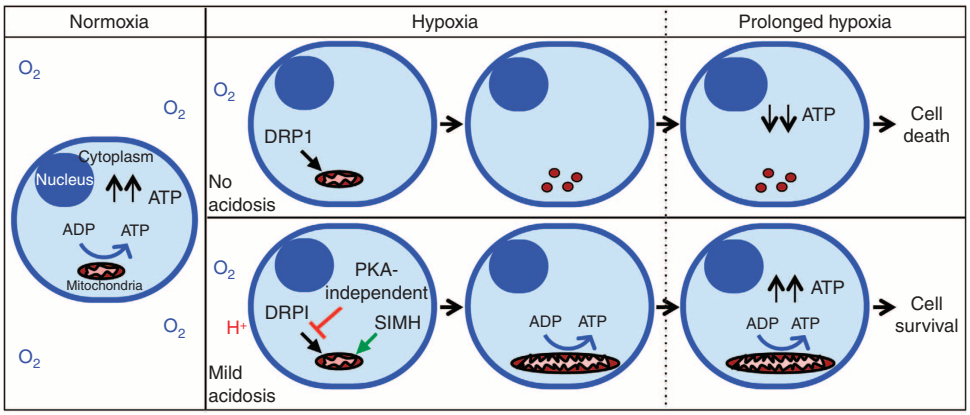

Figure 9 | Mitochondrial restructuring by mild acidosis determines cellular bioenergetics during hypoxia. The cartoon depicts the cascade of events following a decrease in oxygen levels and the role of mild acidosis in triggering mitochondrial restructuring and reprogramming to determine cellular bioenergetics and cell fate. Upper row: hypoxia causes mitochondrial fragmentation, loss of efficient ATP production and eventual cell death. Lower row: mild acidosis during hypoxia prevents DRP1-mediated fission and promotes mitochondrial elongation (in a SIMH-dependent manner) and cristae remodelling to maintain ATP levels and cell survival. In our model and experiments, 'no acidosis' and 'mild acidosis' indicate an extracellular pH of 7.2 and 6.5, respectively; 'hypoxia' indicates incubation at 1% oxygen for 0–12 h, and 'prolonged hypoxia' is considered following 12–21 h of incubation at 1% oxygen.

for mitochondrial ATP generation through mitochondrial respiration. More importantly, a pH-dependent shift in the bioenergetic status of neurons was observed over time, whereby cells in hypoxia at pH 7.2 relied increasingly on oligomycin-insensitive ATP production (that is, glycolysis) while neurons allowed to undergo physiological acidification relied on mitochondrial-dependent ATP production (Fig. 7f). Thus, acidosis sustains efficient mitochondrial ATP production during prolonged hypoxia (Fig. 7f).

An alteration in the metabolic profile of cells in hypoxia–acidosis implies an adaptation of the electron transport chain (ETC) components to maximize mitochondrial efficiency during limited oxygen availability. Several studies have reported the adverse effect of hypoxia on the expression and activity of ETC complexes as well as supercomplex disassembly[55,56]. Expression analysis of subunits encompassing the ETC complexes during acute hypoxia revealed maintained expression of Complex I subunit NDUFA9 as well as ATP synthase subunit ATP5a by mild acidosis (Supplementary Fig. 15). Blue native PAGE (BN-PAGE) analysis of the respiratory chain complexes showed a destabilization of the monomeric ATP synthase multiprotein complex during hypoxia, which is rescued by acidosis (Fig. 8a,b). Only a minor proportion of the ATP synthase is present in its dimeric form in neurons used during our experiments (Fig. 8c and Supplementary Fig. 16). Nonetheless, longer exposure of BN-PAGE from whole cells or BN-PAGE performed on isolated mitochondria revealed a higher molecular weight band corresponding to dimeric forms of the ATP synthase predominantly in hypoxia–acidosis conditions (Fig. 8c,d and Supplementary Fig. 16), indicating a distinct rise in the stability of the enzyme superassembly. The individual multiprotein complexes of the ETC can further associate into super-complexes, known as respirasomes[57,58]. It has been proposed that supercomplex assembly could stabilize the single complexes, enhance the electron flow between complexes and limit generation of oxygen radicals[59–63]. In addition, a distinct role for cristae shape has been recently shown to affect supercomplex assembly and respiratory efficiency[64]. Examination of higher order respiratory complex assembly by BN-PAGE showed a distinct reorganization of Complex I-containing supercomplexes by acidosis regardless of oxygen levels (Fig. 8e), resulting in loss of monomeric complex I and enhanced supercomplex assembly (complex I supercomplex:monomer ratio; Fig. 8h), as well as an increase in the relative levels (Fig. 8f). Detailed analysis of the respiratory supercomplexes showed maintained assembly of Complexes 1, III and IV into supercomplexes in the presence of acidosis during hypoxic conditions (Fig. 8g,h). We hypothesized that the acidosis-mediated changes to the OXPHOS complexes would be accompanied by an enhancement in the respiratory capacity of mitochondria. To test this hypothesis, the bioenergetic profile of mitochondria was assessed in intact neurons exposed to normoxic conditions at pH 7.2 and 6.5. First, basal cellular and mitochondrial oxygen consumption rate (OCR) was similar in both conditions (Fig. 8i,j). Next, the mitochondrial respiration capacity was determined using the uncoupler FCCP, which stimulates maximal mitochondrial respiration by dissipating the mitochondrial membrane potential. We found that acidosis significantly enhances the ability of mitochondria to increase their maximal respiratory capacity (Fig. 8i,j). In addition, analysis of mitochondrial reserve capacity, which signifies the ability of mitochondria to further engage in the production of ATP through OXPHOS, revealed a significant increase at pH 6.5 (Fig. 8i,j). These data coupled with data obtained from ATP studies provide evidence that acidosis maintains mitochondrial function during hypoxic stress. This is achieved through an adaptive reprogramming of mitochondrial respiratory efficiency that occurs as a result of changes in the mitochondrial ultrastructure and cristae shape, respiratory supercomplex assembly and maintenance of monomeric ATP synthase.

Discussion

The ability of post-mitotic cells to adapt and survive physiological or pathological stress, such as that imposed by oxygen deprivation, has been a long-standing question in biology. Here we report that mild extracellular acidosis, a biological consequence of anaerobic metabolism during hypoxia, restructures the mitochondrial network as an adaptive mechanism to enhance mitochondrial function and promote cellular survival. Mitochondrial remodelling by acidosis, through the activation of a dual programme that modulates mitochondrial dynamics and architecture, represents a novel and physiological pathway that sustains mitochondrial integrity and ATP production despite oxygen limitations. Preventing this reversible and homeostatic process results in mitochondrial dysfunction, fragmentation and

cell death. We provide a mechanism underlying the protective nature of mild acidosis, identify a novel physiological regulator of mitochondrial dynamics in post-mitotic cells and propose a role for mitochondrial morphology in the bioenergetic status of cells.

Survival of post-mitotic cells is highly dependent on a sufficient supply of energy to uphold the exhaustive demands incurred by complex molecular networks. The switch to anaerobic metabolism, albeit a critical cellular metabolic adaptation of hypoxic cells, cannot compensate for the loss of mitochondrial respiration during prolonged hypoxia[54,65,66]. As a result, cells faced with prolonged hypoxia will inevitably endure energy failure and cell death if not counteracted with an increase in energy supply. Data presented here demonstrate that post-mitotic cells have evolved a rapid and reversible mechanism to uphold efficient ATP production, via mitochondrial remodelling, that is regulated by acidosis. This is, to our knowledge, the first ascribed function for this metabolic product of anaerobic respiration historically associated with clinical resistance during ischemic insults. We propose a model whereby a threshold accumulation of extracellular protons, acquired through an initial increase in the glycolytic rate during hypoxia, would relay a signal back to mitochondria, potentially via changes in intracellular pH, in order to modulate mitochondrial bioenergetics (Fig. 9).

In recent years, mitochondrial structure and dynamics have emerged as a fundamental aspect for biological life. Our work further highlights this concept in demonstrating the protective nature of mitochondrial restructuring during stress. In addition, we provide a link between mitochondrial morphology and cristae architecture with the metabolic state of cells. The data presented in this study suggest that mitochondrial remodelling can instigate a systemic reconfiguration of mitochondrial efficiency to extract more ATP per oxygen molecule. In essence, acidosis-mediated reorganization of mitochondrial efficiency can override oxygen limitations and allow for the persistence of mitochondrial respiration in an anaerobic environment. This observation refines the well-established role of oxygen as a limiting factor for oxidative phosphosphorylation and puts forth the idea that mitochondrial reprogramming can dictate the bioenergetics of the cell. In view of these findings, the capability of post-mitotic cells to sense and adapt to anaerobic conditions by inducing anaerobic mitochondrial respiration should emerge as a central research theme in the study of physiological and pathological situations that relates to oxygen and energy homeostasis.

Methods

Mice, primary neuronal cultures and cell lines. To generate dorsal telencephalon-specific *MFN1* conditional mutant mice, floxed *MFN1* (Jackson Laboratories) and *Emx1-cre* heterozygous females were bred with floxed *MFN1* homozygous and *MFN2* heterozygous males. Telencephalon-specific *SLP2* conditional mutants were generated by breeding floxed *SLP2* homozygous females with *Foxg1-cre* male mice (provided by Dr Sean Cregan). Cortical neurons were cultured from CD1 wild-type female and male mice (Charles River) and *MFN1* or *SLP2* conditional knockout mice at embryonic day 14.5 or 15.5 (ref. 67). CGNs were cultured from CD1 mice at postnatal day 7 or 8 (ref. 13). All experiments were approved by the University of Ottawa's Animal Care ethics committee adhering to the Guidelines of the Canadian Council on Animal Care. Neurons were maintained in culture for 3–5 days before experimentation. MCF-7 breast carcinoma, A549 lung carcinoma, P19 embryonic teratocarcinoma, Cos7 African green monkey kidney fibroblasts, HeLa and C2C12 myoblasts were obtained from ATCC (Manassas, VA, USA). Primary and transformed MEFs were generated from CD1 mice on embryonic day 13.5. *In vitro* differentiation of C2C12 myoblasts into multinucleated mytotubes was performed by replacing fetal bovine serum (FBS)-containing DMEM with DMEM containing 2% horse serum when myoblasts were at 80% confluency. Media were changed every second day for about 7 days until multinucleated myotubes were formed.

Cell culture. The plating density for each cell population was chosen to optimize the rate of physiological extracellular acidification during hypoxic conditions. Cortical neurons and CGNs were seeded on plates (with or without coverslips) coated with 0.01 mg ml^{-1} poly-D-lysine (BD Bioscience) for all experiments. Cortical neurons were plated onto four-well plates, 35- and 60-mm dishes with 4.0×10^5, 3.0×10^6 and 9.0×10^6 neurons, respectively, and maintained in Neurobasal media (Gibco) that contained 2% B27 (Gibco), 1% N2 (Gibco), 0.6 mM L-glutamine (Gibco) and 1% Pen-Strep (Sigma). CGNs were plated in four- or 12-well plates with 4×10^5 and 8×10^5, respectively, and maintained in DMEM (Wisent Inc.) that contained 10% dialysed FBS (Sigma), 25 mM KCl, 2 mM glutamine (Invitrogen), 25 mM glucose and 0.1 mg ml^{-1} gentamycin (Sigma). MCF-7 and MEFs were plated in 35-mm dishes with 7×10^5 cells and maintained in DMEM containing 5% FBS and 1% Pen-Strep. All cells were maintained at 37 °C under 5% CO_2 environment until experimentation. Hypoxia was achieved by incubation in a hypoxic chamber at 37 °C under a 1% O_2, 5% CO_2 and N_2-balanced atmosphere. Acidosis experiments were conducted as previously described[68], with modifications. For acidosis experiments mimicking physiological conditions, SD or AP media was utilized. Buffer-free and low glucose (5.5 mM) medium (DMEM; Gibco) was freshly prepared and supplemented with B27 and N2 for post-mitotic neurons or 5% FBS for replicating cells. The level of physiological acidification of the extracellular environment is proportional to the cell density and the buffering capacity of the media. $NaHCO_3$ was added at 10 mM (post-mitotic cells) or 35 mM (replicating cells) and the pH was adjusted with HCl to 7.2 (SD media) or 6.5 (AP media). Air was bubbled into both media at 22 °C, which stabilizes the pH at 7.2. Culture media were aspirated and cells were washed × 2 in buffer-free low glucose DMEM to remove all traces of highly buffered culture media. Cells were then placed in AP or SD media. AP media slowly reverted to its original set pH under hypoxia, whereas the SD medium remained at pH 7.2. For acute acidosis experiments in hypoxia or normoxia, 30 mM of MES was used as a buffer and the pH was set and stabilized at the required value.

Viruses and materials. Recombinant adenoviral vectors carrying the DRP1-YFP or GFP expression cassette were prepared using the AdEasy system[12]. Lentivirus vectors carrying photoactivable GFP-ornithine carbamyltransferase (PA-GFP-Oct), Mito-DsRed, shRNA scramble control (shCtr sequence; 5′-CAACAAGATGAAG AGCACCAA-3′), and mouse-specific short-hairpin RNA (shRNA) OPA1 (shOPA1 sequence; 5′-GCCTGACTTTATATGGGAAAT-3′) were prepared using the ViraPower lentiviral expression system (Invitrogen)[13]. For lentiviruses and adenoviruses, neurons were transduced with 2 MOI (multiplicity of infection) or 50–100 MOI, respectively, at time of plating. For all experiments using viruses, neurons were infected with adenovirus or lentivirus for 72 h before experimentation. Oligomycin (10 μM), 6-deoxyglucose (6-DOG, 6 mM), cycloheximide (100 μg ml^{-1}), CPT (20 μM), mdivi-1 (50 μM), H89 (20 μM), forskolin (25 μM) and Monensin (1 μM) were used where indicated.

Immunofluorescence. Cells seeded on coverslips were fixed with 4% paraformaldehyde in PBS for 20 min at room temperature. Primary antibodies used were Tom20 (Santa Cruz; 1:100), Tuj1 (Covance; 1:10,000), MAP2 (Novus Biologicals; 1:200), NeuN (Millipore; 1:1,000), DLP1 (BD Biosciences; 1:100), Cytochrome *c* (BD Biosciences; 1:100) and Bax (Santa Cruz, 1:100). Cells were incubated for 1 h with a primary antibody solution containing 1% bovine serum albumin (BSA), 0.1% Triton-X-100 in PBS. Cells were washed several times in PBS before 1-h incubation with a secondary 594 or 488 Alexa (Invitrogen; 1:400). Hoechst stain 33342 (Sigma) or 4′,6-diamidino-2-phenylindole (DAPI) was added to visualize nuclei and coverslips were mounted using Immunomount (Thermo Scientific).

Immunohistochemistry. Coronal hippocampal slice preparations (200 μm) were incubated in oxygenated artificial cerebrospinal fluid (ACSF) buffered with PIPES to pH 7.2 or 6.5 for 4 h. Hippocampal slices were fixed for 20 min with ice-cold 4% paraformaldehyde in 1 × PBS and then rinsed twice with 1 × PBS. Slices were incubated in 10% sucrose and embedded in OCT and then sectioned using a microtome to 15-μm sections. Sections were stained with primary antibodies specific to Tom20 and NeuN in 10% normal goat serum-0.1% TritonX/0.1% Tween-20 in PBS overnight at 4 °C followed by 3 × 5 min washes with 1 × PBS. Sections were incubated with secondary antibodies in PBS for 1 h, washed for 5 min, stained with DAPI for 5 min, and then washed with 1 × PBS for 3 × 5 min. Slides were mounted using Immunomount (Thermo Scientific). Representative samples were imaged using a Zeiss Axiovert 100 (Oberkochen, Germany) confocal microscope equipped with a QiCam Digital camera (QImaging Corporation) and Zen software.

Mitochondrial length. Mitochondrial length was assessed by staining with Tom20 (translocase of outer mitochondria). Mitochondrial length was measured by tracing the mitochondria using the ImageJ software. Mitochondrial length was either binned into different categories (<0.5 μm, 0.5–1 μm, 1–2 μm, >2 μm) or taken as an average.

Intracellular pH measurements. Changes in intracellular pH was determined utilizing the ratiometric fluorescent intracellular pH indicator BCECF-AM (Invitrogen). Intracellular pH measurements were performed on cultured cortical neurons plated in 96-well black microplates that were treated for 6 h in the

appropriate experimental media and subsequently loaded with BCECF-AM (1 μM) for 30–45 min at 37 °C. A dual-excitation ratio of 480 and 440 nm and fixed emission at 535 nm was used to measure changes in BCECF-AM fluorescence. Since these experiments were designed to determine the effect of extracellular acidosis on intracellular pH, the measurements had to be performed while the cells were maintained in the respective experimental media (that is, media at pH 7.2 or pH 6.5). For this reason, the use of BCECF-AM was first validated by performing a calibration curve, using the high K+ Nigericin technique, to ensure that intracellular changes in pH can be detected in the experimental media. MES-buffered DMEM media was supplemented with 130 mM KCl and the pH was set to 6.0, 6.5, 7.0, 7.5 and 8.0 using KOH. The media of cells previously loaded with BCECF-AM (for 30–45 min) was replaced with the high K+ MES-buffered media supplemented with the ionophore Nigericin (Molecular Probes, 10 μM) and incubated for 10 min to allow for equilibration of the intracellular pH with the controlled extracellular medium. BCECF-AM fluorescence was measured as described above.

Immunoblot. For total cell lysates, cells were washed with PBS, lysed with 4% SDS in PBS, boiled for 5 min and the DNA was sheared by passage through a 26-gauge needle. Primary antibodies recognizing Complex I subunit NDUFA9 (Invitrogen; 1:1,000), Complex II 70-KDa Fp subunit (Invitrogen; 1: 10,000), ATP5a (Abcam; 1:1,000), Complex IV subunit 1 (Invitrogen; 1:1,000), Complex III core protein 2 (UQCRC2, Abcam; 1:1,000), DLP1 (DRP1, BD Transduction Laboratories; 1:1,000), Phoso-DRP1 S637 and S616 (Cell Signaling; 1:1,000), Fis1 (Biovision; 1:500), OPA1 (Abcam; 1:1,000), MFN1 and 2 (Abcam; 1:1,000), VDAC (Abcam; 1:1,000), mitochondrial heat-shock protein 70 (mtHSP70, Thermo Scientific; 1:5,000) and Actin (Santa Cruz; 1:1,000) were used. A secondary antibody conjugated to horseradish peroxidase (Jackson ImmunoResearch) was used and detected using Western Lightning Chemiluminescence Reagent Plus (Perkin Elmer). Representative full-gel bots are shown in Supplementary Fig. 17.

Immunoprecipitation. Cells were lysed in RIPA buffer (50 mM Tris (pH 7.2), 150 mM NaCl, 10% NP40 and 1 mM sodium orthovanadate with a protease inhibitor cocktail (PIC)). Cell lysates were incubated with anti-DRP1 antibody (BD Transduction Laboratories) for 1 h while tumbling at 4 °C, followed by overnight incubation with Sepharose A/G beads blocked in 2% BSA. Beads were washed 4 × in 1 × Tris-buffered saline and eluted by boiling at 95 °C for 4 min.

Time-lapse imaging and mitochondrial fusion assay. Cortical neurons were seeded on 35-mm dishes with coverslip bottoms (MatTek) coated with poly-D-lysine (VWR International) and infected with 2 MOI of the photoactivable GFP tagged to ornithine carbamyltransferase (PA-GFP-Oct) and Mito-DsRed. Following 2-h incubation in MES-buffered media at pH 7.2 or 6.5, plates were mounted in a temperature-controlled chamber (37 °C) and visualized with an LSM-510 confocal laser-scanning microscope (Axiovert 200), with a × 63 oil immersion objective. Mitochondrial fusion assays were performed as described previously with modifications[13]. Briefly, PA-GFP-Oct was first pre-imaged and scanned to ensure that there is no spontaneous activation. PA-GFP-Oct was then photoactivated with a 405-nm laser and the spreading of the signal was imaged every 2 min using a 488-nm line for a total of 22 min. Mito-DsRed was excited at 543 nm and was used a guide to ensure that the ROI for PA-GFP-Oct activation was within the mitochondria. The fusion rate was expressed as a relative measure of pixel intensity at the indicated time over that at $t = 0$ min (where 0 min represents the signal detected after 2 min of photoactivation and equilibration of GFP signal).

OPA1 crosslinking. *In vivo* crosslinking reactions were performed at 37 °C with 10 mM BMH crosslinker (Fisher Scientific) for 20 min. Reactions were terminated by adding 0.001% β-mercaptoethanol. Cells were lysed following crosslinking, and analysed by gradient gel electrophoresis using NuPAGE Novex 3–8% Tris-acetate gradient gels (Life Technologies), followed by western blotting against OPA1.

(TEM) and cristae analyses. Mitochondrial ultrastructure was analysed from whole cells of cultured cortical neurons following 6-h treatment in the appropriate conditions. Briefly, plated neurons were rapidly washed in PBS and harvested by scraping very lightly. Neurons were fixed in 2% gluteraldehyde for 20 min at room temperature and stored immediately at 4 °C for processing as previously described[69]. Cristae analysis was performed using ImageJ and a minimum of 100 mitochondria were analysed. For each individual cristae, the average diameter was measured from three representative regions.

Cytochrome *c* release. Neurons were treated with 20 μM CPT for the indicated times, fixed and stained with cytochrome *c* and Tom20-specific antibodies. For each replicate, a total of 100 neurons were counted from three to five different fields using a Zeiss 510 meta confocal microscope. A diffused cytochrome *c* staining or complete lack of staining was identified as release.

Cell viability assay. Following 30 h of incubation under the indicated conditions, cells were subjected to a live–dead assay (Invitrogen) by staining with calcein (live cells) and ethidium homodimer-1 (dead cells) for 10–15 min at 37 °C. In each replicate, three to five different fields were randomly chosen and imaged per treatment group. Cell death was expressed as a percentage of total cells. Calcein and ethidium homodimer-1 dyes are unaffected by pH as neutralization of an acidic set or acidification of a neutral set immediately before addition of the dyes yielded the same results.

Mitochondrial membrane potential. Neurons were seeded in 96-well black microplates. Following the appropriate treatment, 50 nM TMRE was added and cells were incubated for 30 min at 37 °C under normoxia (control) or hypoxia. FCCP (1 μM) was added to the appropriate wells 10 min before addition of TMRE. Neurons were washed in PBS and TMRE fluoresence was measured in a plate reader at Ex 510 nM an Em 590 nM.

ATP assay. ATP concentrations were measured with the CellTiter-Glo Luminescent Assay (Promega) using a LUMIstar Galaxy luminometer (BMG Labtechnologies) according to the manufacturer's protocol. Data were collected from multiple replicate wells for each experiment. Viability of cells under all conditions was ensured by PI staining.

Blue-native PAGE. ETC supercomplexes and ATP synthase assembly were analysed from whole cells or isolated mitochondria[70]. For whole cells, following the indicated treatments, cells were harvested in PBS on ice, pelleted at 960 *g* for 5 min at 4 °C. For isolated mitochondria, cells were washed with PBS and lysed in mitochondrial isolation buffer (200 mM mannitol, 70 mM sucrose, 10 mM HEPES, pH 7.4, 1 mM EGTA, PIC 1:1,000) on ice using a 25-G needle. Following centrifugation at 110 *g* for 9 min to remove nuclei and cellular debris, the supernatant was centrifuged at 8,600 *g* for 9 min to pellet mitochondria. This differential centrifugation step was repeated to further purify the mitochondrial fraction. For BN-PAGE analysis, pellets of whole cells or isolated mitochondria were resuspended in digitonin extraction buffer (50 mM imidazole/HCl pH 7.0, 50 mM NaCl, 5 mM 6-aminohexanoic acid, 1 mM EDTA and the appropriate ratio of digitonin). A 1% digitonin ratio was used for Complex-1 and supercomplexes, and 2% was used for ATP synthase assembly. One hundred fifty micrograms were loaded with 5% glycerol and 1:10 dye:digitonin ratio of coomassie dye in 500 mM 6-aminohexanoic acid on 3–13% large acrylamide gradient gels. Gels were transferred to nitrocellulose membranes and the resulting membranes were subjected to immunoblotting.

Oxygen consumption. The Seahorse XF24 Extracellular Flux Analyzer (Seahorse Biosciences; North Billerica, MA, USA) was used to measure oxygen consumption in cells. Cortical neurons were seeded onto 24-well Seahorse plates at a density of 1.5×10^5 cells per well. Following treatment, cells were washed with modified Kreb's Ringer Buffer (128 mM NaCl, 4.8 mM KCl, 1.2 mM KH_2PO_4, 1.2 $MgSO_4$, 25 mM $CaCl_2$, 0.1% BSA (fatty acid-free), 10 mM glucose and 1 mM sodium pyruvate, pH 7.4) and placed in Kreb's Ringer Buffer for 15 min at 37 °C before loading into the XF Analyser. Following mesurements of resting respiration, cells were treated sequentially with the following: oligomycin (0.2 μg μl^{-1}), to measure the nonphosphorylating OCR; FCCP (1 μM), to get the maximal OCR; and antimycin A (2.5 μM) and rotenone (1 μM), to measure the extramitochondrial OCR. Each measurement was taken over a 2-min interval followed by 2 min mixing and 2 min incubation. Three measurements were taken for the resting OCR, three after oligomycin treatment, two after FCCP and two after antimycin A and rotenone.

Quantification and statistical analysis. For mitochondrial length measurements, all mitochondria in a field were measured as per condition and a minimum of 1,000 mitochondria were measured for each treatment. For cell death studies, a minimum of 300 cells per field (minimum five fields) were scored for each treatment at the indicated time points. The data represent mean values ± s.d. from three independent experiments ($n = 3$) unless otherwise noted. *P*-values were obtained using a two-tailed Student's *t*-test.

References

1. Lin, M. T. & Beal, M. F. Mitochondrial dysfunction and oxidative stress in neurodegenerative diseases. *Nature* **443,** 787–795 (2006).
2. Terman, A., Kurz, T., Navratil, M., Arriaga, E. A. & Brunk, U. T. Mitochondrial turnover and aging of long-lived postmitotic cells: the mitochondrial-lysosomal axis theory of aging. *Antioxid. Redox. Signal* **12,** 503–535.
3. Newmeyer, D. D. & Ferguson-Miller, S. Mitochondria: releasing power for life and unleashing the machineries of death. *Cell* **112,** 481–490 (2003).
4. Detmer, S. A. & Chan, D. C. Functions and dysfunctions of mitochondrial dynamics. *Nat. Rev. Mol. Cell Biol.* **8,** 870–879 (2007).
5. Youle, R. J. & van der Bliek, A. M. Mitochondrial fission, fusion, and stress. *Science* **337,** 1062–1065 (2012).
6. Gomes, L. C., Di Benedetto, G. & Scorrano, L. During autophagy mitochondria elongate, are spared from degradation and sustain cell viability. *Nat. Cell Biol.* **13,** 589–598 (2011).

7. Tondera, D. *et al.* SLP-2 is required for stress-induced mitochondrial hyperfusion. *EMBO J.* **28,** 1589–1600 (2009).
8. Barsoum, M. J. *et al.* Nitric oxide-induced mitochondrial fission is regulated by dynamin-related GTPases in neurons. *EMBO J.* **25,** 3900–3911 (2006).
9. Frank, S. *et al.* The role of dynamin-related protein 1, a mediator of mitochondrial fission, in apoptosis. *Dev. Cell* **1,** 515–525 (2001).
10. Knott, A. B., Perkins, G., Schwarzenbacher, R. & Bossy-Wetzel, E. Mitochondrial fragmentation in neurodegeneration. *Nat. Rev. Neurosci.* **9,** 505–518 (2008).
11. Scheckhuber, C. Q. *et al.* Reducing mitochondrial fission results in increased life span and fitness of two fungal ageing models. *Nat. Cell Biol.* **9,** 99–105 (2007).
12. Jahani-Asl, A. *et al.* Mitofusin 2 protects cerebellar granule neurons against injury-induced cell death. *J. Biol. Chem.* **282,** 23788–23798 (2007).
13. Jahani-Asl, A. *et al.* The mitochondrial inner membrane GTPase, optic atrophy 1 (Opa1), restores mitochondrial morphology and promotes neuronal survival following excitotoxicity. *J. Biol. Chem.* **286,** 4772–4782 (2011).
14. Wang, J. X. *et al.* miR-499 regulates mitochondrial dynamics by targeting calcineurin and dynamin-related protein-1. *Nat. Med.* **17,** 71–78 (2011).
15. Chandel, N. S., Budinger, G. R. & Schumacker, P. T. Molecular oxygen modulates cytochrome c oxidase function. *J. Biol. Chem.* **271,** 18672–18677 (1996).
16. Wilson, D. F., Rumsey, W. L., Green, T. J. & Vanderkooi, J. M. The oxygen dependence of mitochondrial oxidative phosphorylation measured by a new optical method for measuring oxygen concentration. *J. Biol. Chem.* **263,** 2712–2718 (1988).
17. Solaini, G., Baracca, A., Lenaz, G. & Sgarbi, G. Hypoxia and mitochondrial oxidative metabolism. *Biochim. Biophys. Acta* **1797,** 1171–1177 (2010).
18. Jezek, P. & Plecita-Hlavata, L. Mitochondrial reticulum network dynamics in relation to oxidative stress, redox regulation, and hypoxia. *Int. J. Biochem. Cell Biol.* **41,** 1790–1804 (2009).
19. Zanelli, S. A., Trimmer, P. A. & Solenski, N. J. Nitric oxide impairs mitochondrial movement in cortical neurons during hypoxia. *J. Neurochem.* **97,** 724–736 (2006).
20. Siemkowicz, E. & Hansen, A. J. Brain extracellular ion composition and EEG activity following 10 minutes ischemia in normo- and hyperglycemic rats. *Stroke* **12,** 236–240 (1981).
21. Kaku, D. A., Giffard, R. G. & Choi, D. W. Neuroprotective effects of glutamate antagonists and extracellular acidity. *Science* **260,** 1516–1518 (1993).
22. Meyer, F. B., Anderson, R. E., Sundt, Jr. T. M. & Yaksh, T. L. Intracellular brain pH, indicator tissue perfusion, electroencephalography, and histology in severe and moderate focal cortical ischemia in the rabbit. *J. Cereb. Blood Flow. Metab.* **6,** 71–78 (1986).
23. Allen, D. & Westerblad, H. Physiology. Lactic acid--the latest performance-enhancing drug. *Science* **305,** 1112–1113 (2004).
24. Bing, O. H., Brooks, W. W. & Messer, J. V. Heart muscle viability following hypoxia: protective effect of acidosis. *Science* **180,** 1297–1298 (1973).
25. Currin, R. T., Gores, G. J., Thurman, R. G. & Lemasters, J. J. Protection by acidotic pH against anoxic cell killing in perfused rat liver: evidence for a pH paradox. *FASEB J.* **5,** 207–210 (1991).
26. Morimoto, Y., Morimoto, Y., Kemmotsu, O. & Alojado, E. S. Extracellular acidosis delays cell death against glucose-oxygen deprivation in neuroblastoma x glioma hybrid cells. *Crit. Care. Med.* **25,** 841–847 (1997).
27. Nielsen, O. B., de Paoli, F. & Overgaard, K. Protective effects of lactic acid on force production in rat skeletal muscle. *J. Physiol.* **536,** 161–166 (2001).
28. Penttila, A. & Trump, B. F. Extracellular acidosis protects Ehrlich ascites tumor cells and rat renal cortex against anoxic injury. *Science* **185,** 277–278 (1974).
29. Tombaugh, G. C. & Sapolsky, R. M. Evolving concepts about the role of acidosis in ischemic neuropathology. *J. Neurochem.* **61,** 793–803 (1993).
30. Fan, Y. Y. *et al.* A novel neuroprotective strategy for ischemic stroke: transient mild acidosis treatment by CO inhalation at reperfusion. *J. Cereb. Blood Flow Metab.* **34,** 275–283 (2013).
31. Inserte, J., Ruiz-Meana, M., Rodriguez-Sinovas, A., Barba, I. & Garcia-Dorado, D. Contribution of delayed intracellular pH recovery to ischemic postconditioning protection. *Antioxid. Redox Signal.* **14,** 923–939 (2011).
32. Fujita, M. *et al.* Prolonged transient acidosis during early reperfusion contributes to the cardioprotective effects of postconditioning. *Am. J. Physiol. Heart Circ. Physiol.* **292,** H2004–H2008 (2007).
33. Lam, T. I. *et al.* Intracellular pH reduction prevents excitotoxic and ischemic neuronal death by inhibiting NADPH oxidase. *Proc. Natl Acad. Sci. USA* **110,** E4362–E4368 (2013).
34. Wu, S. Y. *et al.* Protective effect of hypercapnic acidosis in ischemia-reperfusion lung injury is attributable to upregulation of heme oxygenase-1. *PLoS One* **8,** e74742 (2013).
35. McCarty, M. F. & Whitaker, J. Manipulating tumor acidification as a cancer treatment strategy. *Altern. Med. Rev.* **15,** 264–272 (2010).
36. Bouyer, P. *et al.* Effect of extracellular acid-base disturbances on the intracellular pH of neurones cultured from rat medullary raphe or hippocampus. *J. Physiol.* **559,** 85–101 (2004).
37. Henrich, M. & Buckler, K. J. Effects of anoxia, aglycemia, and acidosis on cytosolic Mg2+, ATP, and pH in rat sensory neurons. *Am. J. Physiol. Cell Physiol.* **294,** C280–C294 (2008).
38. Liu, X. & Hajnoczky, G. Altered fusion dynamics underlie unique morphological changes in mitochondria during hypoxia-reoxygenation stress. *Cell Death Differ.* **18,** 1561–1572 (2011).
39. Ong, S. B. *et al.* Inhibiting mitochondrial fission protects the heart against ischemia/reperfusion injury. *Circulation* **121,** 2012–2022 (2010).
40. Smirnova, E., Griparic, L., Shurland, D. L. & van der Bliek, A. M. Dynamin-related protein Drp1 is required for mitochondrial division in mammalian cells. *Mol. Biol. Cell* **12,** 2245–2256 (2001).
41. Cassidy-Stone, A. *et al.* Chemical inhibition of the mitochondrial division dynamin reveals its role in Bax/Bak-dependent mitochondrial outer membrane permeabilization. *Dev. Cell* **14,** 193–204 (2008).
42. Loson, O. C., Song, Z., Chen, H. & Chan, D. C. Fis1, Mff, MiD49, and MiD51 mediate Drp1 recruitment in mitochondrial fission. *Mol. Biol. Cell* **24,** 659–667 (2013).
43. Yoon, Y., Krueger, E. W., Oswald, B. J. & McNiven, M. A. The mitochondrial protein hFis1 regulates mitochondrial fission in mammalian cells through an interaction with the dynamin-like protein DLP1. *Mol. Cell Biol.* **23,** 5409–5420 (2003).
44. Cribbs, J. T. & Strack, S. Reversible phosphorylation of Drp1 by cyclic AMP-dependent protein kinase and calcineurin regulates mitochondrial fission and cell death. *EMBO Rep.* **8,** 939–944 (2007).
45. Qi, X., Disatnik, M. H., Shen, N., Sobel, R. A. & Mochly-Rosen, D. Aberrant mitochondrial fission in neurons induced by protein kinase C{delta} under oxidative stress conditions *in vivo*. *Mol. Biol. Cell* **22,** 256–265 (2011).
46. Meeusen, S. *et al.* Mitochondrial inner-membrane fusion and crista maintenance requires the dynamin-related GTPase Mgm1. *Cell* **127,** 383–395 (2006).
47. Cipolat, S., Martins de Brito, O., Dal Zilio, B. & Scorrano, L. OPA1 requires mitofusin 1 to promote mitochondrial fusion. *Proc. Natl Acad. Sci. USA* **101,** 15927–15932 (2004).
48. Chen, H. *et al.* Mitofusins Mfn1 and Mfn2 coordinately regulate mitochondrial fusion and are essential for embryonic development. *J. Cell Biol.* **160,** 189–200 (2003).
49. Frezza, C. *et al.* OPA1 controls apoptotic cristae remodeling independently from mitochondrial fusion. *Cell* **126,** 177–189 (2006).
50. Frey, T. G. & Mannella, C. A. The internal structure of mitochondria. *Trends Biochem. Sci.* **25,** 319–324 (2000).
51. Olichon, A. *et al.* Loss of OPA1 perturbates the mitochondrial inner membrane structure and integrity, leading to cytochrome c release and apoptosis. *J. Biol. Chem.* **278,** 7743–7746 (2003).
52. Arnoult, D., Grodet, A., Lee, Y. J., Estaquier, J. & Blackstone, C. Release of OPA1 during apoptosis participates in the rapid and complete release of cytochrome c and subsequent mitochondrial fragmentation. *J. Biol. Chem.* **280,** 35742–35750 (2005).
53. Scorrano, L. *et al.* A distinct pathway remodels mitochondrial cristae and mobilizes cytochrome c during apoptosis. *Dev. Cell* **2,** 55–67 (2002).
54. Semenza, G. L. Targeting HIF-1 for cancer therapy. *Nat. Rev. Cancer* **3,** 721–732 (2003).
55. Galkin, A., Abramov, A. Y., Frakich, N., Duchen, M. R. & Moncada, S. Lack of oxygen deactivates mitochondrial complex I: implications for ischemic injury? *J. Biol. Chem.* **284,** 36055–36061 (2009).
56. Piruat, J. I. & Lopez-Barneo, J. Oxygen tension regulates mitochondrial DNA-encoded complex I gene expression. *J. Biol. Chem.* **280,** 42676–42684 (2005).
57. Acin-Perez, R., Fernandez-Silva, P., Peleato, M. L., Perez-Martos, A. & Enriquez, J. A. Respiratory active mitochondrial supercomplexes. *Mol. Cell* **32,** 529–539 (2008).
58. Schagger, H. & Pfeiffer, K. Supercomplexes in the respiratory chains of yeast and mammalian mitochondria. *EMBO J.* **19,** 1777–1783 (2000).
59. Lapuente-Brun, E. *et al.* Supercomplex assembly determines electron flux in the mitochondrial electron transport chain. *Science* **340,** 1567–1570 (2013).
60. Acin-Perez, R. *et al.* Respiratory complex III is required to maintain complex I in mammalian mitochondria. *Mol. Cell* **13,** 805–815 (2004).
61. Diaz, F., Fukui, H., Garcia, S. & Moraes, C. T. Cytochrome c oxidase is required for the assembly/stability of respiratory complex I in mouse fibroblasts. *Mol. Cell Biol.* **26,** 4872–4881 (2006).
62. Schagger, H. Respiratory chain supercomplexes. *IUBMB Life* **52,** 119–128 (2001).
63. Suthammarak, W., Morgan, P. G. & Sedensky, M. M. Mutations in mitochondrial complex III uniquely affect complex I in *Caenorhabditis elegans*. *J. Biol. Chem.* **285,** 40724–40731.
64. Cogliati, S. *et al.* Mitochondrial cristae shape determines respiratory chain supercomplexes assembly and respiratory efficiency. *Cell* **155,** 160–171 (2013).
65. Unno, N. *et al.* Hyperpermeability and ATP depletion induced by chronic hypoxia or glycolytic inhibition in Caco-2BBe monolayers. *Am. J. Physiol.* **270,** G1010–G1021 (1996).

66. Iyer, N. V. *et al.* Cellular and developmental control of O2 homeostasis by hypoxia-inducible factor 1 alpha. *Genes Dev.* **12,** 149–162 (1998).
67. Cregan, S. P. *et al.* Bax-dependent caspase-3 activation is a key determinant in p53-induced apoptosis in neurons. *J. Neurosci.* **19,** 7860–7869 (1999).
68. Mekhail, K., Gunaratnam, L., Bonicalzi, M. E. & Lee, S. HIF activation by pH-dependent nucleolar sequestration of VHL. *Nat. Cell Biol.* **6,** 642–647 (2004).
69. Cheung, E. C. *et al.* Dissociating the dual roles of apoptosis-inducing factor in maintaining mitochondrial structure and apoptosis. *EMBO J.* **25,** 4061–4073 (2006).
70. Wittig, I., Braun, H. P. & Schagger, H. Blue native PAGE. *Nat. Protoc.* **1,** 418–428 (2006).

Acknowledgements

We thank Dr Stephen Lee for critical review of the manuscript, as well as Linda Jui, Peter Rippstein, Vincent Paupe, Alysen Clark and Delphie Dugal-Tessier for excellent technical assistance. This research was funded by grants from the Heart and Stroke Foundation of Canada (HSFO) and Brain Canada/Krembil Foundation to R.S.S. M.K. was supported by fellowships from the Canadian Partnership for Stroke Recovery and the Heart and Stroke Foundation of Canada. D.P. was supported by Ontario Graduate Scholarship (OGS). Equipment was supported by the Canadian Partnership for Stroke Recovery.

Author contributions

All authors reviewed the manuscript. M.K. conceptualized the study, designed and performed experiments, analysed data and wrote the paper; M.T. assisted, performed and analysed experiments; D.P. assisted in the BN-PAGE and Seahorse experiments and interpreted the data; P.K. designed and performed *in vivo* experiments and interpreted the data; J.M. provided technical assistance and generated tools for the study; J.G. performed SLP2 experiments; R.B. supervised *in vivo* experiments; S.P.C. provided the SLP2 conditional mice, supervised and performed SLP2 experiments; M.E.H. provided the Seahorse Analyzer, reagents and interpreted the data; D.P. provided reagents and interpreted the data; and R.S.S. supported and directed the research.

Additional information

Supplementary Information accompanies this paper at http://www.nature.com/naturecommunications

Competing financial interests: The authors declare no competing financial interests.

Reprints and permission information is available online at http://npg.nature.com/reprintsandpermissions/

How to cite this article: Khacho, M. *et al.* Acidosis overrides oxygen deprivation to maintain mitochondrial function and cell survival. *Nat. Commun.* 5:3550 doi: 10.1038/ncomms4550 (2014).

SYNAPSE 65:1181–1195 (2011)

Chronically Saturating Levels of Endogenous Glycine Disrupt Glutamatergic Neurotransmission and Enhance Synaptogenesis in the CA1 Region of Mouse Hippocampus

WAFAE BAKKAR,[1,2] CHUN-LEI MA,[3] MOHAN PABBA,[1,2] PAMELA KHACHO,[1,2] YONG-LI ZHANG,[1] EMILIE MULLER,[1] MARZIA MARTINA,[4] AND RICHARD BERGERON[1,2,5]*

[1]*Ottawa Hospital Research Institute, Ottawa, Ontario, Canada*
[2]*Department of Cellular and Molecular Medicine, University of Ottawa, Ottawa, Ontario, Canada*
[3]*Department of Physiology Binzhou Medical College, Yantai Campus #346 Guanhai Road, Laishan District, Yantai City. Shandong Province, 264003, China*
[4]*National Research Council of Canada, Ottawa, Ontario, Canada*
[5]*Department of Psychiatry, University of Ottawa, Ottawa, Ontario, Canada*

KEY WORDS glutamate; NMDA receptor; mEPSC; glycine encephalopathy; whole-cell patch-clamp; Ifenprodil

ABSTRACT Glycine serves a dual role in neurotransmission. It is the primary inhibitory neurotransmitter in the spinal cord and brain stem and is also an obligatory coagonist at the excitatory glutamate, *N*-methyl-D-aspartate receptor (NMDAR). Therefore, the postsynaptic action of glycine should be strongly regulated to maintain a balance between its inhibitory and excitatory inputs. The glycine concentration at the synapse is tightly regulated by two types of glycine transporters, GlyT1 and GlyT2, located on nerve terminals or astrocytes. Genetic studies demonstrated that homozygous (GlyT1−/−) newborn mice display severe sensorimotor deficits characterized by lethargy, hypotonia, and hyporesponsivity to tactile stimuli and ultimately die in their first postnatal day. These symptoms are similar to those associated with the human disease glycine encephalopathy in which there is a high level of glycine in cerebrospinal fluid of affected individuals. The purpose of this investigation is to determine the impact of chronically high concentrations of endogenous glycine on glutamatergic neurotransmission during postnatal development using an in vivo mouse model (GlyT1+/−). The results of our study indicate the following; that compared with wild-type mice, CA1 pyramidal neurons from mutants display significant disruptions in hippocampal glutamatergic neurotransmission, as suggested by a faster kinetic of NMDAR excitatory postsynaptic currents, a lower reduction of the amplitude of NMDAR excitatory postsynaptic currents by ifenprodil, no difference in protein expression for NR2A and NR2B but a higher protein expression for PSD-95, an increase in their number of synapses and finally, enhanced neuronal excitability. **Synapse 65:1181–1195, 2011.**

INTRODUCTION

Aside from its role in protein synthesis and metabolism, glycine is a well-established inhibitory neurotransmitter, particularly in the spinal cord and brain stem where it activates strychnine-sensitive ionotropic glycine receptors (GlyRs) (Legendre, 2001; Betz and Laube, 2006; Kirsch, 2006). In addition to its inhibitory function, numerous studies performed in the last two decades showed that glycine is implicated in neurotransmission mediated by glutamate, the major excitatory neurotransmitter in the nervous

Additional Supporting Information may be found in the online version of this article.

V.B. and C.-L. M. have contributed equally to the manuscript

Contract grant sponsor: March of Dimes Foundation; Contract grant number: 6-FY06-327; Contract grant sponsor: Richard Bergeron is also a recipient of the New Investigator Award from the Canadian Institutes of Health Research

*Correspondence to: Richard Bergeron, Ottawa Hospital Research Institute, 725 Parkdale Avenue, Ottawa, ON, Canada K1Y 4E9. E-mail: rbergeron@ohri.ca

Received 3 February 2011; Accepted 18 May 2011

DOI 10.1002/syn.20956

Published online 1 June 2011 in Wiley Online Library (wileyonlinelibrary.com).

system that acts as a coagonist at the *N*-methyl-D-aspartate receptor (NMDAR) (Johnson and Ascher, 1987; Kleckner and Dingledine, 1988; Mayer, Vyklicky, and Clements, 1989; Thomson, Walker, and Flynn, 1989; Gabernet et al., 2005; Bergeron, Meyer, Coyle, and Greene, 1998; Berger, Dieudonne, and Ascher, 1998). It is important to mention that several studies also indicate that D-serine could be the more important coagonist at NMDAR, particularly in the hippocampus (Schell, Molliver, and Snyder, 1995).

Similar to other neurotransmitters, glycine gradients in the nervous system are tightly regulated by specialized transmembrane proteins known as glycine transporters (GlyTs) (Smith et al., 1992; Liu et al., 1992; Zafra et al., 1995; Borowsky, Mezey, and Hoffman, 1993; Liu et al., 1993; Lopez-Corcuera, Alcantara, Vazquez, and Aragon, 1993; Guastella et al., 1992; Jursky and Nelson, 1996; Adams, et al., 1995; Zafra et al., 1995; Eulenburg, Armsen, Betz, and Gomeza, 2005). These ion-driven reuptake pumps have two different genes which code for two GlyT subtypes, GlyT1 and GlyT2 (Borowsky, Mezey, and Hoffman, 1993). The in vivo role of GlyTs contributes to the overall activity of inhibitory GlyRs and glutamatergic neurotransmission as recently demonstrated using genetically altered mice (Gomeza et al., 2003; Gomeza et al., 2003; Aragon and Lopez-Corcuera, 2005). Homozygote GlyT1-/- mice die on their first day of birth (Gomeza et al., 2003; Tsai et al., 2004) due to over-activation of GlyRs, whereas heterozygote (GlyT1+/−) animals develop relatively normally but show a disruption in glutamatergic neurotransmission in the forebrain (Martina et al., 2005; Gabernet et al., 2005; Yee et al., 2006).

NMDARs play a central role in synaptic transmission and plasticity (Lau and Zukin, 2007). These ionotropic receptors, which are gated by glutamate (Cull-Candy, Brickley, and Farrant, 2001; Papadia and Hardingham, 2007), incorporate different subunits from a repertoire of three subtypes: NR1, NR2, and NR3, to form heterotetrameric complexes. There are eight NR1 splice variants, four NR2 subunits (A-D), and two NR3 subunits (A and B). The consensus is that NMDARs on CA1 pyramidal cells (CA1 PCs) are tetraheteromers, typically composed of two glycine-binding NR1 subunits and two glutamate-binding NR2 subunits (Anson et al., 1998; Waxman and Lynch, 2005). NR1 is essential for a functional NMDAR, whereas the identity of the NR2 subunit is critical in determining many biophysical and pharmacological properties of the receptor. Although NR2B is the predominant subunit at the synapse early in postnatal development (Monyer et al., 1992; Monyer Laurie, Sakmann, and Seeburg, 1994; Stocca and Vicini, 1998), NR2A expression, which produces the NMDAR current with the fastest kinetics, increases during the postnatal period (Sans, Petralia, Wang, Blahos, Hell, and Wenthold, 2000; Stephenson, 2001).

The purpose of this investigation is to determine the impact of chronic high levels of glycine on different parameters of glutamatergic NMDAR-mediated neurotransmission during the postnatal development in the CA1 region of the mouse hippocampus, using the in vivo mouse model (GlyT1+/−).

Abbreviations

ACSF	artificial cerebrospinal fluid
AMPA	α-amino-3-hydroxy-5-methylisoxazole-4-propionic acid
APV	amino-phosphoro-valeric acid
CNS	central nervous system
GABA	γ-aminobutyric acid
GlyT	glycine transporter
GMS	glycine modulatory site
IR	immunoreactivity
NBQX	1,2,3,4-tetrahydro-6-nitro-2,3-dioxobenzo[f]quinoxaline-7-sulfonamide
NFPS	glycine transporter antagonist type 1
NMDAR	*N*-methyl-D-aspartate receptor
PBS	phosphate buffer saline
QX-314	*N*-ethyl bromide
TTX	tetrodotoxin
WT	wild type mice
EPSC	excitatory postsynaptic current
EDTA	ethylenediaminetetracetic acid
TBS	tris-buffered saline.

EXPERIMENTAL PROCEDURES

Genotyping

All mice used for this investigation were backcrossed at least nine generations to the 129/SvEvTac background, as previously described (Tsai et al., 2004). Genotyping of GlyT1+/− mice has been previously described (Martina et al., 2005; Imamura, Ma, Pabba, and Bergeron, 2008). Briefly, polymerase chain reaction (PCR) amplification of genomic DNA was prepared from mouse tissue. Mouse tail samples were incubated in proteinase K (0.5 mg/ml; Sigma, St. Louis, MO) at 50°C overnight and were centrifuged (20 min) at 1600 g. The supernatant was then added to a double volume of isopropanol to precipitate the genomic DNA. The supernatant was removed and the DNA was washed with 70% ethanol and allowed to dry. DNA was resuspended in 300 μl of water of which 1 μl was added to the PCR mixture.

PCR analysis was done using *Taq* DNA polymerase (Invitrogen Corporation, Carlsbad, CA). Reaction products were run on a 1% agarose gel and visualized using ethidium bromide. Primer sequences (5′-3′) were: Primer 1 GCCTTGGGAAAAGCGCCTCC; Primer 2 CCCCTACTTCATCATGCTGATC; Primer 3 CACCTACCAGTAGTTGCCTT. Cycling conditions (GeneAmp 2400, Perkin-Elmer, Foster City, CA) were 2 min at 95°C followed by 36 cycles at 94°C (melting) for 30 s, 57°C (annealing) for 30 s, and 72°C (extension) for 1 min 40 s.

The reaction solution contained Mg^{2+} (1.5 mM), dNTPs (0.2 mM each), oligonucleotide primers (0.625 μM for Primer 1 and 0.25 μM for Primer 3), *Taq* polymerase (2.5 units), reaction buffer (10×; 2 μl), and 1 μl of solubilized genomic DNA (20 μl final volume) in distilled water. Each mouse was genotyped using one reaction as previously shown (Tsai, Ralph-Williams, Martina et al., 2004). WT mice showed a single band at 1.3 Kb,reas whe the GlyT1+/− mice had an additional band at 1.0 Kb.

Electrophysiology

Hippocampal slices preparation

Prior to decapitation, the animals were anesthetized with isofluorane in agreement with the guidelines of the Canadian Council of Animal Care. The brain was removed and placed in the oxygenated (95% O_2 and 5% CO_2) artificial cerebrospinal fluid (ACSF) at 4°C containing (mM): 126 NaCl, 2.5 KCl, 1 $MgCl_2$, 26 $NaHCO_3$, 1.25 NaH_2PO_4, 2 $CaCl_2$, and 10 glucose. The ACSF solution was adjusted to. an osmolarity of 300 mOsml/L and the pH adjusted to 7.2. Acute coronal brain slices (300 μm) containing the hippocampus were obtained from GlyT1+/− and WT mice at 2, 3, 4, and 8 weeks of age with a vibrating microtome (Leica VT 1000S, Nassloch, Germany). The slices were then transferred to a chamber containing oxygenated ACSF and maintained at room temperature for at least 1 h prior to the recording.

Data recording and analysis

Electrical stimulation of the Schaffer collaterals with a bipolar microelectrode positioned in the stratum radiatum evoked postsynaptic responses. The stimulation was delivered every 12 s with a pulse duration of 100 μs. The stimulation intensity was set in order to obtain an NMDAR-mediated excitatory postsynaptic current (NMDAR EPSC) amplitude of 30-60 pA at a membrane holding potential of −65 mV.

To minimize the current attenuation of NMDAR EPSC, we performed voltage-clamp experiments with pipettes filled with a solution containing (mM) 130 Cs^+ methanesulphonate, 10 Hepes, 2 $MgCl_2$, 2 ATP-Mg, 0.5 GTP, 1 lignocaine (lidocaine) *N*-ethyl bromide (QX-314), and 2 EGTA. For recordings of spontaneous activity, 0.2 mM EGTA was used instead of 2. To isolate the NMDAR-mediated component of evoked responses, we used ACSF containing a low concentration of $MgCl_2$ (0.1 mM) with osmolarity maintained by $CaCl_2$ (2.9 mM) and added (μM): five 1,2,3,4-tetrahydro-6-nitro-2,3-dioxobenzo[f]quinoxaline-7-sulfonamide (NBQX), 50 picrotoxin, 10 CGP 52,432, and 1 strychnine, to block α-amino-3-hydroxy-5-methylisoxazole-4-propionic acid (AMPA), γ-aminobutyric acid (GABA) $GABA_A$, $GABA_B$ and GlyRs, respectively. All chemicals and drugs were purchased from Sigma-Aldrich, with the exception of NBQX, which was purchased from Tocris Bioscience (Ellisville, MO).

Decay kinetics of NMDAR EPSCs were analyzed on the average of 20 to 25 traces. The decays were fitted with double exponential functions: $y = A_f e^{-t/\tau} + A_s e^{-t/\tau}$ in which A is amplitude, τ is decay time constant, and the subscript f and s denote fast and slow components, respectively. Weighted time constants (τ_{mean}) were calculated using the equation: $\tau_{mean} = [A_f/(A_f + A_s)]\ \tau_f + [A_s/(A_s + A_f)]\ \tau_s$ (Stocca and Vicini, 1998; Stocca and Vicini, 1998).

Miniature EPSCs (mEPSCs) were recorded in presence of tetrodotoxin (TTX; 1 μM). Amino-phosphonovaleric acid (APV) and NBQX were not included in the ACSF. Results were analyzed off-line using the mini analysis program written by Justin Lee (Synaptosoft Inc., Decatur, GA). Data were collected using pClamp 9 software (Axon Instrument, Foster City, CA). Analysis was performed off-line with Clampfit 9.0 software (Axon Instruments).

Current-clamp experiments were performed using mutant and WT mice at 4 and 8 weeks of age. These current-clamp experiments required an internal solution containing the same chemicals as described above with the exception of QX-314 which was omitted and 130 Cs^+ methanesulphonate was replaced by 130 K+- gluconate. The ACSF contained a low Mg^{2+} concentration of $MgCl_2$ (0.1 mM), bicuculline (20 μM), picrotoxin (50 μM), CGP-52,532 (10 μM), strychnine (1 μM), and NBQX (5 μM).

Morphological identification of CA1 PCs

In some experiments, the recording pipette was filled with 2 mM Lucifer Yellow. The slices were removed from the chamber after recordings and fixed in 4% paraformaldehyde in a 0.1 M phosphate buffer solution (PBS; 0.1 M, pH 7.2) for 1 to 3 days. Slices were then washed with dimethyl-sulfoxide for 1 h. An LSM 510 confocal laser-scanning microscope (Zeiss, Germany) was used to visualize the CA1 PCs using 10× and 40× water immersion objectives. A three-dimensional structure of the neurons was obtained from the z-series data using the confocal system software. The scanned neurons were reconstructed with Adobe Photoshop7.0 (San Jose, CA) and the dendritic branches were counted manually.

Immunoblotting

Mice were sacrificed under anesthesia using isoflurane, in agreement with the guidelines of the Canadian Council of Animal Care. The hippocampal region (CA1 area) from each hemisphere was dissected on ice and homogenized by dounce tissue homogenizer

using ice-cold TEVP lysis buffer (10 mM Tris-HCl, 5 mM Sodium fluoride (NaF), 5 mM Sodium orthovanadate (Na_3VO_4), 5 mM ethylenediaminetetracetic acid (EDTA), pH 7.4). The hippocampal tissue of 24 different animals (12 mutant and 12 WT mice) was pooled in two different groups. For the NR2A and NR2B subunits, the CA1 regions from 24 different animals (four mutant and four WT mice at 2, 4, and 8 weeks of age) were dissected on ice and homogenized by dounce tissue homogenizer using ice-cold TEVP lysis buffer (10 mM Tris-HCl, 5 mM sodium fluoride (NaF), 5 mM sodium Orthovanadate (Na_3VO_4), 5 mM EDTA, pH 7.4. The lysed tissue was centrifuged at 5000 g for 10 min at 4°C. Twenty-four animals at 2, 4, and 8 weeks of age (12 mutant and 12 WT mice) were also used for the PSD-95 protein measurement.

The pellet (P1) containing nuclei and other debris was discarded and the supernatant (S1) was collected. The S1 was then centrifuged at 15,000 rpm for 15 min at 4°C and the resulting pellet (P2) was collected by discarding the supernatant (S2). The collected pellet (P2) was dissolved in ice-cold TEVP buffer containing a Mini-EDTA free protease inhibitor cocktail tablet (Roche, Basel, Switzerland), 1 mM phenylmethylsulphonyl fluoride, 1% Nonidet P-40, 0.5% Sodium deoxycholate and 0.1% SDS. Protein concentration was determined using a BCA protein assay and bovine serum albumin was used as a standard (Pierce, Biotechnology Inc., Rockford, IL).

Fifty micrograms of membrane proteins from GlyT1+/− and WT mice were diluted with sample loading buffer (10% SDS, 100 μM dithiothreitol (DTT), 10% glycerol (v/v), 0.001% bromophenol blue, 25 mM Tris pH 6.8) and boiled for 3 min at 95°C. The proteins were separated in 7.5% SDS-polyacrylamide gel. Subsequently, proteins were transferred to a polyvinylidene difluoride (PVDF) membrane using a mini trans-blot cell (Bio-Rad, Hercules CA). Membranes were then blocked with 5% nonfat milk in tris-buffered saline (TBS; 50 mM Tris pH 8.0, 148 mM NaCl) for 1 h at room temperature.

Membranes were incubated overnight at 4°C with primary antibodies diluted in 5% nonfat milk in TBS. The antibody dilution used was 1:1000 for rabbit polyclonal anti-NR2A antibodies; 1:7500 for rabbit polyclonal anti-NR2B antibodies; 1:4000 for rabbit polyclonal anti-PSD-95 antibodies; 1:5000 for rabbit polyclonal anti-GAPDH antibodies. The antibodies for NR2A, NR2B and GAPDH were purchased from Abcam, Cambridge, MA, whereas the antibody for PSD-95 was purchased from Cell Signaling Technology, Beverly, MA.

The membranes were washed 3 times in TBS containing 0.1% NP-40 for a total of 20 min, and then incubated with goat antirabbit IgG secondary antibody which is conjugated with horseradish peroxidase (1:3000; Santa Cruz Biotechnology, Inc, CA) for 1 h at room temperature. The membranes were washed again and then incubated in ECL solution (Amersham Biosciences, Baie d'Urfé, QC, Canada). The bands were visualized on Amersham Hyperfilm (Amersham Biosciences).

Immunohistochemistry

GlyT1+/− and age matching WT mice (4 and 8 weeks of age) were anesthetized with an overdose of pentobarbital (60 mg/kg) and intracardiacally perfused with 4% paraformaldehyde in PBS solution. After 30 min postfixation at 4°C, the brain was put into 30% sucrose/PBS solution until it sunk. The brain was then frozen at −80°C. The brain was sliced with a cryostat (Leica CM 3050S, Nassloch, Germany) to obtain hippocampal coronal slices of 14 μm. The slices were quenched with 50 mM NH_4Cl in PBS for 30 min and permeabilized with 0.2% triton and 0.25% fish gelatin in PBS for 30 min to enhance the penetration of the primary antibody and reduce nonspecific binding. The slices were then incubated with a mouse antisynaptophysin (1:750; Sigma) and guinea pig anti-VGLUT 1, 2, 3 (VGLUTs; 1:500; Millipore/Chemicon, Temecula, CA) primary antibodies in 0.25% gelatin and 0.2% triton PBS solution (PBSGT) overnight at 4°C. The slices were then rinsed thoroughly in PBSGT and subsequently incubated with secondary antibodies: Cy3-conjugated goat antimouse IgG (1:500; Jackson ImmunoResearch Laboratories, Inc., West Grove, PA) and an FITC-conjugated goat antiguinea pig (1:250; Jackson ImmunoResearch) in PBSGT for 2 h at room temperature. Slices were rinsed and mounted with Vectashield mounting medium (Vector Laboratories Inc., Burlingame, CA). Control slices, minus the primary antibodies were examined for background staining.

Confocal microscopy and imaging

We acquired fluorescent images of hippocampal slices using an LSM 510 confocal laser-scanning microscope (Zeiss, Germany) with a 63× oil-immersion objective (numerical aperture 1.4) at the resolution of 1024 × 1024 pixels. The stratum pyramidale of the CA1 region of the hippocampus were scanned twice to optimize the signal-to-noise ratio. Three parallel regions of each slice were selected for quantification and the density of clusters was determined by using Image J software (NIH, Bethesda, MD).

Statistical analysis

Student's t tests (two-tailed) or Kolmogorov-Smirnov two-sample test were used to determine the statistical significance of the results. All values are

TABLE I. Decay time constants of NMDAR EPSCs in GlyT1+/− and WT mice

	Control					Ifenprodil
(*n*)	τ_s (ms)	τ_f (ms)	A_s (%)	A_f (%)	τ_{mean} (ms)	τ_{mean} (ms)
2 weeks						
WT (18)	648 ± 49.33	114.0 ± 12.74	26.4 ± 2.18	73.6 ± 2.19	234.7 ± 13.93	151.0 ± 8.80 (7)
GlyT1+/− (18)	457 ± 30.20*	71.8 ± 4.85*	29.5 ± 2.23	70.5 ± 2.28	185.9 ± 10.9*	151.6 ± 9.60 (13)
3 weeks						
WT (18)	654 ± 55.33	111.9 ± 9.48	21.4 ± 2.16	75.2 ± 2.16	205.3 ± 10.92	161.2 ± 10.03 (9)
GlyT1+/− (19)	548 ± 7.20*	83.4 ± 1.37*	20.8 ± 0.61	79.2 ± 0.58	171.6 ± 2.14*	165.4 ± 8.15 (15)
4 weeks						
WT (15)	563 ± 28.53	84.74 ± 4.48	18.3 ± 1.87	81.6 ± 1.68	167.7 ± 5.58	122.1 ± 4.40 (6)
GlyT1+/− (20)	465 ± 31.50*	71.31 ± 3.77*	17.2 ± 1.84	82.8 ± 1.84	139.3 ± 6.91*	124.9 ± 5.94 (9)
8 weeks						
WT (18)	559 ± 27.47	83.89 ± 3.43	14.9 ± 1.68	85.1 ± 1.68	152.4 ± 5.45	115.6 ± 6.10 (7)
GlyT1+/− (18)	411 ± 20.20*	76.44 ± 2.78*	19.6 ± 1.68	80.4 ± 1.88	138.2 ± 3.90*	123.8 ± 14.01 (7)

Values are mean ± SEM. NMDAR EPSCs were recorded in absence (control) and presence of ifenprodil (3 μM). The slow and fast decay components are designated by τ_s and τ_f, respectively, and the weighted time constant by τ mean.
*Significant difference between WT and GlyT1+/− mice ($p < 0.05$).

expressed as means ± SEM, and a *P* value of <0.05 was considered significant.

RESULTS

Biophysical properties of NMDAR EPSCs in GlyT1+/− and WT mice during postnatal development

Previous data from our laboratory showed that in GlyT1+/− mice (12-13 weeks of age), the glycine modulatory site of the NMDAR at the synapse is saturated as suggested by the finding that exogenous application of glycine (10 μM) or D-serine (10 μM) does not modify the amplitude of NMDAR EPSC, whereas the same dose of glycine enhances NMDAR EPSC amplitude by approximately 40% in WT mice (Tsai et al., 2004). We have also previously reported that NMDAR EPSCs in GlyT1+/− mice (12-13 weeks of age) have faster decay kinetics compared to their age matching WT mice (Martina et al., 2005). We recorded NMDAR EPSCs in hippocampal CA1 PCs from both GlyT1+/− and WT mice at 2, 3, 4, and 8 weeks of age in order to explore whether this difference originates early in the postnatal period.

No significant differences were noted in the 10-90% rise time of NMDAR EPSCs between mutant and WT mice at 2 (GlyT1+/−: 18.03 ± 1.86 ms, $n = 20$; WT: 21.6 ± 2.45 ms, $n = 11$), 3 (GlyT1+/−: 26.51 ± 5.83 ms, $n = 11$; WT: 24.01 ± 7.02 ms, $n = 12$), 4 (GlyT1+/−: 26.7 ± 3.9 ms, $n = 21$; WT: 22.1 ± 3.4 ms, $n = 9$), and 8 (GlyT1+/−: 18.36 ± 2.22 ms, $n = 7$; WT: 19.6 ± 2.6 ms, $n = 7$) weeks of age. However, the averaged τ_s and τ_f of GlyT1 ± mice at all ages are consistently faster than those of WT mice (Table I). The weighted time constant is significantly faster in GlyT1+/− compared to that of WT mice (Figs. 1A and 1B; Table I). From these data, we cannot conclude that this is a higher expression of NR2A or a lower expression of NR2B subunits in the CA1 region of mutant mice, however, one could argue that this possibility should be addressed.

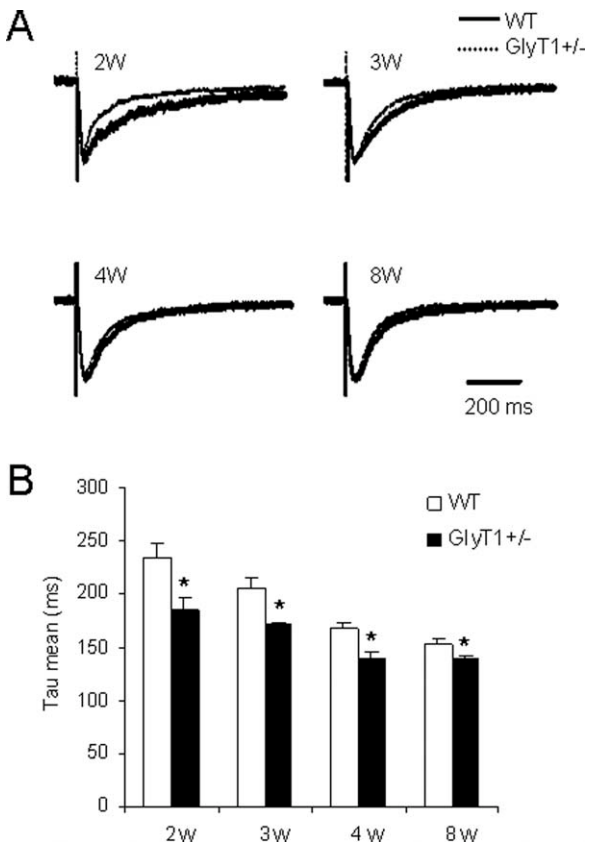

Fig. 1. Biophysical properties of NMDAR EPSCs recorded from CA1 PCs of GlyT1+/− and WT mice. **A**: Traces of NMDAR EPSCs recorded from CA1 PCs of GlyT1+/− (dashed line) and WT (thick line) mice at 2 (2W), 3 (3W), 4 (4W), and 8 (8W) weeks of age. **B**: Histogram showing the weighted time constants (τ_{mean}) of NMDAR EPSCs of CA1 PCs in GlyT1+/− (full bar) and WT mice (empty bar) at 2, 3, 4, and 8 postnatal weeks. *Indicates statistically significant differences in the τ_{mean} between GlyT1+/− and WT mice ($P < 0.05$).

Antagonistic effect of Ifenprodil on NMDAR EPSCs in GlyT1+/− and WT mice during postnatal development

A limited number of drugs can selectively distinguish between certain subunits of NMDARs, of which

ifenprodil is the most characterized. This drug has an IC_{50} that is approximately 400-fold lower for NR2B subunit compared to that of other NMDAR subunits (Williams, 1993). The antagonistic effect of ifenprodil on NMDAR EPSCs correlates with developmental changes in NMDAR composition such that NMDAR activity in immature neurons is almost completely inhibited by ifenprodil (Kew, Richards, Mutel, and Kemp, 1998; Sinor et al., 2000). Because higher levels of endogenous glycine in GlyT1+/− mice could reduce the antagonistic effect of ifenprodil, we used 3 μM of ifenprodil, a concentration that is glycine independent (Legendre and Westbrook, 1991).

Immunoblotting for NR2A, NR2B, PSD-95 in the CA1 region in GlyT1+/− and WT mice during postnatal development

We found that the reduction in the amplitude of NMDAR EPSCs induced by ifenprodil is significantly smaller in GlyT1+/− mice at 2, 3, 4 and 8 weeks of ages compared to their WT littermates ($P < 0.05$; Figs. 2A and 2B). This occurrence may reflect a lower expression of NR2B in mutant mice. Nevertheless, ifenprodil significantly reduces the NMDAR EPSC amplitudes of CA1 PCs in GlyT1+/− mice by 51.99 ± 5.60% ($n = 12$; $P < 0.05$) at 2 weeks, 45.01 ± 2.51% ($n = 23$; $P < 0.05$) at 3 weeks, 38.13 ± 4.32% ($n = 14$; $P < 0.05$) at 4 weeks, and 32.61 ± 5.61% ($n = 8$; $P < 0.05$) at 8 weeks of age, as well we noted further reduction of NMDAR EPSC amplitudes of WT by 67.91 ± 4.63% ($n = 18$; $P < 0.05$) at 2 weeks, 57.66 ± 2.99% ($n = 14$; $P < 0.05$) at 3 weeks, 52.05 ± 5.17% ($n = 12$; $P < 0.05$) at 4 weeks, and 47.15 ± 4.66% ($n = 10$; $P < 0.05$) at 8 weeks of age.

Since NR2B-containing NMDARs have slower decay kinetics compared to NR2A-containing NMDARs, we speculate that ifenprodil could also reduce the τ_{mean} and consequently accelerate NMDAR EPSC decay. Indeed, we find that ifenprodil drastically reduces the values of the τ_{mean} in both GlyT1+/− and WT mice at all ages examined (Fig. 2C and Table I). However, the τ_{mean} of WT mice significantly reduces upon ifenprodil treatment compared GlyT1+/− mice ($P < 0.05$).

Differences observed in the antagonistic effect of ifenprodil on NMDAR EPSC amplitudes and the decay kinetics between the two types of mice suggest a lower expression of NR2B or a higher expression of NR2A in GlyT1+/− mice. To test this hypothesis, we performed immunoblotting experiments to measure NR2A and NR2B protein expression in the CA1 region of the hippocampus of GlyT1+/− and WT mice at 2, 4, and 8 weeks of age (Fig. 3). Consistent with the literature, our results show that NR2B protein expression remains relatively unchanged during postnatal development (Liu, Murray, and Jones, 2004; von Engelhardt, Doganci, Seeburg, and Monyer, 2009),

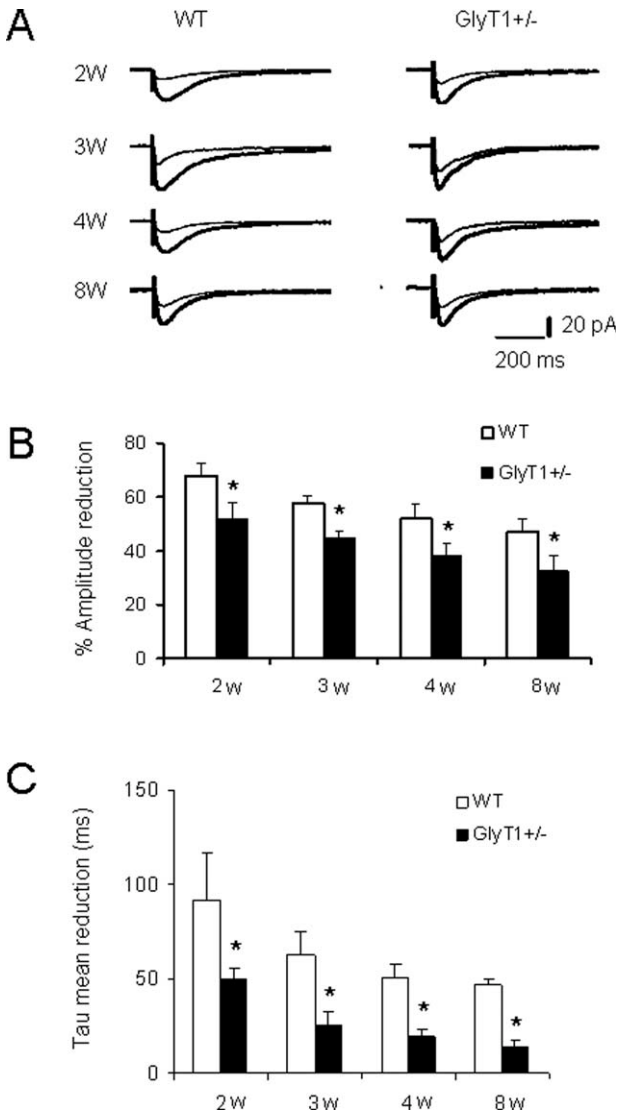

Fig. 2. Effect of ifenprodil on NMDAR EPSCs of CA1 PCs in GlyT1+/− and WT mice. **A**: Traces of NMDAR EPSCs recorded from CA1 PCs in GlyT1+/− and WT mice in the absence (thick line) and presence of ifenprodil (3 μM; thin line). **B**: Histogram showing the effect of ifenprodil on the amplitude of NMDAR EPSCs in GlyT1+/− (full bar) and WT mice (empty bar) at 2, 3, 4, and 8 weeks of age. Note that the antagonistic effect of ifenprodil on NMDAR EPSC amplitude decreased with age in both GlyT1+/− and WT mice. **C:** Histogram showing the effect of ifenprodil on Tau mean reduction in GlyT1+/− (full bar) and WT mice (empty bar) at 2, 3, 4, and 8 weeks of age. *Indicates statistically significant differences between GlyT1+/− and WT mice ($P < 0.05$).

whereas NR2A protein expression becomes more prominent with ages (Monyer et al., 1992; Monyer, et al., 1994; Stocca and Vicini, 1998). However, when comparing GlyT1+/− mice to WT littermates of the same age, no significant difference is observed in the protein expression of either NR2A or NR2B; $n = 4$ for each group.

We also investigated PSD-95 expression, a protein that exists at the excitatory postsynaptic region is known to be coupled with NMDARs, especially with

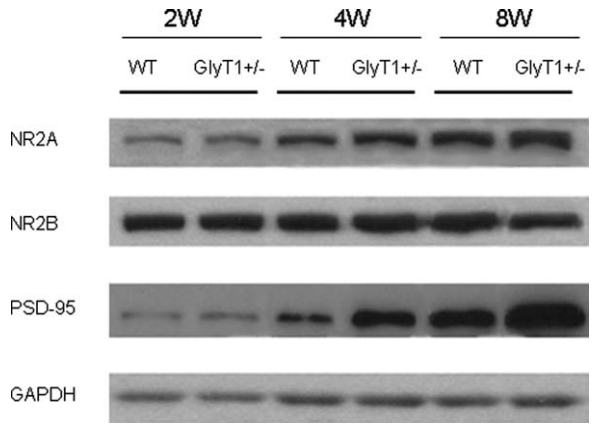

Fig. 3. Expression of NR2A and NR2B protein in whole hippocampus of GlyT1+/− and WT mice. Whole hippocampus (n = 24) was used to determine the protein expression of NR2A, NR2B, and PSD-95 in mutant and WT mice at 2, 4, and 8 weeks of age. During postnatal development, NR2A and PSD-95 protein expression increases with age. When comparing both types of mice, we find a higher expression of PSD-95 protein in GlyT1+/− mice, whereas there is no obvious increase in NR2A protein expression. NR2B protein expression remains relatively constant. GAPDH was used as an internal control for protein loading.

those containing the NR2A subunit (Elias et al., 2008). This protein plays a pivotal role in preventing NR2A-containing NMDARs to internalize (Lin et al., 2004; Rao and Craig, 1997). In both types of mice, we found a PSD-95 protein expression increase with age during postnatal development. Moreover, compared to WT mice, there is a significantly higher protein expression of PSD-95 in mutants at 4 and 8 weeks of age (n = 4 for each group; Fig. 3). Overall, our data suggest that PSD-95 in mutant mice anchors NR2A-containing NMDARs at the synapse, thereby explaining the faster decay kinetics observed in GlyT1+/− animals.

Morphological properties of CA1 PCs in GlyT1+/− and WT mice during postnatal development

We previously reported that there was no significant difference in the morphology of CA1 PCs between GlyT1+/− and WT adult mice (12-13 weeks of age). However, in that case no quantification of dendritic branches was performed (Martina et al., 2005; Martina et al., 2005). To further characterize the morphological properties of CA1 PCs in GlyT1+/− and WT mice during postnatal development (2, 3, 4, and 8 weeks of age) we labeled them by filling the recording electrodes with Lucifer Yellow. We obtained the morphology of CA1 PCs using confocal microscopy following the electrophysiological recordings.

Our findings show that the number of apical and basal dendritic segments in CA1 PCs is significantly higher in mutant compared to WT mice at 2, 3, and 4 weeks of age (Fig. 4 and Table II), whereas no significant difference is observed at 8 weeks of age. These data suggest that during the early stages of postnatal development, CA1 PCs in GlyT1+/− mice undergo morphological changes which may impact network excitability.

Miniature excitatory postsynaptic currents in GlyT1+/− and WT mice during postnatal development

We studied mEPSCs to investigate whether in GlyT1+/− mice, changes in the number of functional synaptic contacts could occur during postnatal development. The averaged amplitude of mEPSCs indicates a single quantum of transmitter release at an individual synapse (or number of postsynaptic glutamatergic receptors), whereas their frequency corresponds to the number/density of synapses (El Husseini et al., 2000) or to the probability of release (Hopf, Waters, Mehta, and Smith, 2002).

Our findings indicate that in GlyT1+/− mice, the average of mEPSC amplitudes (pA) at 2 weeks (7.89 ± 0.24, n = 8), 3 weeks (7.95 ± 0.29, n = 11), 4 weeks (8.67 ± 0.24, n = 7), and 8 weeks (8.71 ± 0.27, n = 6) of age is not significantly different compared to WT mice at 2 (8.26 ± 0.35, n = 6; $P > 0.05$), 3 (8.66 ± 0.30, n = 6; $P > 0.05$), 4 (8.64 ± 0.43, n = 10; $P > 0.05$), and 8 weeks (9.10 ± 0.24, n = 6; $P > 0.05$; Figs. 5A, 5B, and 5D and Supporting Information Fig. 1) of age. These results suggest that there is no difference in the number of glutamatergic postsynaptic receptors (AMPARs and NMDARs) between GlyT1+/− and WT mice.

Interestingly, our observations show that the frequency (Hz) of mEPSCs is significantly higher in GlyT1+/− mice at 4 (0.627 ± 0.06, n = 7) and 8 weeks (0.654 ± 0.07, n = 6) of age compared with their matching WT littermates (4 weeks: 0.455 ± 0.03, n = 10; $P < 0.05$; 8 weeks: 0.520 ± 0.06, n = 6; $P < 0.05$; Figs. 5A, 5C, and 5E and Supporting Information Fig. 2). In contrast, there is no significant difference in the frequency of mEPSCs at 2 and 3 weeks of age between GlyT1+/− (2 weeks: 0.310 ± 0.05, n = 8; 3 weeks: 0.560 ± 0.07, n = 11) and WT mice (2 weeks: 0.284 ± 0.07, n = 6; $P > 0.05$; 3 weeks: 0.470 ± 0.08, n = 6; $P > 0.05$; Kolmogorov-Smirnov test).

We conducted the paired-pulse (PP) protocol to determine the release probability to test whether the high frequency of mEPSC in mutant mice (at 4 and 8 weeks of age) was not due to a higher release of glutamate from presynaptic terminals, (Hsia, Malenka, and Nicoll, 1998; Wasling, Hanse, and Gustafsson, 2004). We performed PP stimulation to Schaffer collateral terminals using a pulse interval of 40, 80, and 100 ms and recorded the NMDAR-mediated paired-response in CA1 PCs. We found that there was a significantly higher PP ratio in GlyT1+/− mice at 3, 4, and 8 weeks of age compared to those of WT litter-

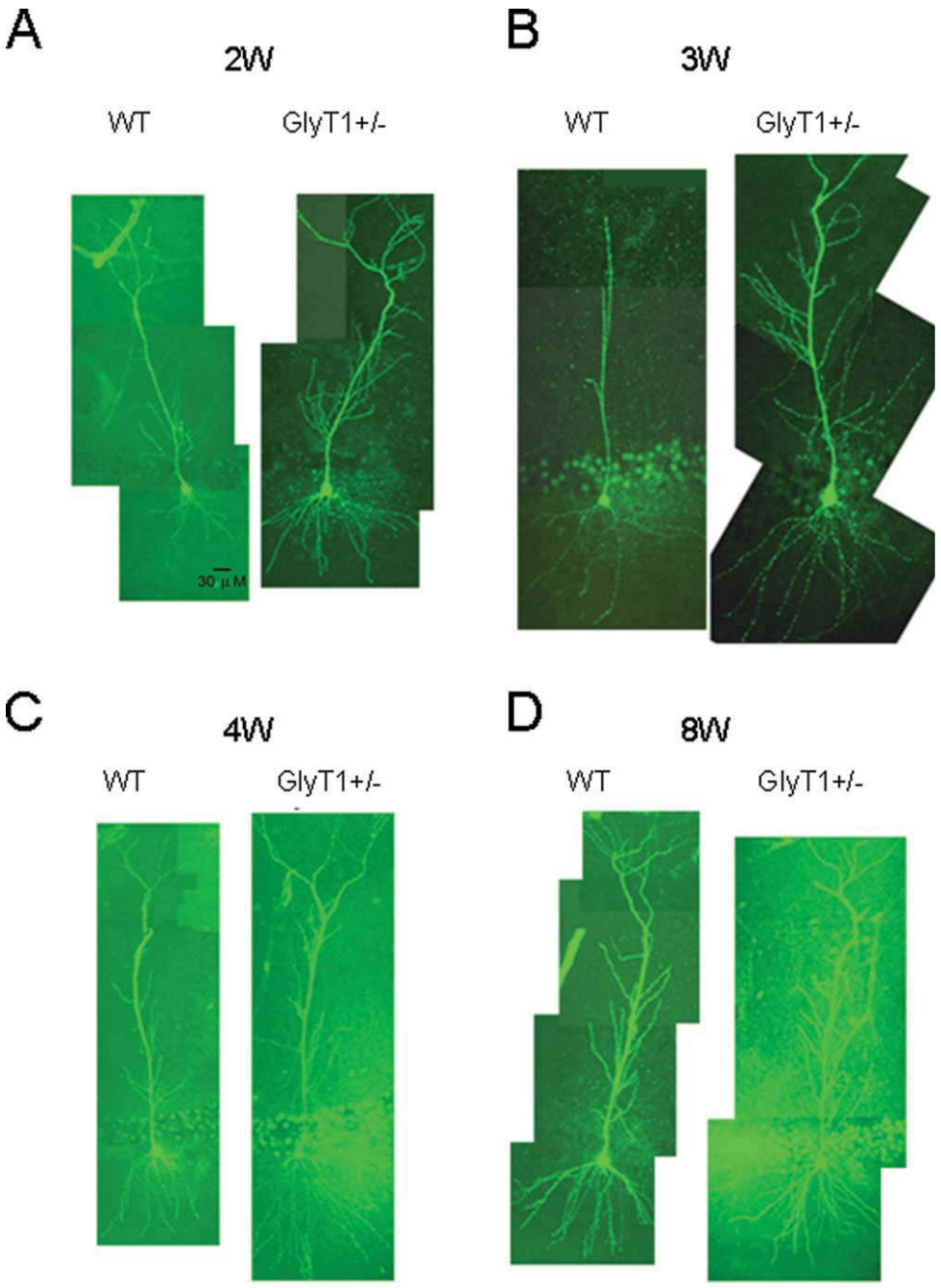

Fig. 4. Morphological properties of CA1 PCs in GlyT1+/− and WT mice during different stages of postnatal development (**A**–**D**) Lucifer yellow-labeled CA1 PCs obtained from GlyT1+/− and WT mice at 2, 3, 4 and 8 weeks of age showed that mutants have a higher number of dendritic branching than WT littermates (see Table II for details). [Color figure can be viewed in the online issue, which is available at wileyonlinelibrary.com.]

mates (Supporting Information Fig. 1; $P < 0.05$). This suggests a lower release probability in GlyT1+/− compared to WT mice (Supporting Information Fig. 1) and may argue in favor of a higher density of synapses in mutant mice at 4 and 8 weeks of age. It is worth mentioning that the above findings, such as the amplitude and frequency of the mEPSCs as well as the paired pulse ratio are not reversed by the GlyR antagonist strychnine at the dose of 1 μM but are blocked by APV (20 μM).

Synaptic organization in GlyT1+/− and WT mice

NMDAR activation is required for early synapse formation and neural development. Blocking NMDAR

TABLE II. Morphological properties of CA1 PCs labeled with Lucifer yellow in GlyT1+/− and WT mice during different stages of postnatal development

	Apical dendrites				Basal dendrites		
(n)	II	III	IV	V	I	II	III
2 weeks							
WT	8.42 ± 1.05 (12‖	11.83 ± 1.55 (12)	6.45 ± 0.62 (11)	7.33 ± 1.76 (3)	3.90 ± 0.31 (10)	7.40 ± 0.58 (10)	11.89 ± 1.41 (9)
GlyT1+/−	6.25 ± 0.99 (16)	16.25 ± 1.54 (16)*	10.88 ± 2.32 (16)*	5.78 ± 0.94 (9)	4.36 ± 0.28 (11)	9.45 ± 0.59 (11)*	12.88 ± 1.36 (8)
3 weeks							
WT	6.67 ± 1.86 (3)	10.0 ± 1.0 (2)	4 (1)	n/a	3.50 ± 1.50 (2)	9.50 ± 3.5 (2)	10.40 ± 4.0 (2)
GlyT1+/−	12.78 ± 0.9 (9)*	21.44 ± 1.5 (9)*	9.63 ± 1.55 (8)	5.0 ± 1.0 (2)	4.62 ± 0.52 (8)	11.75 ± 1.68 (8)	14.88 ± 0.67 (8)*
4 weeks							
WT	8.0 ± 0.82 (6)	10.17 ± 1.62 (6)	4.33 ± 0.76 (6)	5.75 ± 0.85 (4)	3.80 ± 0.37 (5)	9.00 ± 0.89 (5)	7.60 ± 1.33 (5)
GlyT1+/−	12.50 ± 2.1 6 (6)*	15.33 ± 1.84 (6)*	9.17 ± 1.64 (6)*	7.60 ± 1.21 (5)	4.20 ± 0.49 (5)	9.4 ± 1.33 (5)	14.0 ± 2.07 (5)*
8 weeks							
WT	7.00 ± 4.9 (7)	11.10 ± 1.12 (7)	6.86 ± 1.32 (7)	6.50 ± 0.26 (2)	4.28 ± 0.43 (7)	10.14 ± 0.19 (7)	11.86 ± 0.19 (7)
GlyT1+/−	8.86 ± 2.20 (7)	13.14 ± 1.14 (7)	7.14 ± 1.03 (7)	7.00 ± 0.54 (2)	4.14 ± 0.46 (7)	9.0 ± 0.82 (7)	13.43 ± 1.46 (7)

Values are mean ± SEM. CA1 PCs labeled with Lucifer yellow were recorded frome GlyT1+/− and WT mice at 2, 3, 4, and 8 weeks of age. We identified (I) as the first dendritic segments leaving the soma, (II) the dendritic segments branching from (I), (III) the dendritic segments branching from (II), etc.
*Significant difference between GlyT1+/− and WT mice ($P < 0.05$).

activity inhibits dendritic arbor growth (Rajan and Cline, 1998). We performed double immunostaining using synaptophysin, a protein involved in the presynaptic exocytosis machinery and vesicular glutamate transporter subtypes (VGLUT1, 2, 3; VGLUTs), the specific molecular markers of glutamatergic vesicles to compare the density of excitatory synapses at Schaffer collaterals/CA1 synapses between GlyT1+/− and WT mice at 4 and 8 weeks of age. Colocalization of synaptophysin and VGLUTs formed bright fluorescent clusters that are uniformly distributed in the *stratum pyramidale* in both GlyT1+/− and WT mice (Figs. 6A–6D). The density of synaptophysin and VGLUTs clusters as well the density of coclusters is much higher in GlyT1+/− mice at 4 and 8 weeks of age compared with that of WT littermates (Supporting Information Figs. 4A–4C). These findings suggest a higher density of excitatory presynaptic terminals and further suggest a higher number of synaptic contacts at Schaffer collaterals/CA1 synapses in mutant mice.

Neuronal excitability in GlyT1+/− and WT mice

Thus far, the results of our study suggest that in the hippocampal network of mutant mice, there is a higher level of synaptic contact which could lead to higher excitability. In the last series of experiments, we sought to investigate this hypothesis by assessing the firing frequency of action potentials of CA1 PCs at 4 and 8 weeks in both types of mice. If indeed the neuronal network is more excitable in mutant mice, the frequency of action potentials should increase when compared to WT mice. We recorded CA1 pyramidal neurons in current-clamp mode. Cs methanesulfonate was not used because it would inhibit potassium channels. For these experiments, K+ gluconate was used instead of Cs methanesulfonate. As illustrated in Figures 7A and 7B, there is a significant increase in the frequency of action potentials in GlyT1+/− mice at 4 and 8 weeks. Interestingly, we do not find any significant change in resting membrane potential. Moreover, in both GlyT1+/− and WT mice at 8 weeks of age, the firing frequency was reduced upon bath application of the competitive NMDAR antagonist, APV (Fig. 7C).

DISCUSSION

In this study, using GlyT1+/− mice, we investigated the impact of chronic high levels of endogenous glycine on important parameters of glutamatergic neurotransmission involving NMDARs. Our results indicate that throughout postnatal development, compared with control animals, mutant mice undergo major changes with respect to the pharmacological properties and functionality of NMDARs in CA1 PCs. More precisely, differences observed in GlyT1+/− mice are the following: (1) a faster decay kinetic of NMDAR EPSCs; (2) a reduction of the antagonistic effect of ifenprodil; (3) a higher protein expression of PSD-95; (4) an increase in dendritic branching and glutamatergic presynaptic terminals; (5) a higher frequency of mEPSC; and (6) higher network excitability.

During early postnatal development, NMDARs at the synapse are predominantly composed of NR2B subunits, whereas NR2A subunits are gradually inserted into the synapse at maturation (Monyer, et al., 1994; Sheng et al., 1994; Flint et al., 1997), a transition that is reflected by the acceleration of the decay kinetics of NMDAR EPSCs (Hestrin, 1992; Cathala, Misra, and Cull-Candy, 2000) and the loss of ifenprodil sensitivity (Tovar and Westbrook, 1999; Williams, 2001). Accordingly, in both mutant and WT mice, we observed a developmental decrease in the decay kinetics of NMDAR EPSCs, however, GlyT1+/− mice exhibited significantly faster decay kinetics compared with WT littermates at all studied ages. Consist-

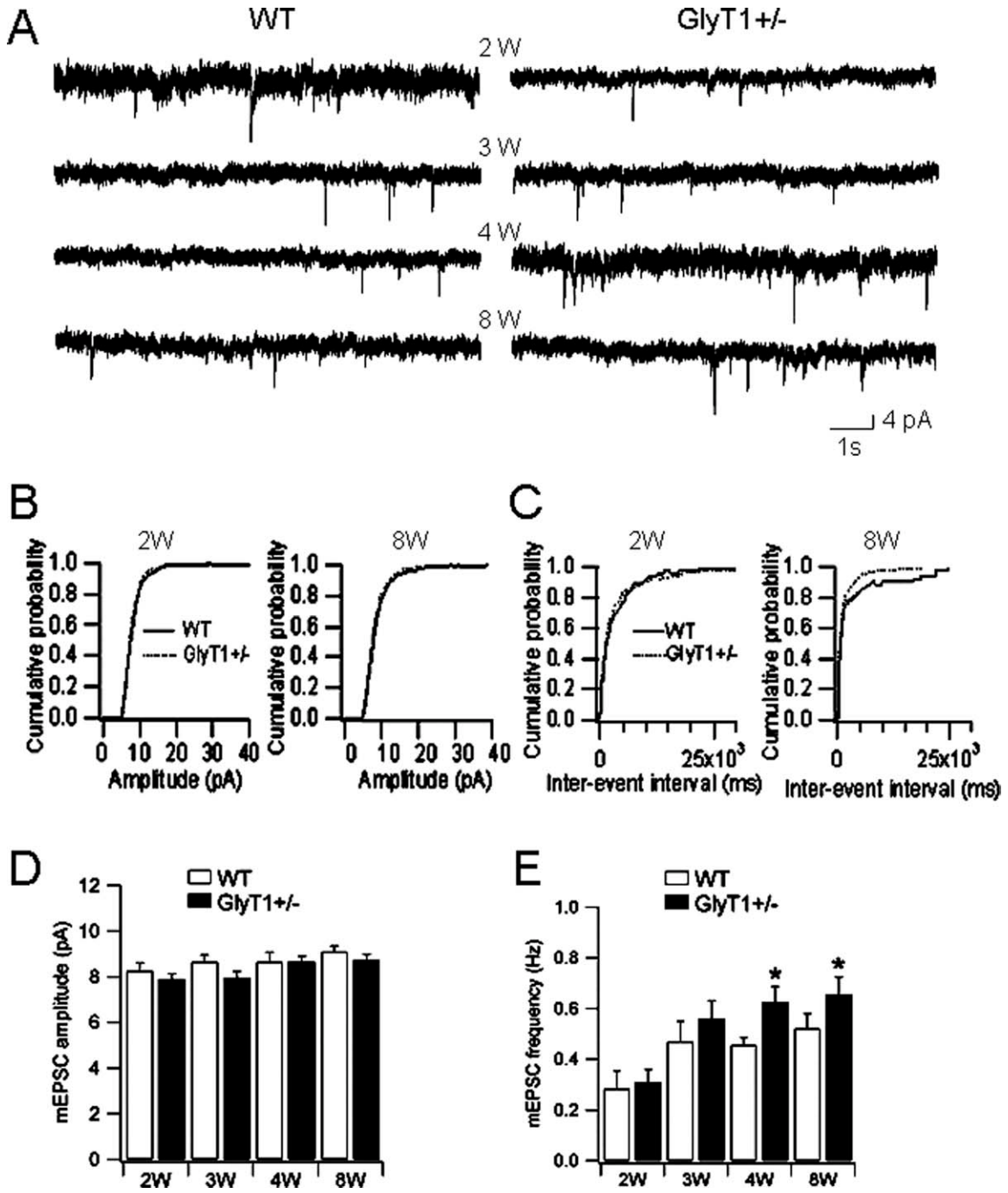

Fig. 5. mEPSCs of CA1 PCs in GlyT1+/− and WT mice during postnatal development. **A**: mEPSCs recorded from CA1 PCs of GlyT1+/− (right panel) and WT (left panel) mice at 2, 3, 4, and 8 weeks of age. **B** and **D**: Both types of mice had no significant difference in mEPSCs amplitudes at 2, 3, 4, and 8 weeks of age. **C** and **E**: The frequency of mEPSCs was significantly higher in mutants at 4 and 8 weeks of age. *Indicates statistically significant differences between GlyT1+/− and WT mice ($P < 0.05$).

ent with previous reports (Monyer et al., 1994; Sheng et al., 1994; Flint et al., 1997), the results of our immunoblotting experiments confirmed an increase in NR2A protein expression with age in both GlyT1+/− and WT mice. However, our results did not reveal any significant difference in protein expression of NR2A between GlyT1+/− and WT mice at any studied time points. Our observation that decay kinetics of NMDAR EPSCs is faster in mutant mice cannot be explained by a difference in NR2A or NR2B protein expression. In agreement with other studies (Stocca and Vicini, 1998), our data from immunoblotting experiments revealed that NR2B protein expression remains relatively constant despite the faster decay kinetics of

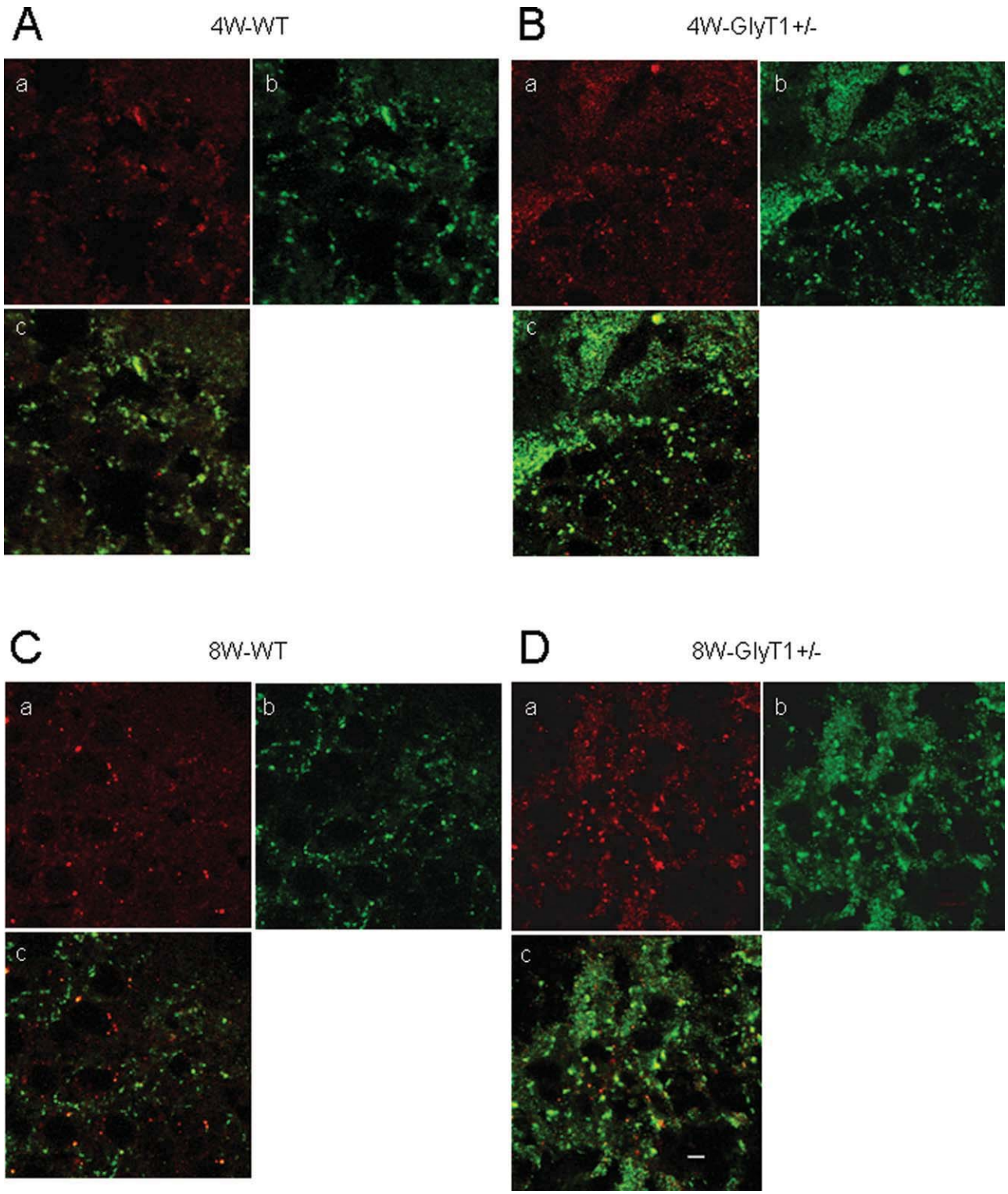

Fig. 6. Immunohistochemistry detection of synaptophysin and VGLUTs in the *stratum pyramidale* of GlyT1+/− and WT mice at 4 and 8 weeks of age. **A–D**: Immunofluorescent confocal sections of CA1 PCs layer in the hippocampus, double labeled for (a) synaptophysin, (b) VGLUTs in GlyT1+/− and WT mice at 4 and 8 weeks of age and (c) merged image. Scale bar is 5 μm. [Color figure can be viewed in the online issue, which is available at wileyonlinelibrary.com.]

NMDAR EPSCs and the decrease in ifenprodil sensitivity, suggesting that NR2A subunits are inserted into these synapses forming heteromerics complexes.

A core component of the postsynaptic density at excitatory synapses during postnatal development is that PSD-95 protein expression parallels that of

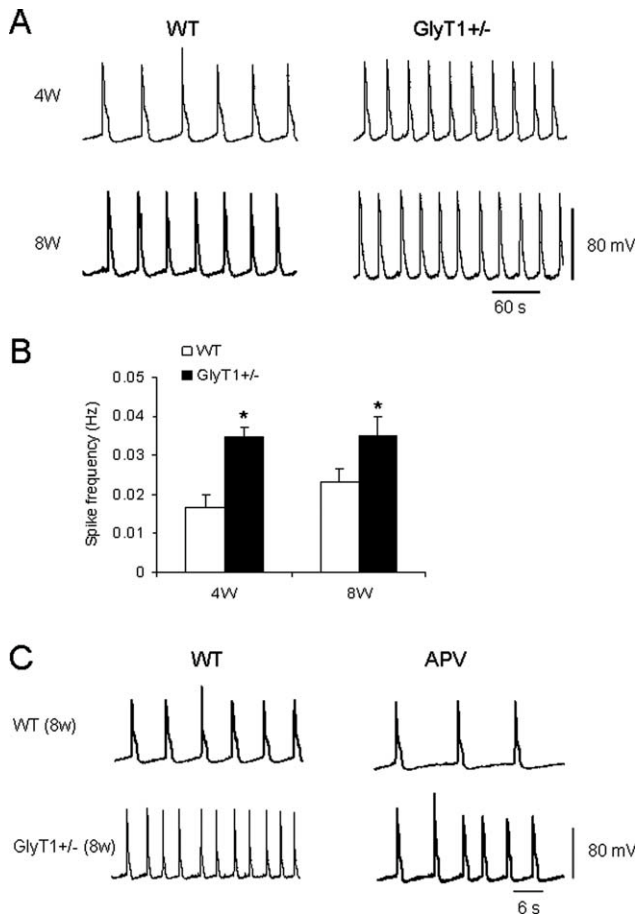

Fig. 7. Neuronal excitability in GlyT1+/− and WT mice. **A**: Traces representing spontaneous NMDAR-dependent activity in CA1 PCs recorded in current-clamp mode. We observed a higher frequency of action potentials in mutants compared to WT mice at 4 and 8 weeks of age. **B**: Bar histogram shows a significantly higher frequency of action potentials in GlyT1+/− mice compared with WT littermates. **C**: The action potential frequency in mutants (8W) and WT animals (8W) was reduced upon bath application of NMDAR antagonist APV (50 μM). *Indicates statistically significant differences between GlyT1+/− and WT mice ($P < 0.05$).

NR2A. Indeed, a past study shows that over-expression of PSD-95 in cultured cerebellar granule cells promotes NR2A synaptic expression (Losi et al., 2003). Therefore, the faster decay kinetics observed in GlyT1+/− mice could be explained by the increased expression of PSD-95, which is involved in the trafficking and stabilization of NR2A subunits at the synapse (Elias et al., 2008). Previous reports have already shown the molecular mechanisms that could be involved in the phenomenon (Tovar and Westbrook, 1999; Fox, Henley, and Isaac, 1999; MacDonald, Jackson, and Beazely, 2006; Hoffmann, Gremme, Hatt, and Gottmann, 2000).

We observed that throughout postnatal development, GlyT1+/− mice exhibited a higher number of dendritic branching (Fig. 4 and Table II) as well as a higher density of excitatory glutamatergic synapses (Fig. 6 and Supporting Information Fig. 4) in the CA1 region of the hippocampus compared to WT mice. Indeed, the results of our investigation are consistent with those of previous reports in which focal application of glutamate lead to a dramatic increase in the length of the shaft filopodia leading to dendritic growth and branching during neuronal development (Portera-Cailliau, Pan, and Yuste, 2003). Moreover, numerous studies highlight that neuronal activity mediated by the NMDARs promotes dendritic arbor growth (Niell, Meyer, and Smith, 2004; Sin, Haas, Ruthazer, and Cline, 2002), whereas blocking NMDARs reduces dendritic growth (Rajan and Cline, 1998). Recently, Cline and coworkers showed that NR2A and NR2B subunits have specific functions in the morphological development of tectal neurons in the living Xenopus and found that NR2A but not NR2B increased dendritic branch clusters (Ewald, Keuren-Jensen, Aizenman, and Cline, 2008). GlyT1+/− mice exhibited a higher degree of synaptic connectivity (Fig. 5 and Supporting Information Fig. 2) as well as a higher degree of network excitability in the CA1 region of the hippocampus compared to WT mice (Fig. 7). Several mechanisms could explain this occurrence. First, the higher synaptic expression of NR2A in mutants endows the NMDAR channel with a higher open probability (Po; 5-fold higher) as well as a higher peak open probability than NR2B-containing NMDARs (Erreger et al., 2005; Mellor, Nicoll, and Schmitz, 2002), resulting in a higher degree of synaptic excitability. Second, NR2A-containing NMDARs have a faster glutamate unbinding rate (30-fold faster) than NR2B-containing NMDARs; this attribute reduces the degree of receptor desensitization, thereby enabling the receptor to respond promptly to repetitive synaptic signal inputs, especially during high frequency stimulation (Erreger et al., 2005). Finally, the morphological findings in our study, e.g., the higher number of postsynaptic dendritic branching in GlyT1+/− mice and higher density of synapses, provide the postsynaptic neurons with a stronger ability for integration of multiple synaptic inputs by temporal and spatial summation, altogether facilitating the generation of action potentials (Xu, Ye, Poo, and Zhang, 2006; Hausser, Spruston, and Stuart, 2000; Magee, 2000). These mechanisms could explain, at least in part, the higher network excitability encountered in mutant mice.

One of the more interesting and intriguing findings of our work is that there is a higher expression of PSD-95 protein in the hippocampus of mutant compared with WT mice. PSD-95 has been particularly studied because in the central nervous system it is one of the major constituents of excitatory PSDs (Chen et al., 2005), and it is directly involved in synaptic plasticity (Migaud et al., 1998). It is well documented that this abundant postsynaptic scaffold, PSD-95, regulates the formation of excitatory

synapses. PSD-95 is essential for synaptogenesis and for neurons to establish correct connectivity. PSD-95 protein plays major roles in synapse organization and function (Funke, Dakoji, and Bredt, 2005). Overexpression of PSD-95 in neurons is associated with modifications in the properties of synaptic transmission and has also been proposed to affect synapse maturation and stabilization (El-Husseini, Schnell, Chetkovich, Nicoll and Bredt, 2000) and, thus, synapse number. Acute knockdown of PSD-95 reduces the development of synaptic structures (Ehrlich, Klein, Rumpel, and Malinow, 2007), and PSD-95 mutant mice exhibit variations in spine densities in several brain regions (Vickers et al., 2006).

Morphological properties of excitatory synapses upon over-expression of PSD-95 reveals important new functions of this protein in regulating spine synapse formation and plasticity. The expression of PSD-95 resulted in changes in spine shape, a marked increase of the spine volume, and an enlargement of the PSD, resulting in the formation of synapses with complex and perforated or segmented PSDs. The effect is very significant because, on average, the PSD area increased by a factor of six to eight, and the spine volume increased about 3-fold, emphasizing the close relationship existing between spine volume and PSD size (Harris and Stevens, 1989). Moreover, PSD-95 has diverse synaptic functions. One such function is to interact with membrane proteins and regulate their synaptic localization. PSD-95 seems to stabilize interacting membrane proteins at synapses by suppressing their lateral diffusion or internalization (Roche et al., 2001; Prybylowski et al., 2005). In addition to its role in protein trafficking, PSD-95 can regulate the functional properties of interacting membrane proteins, as shown by PSD-95-dependent changes in the gating of NMDA receptors (Lin et al., 2006).

Glycinergic neurotransmission is known to control motor functions and arousal states (Legendre, 2001; Betz et al., 2006) while glutamatergic neural pathways are involved in the regulation of cognitive processes such as learning and memory storage (Citri and Malenka, 2008; MacDonald, Jackson, and Beazely, 2006; Citri and Malenka, 2008). Presumably, GlyT1 disruption affects one or more of these processes. This could likely play a role in glycine encephalopathy (GE) pathophysiology. This disease is believed to result from a shortage of an enzyme that normally breaks down glycine in the body. This defect allows excess glycine to build up in tissues and organs, particularly in the brain, leading to serious medical complications. Typically, neonatal individuals suffering from GE display a number of neuropsychological symptoms including hypotonia, convulsions and even coma, while mental retardation, psychomotor limitations, and behavioral abnormalities are usually observed later during childhood (Hayasaka et al., 1982; Hayasaka, Tada, Fueki, and Aikawa, 1990; Agamanolis, Potter, and Lundgren, 1993; Kikuchi, Motokawa, Yoshida, and Hiraga, 2008). Most GE individuals die as newborns but the rare ones that survive demonstrate lack of neurological development, intractable seizures and many neuropsychiatric symptoms including learning disabilities and mental retardation (Applegarth and Toone, 2001; Toone, et al., 2003; Applegarth and Toone, 2004).

GlyT1 knockout mouse models (Gomeza et al., 2003; Tsai et al., 2004) suggest the intriguing possibility that mutations in the corresponding gene in humans could cause GE. It is tempting to speculate that many of the symptoms present in GE patients could be explained by some of the new findings that we are reporting in our study. However, it is worth mentioning that all animal models of any human disease must be viewed with some scepticism. Indeed, homozygous GlyT1 deficient mice display most of the symptoms observed in individuals with GE, however, one would argue that the phenotype of heterozygous GlyT1 mice is relatively normal compared with WT mice. Indeed, GlyT1+/− are quite healthy, rarely exhibit seizures and perform relatively well in the Morris Water Maze (Tsai et al., 2004). However, GlyT1+/− mice have higher levels of glycine in their brain, blood, and urine, similar to what has been reported in GE patients that survive until early adulthood (Agamanolis, Potter, and Lundgren, 1993; Hardingham, 2009; Gomeza et al., 2003). NMDAR antagonists as a first line treatment for patients with GE have been used by several groups (Ohya, et al., 1991). The results of our investigations are indeed in support of this approach. However, one should never minimize the potential side effects of this type of treatment and the use of NMDAR antagonists should be done with caution.

ACKNOWLEDGMENTS

The authors thank Dr J.T. Coyle for providing the transgenic mice and Adrian Wong for his critical input. We also thank Chris Métivier and Jonathan Boyd for technical assistance.

REFERENCES

Adams RH, Sato K, Shimada S, Tohyama M, Puschel AW, Betz H. 1995. Gene structure and glial expression of the glycine transporter GlyT1 in embryonic and adult rodents. J Neurosci 15:2524–2532.

Agamanolis DP, Potter JL, Lundgren DW. 1993. Neonatal glycine encephalopathy: biochemical and neuropathologic findings. Pediatr Neurol 9:140–143.

Anson LC, Chen PE, Wyllie DJ, Colquhoun D, Schoepfer R. 1998. Identification of amino acid residues of the NR2A subunit that control glutamate potency in recombinant NR1/NR2A NMDA receptors. J Neurosci 18:581–589.

Applegarth DA, Toone JR. 2001. Nonketotic hyperglycinemia (glycine encephalopathy): laboratory diagnosis. Mol Genet Metab 74:139–146.

Applegarth DA, Toone JR. 2004. Glycine encephalopathy (nonketotic hyperglycinaemia) : review and update. J Inherit Metab Dis 27:417–422.
Aragon C, Lopez-Corcuera B. 2005. Glycine transporters: crucial roles of pharmacological interest revealed by gene deletion. Trends Pharmacol Sci 26:283–286.
Berger AJ, Dieudonne S, Ascher P. 1998. Glycine uptake governs glycine site occupancy at NMDA receptors of excitatory synapses. J Neurophysiol 80:3336–3340.
Bergeron R, Meyer TM, Coyle JT, Greene RW. 1998. Modulation of N-methyl-D-aspartate receptor function by glycine transport. Proc Natl Acad Sci U S A 95:15730–15734.
Betz H, Gomeza J, Armsen W, Scholze P, Eulenburg V. 2006. Glycine transporters: essential regulators of synaptic transmission. Biochem Soc Trans 34:55–58.
Betz H, Laube B. 2006. Glycine receptors: Recent insights into their structural organization and functional diversity. J Neurochem 97:1600–1610.
Borowsky B, Mezey E, Hoffman BJ. 1993. Two glycine transporter variants with distinct localization in the CNS and peripheral tissues are encoded by a common gene. Neuron 10:851–863.
Cathala L, Misra C, Cull-Candy S. 2000. Developmental profile of the changing properties of NMDA receptors at cerebellar mossy fiber-granule cell synapses. J Neurosci 20:5899–5905.
Chen X, Vinade L, Leapman RD, Petersen JD, Nakagawa T, Phillips TM, Sheng M, Reese TS. 2005. Mass of the postsynaptic density and enumeration of three key molecules. Proc Natl Acad Sci U S A 102:11551–11556.
Citri A, Malenka RC. 2008. Synaptic plasticity: Multiple forms, functions, and mechanisms. Neuropsychopharmacology 33:18–41.
Cull-Candy S, Brickley S, Farrant M. 2001. NMDA receptor subunits: Diversity, development and disease. Curr Opin Neurobiol 11:327–335.
Ehrlich I, Klein M, Rumpel S, Malinow R. 2007. PSD-95 is required for activity-driven synapse stabilization. Proc Natl Acad Sci U S A 104:4176–4181.
El Husseini AE, Schnell E, Chetkovich DM, Nicoll RA, Bredt DS. 2000. PSD-95 involvement in maturation of excitatory synapses. Science 290:1364–1368.
Elias GM, Elias LA, Apostolides PF, Kriegstein AR, Nicoll RA. 2008. Differential trafficking of AMPA and NMDA receptors by SAP102 and PSD-95 underlies synapse development. Proc Natl Acad Sci U S A 105:20953–20958.
Erreger K, Dravid SM, Banke TG, Wyllie DJ, Traynelis SF. 2005. Subunit-specific gating controls rat NR1/NR2A and NR1/NR2B NMDA channel kinetics and synaptic signalling profiles. J Physiol 563:345–358.
Eulenburg V, Armsen W, Betz H, Gomeza J. 2005. Glycine transporters: essential regulators of neurotransmission. Trends Biochem Sci 30:325–333.
Ewald RC, Keuren-Jensen KR, Aizenman CD, Cline HT. 2008. Roles of NR2A and NR2B in the development of dendritic arbor morphology in vivo. J Neurosci 28:850–861.
Flint AC, Maisch US, Weishaupt JH, Kriegstein AR, Monyer H. 1997. NR2A subunit expression shortens NMDA receptor synaptic currents in developing neocortex. J Neurosci 17:2469–2476.
Fox K, Henley J, Isaac J. 1999. Experience-dependent development of NMDA receptor transmission. Nat Neurosci 2:297–299.
Funke L, Dakoji S, Bredt DS. 2005. Membrane-associated guanylate kinases regulate adhesion and plasticity at cell junctions. Annu Rev Biochem 74:219–245.
Gabernet L, Pauly-Evers M, Schwerdel C, Lentz M, Bluethmann H, Vogt K, Alberati D, Mohler H, Boison D. 2005. Enhancement of the NMDA receptor function by reduction of glycine transporter-1 expression. Neurosci Lett 373:79–84.
Gomeza J, Hulsmann S, Ohno K, Eulenburg V, Szoke K, Richter D, Betz H. 2003. Inactivation of the glycine transporter 1 gene discloses vital role of glial glycine uptake in glycinergic inhibition. Neuron 40:785–796.
Gomeza J, Ohno K, Hulsmann S, Armsen W, Eulenburg V, Richter DW, Laube B, Betz H. 2003. Deletion of the mouse glycine transporter 2 results in a hyperekplexia phenotype and postnatal lethality. Neuron 40:797–806.
Guastella J, Brecha N, Weigmann C, Lester HA, Davidson N. 1992. Cloning, expression, and localization of a rat brain high-affinity glycine transporter. Proc Natl Acad Sci U S A 89:7189–7193.
Hardingham GE. 2009. Coupling of the NMDA receptor to neuroprotective and neurodestructive events. Biochem Soc Trans 37:1147–1160.
Harris KM, Stevens JK. 1989. Dendritic spines of CA 1 pyramidal cells in the rat hippocampus: serial electron microscopy with reference to their biophysical characteristics. J Neurosci 9:2982–2997.
Hausser M, Spruston N, Stuart GJ. 2000. Diversity and dynamics of dendritic signaling. Science 290:739–744.
Hayasaka K, Narisawa K, Satoh T, Tateda H, Metoki K, Tada K, Hiraga K, Aoki T, Kawakami T, Akamatsu H, Matsuo N. 1982. Glycine cleavage system in ketotic hyperglycinemia: a reduction of H-protein activity. Pediatr Res 16:5–7.
Hayasaka K, Tada K, Fueki N, Aikawa J. 1990. Prenatal diagnosis of nonketotic hyperglycinemia: enzymatic analysis of the glycine cleavage system in chorionic villi. J Pediatr 116:444–445.
Hestrin S. 1992. Developmental regulation of NMDA receptor-mediated synaptic currents at a central synapse. Nature 357:686–689.
Hoffmann H, Gremme T, Hatt H, Gottmann K. 2000. Synaptic activity-dependent developmental regulation of NMDA receptor subunit expression in cultured neocortical neurons. J Neurochem 75:1590–1599.
Hopf FW, Waters J, Mehta S, Smith SJ. 2002. Stability and plasticity of developing synapses in hippocampal neuronal cultures. J Neurosci 22:775–781.
Hsia AY, Malenka RC, Nicoll RA. 1998. Development of excitatory circuitry in the hippocampus. J Neurophysiol 79:2013–2024.
Imamura Y, Ma CL, Pabba M, Bergeron R. 2008. Sustained saturating level of glycine induces changes in NR2B-containing-NMDA receptor localization in the CA1 region of the hippocampus. J Neurochem 105:2454–2465.
Johnson JW, Ascher P. 1987. Glycine potentiates the NMDA response in cultured mouse brain neurons. Nature 325:529–531.
Jursky F, Nelson N. 1996. Developmental expression of the glycine transporters GLYT1 and GLYT2 in mouse brain. J Neurochem 67:336–344.
Kew JN, Richards JG, Mutel V, Kemp JA. 1998. Developmental changes in NMDA receptor glycine affinity and ifenprodil sensitivity reveal three distinct populations of NMDA receptors in individual rat cortical neurons. J Neurosci 18:1935–1943.
Kikuchi G, Motokawa Y, Yoshida T, Hiraga K. 2008. Glycine cleavage system: reaction mechanism, physiological significance, and hyperglycinemia. Proc Jpn Acad Ser B Phys Biol Sci 84:246–263.
Kirsch J. 2006. Glycinergic transmission. Cell Tissue Res 326:535–540.
Kleckner NW, Dingledine R. 1988. Requirement for glycine in activation of NMDA-receptors expressed in Xenopus oocytes. Science 241:835–837.
Lau CG, Zukin RS. 2007. NMDA receptor trafficking in synaptic plasticity and neuropsychiatric disorders. Nat Rev Neurosci 8:413–426.
Legendre P. 2001. The glycinergic inhibitory synapse. Cell Mol Life Sci 58:760–793.
Legendre P, Westbrook GL. 1991. Ifenprodil blocks N-methyl-D-aspartate receptors by a two-component mechanism. Mol Pharmacol 40:289–298.
Lin Y, Jover-Mengual T, Wong J, Bennett MV, Zukin RS. 2006. PSD-95 and PKC converge in regulating NMDA receptor trafficking and gating. Proc Natl Acad Sci U S A 103:19902–19907.
Lin Y, Skeberdis VA, Francesconi A, Bennett MV, Zukin RS. 2004. Postsynaptic density protein-95 regulates NMDA channel gating and surface expression. J Neurosci 24:10138–10148.
Liu QR, Lopez-Corcuera B, Mandiyan S, Nelson H, Nelson N. 1993. Cloning and expression of a spinal cord- and brain-specific glycine transporter with novel structural features. J Biol Chem 268:22802–22808.
Liu QR, Nelson H, Mandiyan S, Lopez-Corcuera B, Nelson N. 1992. Cloning and expression of a glycine transporter from mouse brain. FEBS Lett 305:110–114.
Liu XB, Murray KD, Jones EG. 2004. Switching of NMDA receptor 2A and 2B subunits at thalamic and cortical synapses during early postnatal development. J Neurosci 24:8885–8895.
Lopez-Corcuera B, Alcantara R, Vazquez J, Aragon C. 1993. Hydrodynamic properties and immunological identification of the sodium- and chloride-coupled glycine transporter. J Biol Chem 268:2239–2243.
Losi G, Prybylowski K, Fu Z, Luo J, Wenthold RJ, Vicini S. 2003. PSD-95 regulates NMDA receptors in developing cerebellar granule neurons of the rat. J Physiol 548:21–29.
MacDonald JF, Jackson MF, Beazely MA. 2006. Hippocampal long-term synaptic plasticity and signal amplification of NMDA receptors. Crit Rev Neurobiol 18:71–84.
Magee JC. 2000. Dendritic integration of excitatory synaptic input. Nat Rev Neurosci 1:181–190.
Martina M, Turcotte ME, Halman S, Tsai G, Tiberi M, Coyle JT, Bergeron R. 2005. Reduced glycine transporter type 1 expression

leads to major changes in glutamatergic neurotransmission of CA1 hippocampal neurones in mice. J Physiol 563:777–793.
Mayer ML, Vyklicky L Jr, Clements J. 1989. Regulation of NMDA receptor desensitization in mouse hippocampal neurons by glycine. Nature 338:425–427.
Mellor J, Nicoll RA, Schmitz D. 2002. Mediation of hippocampal mossy fiber long-term potentiation by presynaptic Ih channels. Science 295:143–147.
Migaud M, Charlesworth P, Dempster M, Webster LC, Watabe AM, Makhinson M, He Y, Ramsay MF, Morris RG, Morrison JH, O'Dell TJ, Grant SG. 1998. Enhanced long-term potentiation and impaired learning in mice with mutant postsynaptic density-95 protein. Nature 396:433–439.
Monyer H, Burnashev N, Laurie DJ, Sakmann B, Seeburg PH. 1994. Developmental and regional expression in the rat brain and functional properties of four NMDA receptors. Neuron 12:529–540.
Monyer H, Sprengel R, Schoepfer R, Herb A, Higuchi M, Lomeli H, Burnashev N, Sakmann B, Seeburg PH. 1992. Heteromeric NMDA receptors: Molecular and functional distinction of subtypes. Science 256:1217–1221.
Niell CM, Meyer MP, Smith SJ. 2004. In vivo imaging of synapse formation on a growing dendritic arbor. Nat Neurosci 7:254–260.
Ohya Y, Ochi N, Mizutani N, Hayakawa C, Watanabe K. 1991. Nonketotic hyperglycinemia: treatment with NMDA antagonist and consideration of neuropathogenesis. Pediatr Neurol 7:65–68.
Papadia S, Hardingham GE. 2007. The dichotomy of NMDA receptor signaling. Neuroscientist 13:572–579.
Portera-Cailliau C, Pan DT, Yuste R. 2003. Activity-regulated dynamic behavior of early dendritic protrusions: evidence for different types of dendritic filopodia. J Neurosci 23:7129–7142.
Prybylowski K, Chang K, Sans N, Kan L, Vicini S, Wenthold RJ. 2005. The synaptic localization of NR2B-containing NMDA receptors is controlled by interactions with PDZ proteins and AP-2. Neuron 47:845–857.
Rajan I, Cline HT. 1998. Glutamate receptor activity is required for normal development of tectal cell dendrites in vivo. J Neurosci 18:7836–7846.
Rao A, Craig AM. 1997. Activity regulates the synaptic localization of the NMDA receptor in hippocampal neurons. Neuron 19:801–812.
Roche KW, Standley S, McCallum J, Dune Ly C, Ehlers MD, Wenthold RJ. 2001. Molecular determinants of NMDA receptor internalization. Nat Neurosci 4:794–802.
Sans N, Petralia RS, Wang YX, Blahos J, Hell JW, Wenthold RJ. 2000. A developmental change in NMDA receptor-associated proteins at hippocampal synapses. J Neurosci 20:1260–1271.
Schell MJ, Molliver ME, Snyder SH. 1995. D-serine, an endogenous synaptic modulator: localization to astrocytes and glutamate-stimulated release. Proc Natl Acad Sci U S A 92:3948–3952.
Sheng M, Cummings J, Roldan LA, Jan YN, Jan LY. 1994. Changing subunit composition of heteromeric NMDA receptors during development of rat cortex. Nature 368:144–147.
Sin WC, Haas K, Ruthazer ES, Cline HT. 2002. Dendrite growth increased by visual activity requires NMDA receptor and Rho GTPases. Nature 419:475–480.
Sinor JD, Du S, Venneti S, Blitzblau RC, Leszkiewicz DN, Rosenberg PA, Aizenman E. 2000. NMDA and glutamate evoke excitotoxicity at distinct cellular locations in rat cortical neurons in vitro. J Neurosci 20:8831–8837.
Smith KE, Borden LA, Hartig PR, Branchek T, Weinshank RL. 1992. Cloning and expression of a glycine transporter reveal colocalization with NMDA receptors. Neuron 8:927–935.
Stephenson FA. 2001. Subunit characterization of NMDA receptors. Curr Drug Targets 2:233–239.
Stocca G, Vicini S. 1998. Increased contribution of NR2A subunit to synaptic NMDA receptors in developing rat cortical neurons. J Physiol 507(Pt 1):13–24.
Thomson AM, Walker VE, Flynn DM. 1989. Glycine enhances NMDA-receptor mediated synaptic potentials in neocortical slices. Nature 338:422–424.
Toone JR, Applegarth DA, Levy HL, Coulter-Mackie MB, Lee G. 2003. Molecular genetic and potential biochemical characteristics of patients with T-protein deficiency as a cause of glycine encephalopathy (NKH). Mol Genet Metab 79:272–280.
Tovar KR, Westbrook GL. 1999. The incorporation of NMDA receptors with a distinct subunit composition at nascent hippocampal synapses in vitro. J Neurosci 19:4180–4188.
Tsai G, Ralph-Williams RJ, Martina M, Bergeron R, Berger-Sweeney J, Dunham KS, Jiang Z, Caine SB, Coyle JT. 2004. Gene knockout of glycine transporter 1: Characterization of the behavioral phenotype. Proc Natl Acad Sci U S A 101:8485–8490.
Vickers CA, Stephens B, Bowen J, Arbuthnott GW, Grant SG, Ingham CA. 2006. Neurone specific regulation of dendritic spines in vivo by post synaptic density 95 protein (PSD-95). Brain Res 1090:89–98.
von Engelhardt J, Doganci B, Seeburg PH, Monyer H. 2009. Synaptic NR2A- but not NR2B-containing NMDA receptors increase with blockade of ionotropic glutamate receptors. Front Mol Neurosci 2:1–14.
Wasling P, Hanse E, Gustafsson B. 2004. Developmental changes in release properties of the CA3-CA1 glutamate synapse in rat hippocampus. J Neurophysiol 92:2714–2724.
Waxman EA, Lynch DR. 2005. N-methyl-D-aspartate receptor subtypes: Multiple roles in excitotoxicity and neurological disease. Neuroscientist 11:37–49.
Williams K. 1993. Ifenprodil discriminates subtypes of the N-methyl-D-aspartate receptor: selectivity and mechanisms at recombinant heteromeric receptors. Mol Pharmacol 44:851–859.
Williams K. 2001. Ifenprodil, a novel NMDA receptor antagonist: Site and mechanism of action. Curr Drug Targets 2:285–298.
Xu NL, Ye CQ, Poo MM, Zhang XH. 2006. Coincidence detection of synaptic inputs is facilitated at the distal dendrites after long-term potentiation induction. J Neurosci 26:3002–3009.
Yee BK, Balic E, Singer P, Schwerdel C, Grampp T, Gabernet L, Knuesel I, Benke D, Feldon J, Mohler H, Boison D. 2006. Disruption of glycine transporter 1 restricted to forebrain neurons is associated with a procognitive and antipsychotic phenotypic profile. J Neurosci 26:3169–3181.
Zafra F, Aragon C, Olivares L, Danbolt NC, Gimenez C, Storm-Mathisen J. 1995. Glycine transporters are differentially expressed among CNS cells. J Neurosci 15:3952–3969.
Zafra F, Gomeza J, Olivares L, Aragon C, Gimenez C. 1995. Regional distribution and developmental variation of the glycine transporters GLYT1 and GLYT2 in the rat CNS. Eur J Neurosci 7:1342–1352.